Fitness strategies of fastidious prokaryotes

by

Marcus Vinicius Merfa e Silva

A dissertation submitted to the Graduate Faculty of
Auburn University
in partial fulfillment of the
requirements for the Degree of
Doctor of Philosophy

Auburn, Alabama
December 11, 2021

Keywords: '*Candidatus* Liberibacter asiaticus', *Xylella fastidiosa*, HLB, culturing, natural competence, type IV pili

Approved by

Leonardo De La Fuente, Chair, Professor of Plant Pathology
Neha Potnis, Assistant Professor of Plant Pathology
John Beckmann, Assistant Professor of Entomology
Paul A. Cobine, Professor of Biological Sciences

Abstract

Fastidious prokaryotes are slow-growing bacteria that either require specific media to grow or are not able to grow axenically. '*Candidatus* Liberibacter asiaticus' (CLas) and *Xylella fastidiosa* are important fastidious plant pathogenic bacteria that threaten agriculture worldwide. CLas is associated with Huanglongbing, the most devastating disease of citrus globally, whereas *X. fastidiosa* harms many economically important crops worldwide, including grapevine, citrus, and olive. In this study, we sought to understand the fitness of CLas in its natural environments based on published studies and aimed to replicate these conditions in vitro to increase its culturability, since CLas is hitherto unculturable axenically. Commercial grapefruit juice (GJ), which was used as base culture medium, was amended with a wide range of compounds, and incubated under different conditions to evaluate the optimization of CLas growth. A reproducible growth behavior in which CLas growth ratios were inversely proportional to the initial inoculum concentration was observed. Additionally, strategies to reduce the cell density allowed CLas to reach maximum growth as fast as 3 days post inoculation, but with no sustained exponential growth over time. Conversely, we performed a complete functional analysis of the molecular components of the type IV pili (TFP) machinery of *X. fastidiosa* that mediates both its twitching motility and natural competence, an important mechanism to generate genetic diversity and likely modulate its fitness within natural hosts. We determined the core components of TFP involved in these two traits, as well as screened the role for virulence in planta for some of these components. Remarkably, we identified a novel minor pilin, FimT3, which is the DNA receptor of the *X. fastidiosa* TFP, being thus essential for its natural competence by binding DNA. Moreover, we identified recently recombined genes within *X. fastidiosa* strains by performing whole genome analyses. Identified genes are involved in host colonization, regulation and

signaling, host evasion, and nutrient acquisition, which are all important for the ecology of *X. fastidiosa*. We hope our results may help to better understand the fitness of these two pathogens, which may aid the development of strategies for controlling them.

Acknowledgments

I would like to express my most sincere gratitude to Dr. Leonardo De La Fuente for giving me the opportunity to join his lab and for his continuous support and guidance. His motivation, patience and enthusiasm constantly inspired me to do my utmost.

I am also grateful to Dr. Neha Potnis, Dr. Paul A. Cobine and Dr. John Beckmann for serving on my Graduate Committee and for their valuable suggestions, guidance, and collaboration towards my work. In addition, I thank the outside university reader Dr. Yi Wang for his constructive suggestions.

I would like to extend my gratitude to my current and former lab mates and friends Laura Gómez, Balapuwaduge H. Mendis, Eber Naranjo, Qing Ge, Deepak Shantharaj, Noel Claudio, Ranlin Liu, Hongyu Chen, Sy Traore, Edel Pérez-López and Prem Kandel for kindly sharing their experiences with me and helping me to accomplish this work.

I am deeply grateful to my family for unconditionally supporting me throughout this journey, especially my parents Luis Claudio da Silva and Marta de Oliveira Merfa da Silva. Thank you for making my path easier and helping me in every possible way.

I dedicate this work to my beloved Gabriela Augusto Koyama for her unconditional patience and support. Thank you for always believing and encouraging me.

Table of Contents

Abstract ii

Acknowledgments iv

List of Tables ix

List of Figures xi

Chapter 1. Introduction to plant pathogenic fastidious bacteria 1

Bacterial plant pathogens 1

Fastidious plant pathogenic bacteria 1

Bacterial fitness 2

Overall goal 2

References 3

Chapter 2. Progress and obstacles in culturing '*Candidatus* Liberibacter asiaticus', the bacterium associated with Huanglongbing 4

Abstract 4

Introduction 5

Vasculature-restricted pathogens successfully cultured 7

CLas transient cultures 8

Available nutrients in CLas hosts 10

Beyond nutrients: conditions to consider for CLas culture 20

Genetic components 21

Bacteriophage genes in CLas 23

Cell culture infection models and bacterial co-cultures as valuable tools 24

Liberibacter crescens, a model system 26

Concluding remarks: What have we learned? 27
Long-term goal 28
Specific objective 28
Hypothesis 28
Acknowledgments 28
References 29
Chapter 3. Growth of '*Candidatus* Liberibacter asiaticus' in commercial grapefruit juice-based media formulations reveals common cell density-dependent transient behaviors 35
Abstract 35
Introduction 36
Materials and methods 40
Results 51
Discussion 65
Acknowledgments 73
References 75
Supplementary material for chapter 3 81
Chapter 4. Overview of *Xylella fastidiosa*: main features, adaptation to the xylem, type IV pili, and natural competence 94
Xylella fastidiosa 94
Pathogen transmission and disease development 95
Adaptation of *X. fastidiosa* to the xylem environment 98
X. fastidiosa taxonomy and distribution 105
Intersubspecific homologous recombination in *X. fastidiosa* 107

Natural competence: from discovery to current knowledge 108
Natural competence mechanisms: the role of type IV pili 110
The role of natural competence in evolution and adaptation 114
Naturally competent plant pathogenic bacteria 114
The natural competence of *X. fastidiosa* 115
Long-term goal 116
Specific objectives 117
Hypotheses 117
References 118
Chapter 5. Movement and evolution: complete functional analysis of type IV pilus of a re-emergent plant pathogen reveals a unique DNA receptor 130
Abstract 130
Significance statement 131
Introduction 131
Materials and methods 135
Results 140
Discussion 152
Acknowledgments 157
References 158
Supplementary material for chapter 5 164
Chapter 6. Patterns of inter- and intra-subspecific homologous recombination inform eco-evolutionary dynamics of *Xylella fastidiosa* 234
Abstract 234

Introduction 235
Materials and methods 238
Results and discussion 242
Conclusions 263
Acknowledgments 264
References 265
Supplementary material for chapter 6 271
Chapter 7. Concluding remarks 300

List of Tables

Table 2-1. Genome size and GC content of several vascular bacterial pathogens and insect symbionts 8

Table 2-2. Main common compounds found in citrus phloem sap, psyllid hemolymph, and G medium (grapefruit juice), based on studies referenced in the main text 11

Table 3-1. Contribution of different compounds and incubation conditions to CLas growth 60

Table S3-1. Experiments conducted from 2017 to 2021 93

Table S5-1. Bacterial strains and plasmids used in this study 202

Table S5-2. List of PCR primers and qPCR primers and probe used in this study 205

Table S5-3. List of *pil* and associated genes deleted in *X. fastidiosa* strain TemeculaL 221

Table S5-4. Genomic organization of *pil* and associated genes in *X. fastidiosa* TemeculaL ... 224

Table S5-5. Pearson's correlation results for the analyzed phenotypic traits of *X. fastidiosa* .. 225

Table S5-6. DNA-binding probability of amino acid residues from FimT3 226

Table S5-7. Homologs of FimT3 are found in many members of the Xanthomonadaceae and few *Pseudomonas* spp. 227

Table 6-1. List of recent recombination events in genes/categories identified in WT strains and their possible ecological role in host adaptation 248

Table S6-1. Strains, mutants, and recombinants used in this study 282

Table S6-2. Sequencing and assembly statistics of the genomes sequenced in this study 288

Table S6-3. Annotation results of the genomes sequenced in this study 289

Table S6-4. Extent and origin of recent recombination in each strain of *X. fastidiosa* analyzed in this study using fastGEAR 290

Table S6-5. Ancestral recombination events in the core genome of *X. fastidiosa* predicted by fastGEAR 292

Table S6-6. Complete list of genes under recent recombination used for Table 6-1, organized by COG numbers and description 293

Table S6-7. Frequency of recent recombination events per gene of strains belonging to each *X. fastidiosa* subspecies ..... Available online

List of Figures

Figure 2-1. Summary of conditions for growth of '*Candidatus* Liberibacter asiaticus' (CLas) in nature in plant host and insect vectors 13

Figure 3-1. Growth of CLas inoculated into grapefruit juice in 24-well plates..... 53

Figure 3-2. Growth of CLas among subcultures in modified grapefruit juice in 24-well plates 54

Figure 3-3. Growth of CLas when incubated using the flow system..... 56

Figure 3-4. Growth of CLas when subcultured at 3-day intervals..... 57

Figure 3-5. Assessment of CLas growth on solid grapefruit juice plates 58

Figure 3-6. Growth of CLas within periwinkle callus culture 64

Figure 3-7. Detection of CLas within periwinkle calli by immune tissue printing 65

Figure S3-1. System used to assess CLas growth under flow conditions..... 81

Figure S3-2. qPCR standard curve used to quantify '*Ca.* Liberibacter asiaticus' in each sample as genome equivalents..... 82

Figure S3-3. CLas population in citrus seeds used as inoculum source throughout this study .. 83

Figure S3-4. Comparison of CLas growth in different pH of grapefruit juice 84

Figure S3-5. Effect of adding ATP to GJ on CLas growth..... 85

Figure S3-6. Assessing the contribution of *Wolbachia* repressor protein (Wrp) to CLas growth86

Figure S3-7. CLas growth in mGJ amended with TNM-FH insect medium, BSA and ATP..... 87

Figure S3-8. Comparison of CLas growth in mGJ and amended mGJ 88

Figure S3-9. Determining the contribution of adding exogenous DNA to CLas growth 89

Figure S3-10. Comparison of CLas growth in flow conditions at 28 ºC and room temperature 90

Figure S3-11. CLas and Lcr growth in coculture 91

Figure S3-12. CLas growth in coculture with SF9 insect cell line 92

Figure 4-1. General TFP structure and mechanism required for twitching motility and natural competence in Gram-negative bacteria 113
Figure 5-1. Natural competence and twitching motility phenotypes of *X. fastidiosa* mutant strains used in this study 142
Figure 5-2. FimT3 DNA binding activity 147
Figure 5-3. Phylogenetic tree based on FimT3 amino acid sequences from Xanthomonadaceae bacterial strains with whole-genome sequences 152
Figure 5-4. Schematic representation of the functional role of TFP molecular components in natural competence and twitching motility of *X. fastidiosa* 153
Figure S5-1. Recombination frequencies obtained through natural competence of *X. fastidiosa* mutant strains used in this study 186
Figure S5-2. Fringe width measurements of the twitching motility phenotypes of *X. fastidiosa* mutant strains used in this study 187
Figure S5-3. Figure panel with representative pictures of the twitching motility phenotypes of *X. fastidiosa* mutant strains used in this study 188
Figure S5-4. Growth curves of *X. fastidiosa* mutant strains used in this study 189
Figure S5-5. Growth rates of *X. fastidiosa* mutant strains used in this study 190
Figure S5-6. Total number of viable CFU/ml of *X. fastidiosa* mutant strains used in this study after growth during natural competence assays 191
Figure S5-7. Biofilm formation of *X. fastidiosa* mutant strains used in this study 192
Figure S5-8. Planktonic growth of *X. fastidiosa* mutant strains used in this study 193
Figure S5-9. Settling rates of *X. fastidiosa* mutant strains used in this study 194
Figure S5-10. Deletion of *pil* genes negatively affects virulence of *X. fastidiosa* 195

Figure S5-11. *X. fastidiosa* cells take up Cy-3 labeled DNA into a DNase I resistant state 197

Figure S5-12. Percentage of *X. fastidiosa* cells that acquired DNA from the extracellular environment during DNA uptake assays in the different analyzed strains 198

Figure S5-13. FimT3 DNA binding activity in different DNA sequences 199

Figure S5-14. Alignment of FimT3 from *X. fastidiosa* to DNA-binding minor pilins from *Neisseria meningitidis* (ComP) and *Vibrio cholerae* (VC0858) 200

Figure S5-15. The DNA-binding residues of FimT3 is majorly conserved within bacterial members of the Xanthomonadaceae family encoding this protein 201

Figure 6-1. Diagram summarizing the lineage of the recombinant strains used in this study .. 242

Figure 6-2. Maximum likelihood phylogeny of the core genome alignment of 13 strains of *X. fastidiosa* in vitro recombinants and their donor and recipient parental strains before (A) and after (B) recombination filtering 244

Figure 6-3. Detection of recombinogenic regions in the core genomes of *X. fastidiosa* in vitro recombinants and their parental strains using BratNextGen 245

Figure 6-4. Population structure of *X. fastidiosa* 252

Figure 6-5. Interlineage recombination 254

Figure 6-6. Distribution of length of recombinant fragments and the number of recombination events for each subspecies of *X. fastidiosa* 256

Figure 6-7. Diagram illustrating the ecological role of genes found to be under recent recombination in *Xylella fastidiosa* 261

Figure S6-1. Pipeline to determine the number and frequency of recent recombination events of each gene per *X. fastidiosa* strain 277

Figure S6-2. Detection of intersubspecific recombination in the flanking region of the Kanamycin (Km)-resistance insertion site in the in vitro recombinants produced by mixing live cells of TemeculaL with heat-killed cells of AlmaEM3(NS1::Km^R) 278

Figure S6-3. Recombination analysis performed using BratNextGen on the core genome alignment of 55 *X. fastidiosa* strains analyzed in this study 279

Figure S6-4. Distribution, origin and proportion of recent recombination events across the *X. fastidiosa* core genome of 57 strains as predicted by fastGEAR as described in materials and methods and Fig. 6-5..... 280

Figure S6-5. Maximum likelihood phylogeny of core genome alignment of *X. fastidiosa* strains including intercepted strains PD7202 and PD7211 281

Chapter 1

Introduction to plant pathogenic fastidious bacteria

Bacterial plant pathogens

A wide range of bacterial species colonize and cause diseases in economically important crops worldwide (Kannan et al. 2015; Strange and Scott 2005). In fact, it is estimated that around 150 bacterial species may cause plant diseases (Kannan et al. 2015). Plant pathogenic bacteria affect all crops by colonizing either their tissues or surface and causing a variety of symptoms including cankers, spots, tissue rots, blights, and hormone imbalances that result in plant stunting or overgrowth, leaf epinasty and root branching (Kannan et al. 2015; Strange and Scott 2005). Collectively, bacterial plant diseases cause losses of over $1 billion worldwide every year, impacting plants on a quantitative and qualitative level and negatively affecting the global food production chain (Kannan et al. 2015; Mansfield et al. 2012).

Fastidious plant pathogenic bacteria

The term fastidious plant pathogenic bacteria refers to bacterial plant pathogens that are usually limited to either the phloem or xylem of plant hosts and are transmitted from plant to plant by insect vectors, which are also hosts of these bacteria (Davis 1992). In addition, fastidious bacteria are slow-growing and either cannot grow in any available media or require very specific media to be cultured (Chang et al. 2013). Due to the vascular-limited nature of these pathogens, management of their caused diseases is challenging (Jiang et al. 2019; Yadeta and Thomma 2013). Moreover, the research of fastidious plant pathogens is difficult due to their slow-growth behavior, lack of culturing of multiple species, need of an insect vector for

transmission and absence of model systems (Jiang et al. 2019). '*Candidatus* Liberibacter asiaticus' (CLas) and *Xylella fastidiosa* are two important fastidious plant pathogenic bacteria that harm economically important crops worldwide (Bové 2006; Chatterjee et al. 2008) and are the focus of this study.

Bacterial fitness

Bacterial fitness is the ability of individuals (or genotypes) to modulate their metabolism for growth and survival according to environmental conditions, which also includes their ability to reproduce within hosts, be transmitted, and overcome host defenses (Laurent et al. 2001; Pope et al. 2010). Therefore, in this study, we aimed to i. explore conditions and compounds that contribute to the fitness of CLas in its plant hosts and insect vectors and replicate these features in vitro to increase the in vitro viability of this hitherto unculturable pathogen (Wang and Trivedi 2013); and ii. investigate the role of type IV pili in the natural competence mechanism of *X. fastidiosa*, as well as identify genes that have been recombined by intersubspecific homologous recombination within this pathogen, both of which likely contribute to modulate the fitness of this bacterium within its hosts. A detailed description of each pathogen and results of this study are described in the following chapters of this dissertation.

Overall goal

Understand processes that contribute to the fitness of fastidious prokaryotes.

References

Bové, J. M. 2006. Huanglongbing: A destructive, newly-emerging, century-old disease of citrus. Journal of Plant Pathology 88:7-37.

Chang, C. J., Shih, H. T., Su, C. C., and Jan, F. J. 2013. Fastidious prokaryotes and plant health. Plant Pathology Bulletin 22:233-243.

Chatterjee, S., Almeida, R. P. P., and Lindow, S. 2008. Living in two worlds: the plant and insect lifestyles of *Xylella fastidiosa*. Annu Rev Phytopathol 46:243-271.

Davis, M. J. 1992. Fastidious bacteria of plant vascular tissues and their invertebrate vectors. Pages 4030-4049 in: The Prokaryotes. A. Balows, H. G. Trüper, M. Dworkin, W. Harder and K. H. Schleifer, eds. Springer, New York, NY.

Jiang, Y., Zhang, C. X., Chen, R., and He, S. Y. 2019. Challenging battles of plants with phloem-feeding insects and prokaryotic pathogens. Proc Natl Acad Sci U S A 116:23390-23397.

Kannan, V., Bastas, K., and Devi, R. 2015. Scientific and economic impact of plant pathogenic bacteria. Pages 369-392 in: Sustainable approaches to controlling plant pathogenic bacteria. R. V. Kannan and K. K. Bastas, eds. CRC Press, Boca Raton, FL.

Laurent, F., Lelièvre, H., Cornu, M., Vandenesch, F., Carret, G., Etienne, J., and Flandrois, J. P. 2001. Fitness and competitive growth advantage of new gentamicin-susceptible MRSA clones spreading in French hospitals. J Antimicrob Chemother 47:277-283.

Mansfield, J., Genin, S., Magori, S., Citovsky, V., Sriariyanum, M., Ronald, P., Dow, M., Verdier, V., Beer, S. V., Machado, M. A., Toth, I., Salmond, G., and Foster, G. D. 2012. Top 10 plant pathogenic bacteria in molecular plant pathology. Mol Plant Pathol 13:614-629.

Pope, C. F., McHugh, T. D., and Gillespie, S. H. 2010. Methods to determine fitness in bacteria. Pages 113-121 in: Antibiotic Resistance Protocols. Methids in Molecular Biology (Methods and Protocols), vol. 642. S. Gillespie and T. McHugh, eds. Humana Press.

Strange, R. N., and Scott, P. R. 2005. Plant disease: a threat to global food security. Annu Rev Phytopathol 43:83-116.

Wang, N., and Trivedi, P. 2013. Citrus Huanglongbing: a newly relevant disease presents unprecedented challenges. Phytopathology 103:652-665.

Yadeta, K. A., and Thomma, B. P. H. J. 2013. The xylem as battleground for plant hosts and vascular wilt pathogens. Front Plant Sci 4:97.

Chapter 2

Progress and obstacles in culturing '*Candidatus* Liberibacter asiaticus', the bacterium associated with Huanglongbing

Note – This study was previously published with the following citation:

MERFA, M. V., Pérez-López, E., Naranjo, E., Jain, M., Gabriel, D. W., and De La Fuente, L. 2019. Progress and obstacles in culturing '*Candidatus* Liberibacter asiaticus', the bacterium associated with Huanglongbing. Phytopathology 109:1092-1101.

This work performed in collaboration with other authors. My part of the collaboration was to coordinate the sections and writing of the manuscript and write the following sections: 'Abstract', 'CLas transient cultures', 'Available nutrients in CLas hosts', 'Beyond nutrients: conditions to consider for CLas culture' and collaborate with the section 'Concluding remarks: what have we learned?'. In addition, I was responsible for doing **Table 2-2** and **Fig. 2-1**. The entire manuscript is included in this chapter to maintain its cohesion and understanding.

Abstract

In recent decades, '*Candidatus* Liberibacter spp.' have emerged as a versatile group of psyllid-vectored plant pathogens and endophytes capable of infecting a wide range of economically important plant hosts. The most notable example is '*Candidatus* Liberibacter asiaticus' (CLas) associated with Huanglongbing (HLB) in several major citrus-producing areas of the world. CLas is a phloem-limited α-proteobacterium that is primarily vectored and transmitted among citrus species by the Asian citrus psyllid (ACP) *Diaphorina citri*. HLB was first detected in North America in Florida (USA) in 2005, following introduction of the ACP to

the State in 1998. HLB rapidly spread to all citrus growing regions of Florida within three years, with severe economic consequences to growers and considerable expense to taxpayers of the state and nation. Inability to establish CLas in culture (except transiently) remains a significant scientific challenge towards effective HLB management. Lack of axenic cultures has restricted functional genomic analyses, transfer of CLas to either insect or plant hosts for fulfilment of Koch's postulates, characterization of host-pathogen interactions and effective screening of antibacterial compounds. In the last decade, substantial progress has been made towards CLas culturing: (a) three reports of transient CLas cultures were published, (b) a new species of *Liberibacter* was identified and axenically cultured from diseased mountain papaya (*L. crescens* strain BT-1), (c) psyllid hemolymph and citrus phloem sap were biochemically characterized, (d) CLas phages were identified and lytic genes possibly affecting CLas growth were described, and (e) genomic sequences of fifteen CLas strains were made available. In addition, development of *L. crescens* as a surrogate host for functional analyses of CLas genes, has provided valuable insights into CLas pathogenesis and its physiological dependence on the host cell. In this review we summarize the conclusions from these important studies.

Introduction

'*Candidatus* Liberibacter asiaticus' (CLas), '*Ca.* Liberibacter americanus' (CLam) and '*Ca.* Liberibacter africanus' (CLaf) are Gram-negative bacteria in the α subdivision of Proteobacteria (Jagoueix et al. 1994). These three '*Ca.* Liberibacter spp.' have been associated with Citrus Huanglongbing (HLB), a devastating disease considered one of the most damaging plant diseases worldwide, causing substantial economic losses in Asia, Africa, Oceania, and the Americas (Bové 2014). CLas is widespread in all continents affected by HLB, including the

Americas with reports in United States, Mexico, Brazil, and Cuba; Africa with reports in Ethiopia, and Reunion Island; and Oceania (Wang et al. 2017).

The term '*Candidatus*' is used to record putative prokaryotic taxa, where the identifying information is obtained from genomic sequencing of natural samples and supported by observation of cells. However, traditional taxonomic description of such organisms in pure culture is still missing (Murray and Stackebrandt 1995). Besides the taxonomical problem, the lack of critical molecular and physiological information of '*Candidatus*' organisms hamper the understanding of the biological interactions, and subsequent development of control strategies for pathogens like CLas (Stewart 2012).

Despite very limited success towards growing CLas in vitro (Davis et al. 2008; Parker et al. 2014; Sechler et al. 2009), not one of the pathogenic Liberibacters has been maintained in continuous axenic culture to date. The aim of this review is to critically summarize the advances in CLas culturing and integrate recent molecular and chemical information that provides insight into the requirements for free-living growth of Liberibacters in culture. We have compared and consolidated information from completely sequenced genomes of CLas (Duan et al. 2009; Katoh et al. 2014), CLam (Wulff et al. 2014), CLaf (Lin et al. 2015) and the cultured but not evidently pathogenic *Liberibacter crescens* (Lcr) genome (Leonard et al. 2012). Also included are plant host and insect vector metabolomic analyses (Killiny 2016, 2017; Killiny et al. 2017b), and recent discoveries using *L. crescens* as a surrogate (Jain et al. 2017a, b) to identify traits that may be hampering CLas culturing. The ability of culturing CLas (and other '*Ca.* Liberibacter spp.') will be fundamental help to: i) fulfill Koch's postulates; ii) efficiently assess virulence across

different CLas genotypes; iii) screen efficiently antibacterial compounds; iv) conduct functional studies to understand the basis of CLas pathogenicity and insect transmission; and v) use this information to allow development of novel control methods based on the molecular pathogen-plant-insect interactions.

Vasculature-restricted citrus pathogens successfully cultured

Several fastidious bacteria besides CLas have been associated with citrus diseases (Davis and Brlansky 2007). The phloem-inhabiting *Spiroplasma citri*, which is a citrus plant pathogen associated with citrus stubborn disease, was the first phloem-limited fastidious prokaryote isolated in axenic culture (Saglio et al. 1971). The second fastidious prokaryote isolated in axenic culture was the xylem-limited *Xylella fastidiosa*, which is the causal agent of Pierce's disease of grapevines (Davis et al. 1978). *Xylella fastidiosa* subsp. *pauca,* which infects citrus was cultured several years later (Chang et al. 1993). Successful culturing of these vasculature-limited, fastidious plant pathogens relied on a nutritionally complex culture medium containing undefined components (Davis et al. 1978). The highly restricted nutritive value of xylem sap and significantly larger genome size of *X. fastidiosa* (2.5 Mb) (**Table 2-1**) may be contrasted to the nutritional environment of CLas, given that phloem is physiologically and nutritionally more complex than xylem. Pathogenic Liberibacters in general have undergone reductive genome evolution with an average genome size of 1.2 Mb, but *S. citri* has a small genome (1.6 Mb) as well (**Table 2-1**), and nevertheless it has been cultured in vitro.

Table 2-1. Genome size and GC content of several vascular bacterial pathogens and insect symbionts.

Strain[a]	Genome size (bp)	GC content (%)	GenBank Accession no.
CLas			
Psy62	1,227,204	36.5	NC_012985.3
Ishi-1	1,190,853	36.32	AP014595
CLso			
CLso-ZC1	1,258,278	35.24	NC_014774
LsoNZ1	1,312,416	35.32	JMTK01000000
CLam			
PW_SP	1,176,071	31	AOFG00000000
Sao Paulo	1,195,201	31.1	NC_022793.1
CLaf			
PTSAPSY	1,192,232	34.5	NZ_CP004021.1
Lcr			
BT-1	1,504,659	35.36	NC_019907.1
Xylella fastidiosa			
Temecula 1	2,519,802	51.8	NC_004556
Spiroplasma citri			
R8-A2	1,599,709	25.1	NZ_CP013197.1
***'Candidatus* Carsonella ruddii'**			
NHV	159,923	15.6	NC_018418.1
Thao2000	162,504	14.2	NC_018415.1

[a]'*Ca.* Liberibacter spp.': '*Candidatus* Liberibacter asiaticus' (CLas), '*Ca.* Liberibacter americanus' (CLam), '*Ca.* Liberibacter africanus' (CLaf), and '*Ca.* Liberibacter solanacearum' (CLso). Lcr: *Liberibacter crescens*. Fastidious bacteria *Xylella fastidiosa* and *Spiroplasma citri* were initially identified as unculturable plant pathogens. *'Candidatus* Carsonella ruddii*'* is a primary *Diaphorina citri* symbiont. Whenever multiple genomes of the same species were available, only a representative genome in terms of size and GC content was included here.

CLas transient cultures

CLas has not yet been established in culture except transiently. In the past decade, three main studies (Davis et al. 2008; Parker et al. 2014; Sechler et al. 2009) have contributed to the progress towards the goal of culturing CLas. Davis et al. (2008) reported that co-cultivation of CLas was possible in the presence of another accidentally contaminant bacterium, *Propionibacterium acnes*. Although CLas/*P. acnes* survived multiple passages in vitro, CLas was not able to grow in pure culture without *P. acnes*. However, confirmation of CLas growth in vitro outside its plant or vector hosts remains a seminal contribution. The authors also suggested that through a mutualistic relationship with another bacterium, CLas could obtain requisite nutrients and/or chemical signals required for its growth. A few years later, Parker et al. (2014)

reported viable CLas cultures in vitro for several weeks in a medium containing commercial grapefruit juice, also in the presence of other microflora found in grapefruit seeds. Moreover CLas was found to remain viable for several months inside biofilms formed by other bacteria (Parker et al. 2014). However, in the absence of continuous CLas growth, no bona fide independent 'cultivation' was claimed. These results also contributed to the belief that CLas is able to survive independently of either plant or insect hosts. The CLas growth pattern oscillated over time, resembling cryptic growth and indicating depletion of specific nutritional or signaling components from the growth medium, causing partial loss of bacterial population, followed by revival of the persisting population using the content of dead cells as growth stimulators (Parker et al. 2014).

In 2009, Sechler et al. reported that CLas and CLam were grown in pure culture in vitro to the point where these strains "grown on Liber A medium were pathogenic on citrus", thus "partially fulfilling Koch's postulates". A cursory reading of Sechler et al. (2009) would suggest that sustainable culturing had been achieved, but no such claim was made. The claim of partial fulfillment of Koch's postulates was greeted with skepticism and is now regarded by consensus as unreproducible. No follow-up publications using this approach to culture CLas are available. Very recently, Fujiwara et al. (2018) reported a co-culture of CLas strain Ishi-1 (that has no phages according to genomic data) in vitro associated with phloem-associated microbiota. The authors followed the population of CLas by DNA quantification, and observed increase in DNA amounts over time, therefore suggesting growth; but no direct quantification of viability was provided. In agar plates the authors could not see distinctive colonies, but a few cells were found after microscopic observations. In their manuscript the authors conclude that CLas needs other

microflora for effective growth, based on suppression of certain 'helper' bacteria by antibiotics. The authors conclude that CLas is resistant to oxytetracycline and many other antibiotics, which contradicts previous reports (Zhang et al. 2018). Reproducibility of these findings by other research groups is needed.

Available nutrients in CLas hosts

The CLas genome encodes a large repertoire of transporter proteins (137 transporter proteins, including 40 ABC-type), enabling uptake and assimilation of all requisite nutrients from its extracellular environment, either from the host or culture medium (Wang and Trivedi 2013). In plants, CLas is strictly intracellular and phloem-limited. Following insect acquisition via feeding, however, CLas becomes extracellular, then enters, traverses and exits the midgut epithelial cell layer and the basement membrane, emerging into the insect host hemolymph (Ghanim et al. 2017). CLas colonizes the psyllid host as a systemic, circulative and propagative endosymbiont, both inter- and intracellularly, across several organs *en route* to the salivary glands, which it penetrates to again become intracellular, prior to emergence into the salivary gland lumen, from which it can be secreted into plant hosts (Ammar et al. 2011).

The capacity to cross multiple membrane barriers and survive both intra- and extra-cellularly suggests regulatory and mechanistic complexity and capacity to cope with multiple microenvironments. Nevertheless, CLas has a highly reduced genome, lost multiple enzymes and entire biosynthetic pathways, as well as secretion systems from its genome (Duan et al. 2009). CLas therefore apparently has a stringent metabolic dependence on phloem sieve tube, psyllid

cell and hemolymph contents to support its physiological and reproductive requirements (Killiny et al. 2017b).

In recent years, the chemical composition of psyllid hemolymph and the phloem sap of fourteen citrus varieties and periwinkle (*Catharanthus roseus*, an alternate laboratory host of CLas) have been characterized in detail (Killiny 2016, 2017; Hijaz and Killiny 2014; Killiny et al. 2017b). **Table 2-2** summarizes these results in comparison with Medium G, used for transient cultures of CLas (Parker et al. 2014), since it is the only CLas medium for which chemical characterization is available. A critical appraisal of these data is fundamental and crucial for identification of metabolic requirements for maintaining CLas viability and sustained free living growth in vitro.

Table 2-2. Main common compounds found in citrus phloem sap, psyllid hemolymph, and G medium (grapefruit juice), based on studies referenced in the main text.

Compounds[a]	Periwinkle	Psyllid	Citrus	G medium[b]
Sugars[c]				
Glucose	✔	✔	✔	✔
Fructose	✔	✔	✔	✔
Sucrose	✔	✔	✔	✔
Myo-inositol	✔	✔	✔	✔
Scyllo-inositol	✔	✔	✔	NF
Chiro-inositol	✔	✔	✔	NF
Organic acids				
2-ketoglutaric acid	✔	✔	✔	NF
Lactic acid	✔	✔	✔	NF
Glycolic acid	✔	✔	✔	NF
Fumaric acid	✔	✔	✔	NF
Succinic acid	✔	✔	✔	✔
Malic acid	✔	✔	✔	✔
Citric acid	✔	✔	✔	✔
Iso-citric acid	✔	✔	✔	✔

GABA	✔	✔	✔	✔
Amino acids				
Leucine	✔	✔	✔	✔
Tryptophan	✔	✔	✔	✔
Isoleucine	✔	✔	✔	✔
Tyrosine	✔	✔	✔	✔
Valine	✔	✔	✔	✔
Histidine	✔	✔	✔	NF
Asparagine	✔	✔	✔	NF
Methionine	✔	✔	✔	✔
Alanine	✔	✔	✔	✔
Proline	✔	✔	✔	✔
Energy compounds				
ATP	NA	✔	✔	NA
ADP	NA	✔	✔	NA
AMP	NA	✔	✔	NA
GTP	NA	✔	✔	NA
GDP	NA	✔	✔	NA
NAD	NA	✔	✔	NA
NADP	NA	✔	✔	NA
FAD	NA	✔	✔	NA

[a]These compounds were selected based on the characterizations made by Killiny 2016, 2017; Hijaz and Killiny 2014; Killiny et al. 2017; Parker et al. 2014.
[b]Medium G refers to grapefruit juice used and characterized by Parker et al. 2014.
[c]Although these sugars are present in the environments where CLas lives, it probably does not use them as carbon and energy sources, since it lacks key genes of the glycolysis pathway, a sucrose transporter, and a methylghyoxal detoxifying system.
✓: compound identified; NF: not found; NA: not analyzed.

The major compounds found in these environments are discussed below (**Fig. 2-1**). Hypotheses on the ability of CLas to utilize certain compounds is based mainly in genomic annotation, since in all cases functional data demonstrating ability to assimilate these compounds has not been tested, due to the limitation of non-available CLas axenic cultures. Information was included below whenever functionality of certain genes was demonstrated in surrogate bacterial systems.

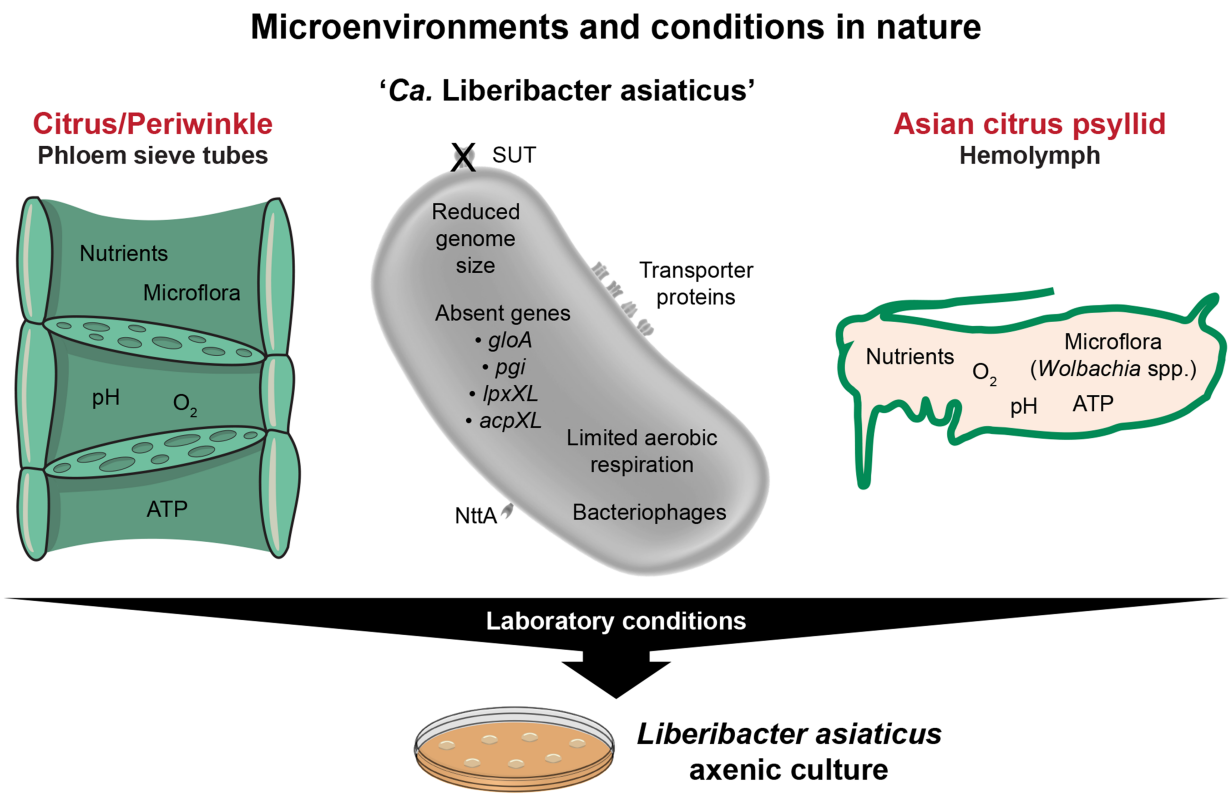

Fig. 2-1. Summary of conditions for growth of '*Candidatus* Liberibacter asiaticus' (CLas) in nature in plant host and insect vectors. The environmental conditions in the phloem sieve tubes of plant hosts and insect vectors hemolymph are discussed in the manuscript and should be taken into consideration for development of culture medium supporting axenic growth of CLas. SUT: sucrose uptake transporter; NttA: ATP/ADP translocase; *gloA*: glyoxalase; *pgi*: phosphoglucoisomerase; *lpxXL*: lipid A C28 acyltransferase; *acpXL:* acyl carrier protein. See text for details.

i) Sugars. Sugars are the most abundant energy-rich compounds found in the phloem sap of different citrus varieties and periwinkle, as well as in the hemolymph of ACP. The main sugars present in these environments are glucose, fructose and sucrose (Killiny 2016, 2017; Hijaz and Killiny 2014; Killiny et al. 2017b). Bioinformatic analyses of the CLas genome indicated that sugars such as glucose and fructose could be internalized via an ABC transporter (glucose/galactose MSF transporter) and utilized through glycolysis and downstream tricarboxylic acid (TCA) cycle (Duan et al. 2009; Wang and Trivedi 2013). It was hypothesized that in the absence of pyruvate biosynthetic enzymes, the majority of pyruvate production in

CLas could possibly be via glycolytic breakdown of glucose (Wang and Trivedi 2013). Glycolytic utilization of sugars in CLas for production of pyruvate was, however, ruled out owing to the absence of phosphoglucoisomerase (PGI), the key rate limiting enzyme of glycolysis (Jain et al. 2017b). Further supporting the lack of glycolysis is the fact that CLas, unlike *L. crescens*, lacks a functional glyoxalase system, required for detoxifying methylglyoxal, a highly cytotoxic, non-enzymatic byproduct of glycolysis (Jain et al. 2017b). Pyruvate and other organic acids are abundantly available in the phloem sap and hemolymph environments, therefore it is likely that CLas can readily absorb and assimilate pyruvic acid and other organic acids as primary carbon source. CLas was also found to be deficient in a sucrose transporter gene (*sut*), which was functionally characterized to be present only in the culturable *L. crescens* (Jain et al. 2017b).

Some sugar derivatives are also abundantly present in both CLas host environments assessed, including sugar alcohols such as myo-inositol, scyllo-inositol and chiro-inositol (Killiny 2016, 2017; Hijaz and Killiny 2014; Killiny et al. 2017b). Killiny and coworkers hypothesized that the high sugar alcohol content and multiple isomeric forms of these compounds in phloem sap and hemolymph is indicative of an important role in the survival and/or pathogenicity of CLas. Nevertheless, there is still no evidence that these sugar alcohols can be used by CLas as a carbon source, and there is no direct correlation between the sugar alcohol levels and relative susceptibility of citrus varieties towards HLB (Killiny 2017).

ii) O*rganic acids.* Organic acids are abundant in citrus and periwinkle phloem sap as well as in ACP hemolymph, represented by mono-, di and tricarboxylic acids. The main organic acids

present in both these environments are lactic, glycolic, pyruvic, fumaric, succinic, malic, citric, isocitric and 2-ketoglutaric acids (Killiny 2016, 2017; Killiny et al. 2017b). *Liberibacter crescens* can utilize 2-ketoglutarate as the primary carbon source (Fagen et al. 2014a, b). CLas genome encodes the necessary enzymes to use malate, fumarate and succinate (Wang and Trivedi 2013). Many of these organic acids are intermediates in the TCA cycle and could be directly used by CLas to produce energy (Fernie et al. 2004). The presence of a malate hydrogenase in the genome of CLas should allow the oxidation of malate to oxaloacetate, thus feeding the TCA cycle. CLas lacks isocitrate lyase and malate synthase enzymes in its genome, indicating that CLas may acquire these compounds exogenously from its extracellular environment. The presence of a C4 dicarboxylate transport protein in the CLas genome also supports this prediction (Wang and Trivedi 2013).

As mentioned above, CLas seems to lack glycolysis and could possibly import and utilize extracellular pyruvic acid as the entry point into an intact TCA cycle, since all the TCA cycle enzymes are present in all Liberibacters, providing the reducing equivalents for subsequent ATP synthesis. Jain et al. (2017b), however, argued that non-cyclic or shunted parts of the TCA pathway are more likely to function in CLas, consistent with the abundant availability of ATP (Pitino et al. 2017) and TCA cycle intermediates in its extracellular environment. The cyclic flux of TCA cycle intermediates is dependent upon high energy demand and several bacteria operate non-cyclic variations in the TCA cycle in order to generate biosynthetic precursors for lipids and amino acids under anaerobic or microaerophilic growth conditions (Tian et al. 2005).

iii) Amino acids. CLas is able to use many proteinogenic amino acids as carbon and nitrogen sources, including alanine, glutamate, aspartate, glycine, serine, methionine, cysteine, arginine, proline, histidine, threonine, tyrosine, phenylalanine, and tryptophan (Duan et al. 2009). CLas has the ability to internalize amino acids through ABC-type transporters. It also encodes a number of general L-amino acid permease proteins to import a variety of amino acids, and also a branched-chain proton-glutamate transporter, which can import both glutamate and aspartate from the environment (Duan et al. 2009; Li et al. 2012; Wang and Trivedi 2013). CLas is able to synthesize *de novo* only six of the 20 proteinogenic amino acids, namely, lysine, serine, glycine, glutamine, threonine, and arginine. Therefore, CLas must overcome the lack of the remaining *de novo* amino acid biosynthesis by acquiring these from the surrounding environment. The phloem sap of sweet orange and the hemolymph of ACP have all the amino acids necessary to meet the growth and metabolic requirements of CLas (Hijaz and Killiny 2014; Killiny et al. 2017b). Notably, a high proline-to-glycine ratio was positively correlated with high CLas infectivity in plant hosts (Steamou et al. 2017). These authors also noted a positive association of arginine, gamma-aminobutyric acid (GABA) and proline with CLas susceptibility in various hosts. Although the phloem sap of periwinkle appears to lack leucine, tryptophan, tyrosine, histidine and methionine, CLas grows well in periwinkle (Killiny 2016). Since these amino acids cannot be synthesized *de novo* by CLas, the source of these amino acids for CLas growth in periwinkle is puzzling.

Some non-proteinogenic amino acids, specifically GABA, were present in all host environments supporting CLas growth (Killiny 2016, 2017; Hijaz and Killiny 2014; Killiny et al. 2017b). GABA is an important neurotransmitter in mammals, insects, and other organisms, and

it also accumulates in plants in response to biotic and abiotic stresses (Ham et al. 2012) . It has been proposed that CLas indirectly upregulates the TCA cycle of the plant host via the GABA shunt to satisfy the increased demand for TCA cycle intermediates for supporting CLas growth (Nehela and Killiny 2019). GABA was demonstrated to function environmentally as a cell-to-cell signal mediator by inhibiting the action of acyl-homoserine lactones (quorum sensing molecule) on *Agrobacterium tumefaciens* (Chevrot et al. 2006). If quorum sensing is important for CLas growth and multiplication, as suggested by Yan et al. (2013), it may be important to avoid use of GABA in culture media.

Choline is an essential nutrient derived from serine and is required for biosynthesis of the osmoprotectant glycinebetaine in plants. Extracellular choline is abundant both in xylem as well as phloem exudates (Gout et al. 1990), is critical for phloem development and conductivity (Dettmer et al. 2014), and is important for some plant–pathogen infections (Chen et al. 2013). A phospholipid derivative, phosphatidylcholine (PC) represents almost one half of the total lipid content present in eukaryotic cell membranes. However, PC is present only in bacteria that live in close association with eukaryotic hosts, such as *Agrobacterium tumefaciens*, *Sinorhizobium meliloti* and *Pseudomonas aeruginosa* (Aktas et al. 2010). PC strongly affects the physicochemical properties of bacterial membranes, including fluidity, permeability and membrane potentials. PC-deficient phenotypes of these bacteria are marked by temperature and sodium dodecyl sulfate (SDS) sensitivity, attenuated virulence, loss of Type 4 secretion, reduced growth and motility and increased biofilm formation (Aktas et al. 2010). There are two pathways for PC biosynthesis. The enzyme phospholipid N-methyltransferase catalyzes *de novo* PC biosynthesis via three-fold sequential N-methylations of phosphatidylethanolamine using the

methyl donor S-adenosylmethionine. Alternatively, nutritional choline can also be incorporated into the membrane via the single step enzymatic action of phosphatidylcholine synthase. While proteins for both these pathways exist in (cultured) *L. crescens* (WP_015272535.1 and WP_015272978.1, respectively), CLas lacks the ability to synthesize PC *de novo*. However, CLas encodes a predicted ABC transporter import system with high substrate specificity for choline (CLIBASIA_RS01090) (Li et al. 2012). CLas also encodes a phosphatidylcholine synthase (CLIBASIA_RS03145), indicating that CLas is capable of utilizing extracellular choline, present in both plant and insect hosts. Choline is likely to be a necessary component in CLas culture media.

iv) Fatty acids. Fatty acids are also detected in low amounts in the phloem sap of periwinkle and citrus plants and in high amounts in the hemolymph of ACP (Killiny 2016, 2017; Hijaz and Killiny 2014; Killiny et al. 2017b). Analysis of the genome of CLas showed that this bacterium is not likely able to utilize fatty acids as a carbon source (Wang and Trivedi 2013). However, the recent successful axenic culture of the insect endosymbiont *Spiroplasma paulsonii* required lipid supplementation and was based on observations that the pathogen rapidly depleted specific host lipids (Masson et al. 2018), indicating that lipid supplementation of CLas culture media may require further investigation.

v) Nucleotides and cofactors. Nucleotides are also found in abundance in the phloem sap of sweet orange and hemolymph of ACP, and include all three adenine nucleotides (ATP, ADP, and AMP), two guanine nucleotides (GTP and GDP), two cytosine nucleotides (CDP and CTP), two uridine nucleotides (UDP and UTP), two nicotinamide nucleotides (NAD and NADP) and

flavin nucleotide (FAD) (Hijaz et al. 2016; Killiny et al. 2017b). Because CLas encodes many ABC transport proteins in its genome (Li et al. 2012; Wang and Trivedi 2013), these exogenous sources of nucleotides are likely exploited by CLas as energy sources and as a source of co-factors (Hijaz et al. 2016). CLas lacks enzymes needed for the metabolism of purines and pyrimidines, which must therefore be acquired from the host (Hartung et al. 2011). However, genome analysis shows that CLas is presumably able to salvage nucleotides from the respective nucleoside diphosphates.

One significant and unusual feature found in the genome of CLas (and other pathogenic Liberibacters) is the presence of *nttA*, which has been demonstrated to encode an ATP/ADP translocase (Jain et al. 2017b; Vahling et al. 2010). Since CLas also encodes ATP synthase (Duan et al. 2009), it is likely capable of synthesizing its own ATP, as well as uptake ATP from its extracellular environment. ATP/ADP translocases are present in all plastids (Möhlmann et al. 1998) and are also encoded by only three other prokaryotes, all obligate and intracellular pathogens: *Chlamydia psittaci*, *Rickettsia prowazekii* and *Lawsonia intracellularis*. ATP/ADP translocases catalyze the highly specific uptake of host ATP in exchange for the bacterial ADP (energy parasitism) (Schmitz-Esser et al. 2008).

CLas possibly has a limited ability to perform aerobic respiration, since it lacks homologs corresponding to the final stages of oxidative phosphorylation and many diverse terminal oxidases (Duan et al. 2009). In addition to the provision of nucleotides and cofactors, an exogenous supply of ATP in any axenic culture media is likely also important, since increased ATP levels are observed in both insect and plant hosts after CLas infection (Killiny et al. 2017a;

Pitino et al. 2017). It has been suggested that some bacteria, including *Escherichia coli* and *Salmonella* spp., excrete ATP into their surroundings if their respiratory rates and ATP generation exceed their physiological requirements (Mempin et al. 2013). Given that CLas has only been maintained transiently in co-cultures with other bacteria (Davis et al. 2008; Fujiwara et al. 2018; Parker et al. 2014) it is possible that the co-cultured bacteria may be sustaining the ATP requirement for CLas.

Beyond nutrients: conditions to consider for CLas culture

i) pH. The significant levels of organic acids found in the phloem sap of both citrus and periwinkle plants renders these two environments slightly acidic (approximately pH 6.0 for citrus phloem sap and pH 5.85 for periwinkle phloem sap) (Killiny 2016; Hijaz and Killiny 2014). CLas has also been shown to grow inside acidic citrus fruits (Li et al. 2009), indicating that CLas growth may be supported in an acidic (or slightly acidic) environment. Medium G, which supports transient growth of CLas, is composed of 100% commercial grapefruit juice, and was used by Parker et al. (2014) to study the viability of CLas in vitro. It contained several sugars, organic acids and amino acids required for CLas growth and at an extremely acidic pH (close to 3.0).

ii) Oxygen levels. CLas possibly has a limited ability to perform aerobic respiration due to the absence of the terminal oxidase complex (cytochrome bd), but possesses many enzymes with a role in nitrogen metabolism, including NAD+ synthase, glutamine synthetase, and glutaminase, indicating that CLas could rely on nitrogen to generate energy through anaerobic respiration (Duan et al. 2009). However, in a review that included new analyses of the genomes

of CLas, Wang and Trivedi (2013) suggested that CLas does not perform anaerobic respiration because it lacks nitrate, sulphate, fumarate, and trimethylamine reductase systems. The authors argued that the absence of electron acceptors for an anaerobic respiratory chain, such as nitrate or nitrite reductase, prevents this type of respiration in CLas, considering that the enzymes found for nitrogen metabolism by Duan et al. (2009) are insufficient to define a respiratory chain (Wang and Trivedi 2013). This conclusion was supported by the fact that oxygen is present in the phloem of plants, even though at lower concentration than the surrounding atmosphere (Drew 1997). Taken together, the available information indicates that CLas is able to perform aerobic respiration, even under microaerophilic growth conditions. However, because it lacks genes for the biosynthesis of menaquinone and ubiquinone, CLas will need to acquire these compounds exogenously for a functional respiratory chain (Wang and Trivedi 2013).

Genetic components

Comparative genomics and metabolic pathway analyses have revealed a trend for the reduction or complete absence of several biosynthetic pathways, metabolic enzymes, and secretion systems in the genomes of uncultured pathogenic Liberibacters. Genomic comparisons between cultured but likely non-pathogenic *L. crescens* (1.5 Mb) and CLas (1.2 Mb) have provided valuable clues about the genes missing from CLas that would cause growth problems, which may not be readily alleviated by simple media adjustments. As noted above, a functional glyoxalase pathway is absent in all pathogenic (and uncultured) Liberibacters, and present in *L. crescens* (Jain et al. 2017b). The two-enzyme glyoxalase system, consisting of glyoxalase I (GloA; lactoylglutathione lyase) and glyoxalase II (GloB; hydroxyacylglutathione hydrolase), provides the primary cellular defense against methylglyoxal-induced carbonyl stress and

proteome glycation in both prokaryotes and eukaryotes. Methylglyoxal is a highly cytotoxic byproduct of glycolysis and is also produced via protein and lipid degradation. The CLas genome lacks *gloA*, and CLas circumvents a toxic buildup of cellular methylglyoxal pool by preventing sugar uptake and glycolytic utilization and instead scavenges ATP directly from the host cell cytoplasm while infecting either plant or psyllid host (Jain et al. 2017b). An efficient mitigation of carbonyl stress would still be needed for methylglyoxal resulting from cellular metabolic processes in axenically cultured CLas. This could be done by addition of specific methylglyoxal-binding compounds to the culture medium, to mitigate the effects of the methylglyoxal-induced carbonyl stress (Lv et al. 2011). An alternative strategy would be adding the *gloA* gene from Lcr into CLas. However, genetic modification protocols of CLas have not been established to date.

As another example, biochemical analyses revealed the presence of a very long chain fatty acid (VLCFA)-modified lipid A in *L. crescens* LPS (Complex Carbohydrate Research Center, Athens, GA, unpublished data), a unique feature of several bacteria that form chronic intracellular infections within legumes and mammalian hosts. Homologs for both genes coding proteins involved in the biosynthesis of VLCFA-modified lipid A, LpxXL and AcpXL, are present in Lcr (WP_015273388.1 and WP_015273393.1), but both are absent in all pathogenic (and uncultured) Liberibacters, including CLas. Knockout mutations of various Lcr genes have been readily obtained in the past (Jain et al. 2017a, b), but mutations affecting formation of VLCFA-modified lipid A in *L. crescens* have not been successful (Jain & Gabriel, unpublished data), leading to the speculation that VLCFA-modified lipid A may be essential for axenic

growth of pathogenic Liberibacters. Introduction of *lpxXL* and *acpXL* from Lcr into CLas would aid in achieving this goal, if transformation protocols for CLas are developed.

Bacteriophage genes in CLas

CLas strain UF506 carries an excision plasmid prophage, SC2, and a chromosomally integrated prophage, SC1 (Fleites et al. 2014; Zhang et al. 2011). SC1 becomes replicative in planta with expression of lytic genes (Fleites et al. 2014) and forms readily observed bacteriophage particles in periwinkle (Zhang et al. 2011) and citrus (Fu et al. 2015). By contrast, the replicative excision plasmid SC2 lacks lytic genes. SC1 and SC2 encode multiple virulence factors suggested to contribute to the fitness of CLas in its hosts (Jain et al. 2015; Sudhan et al. 2018; Zhang et al. 2011). Fifteen different CLas strains from various geographical locations have been sequenced to date with annotated genome information available in NCBI. Although CLas strains have shown distinguishable genetic features, the genome structure and most of the genes previously identified as essential are conserved in the American and Asian strains (Lai et al. 2016; Yan et al. 2013). However, considerable heterogeneity has been observed in the resident prophage composition, with some strains lacking either or both prophages. For example, the Japanese strain Ishi-1 lacks both prophages (Katoh et al. 2014), and the Chinese strains A4 (Zheng et al. 2014a), YCpsy (Wu et al. 2015), and the American strains HHCA (Zheng et al. 2014b) and FL17 (Zheng et al. 2015) have only a single prophage. South Asian as well as American CLas strains can be differentiated based on prophage gene content (Tomimura et al. 2009; Zheng et al. 2017) and display high variability in the prophage region (Duan et al. 2009; Katoh et al. 2014; Zhang et al. 2011; Zheng et al. 2016, 2017). The suspected role of some of the CLas prophage genes (for example, SC2 peroxidase; Jain et al. 2015) in modulation of host

defense responses might be the driving force behind the high level of genetic variability (Zheng et al. 2016, 2017).

Expression of the SC1-encoded lytic cycle gene encoding holin in *E. coli* inhibited bacterial growth (Fleites et al. 2014), and its expression was demonstrated to be transcriptionally suppressed by a small membrane permeable protein expressed by *Wolbachia* within the psyllid host (Jain et al. 2017a). Since phage particles have been observed only in planta and never in the psyllid host, it has been suggested that activation of the phage lytic cycle may limit CLas growth in vitro in the absence of the *Wolbachia*-expressed repressor protein. Wang and Trivedi (2013) suggested that a lytic burst of CLas inside citrus phloem might trigger apoptotic death of citrus phloem cells, thus explaining the lack of CLas in microscopic observations of citrus leaf midribs during advanced stages of HLB (Folimonova et al. 2009). Based on the studies mentioned above, CLas strains lacking prophages such as Ishi-1 could be ideal for an attempt at culturing in axenic medium *ex situ* (Fujiwara et al. 2018). However, the lack of success culturing Ishi-1 (Fujiwara et al. 2018) may suggest that prophages are not the culprit for the lack of axenic culture. It is difficult to draw conclusions since the attempts to culture different CLas (Davis et al. 2008; Parker et al. 2014; Sechler et al. 2009) have used very different, therefore non-comparable, culture conditions.

Cell culture infection models and bacterial co-cultures as valuable tools

Chlamydia, *Rickettsia* and *Mycobacterium leprae* are obligate intracellular bacteria requiring a host cell for replication and can only be studied in vitro using a cell culture system. Host cell culture strategies for such pathogens have been utilized with some degree of success

(Hanson and Tan 2016). The systematic evaluation of *Coxiella burnetii* metabolic requirements inside the host cell culture system using expression microarrays, genomic reconstruction, and metabolite typing allowed successful isolation of the pathogen in axenic media (Omsland et al. 2013). A similar strategy to culture CLas in host cell lines in vitro has not been published, despite the fact that establishment of primary cell culture lines of ACP has been reported (Marutani-Hert et al. 2009).

Bacterial co-culture is another valuable approach for isolation of bacteria considered recalcitrant to axenic culture methods (Stewart 2012). Niche-specific bacterial communities coexist in complex crosstalk and metabolic relationships that can affect isolation of fastidious unculturable bacteria (Pham and Kim 2012). For this reason several co-culture methods have been used for isolation of several fastidious and previous unculturable bacteria from diverse habitats (Ding et al. 2017; Tanaka and Benno 2015; Vartoukian et al. 2016a). Fujiwara et al. (2018) have recently reported that viability of CLas phage-less strain Ishi-1 in vitro was dependent on the presence of several co-cultured bacteria belonging to *Comamonadaceae*, *Flavobacteriaceae*, *Microbacteriaceae* and *Pseudomonadaceae*, which are members of the core bacterial community in CLas-infected citrus leaves. Davis et al. (2008) also demonstrated that CLas could be maintained in vitro for several weeks in co-culture with accidental contaminant *P. acnes*, indicating a mutually beneficial interrelationship between the two bacteria. Interestingly, *P. acnes*, *P. reudenreichii* and *P. jensenii* have recently been used as helper strains to grow nearly a dozen previously unculturable bacteria (Vartoukian et al. 2016a, b). Notably, *P. acnes* has also been shown to increase the viability of other bacteria such as *Staphylococcus aureus* in co-culture (Tyner and Patel 2016).

***Liberibacter crescens*, a model system**

Liberibacter crescens (Leonard et al. 2012) was isolated in axenic medium from the sap of diseased Babaco mountain papaya (*Carica stipulata* × *C. pubescens*) and has no known plant or insect hosts. *L. crescens* appears to be the most basal Liberibacter lineage, diverging from the other pathogenic '*Ca*. Liberibacter spp.' early during reductive evolution of the genus (Nakabachi et al. 2013). Despite the differences among CLas strains and *L. crescens* based on their genomes (Fagen et al. 2014b), engineering *L. crescens* for functional genomic studies of CLas genes has helped in understanding CLas physiology (Fleites et al. 2014; Jain et al. 2017a, 2018), and informs CLas culturing efforts. Several quite different bacterial strains have been utilized as surrogate hosts for functional characterization of CLas genes. For example, CLas transcriptional activator LdtR was functionally annotated using *Sinorhizobium meliloti* as a surrogate (Pagliai et al. 2014). However, with a genome size of ~6.7 Mb, *S. meliloti* not only possessed a larger repertoire of regulatory proteins as compared to CLas (Pagliai et al. 2014), but also provided a significantly different regulatory context than CLas. The genome content of *L. crescens* is highly similar and syntenic with the pathogenic '*Ca*. Liberibacters spp.' (Nakabachi et al. 2013), and *L. crescens* may therefore be more suitable as a surrogate host for functional genomic studies of CLas genes, particularly in studies involving plant or psyllid inoculation assays.

Interestingly, our recent study demonstrated that *L. crescens* can form biofilms in vitro under modified culture condition, allowing the use of this system to understand the process of biofilm formation in CLas, that has been described only in insect vectors so far (Naranjo et al. 2019). Clearly, either transforming CLas to enable its culturing, or causing *L. crescens* to be

pathogenic by addition of CLas genes are two complimentary approaches to the same end. Although *L. crescens* is readily amenable to genetic transformation, to date CLas has not been transformed. In the absence of ability to transform CLas, axenic growth of this bacterium may be difficult or impossible. Clearly, development of CLas transformation protocols, even if utilizing transient cultures, remains a high priority for culturing efforts.

Concluding remarks: What have we learned?

Despite the fact that more than a century has elapsed since its first reports, CLas remains enigmatic, and its pathogenicity and transmission functions are in many ways unknown. New reports appear regularly in the literature that reveal potential new mechanisms of CLas pathogenicity, details of the interaction between CLas and its citrus host or its psyllid vector host, or CLas associated with HLB affecting new countries or new citrus varieties. Reports of '*Ca.* Liberibacters spp.' infecting other host species, such as tomato, potato and carrots (Nelson et al. 2013), pears (Thompson et al. 2013) or Australian eggplant psyllid (Morris et al. 2017), highlight a deserved focus on this genus as a causal agent of emerging diseases of multiple crops.

A global multiomics and interdisciplinary vision is likely to find the key elements to be taken into account and accomplish the sought-after goal of culturing pathogenic '*Ca.* Liberibacters spp.'. Novel approaches are needed to find a successful method for CLas culturing, since simply testing mixtures of nutrients has proven to only advance the topic to a limited extent. Chemical signals found in the hosts may be missing in these transient cultures, and may be needed to achieve the culturing goal. Time is of the essence, CLas has already reduced citrus production in Florida by over 70% at the time of this writing.

Long-term goal

Develop novel culturing strategies to increase the viability of CLas in in vitro conditions. The establishment of such strategies will enable studies to better understand the physiology and host-interactions of CLas, ultimately leading to the development of novel management approaches to control HLB.

Specific objective

A.1. Determine which compounds and incubation conditions will increase the viability of CLas in in vitro conditions.

Hypothesis

A.1. Supplementing the culture medium used to maintain CLas in transient in vitro cultures with additional compounds to mimic its natural environments and fulfill its nutrient requirements, will increase the viability in vitro of CLas.

Acknowledgments

Agriculture and Food Research Initiative competitive grant no. 2016-70016-24844 and 2015-70016-23010 from the USDA National Institute of Food and Agriculture, Citrus Disease Research and Extension; and HATCH AAES (Alabama Agricultural Experiment Station) program provided to L.D.L.F.

References

Aktas, M., Wessel, M., Hacker, S., Klüsener, S., Gleichenhagen, J., and Narberhaus, F. 2010. Phosphatidylcholine biosynthesis and its significance in bacteria interacting with eukaryotic cells. Eur J Cell Biol 89:888-894.

Ammar, E. D., Shatters, R. G., and Hall, D. G. 2011. Localization of *Candidatus* Liberibacter asiaticus, associated with citrus huanglongbing disease, in its psyllid vector using fluorescence *in situ* hybridization. J Phytopathol 159:726-734.

Bové, J. M. 2014. Huanglongbing or yellow shoot, a disease of Gondwanan origin: Will it destroy citrus worldwide? Phytoparasitica 42:579-583.

Chang, C., Garnier, M., Zreik, L., Rossetti, V., and Bové, J. 1993. Culture and serological detection of the xylem-limited bacterium causing citrus variegated chlorosis and its identification as a strain of *Xylella fastidiosa*. Curr Microbiol 27:137-142.

Chen, C., Li, S., McKeever, D. R., and Beattie, G. A. 2013. The widespread plant-colonizing bacterial species *Pseudomonas syringae* detects and exploits an extracellular pool of choline in hosts. Plant J 75:891-902.

Chevrot, R., Rosen, R., Haudecoeur, E., Cirou, A., Shelp, B. J., Ron, E., and Faure, D. 2006. GABA controls the level of quorum-sensing signal in *Agrobacterium tumefaciens*. Proc Natl Acad Sci U S A 103:7460-7464.

Davis, M. J., and Brlansky, R. 2007. Culturing fastidious prokaryotes - points to consider when working with citrus huanglongbing or greening. Proc Fla State Hort Soc 120:136-137.

Davis, M. J., Mondal, S. N., Chen, H., Rogers, M. E., and Brlansky, R. H. 2008. Co-cultivation of '*Candidatus* Liberibacter asiaticus' with Actinobacteria from citrus with huanglongbing. Plant Dis 92:1547-1550.

Davis, M. J., Purcell, A. H., and Thomson, S. V. 1978. Pierce's disease of grapevines: isolation of the causal bacterium. Science 199:75-7.

Dettmer, J., Ursache, R., Campilho, A., Miyashima, S., Belevich, I., O'Regan, S., Mullendore, D. L., Yadav, S. R., Lanz, C., Beverina, L., Papagni, A., Schneeberger, K., Weigel, D., Stierhof, Y. D., Moritz, T., Knoblauch, M., Jokitalo, E., and Helariutta, Y. 2014. CHOLINE TRANSPORTER-LIKE1 is required for sieve plate development to mediate long-distance cell-to-cell communication. Nat Commun 5:4276.

Ding, Z. W., Lu, Y. Z., Fu, L., Ding, J., and Zeng, R. J. 2017. Simultaneous enrichment of denitrifying anaerobic methane-oxidizing microorganisms and anammox bacteria in a hollow-fiber membrane biofilm reactor. Appl Microbiol Biotechnol 101:437-446.

Drew, M. M. C. 1997. Oxygen deficiency and root metabolism: injury and acclimation under hypoxia and anoxia. Annu Rev Plant Physiol Plant Mol Biol 48:223-250.

Duan, Y., Zhou, L., Hall, D. G., Li, W., Doddapaneni, H., Lin, H., Liu, L., Vahling, C. M., Gabriel, D. W., Williams, K. P., Dickerman, A., Sun, Y., and Gottwald, T. 2009. Complete genome sequence of citrus huanglongbing bacterium, "*Candidatus* Liberibacter asiaticus" obtained through metagenomics. Mol Plant Microbe Interact 22:1011-1020.

Fagen, J. R., Leonard, M. T., Coyle, J. F., McCullough, C. M., Davis-Richardson, A. G., Davis, M. J., and Triplett, E. W. 2014a. *Liberibacter crescens* gen. nov., sp. nov., the first cultured member of the genus *Liberibacter*. Int J Syst Evol Microbiol 64:2461-2466.

Fagen, J. R., Leonard, M. T., McCullough, C. M., Edirisinghe, J. N., Henry, C. S., Davis, M. J., and Triplett, E. W. 2014b. Comparative genomics of cultured and uncultured strains suggests genes essential for free-living growth of *Liberibacter*. PLoS One 9:e84469.

Fernie, A. R., Carrari, F., and Sweetlove, L. J. 2004. Respiratory metabolism: Glycolysis, the TCA cycle and mitochondrial electron transport. Curr Opin Plant Biol 7:254-261.

Fleites, L. A., Jain, M., Zhang, S., and Gabriel, D. W. 2014. "*Candidatus* Liberibacter asiaticus" prophage late genes may limit host range and culturability. Appl Environ Microbiol 80:6023-6030.

Folimonova, S. Y., Robertson, C. J., Garnsey, S. M., Gowda, S., and Dawson, W. O. 2009. Examination of the responses of different genotypes of citrus to huanglongbing (citrus greening) under different conditions. Phytopathology 99:1346-1354.

Fu, S. M., Hartung, J., Zhou, C. Y., Su, H. N., Tan, J., and Li, Z. A. 2015. Ultrastructural changes and putative phage particles observed in sweet orange leaves infected with '*Candidatus* Liberibacter asiaticus.' Plant Dis 99:320-324.

Fujiwara, K., Iwanami, T., and Fujikawa, T. 2018. Alterations of *Candidatus* Liberibacter asiaticus-associated microbiota decrease survival of *Ca.* L. asiaticus in *in vitro* assays. Front Microbiol 9:3089.

Ghanim, M., Achor, D., Ghosh, S., Kontsedalov, S., Lebedev, G., and Levy, A. 2017. '*Candidatus* Liberibacter asiaticus' accumulates inside endoplasmic reticulum associated vacuoles in the gut cells of *Diaphorina citri*. Sci Rep 7:16945.

Gout, E., Bligny, R., Roby, C., and Douce, R. 1990. Transport of phosphocholine in higher plant cells: 31P nuclear magnetic resonance studies. Proc Natl Acad Sci U S A87:4280-4283.

Ham, T., Chu, S., Han, S., and Ryu, S. 2012. c-Aminobutyric acid metabolism in plant under environment stresses. Korean J Crop Sci 57: 144-150.

Hanson, B. R., and Tan, M. 2016. Intra-ChIP: studying gene regulation in an intracellular pathogen. Curr Genet 62:547-551.

Hartung, J. S., Shao, J., and Kuykendall, L. D. 2011. Comparison of the "*Ca.* liberibacter asiaticus" genome adapted for an intracellular lifestyle with other members of the rhizobiales. PLoS One 6:e23289.

Hijaz, F., and Killiny, N. 2014. Collection and chemical composition of phloem sap from *Citrus sinensis* L. Osbeck (sweet orange). PLoS One 9:e101830.

Hijaz, F., Manthey, J. A., Van der Merwe, D., and Killiny, N. 2016. Nucleotides, micro- and macro-nutrients, limonoids, flavonoids, and hydroxycinnamates composition in the phloem sap of sweet orange. Plant Signal Behav 11:e1183084.

Jagoueix, S., Bové, J. M., and Garnier, M. 1994. The phloem-limited bacterium of greening disease of citrus is a member of the subdivision of the Proteobacteria. Int J Syst Bacteriol 44:379-386.

Jain, M., Fleites, L. A., and Gabriel, D. W. 2015. Prophage-encoded peroxidase in '*Candidatus* Liberibacter asiaticus' is a secreted effector that suppresses plant defenses. Mol Plant Microbe Interact 28:1330-1337.

Jain, M., Fleites, L. A., and Gabriel, D. W. 2017a. A small *Wolbachia* protein directly represses phage lytic cycle genes in "*Candidatus* Liberibacter asiaticus" within psyllids. mSphere 2:e00171-17.

Jain, M., Munoz-Bodnar, A., and Gabriel, D. W. 2017b. Concomitant loss of the glyoxalase system and glycolysis makes the uncultured pathogen "*Candidatus* Liberibacter asiaticus" an energy scavenger. Appl Environ Microbiol 83:e01670-17.

Jain, M., Munoz-Bodnar, A., Zhang, S., and Gabriel, D. W. 2018. A secreted '*Candidatus* Liberibacter asiaticus' peroxiredoxin simultaneously suppresses both localized and systemic innate immune responses *in planta*. Mol Plant Microbe Interact 31:1312-1322.

Katoh, H., Miyata, S. I., Inoue, H., and Iwanami, T. 2014. Unique features of a Japanese "*Candidatus* Liberibacter asiaticus" strain revealed by whole genome sequencing. PLoS One 9:e106109.

Killiny, N. 2016. Generous hosts: What makes Madagascar periwinkle (*Catharanthus roseus*) the perfect experimental host plant for fastidious bacteria? Plant Physiol Biochem 109:28-35.

Killiny, N. 2017. Metabolite signature of the phloem sap of fourteen citrus varieties with different degrees of tolerance to *Candidatus* Liberibacter asiaticus. Physiol Mol Plant Pathol 97:20-29.

Killiny, N., Hijaz, F., Ebert, T. A., Rogers, M. E., Alfred, L., and Harold Drake, E. L. 2017a. A plant bacterial pathogen manipulates its insect vector's energy metabolism. Appl Environ Microbiol 83:e03005-16.

Killiny, N., Hijaz, F., El-Shesheny, I., Alfaress, S., Jones, S. E., and Rogers, M. E. 2017b. Metabolomic analyses of the haemolymph of the Asian citrus psyllid *Diaphorina citri*, the vector of huanglongbing. Physiol Entomol 42:134-145.

Lai, K. K., Davis-Richardson, A. G., Dias, R., and Triplett, E. W. 2016. Identification of the genes required for the culture of *Liberibacter crescens*, the closest cultured relative of the *Liberibacter* plant pathogens. Front Microbiol 7:547.

Leonard, M. T., Fagen, J. R., Davis-Richardson, A. G., Davis, M. J., and Triplett, E. W. 2012. Complete genome sequence of *Liberibacter crescens* BT-1. Stand Genomic Sci 7:271-283.

Li, W., Levy, L., and Hartung, J. S. 2009. Quantitative distribution of '*Candidatus* Liberibacter asiaticus' in citrus plants with citrus huanglongbing. Phytopathology 99:139-144.

Li, W., Cong, Q., Pei, J., Kinch, L. N., and Grishin, N. V. 2012. The ABC transporters in *Candidatus* Liberibacter asiaticus. Proteins 80:2614-2628.

Lin, H., Pietersen, G., Han, C., Read, D. A., Lou, B., Gupta, G., and Civerolo, E. L. 2015. Complete genome sequence of "*Candidatus* Liberibacter africanus," a bacterium associated with citrus huanglongbing. Genome Announc 3:e00733-15.

Lv, L., Shao, X., Chen, H., Ho, C. T., and Sang, S. 2011. Genistein inhibits advanced glycation end product formation by trapping methylglyoxal. Chem Res Toxicol 24:579-586.

Marutani-Hert, M., Hunter, W. B., and Hall, D. G. 2009. Establishment of Asian citrus psyllid (*Diaphorina citri*) primary cultures. In Vitro Cell Dev Biol Anim 45:317-320.

Masson, F., Copete, S. C., Schüpfer, F., Garcia-Arraez, G., and Lemaitre, B. 2018. *In Vitro* culture of the insect endosymbiont *Spiroplasma poulsonii* highlights bacterial genes involved in host-symbiont interaction. MBio 9:e00024-18.

Mempin, R., Tran, H., Chen, C., Gong, H., Kim Ho, K., and Lu, S. 2013. Release of extracellular ATP by bacteria during growth. BMC Microbiol 13:301.

Möhlmann, T., Tjaden, J., Schwöppe, C., Winkler, H. H., Kampfenkel, K., and Neuhaus, H. E. 1998. Occurrence of two plastidic ATP/ADP transporters in *Arabidopsis thaliana* L - Molecular characterisation and comparative structural anaysis of similar ATP/ADP translocators from plastids and *Rickettsia prowazekii*. Eur J Biochem 252:353-359.

Morris, J., Shiller, J., Mann, R., Smith, G., Yen, A., and Rodoni, B. 2017. Novel '*Candidatus* Liberibacter' species identified in the Australian eggplant psyllid, *Acizzia solanicola*. Microb Biotechnol 10:833-844.

Murray, R. G. E., and Stackebrandt, E. 1995. Taxonomic note: Implementation of the provisional status *Candidatus* for incompletely described procaryotes. Int J Syst Bacteriol 45:186-

187.
Nakabachi, A., Nikoh, N., Oshima, K., Inoue, H., Ohkuma, M., Hongoh, Y., Miyagishima, S. Y., Hattori, M., and Fukatsu, T. 2013. Horizontal gene acquisition of *Liberibacter* plant pathogens from a bacteriome-confined endosymbiont of their psyllid vector. PLoS One 8:e82612.
Naranjo, E., Merfa, M. V., Ferreira, V., Jain, M., Davis, M. J., Bahar, O., Gabriel D. W., and De La Fuente, L. 2019. *Liberibacter crescens* biofilm formation in vitro: establishment of a model system for pathogenic '*Candidatus* Liberibacter spp.'. Sci Rep 9:5150.
Nehela, Y., and Killiny, N. 2019. *Candidatus* Liberibacter asiaticus and its vector, *Diaphorina citri*, augments the TCA cycle of their host via the GABA shunt and polyamines pathway. Mol Plant Microbe Interact 32:413-427.
Nelson, W. R., Sengoda, V. G., Alfaro-Fernandez, A. O., Font, M. I., Crosslin, J. M., and Munyaneza, J. E. 2013. A new haplotype of "*Candidatus* Liberibacter solanacearum" identified in the Mediterranean region. Eur J Plant Pathol 135:633-639.
Omsland, A., Hackstadt, T., and Heinzen, R. A. 2013. Bringing culture to the uncultured: *Coxiella burnetii* and lessons for obligate intracellular bacterial pathogens. PLoS Pathog 9:e1003540.
Pagliai, F. A., Gardner, C. L., Bojilova, L., Sarnegrim, A., Tamayo, C., Potts, A. H., Teplitski, M., Gonzalez, C. F., Folimonova, S. Y., Lorca, G. L., and Gonzalez, C. F. 2014. The transcriptional activator LdtR from '*Candidatus* Liberibacter asiaticus' mediates osmotic stress tolerance PLoS Pathog 10:e1004101.
Parker, J. K., Wisotsky, S. R., Johnson, E. G., Hijaz, F. M., Killiny, N., Hilf, M. E., and De La Fuente, L. 2014. Viability of '*Candidatus* Liberibacter asiaticus' prolonged by addition of citrus juice to culture medium. Phytopathology 104:15-26.
Pham, V. H. T.,and Kim, J. 2012. Cultivation of unculturable soil bacteria. Trends Biotechnol 30:475-484.
Pitino, M., Armstrong, C. M., and Duan, Y. 2017. Molecular mechanisms behind the accumulation of ATP and H_2O_2 in citrus plants in response to "*Candidatus* Liberibacter asiaticus" infection. Hortic Res 4:17040.
Saglio, P., Laflèche, D., Bonisol, D. C., and Bové, J. M. 1971. Isolement et culture in vitro des mycoplasmes associés au stubborn des agrumes et leur observation au microscope électronique. C R Ac Sci D 272:1387-1390.
Schmitz-Esser, S., Haferkamp, I., Knab, S., Penz, T., Ast, M., Kohl, C., Wagner, M., and Horn, M. 2008. *Lawsonia intracellularis* contains a gene encoding a functional Rickettsia-like ATP/ADP translocase for host exploitation. J Bacteriol 190:5746-5752.
Sechler, A., Schuenzel, E. L., Cooke, P., Donnua, S., Thaveechai, N., Postnikova, E., Stone, A. L., Schneider, W. L., Damsteegt, V. D., and Schaad, N. W. 2009. Cultivation of "*Candidatus* Liberibacter asiaticus", "*Ca.* L. africanus", and "*Ca.* L. americanus" associated with huanglongbing. Phytopathology 99:480-486.
Steamou, M., Olufemi, J. A., Simpson, C. R., and Jiftion, J. L. 2017. Contrasting amino acid profiles among permissive and non-permissive hosts of *Candidatus* Liberibacter asiaticus, putative causal agent of huanglongbing. PLoS One 12:e0187921.
Stewart, E. J. 2012. Growing unculturable bacteria. J Bacteriol 194:4151-4160.
Sudhan, D., Puttamuk, T., Vuttipongchaikij, S., and Chuawong, P. 2018. Cloning, overexpression, and purification of a gene of unknown function of prophage loci from '*Candidatus* Liberibacter asiaticus,' the destructive bacterial pathogen of huanglongbing

disease in citrus plants. Protein Expr Purif 150:72-80.
Tanaka, Y., and Benno, Y. 2015. Application of a single-colony coculture technique to the isolation of hitherto unculturable gut bacteria. Microbiol Immunol 59:63-70.
Thompson, S., Fletcher, J. D., Ziebell, H., Beard, S., Panda, P., Jorgensen, N., Fowler, S. V., Liefting, L. W., Berry, N., and Pitman, A. R. 2013. First report of "*Candidatus* Liberibacter europaeus" associated with psyllid infested Scotch broom. New Dis Rep 27:6.
Tian, J., Bryk, R., Itoh, M., Suematsu, M., and Nathan, C. 2005. Variant tricarboxylic acid cycle in *Mycobacterium tuberculosis*: identification of α-ketoglutarate decarboxylase. Proc Natl Acad Sci U S A 102:10670-10675.
Tomimura, K., Miyata, S. I., Furuya, N., Kubota, K., Okuda, M., Subandiyah, S., Hung, T. H., Su, H. J., and Iwanami, T. 2009. Evaluation of genetic diversity among "*Candidatus* Liberibacter asiaticus" isolates collected in Southeast Asia. Phytopathology 99:1062-1069.
Tyner, H., and Patel, R. 2016. *Propionibacterium acnes* biofilm - A sanctuary for Staphylococcus aureus? Anaerobe 40:63-67.
Vahling, C. M., Duan, Y., and Lin, H. 2010. Characterization of an ATP translocase identified in the destructive plant pathogen "*Candidatus* Liberibacter asiaticus." J Bacteriol 192:834-840.
Vartoukian, S. R., Adamowska, A., Lawlor, M., Moazzez, R., Dewhirst, F. E., and Wade, W. G. 2016a. *In vitro* cultivation of "unculturable" oral bacteria, facilitated by community culture and media supplementation with siderophores. PLoS One 11:e0146926.
Vartoukian, S. R., Moazzez, R. V., Paster, B. J., Dewhirst, F. E., and Wade, W. G. 2016b. First cultivation of health-associated *Tannerella* sp. HOT-286 (BU063). J Dent Res 95:1308-1313.
Wang, N., Pierson, E. A., Setubal, J. C., Xu, J., Levy, J. G., Zhang, Y., Li, J., Rangel, L. T., and Martins, J. 2017. The *Candidatus* Liberibacter–host interface: insights into pathogenesis mechanisms and disease control. Annu Rev Phytopathol 55:451-482.
Wang, N., and Trivedi, P. 2013. Citrus huanglongbing: a newly relevant disease presents unprecedented challenges. Phytopathology 103:652-665.
Wu, F., Zheng, Z., Deng, X., Cen, Y., Liang, G., and Chen, J. 2015. Draft Genome Sequence of "*Candidatus* Liberibacter asiaticus" from *Diaphorina citri* in Guangdong, China. Genome Announc 3:e01316-15.
Wulff, N. A., Zhang, S., Setubal, J. C., Almeida, N. F., Martins, E. C., Harakava, R., Kumar, D., Rangel, L. T., Foissac, X., Bové, J. M., and Gabriel, D. W. 2014. The complete genome sequence of '*Candidatus* Liberibacter americanus', associated with citrus huanglongbing. Mol Plant Microbe Interact 27:163-176.
Yan, Q., Sreedharan, A., Wei, S., Wang, J., Pelz-Stelinski, K., Folimonova, S., and Wang, N. 2013. Global gene expression changes in *Candidatus* Liberibacter asiaticus during the transmission in distinct hosts between plant and insect. Mol Plant Pathol 14:391-404.
Zhang, S., Flores-Cruz, Z., Zhou, L., Kang, B. H., Fleites, L. A., Gooch, M. D., Wulff, N. A., Davis, M. J., Duan, Y. P., and Gabriel, D. W. 2011. '*Ca.* Liberibacter asiaticus' carries an excision plasmid prophage and a chromosomally integrated prophage that becomes lytic in plant infections. Mol Plant Microbe Interact 24:458-468.
Zhang, M., Guo, Y., Powell, C. A., Doud, M. S., Yang, C., and Duan, Y. 2018. Effective antibiotics against '*Candidatus* Liberibacter asiaticus' in HLB-affected citrus plants

identified via the graft-based evaluation. PLoS One 9:e111032.
Zheng, Z., Deng, X., and Chen, J. 2014a. Whole-genome sequence of "*Candidatus* Liberibacter asiaticus" from Guangdong, China. Genome Announc 2:e00273-14.
Zheng, Z., Deng, X., and Chen, J. 2014b. Draft genome sequence of "*Candidatus* Liberibacter asiaticus" from California. Genome Announc 2:e00999-14.
Zheng, Z., Sun, X., Deng, X., and Chen, J. 2015. Whole-genome sequence of "*Candidatus* Liberibacter asiaticus" from a huanglongbing-affected citrus tree in central Florida. Genome Announc 3:e00169-15.
Zheng, Z., Bao, M., Wu, F., Chen, J., and Deng, X. 2016. Predominance of single prophage carrying a CRISPR/cas system in "*Candidatus* Liberibacter asiaticus" strains in southern China. PLoS One 11:e0146422.
Zheng, Z., Wu, F., Kumagai, L., Polek, M., Deng, X., and Chen, J. 2017. Two "*Candidatus* Liberibacter asiaticus" strains recently found in California harbor different prophages. Phytopathology 107:662-668.

Chapter 3

Growth of '*Candidatus* Liberibacter asiaticus' in commercial grapefruit juice-based media formulations reveals common cell density-dependent transient behaviors

Note – This study was previously published with the following citation:

MERFA, M. V., Naranjo, E., Shantharaj, D., and De La Fuente, L. 2021. Growth of '*Candidatus* Liberibacter asiaticus' in commercial grapefruit juice-based media formulations reveals common cell density-dependent transient behaviors. Phytopathology Preprint. doi: 10.1094/PHYTO-06-21-0228-FI.

The development of the periwinkle calli system to grow CLas ex vivo and the attempt to grow CLas in co-culture with the SF9 insect cell line, as described in this chapter, were performed in collaboration with Dr. Deepak Shantharaj.

Abstract

The phloem-restricted, insect-transmitted bacterium '*Candidatus* Liberibacter asiaticus' (CLas) is associated with Huanglongbing (HLB), the most devastating disease of citrus worldwide. The inability to culture CLas impairs the understanding of its virulence mechanisms and the development of effective management strategies to control this incurable disease. Previously, our research group used commercial grapefruit juice (GJ) to prolong the viability of CLas in vitro. In the present study, GJ was amended with a wide range of compounds and incubated under different conditions to optimize CLas growth. Remarkably, results showed that CLas growth ratios were inversely proportional to the initial inoculum concentration. This correlation is likely regulated by a cell density-dependent mechanism, since diluting samples

between subcultures allowed CLas to resume growth. Moreover, strategies to reduce the cell density of CLas, such as subculturing at short intervals and incubating samples under flow conditions, allowed this bacterium to multiply and reach maximum growth as fast as 3 days post inoculation, although no sustained exponential growth was observed under any tested condition. Unfortunately, cultures were only transient, since CLas lost viability over time; nevertheless, we obtained populations of $\approx 10^5$ genome equivalents/ml repeatedly. Finally, we established an ex vivo system to grow CLas within periwinkle calli that could be used to propagate bacterial inoculum in the lab. In this study we determined the influence of a comprehensive set of conditions and compounds on CLas growth in culture. We hope our results will help guide future efforts toward the long-sought goal of culturing CLas axenically.

Introduction

The ability to grow bacteria in pure culture has been the foundation of bacteriology by enabling a wide range of studies towards understanding their biology (Austin 2017; Lagier et al. 2015). However, most bacterial species have not been successfully established in axenic in vitro cultures (Zengler et al. 2002), thus hindering the assessment of their characteristics and understanding of their role in the environment or within their hosts. One relevant hitherto unculturable group of emergent plant pathogenic bacteria is comprised by '*Candidatus* Liberibacter spp.', which are psyllid-transmitted, phloem-limited, fastidious Gram-negative bacteria of the α subdivision of Proteobacteria (Jagoueix et al. 1994; Killiny 2021; Wang and Trivedi 2013). In addition, they are plant pathogens and endophytes that harm a wide range of economically important crops worldwide, including citrus, potato, tomato, carrot and pear (Bové 2014b; Merfa et al. 2019; Nelson et al. 2012; Thompson et al. 2013).

The citrus Huanglongbing (HLB) disease (also known as citrus greening) is currently the most single devastating disease of citrus worldwide, leading to significant economic losses in the Americas, Asia and Africa (Bové 2014b; Gottwald 2010). The disease is characterized by reductions in yield and tree lifespan, and lopsided, bitter fruits (Bové 2006; Wang and Trivedi 2013). In addition, although an ultimate solution to control HLB in the field is yet to be developed (Bové 2006; Wang and Trivedi 2013), substantial progress has recently been made by different studies towards this goal. These include the identification of a stable antimicrobial peptide that both treated and prevented HLB in greenhouse conditions (Huang et al. 2021); a region-wide implementation of roguing of infected trees followed by tree replacement that significantly reduced the incidence of HLB in the Gannan region of China (Yuan et al. 2020); application of streptomycin through trunk injection to reduce the in planta population of the HLB-associated bacterium (Li et al. 2020); assessment of the use of thermotherapy to treat infected trees (Thapa et al. 2021); and the development of an assay for early detection of the HLB-associated bacterium in asymptomatic tissues to aid the management of the disease (Wheatley et al. 2021). Moreover, the development of tools and techniques for the early detection of the associated bacterium in the field is critical for HLB management (Braswell et al. 2020; Gottwald et al. 2020; Pandey and Wang 2019). In the U.S., and in most of the major citrus producing areas globally, HLB is associated with '*Candidatus* Liberibacter asiaticus' (CLas). Nonetheless, different '*Ca.* Liberibacter' species ('*Ca.* L. americanus' and '*Ca.* L. africanus') are also associated with the disease in other parts of the world (Bové 2006, 2014b).

The recalcitrance of CLas to grow axenically has greatly impaired our ability to understand important characteristics such as virulence mechanisms, host-pathogen interactions

and even fulfilment of Koch's postulates for HLB (Bové 2006; Merfa et al. 2019; Wang and Trivedi 2013). These limitations hamper the development of efficient management approaches to control this disease. Since having CLas grown in laboratory conditions is fundamental to advance its research, in the past decade, several efforts have been made to culture this bacterium. Even though a reliable and reproducible method to culture CLas in axenic conditions is yet to be developed, these studies have significantly contributed to advance our knowledge about the nutrient and environmental requirements of CLas. Research approaches have included formulating culture media to mimic the natural environments where CLas lives (Parker et al. 2014; Sechler et al. 2009), coculturing it with one or more bacterial species (Davis et al. 2008; Fujiwara et al. 2018; Ha et al. 2019) and using explants of CLas-infected plant tissues to establish ex vivo systems to grow this bacterium (Attaran et al. 2020; Irigoyen et al. 2020). Data suggest that CLas is able to grow in conditions close to its natural environments, while it may also obtain additional nutrients or chemical signals by establishing mutualistic relationships with other cohabiting bacteria. However, these approaches do not allow CLas to be studied directly due to either the nature of mixed cultures, transient growth of CLas, low number of CLas cells in comparison to the overall population, or growth within plant tissues. Thus, further investigation is needed to elucidate factors that are required to reach the long-sought goal of obtaining pure cultures of CLas.

Previously, our research group established transient cultures of CLas with other microflora by using commercial grapefruit juice (GJ) as culture medium (Parker et al. 2014). Therefore, in this study we aimed at amending GJ using compounds with potential to help CLas growth based on the current literature (Merfa et al. 2019), in addition to testing different

incubation settings to define optimized growth conditions for our system. Compounds and conditions that were tested were chosen based on studies performed with the surrogate bacterium *Liberibacter crescens* (Lcr), the only culturable species of the genus *Liberibacter* (Cruz-Munoz et al. 2019; Fagen et al. 2014b; Jain et al. 2017a), CLas itself (Duan et al. 2009; Vahling et al. 2010; Wang and Trivedi 2013) and considering the composition of the original GJ (Parker et al. 2014). We were able to repeatedly establish transient cultures of CLas, which survived sequential subcultures. However, CLas growth was inversely proportional to the concentration of cells present in the initial inoculum, since higher growth ratios were obtained when the initial inoculum had lower number of cells. Unfortunately, most tested compounds and conditions did not improve CLas growth in our system.

On the other hand, the use of surrogate organisms is a valuable tool that allow advancing our knowledge about fastidious bacteria. In this context, periwinkle (*Catharanthus roseus*) has been used as a surrogate host to study the HLB pathosystem because it carries a higher population of CLas in comparison to citrus plants and produces HLB-like symptoms in a short period of time (Bové 2014a). Studies with this plant host include determining the distribution of CLas in planta (Ding et al. 2015; Li et al. 2018); screening of antimicrobial compounds (Zhang et al. 2010); visualization of CLas-associated phage particles within the phloem (Zhang et al. 2011); analysis of the nutritional requirements of CLas by evaluating the phloem sap composition (Killiny 2016); and assessment of the plant response against CLas by performing transcriptome profiling of infected plants (Liu et al. 2019). Therefore, we established an ex vivo system to grow CLas in calli produced from infected periwinkle leaves to propagate inoculum of CLas in laboratory conditions. Overall, we believe our results demonstrate a set of growth

conditions and nutrient supplements, as well as the establishment of an ex vivo system, that could enhance the axenic growth of CLas.

Materials and methods

Bacterial strains and growth conditions

'*Ca*. L. asiaticus'- infected material was used as initial inoculum in all assays performed in this study. Inoculum was obtained from either CLas-infected sweet orange seeds, periwinkle plants or excised Asian citrus psyllids (ACP, *Diaphorina citri*) guts (details below). Growth assessment was performed in broth media containing grapefruit juice (Simply Grapefruit; Simply Orange Juice Company, Apopka, FL, USA) as the base culture medium. *L. crescens* strain BT-1 was grown on BM7 agar plates at 28 ºC (Fagen et al. 2014a). *L. crescens* cryopreserved stocks (BM7 with 20% glycerol, -80 ºC) were plated on BM7 and grown for 7 days. Then, cultures were restreaked on new BM7 agar plates for a second passage and grown for an additional 7 days prior to the start of the experiments. *Propionibacterium acnes* was grown on Reinforced Clostridial agar plates (HiMedia, Mumbai, India) at 28 ºC in an anerobic chamber for 4 days before use. *Escherichia coli* bearing the pLas16S plasmid, which is used as standard to quantify the CLas population by quantitative polymerase chain reaction (qPCR) (Parker et al. 2014), was grown overnight at 37 ºC on LB medium (Becton, Dickinson and Company, Sparks, MD, USA) amended with kanamycin at a final concentration of 50 µg/ml.

CLas inoculum preparation

Citrus seeds. Sweet orange fruits [*Citrus sinensis* (L.) Osbeck 'Hamlin' and 'Valencia'] were collected from HLB-symptomatic trees in a grove located in Vero Beach, FL (June 2017 to

October 2020) and shipped overnight to Auburn University, Alabama. Experiments started ≈24 h after sample collection, however fruits were stored at 4 ºC in a cold chamber for up to a month and used regularly in assays. No clear differences in CLas growth behavior were observed when fruits were used at time of arrival or after storage at 4 ºC (data not shown). Symptomatic, greenish lopsided fruits were used to obtain CLas inoculum. Fruits were surface sterilized by submerging them in 1.2% sodium hypochlorite solution for 1 min, followed by 70% ethanol solution for 1 min and two subsequent wash steps with sterile deionized water for 1 min each. Seeds were collected aseptically using sterile tweezers and scalpel and weighed. About 200 mg of seed material were used in each assay and aborted seeds were preferentially collected. When there were not enough aborted seeds, only the seed coat of normally developed seeds was collected, since CLas is present more abundantly within this tissue in citrus seeds (Achor et al. 2020; Hilf 2011). The seed material was thoroughly ground using sterile mortar and pestle in 5 ml of broth media and suspended to a final volume of 10 ml. The suspension was then vortexed for 1 min, filtered through a 100-µm nylon net Steriflip Filter Unit (EMD Millipore, Billerica, MA, USA) to remove large seed particles and used as CLas inoculum.

Periwinkle leaves. CLas-infected periwinkle plants (surrogate host) were shipped overnight to Auburn University from USDA Fort Piece, FL and kept in greenhouse conditions (day/night temperatures of 28 ºC/22 ºC, 60 to 80% relative humidity and seasonal day/night photoperiod) at the Plant Science Research Center (Auburn University, Auburn, AL, USA). To propagate infected plants, healthy periwinkle seeds (*Catharanthus roseus* Pacifica XP White; Harris Seeds, Rochester, NY, USA) were germinated in 1206 inserts (Grower's Solution, LLC, Cookeville, TN, USA) using Sunshine Mix #8 (Sun Gro Horticulture Canada Ltd., Vancouver,

Canada), then transferred to 8-inches round pots and regularly fertilized with Osmocote 19-6-12 (The Scotts Company, Marysville, OH, USA) as needed. After ≈1 month of transplant, healthy plants were pruned and grafted with branches of CLas-infected periwinkle plants (1 branch per healthy plant). Grafted plants were bagged for 7 days to keep humidity and then grown until symptoms appeared. Only blotchy mottled leaves were used for inoculum preparation in each assay. Periwinkle leaves were surface sterilized as described above for citrus fruits and the petioles and midribs were collected aseptically using tweezers and scalpel. Leaf material (≈200 mg) was thoroughly ground in 5 ml of broth media using sterile mortar and pestle and suspended to a final volume of 10 ml. Then, the suspension was vortexed for 1 min, filtered through a 100-µm nylon net Steriflip Filter Unit (EMD Millipore, Billerica, MA, USA) to remove large leaf particles and finally used as CLas inoculum.

ACP guts. Psyllids (*Diaphorina citri* Kuwayama) were reared on CLas-infected citrus plants in the Citrus Research and Education Center (University of Florida, Lake Alfred, FL, USA) and shipped overnight to Auburn University. Experiments started ≈24 h after psyllids collection and 20 to 40 ACPs were used in each assay. Prior to starting inoculum preparation, the insects were inactivated temporarily by incubation at -20 ºC for 1 min. Then, ACPs were transferred to a 1.5 ml tube on ice and surface sterilized by adding 1 ml of ice cold 70% ethanol and vigorously inverting the tube for few seconds. Next, the ethanol was discarded, and psyllids were washed 20 times with 1 ml of ice cold sterile deionized water by vigorously inverting the tube for few seconds. The insects were then individually placed on 10 µl drops of sterile deionized water on a petri dish lid and dissected with the aid of an Olympus SZ3060 stereo microscope (Olympus, Tokyo, Japan) using a pair of surface sterilized Dumont tweezers 4 and 5

(Electron Microscopy Sciences, Hatfield, PA, USA) to recover their guts. Guts were placed in 1 ml of broth media and vortexed twice for 1 min to release CLas cells. Finally, the inoculum was briefly centrifuged at 5,000 rpm for 2 seconds to pellet guts, and only the supernatant was used in experiments.

All inocula used in this study were tested by qPCR (described below) to determine presence and total population of CLas at the beginning and throughout development of assays.

Culture media

Commercially available grapefruit juice was used as the base culture medium throughout all assays described here (Parker et al. 2014), and was purchased at different times during the course of this study. Before using it as culture medium, GJ was centrifuged at 20,000 rpm for 30 min to pellet solid particles, filtered using a 0.45-µm polyethersulfone (PES) membrane (Pall Corporation, Port Washington, NY, USA) and then filter sterilized using a 0.2-µm PES filter Unit (VWR, Radnor, PA, USA). This processed GJ was stored at -20 ºC as 45 ml aliquots and thawed at room temperature before use. When needed, the pH of GJ was adjusted to 5.85 using 5 M NaOH (the regular pH of the processed GJ is ≈3.2 to 3.5). In addition, solid GJ plates were prepared by autoclaving Gelrite (10 g/l; Research Products International Corp., Mt. Prospect, IL, USA) in deionized water and supplementing with sterile grapefruit juice to a final concentration of 50%. The autoclaved Gelrite and GJ were brought to 40 ºC before mixing.

The most common amendments used here to modify GJ broth medium were: α-ketoglutaric acid (2 g/L), L-asparagine (1 g/L), L-histidine (0.05 g/L), monosodium phosphate

monohydrate (1.5 g/L) and cycloheximide (200 µg/ml), with pH adjusted to 5.85. This culture medium was hereafter named mGJ, for modified grapefruit juice. We chose to add these compounds to GJ based on studies about the nutritional requirements of CLas and Lcr and considering the composition of GJ itself (Cruz-Munoz et al. 2019; Duan et al. 2009; Fagen et al. 2014a; Parker et al. 2014; Wang and Trivedi 2013). Cycloheximide was added to mitigate eukaryotic (mainly fungal) contamination, mostly observed when ACP guts were used as source of CLas inoculum. Other growth conditions and/or compounds added to GJ or mGJ, as well as the concentrations used and rationale for testing them, are reported throughout this study (**Table 3-1**). All compounds mentioned here were dissolved directly in GJ and the broth medium was once again filter sterilized by using a 0.2-µm PES filter Unit (VWR, Radnor, PA, USA).

CLas culturing conditions

24-well plates. To assess CLas growth under different media formulations and growth conditions, CLas suspensions obtained from the different inoculum sources were inoculated (1.8 ml of broth media + 200 µl of CLas inoculum) into GJ, mGJ or other amended grapefruit juice formulations in polystyrene 24-well plates (VWR, Radnor, PA, USA) as 10-fold serial dilutions. Plates were incubated at 28 ºC for 21 days in the dark without agitation. Then, samples were subcultured into fresh broth medium and 200 µl aliquots from each sample were collected to assess total CLas population by qPCR. The OD_{600nm} of cultures was also measured at initial and final time points of assays using a plate reader (Cytation 3 Image Reader spectrophotometer; Biotek Instruments Inc., Winooski, VT, USA). However, data from these readings were not informative about CLas growth, since number of cells were usually below the detection limit, which is also an indication of lack of contamination with fast growing microflora (data not

shown). Thus, only qPCR was used to evaluate CLas growth over time in the different assessed culturing conditions. A total of 3 to 4 subcultures were performed in each assay at 21-day intervals. In all experiments conducted in 24-well plates, samples were diluted by 10-fold serial dilutions using broth media until 10^{-4}. All dilutions, including the concentrated suspension, were inoculated into 24-well plates to assess CLas growth in each tested condition. During the time series assays, plates were regularly inspected for visual presence of cocultured bacteria (non-CLas) by assessing any sudden increase in the turbidity of the medium. These were presumed to be contaminating fast-growing bacteria.

Flow system. CLas growth was also evaluated in a condition that allowed for constant broth medium replenishment over time, by incubating cells in a flow system (**Fig. S3-1**). For that, broth culture medium was put in a 1-ml plastic syringe (Becton, Dickinson and Company, Franklin Lakes, NJ, USA), while 1 ml of CLas inoculum was placed in a 5-ml plastic syringe barrel (Henke Sass Wolf, Tuttlingen, Germany), which served as collection tube, and was capped by using autoclaved cotton plugs. Both syringes were connected to each other using a polytetrafluoroethylene (PTFE) tubing with a nominal inside diameter of 0.022-inches (Weico Wire & Cable, Inc., Edgewood, NY, USA). The loaded 1-ml syringes were then inserted into an automated syringe pump (11 Plus; Harvard Apparatus, Holliston, MA, USA) and the broth medium was supplied at a constant flow rate of 0.25 µl/min. During the experiments, broth culture medium was replenished in 1-ml syringes as required (usually every 3 days). Samples were incubated for 12 days at room temperature and 200 µl aliquots were taken every 3 days to assess CLas population by qPCR. Finally, in experiments that required incubation of cells at a constant temperature, samples were placed inside a Styrofoam box filled with deionized water in

which the temperature was kept at 28 ºC by a 50 W aquarium heater (Aqueon, Franklin, WI, USA).

Subculturing at 3-day intervals. To evaluate if CLas could grow in a shorter period than 21 days, subculturing of samples was performed at 3-day intervals, as described above for assays in 24-well plates. Accordingly, samples were incubated in 24-well plates at 28 ºC for a total of 15 days, while at every 3 days, subcultures were performed and 200 µl aliquots were taken to assess CLas population by qPCR. The CLas population was only assessed in each subculture after the 3 days incubation period and not throughout the entire 15 days. Inocula used in these assays were taken from CLas samples previously incubated in 24-well plates for 21 days (see above). Only samples that had previously presented growth were used to perform assays with subculturing at 3-day intervals.

Solid GJ plates. CLas samples were plated in solid GJ plates to assess for colony and/or microcolony growth. For this purpose, 100 µl of CLas inocula obtained from citrus seeds or periwinkle plants (as described above) were spread on GJ Gelrite plates and incubated at 28 ºC. Growth of bacteria was visually assessed at weekly intervals for the presence of colony formation units. At the final time point of assays (14-, 21- and 28- days post incubation), cells were harvested by scrapping the medium using 500 µl of sterile grapefruit juice and transferring them to 2 ml microcentrifuge tubes. CLas growth was then analyzed by qPCR.

Periwinkle callus culture

Induction and propagation of periwinkle calli were performed according to well established protocols (Pietrosiuk et al. 2007; Singh 2011). In summary, leaves from CLas-infected periwinkle plants were collected and surface sterilized as described above. Then, cross sections of leaves were taken using a sterile blade and transferred to culture media for callus induction and propagation. Three different culture media that differ in ammonium and nitrate concentration ratios were tested: Murashige & Skoog basal medium (Murashige and Skoog 1962), Gamborg's basal medium (Gamborg et al. 1968) and Nitsch & Nitsch (Nitsch and Nitsch 1969). Basal media were supplemented with Gamborg's B5 vitamins, indole-3-acetic acid (IAA; 1 mg/ml), benzyl adenine (BAP; 0.1 mg/ml), sucrose (30 g/l) and 0.8% phytagel (chemicals were purchased from PhytoTech Labs, Lenexa, KS, USA). Inoculated plates (containing ≈10 explants each) were incubated at room temperature and humidity conditions under a 12:12 h (light:dark) photoperiod using fluorescent tube light (intensity of light ≈200 lux). Plates were placed ≈1.5 meters away from the light source. Controls using healthy periwinkle leaves were also used.

Periwinkle cell proliferation and callus formation were monitored weekly for 6 weeks from the initial date after the explant transfer to the culture media and eventually subcultured by transferring to new culture medium plates. When contamination was present, non-contaminated explants were transferred to new plates, while contaminated samples were discarded. At select time points, as well as in the source plant material that contains the initial inoculum, the total CLas population was determined by extracting DNA (detailed below) from ≈200 mg of callus material and submitting samples to qPCR. The presence of CLas within samples was also analyzed by immune tissue printing (Ding et al. 2017a).

CLas detection within periwinkle calli through immune tissue printing

Detection of CLas via immune tissue printing was performed as described elsewhere (Ding et al. 2017a). Briefly, 5- to 6-week-old periwinkle calli obtained as described above, including calli obtained from both CLas-infected and healthy leaves, were cut aseptically into slices and imprinted onto activated 0.2-µm PVDF membranes (Bio-Rad Laboratories Inc., Hercules, CA, USA; protein binding capacity of 150–160 µg/cm^2) until dried. Membranes were processed for immunodetection at 37 ºC using a reciprocal shaker (80 rpm) incubator (Thermo Scientific, MaxQ 6000, Swedesboro, NJ, USA). Initially, membranes were reactivated in 95% methanol for 1 min and transferred to phosphate-buffered saline (PBS) + 0.05% Tween-20 (PBST) at room temperature and washed twice (5 mins each). Later, membranes were blocked in PBST + 5% fat-free skim milk (SACO Foods Inc., Middleton, WI, USA) for 1 h. Membranes were then treated with rabbit anti-OmpA primary antibody (Abnova, Taipei City, Taiwan) (1:500 dilution in PBST), which detects the outer membrane protein OmpA of CLas (Ding et al. 2015), by overnight incubation, washed three times with PBST (10 mins each), treated with goat anti-rabbit secondary antibody coupled to horseradish peroxidase (HRP; Promega Corporation, Madison, WI, USA) at a 1:10,000 dilution in PBST for 1 hour, and washed again three times with PBST (10 mins each). Finally, membranes were developed using 1 ml of 3,3′,5,5′-Tetramethylbenzidine (TMB) substrate (Agdia, Elkhart, IN, USA) added at room temperature. Incubation was stopped when the blue-purple color developed on the prints by washing in sterile deionized water. In addition, total proteins in each sample were visualized by staining membranes with Ponceau S (0.1% w/v in 0.5% acetic acid) (Amresco, Solon, OH, USA) for 5 mins and destaining in 0.5% acetic acid.

qPCR analyses

DNA from all samples was extracted using a modified cetyltrimethylammonium bromide (CTAB) procedure (Doyle and Doyle 1987). Then, qPCR was performed using the previously described HLBas/HLBr/HLBp pair of primers and TaqMan probe set (Li et al. 2006) to quantify CLas population in each sample as genome equivalents. DNA amplifications were performed in 20 µl reactions containing 1× ABsolute Blue QPCR ROX Mix (Thermo Scientific, Waltham, MA, USA), 250 nM of each primer, 150 nM of the probe (labeled 5′-6FAM, 3′-BHQ1), and 1 µl of DNA template, and carried out using a C1000 thermal cycler base with a CFX96 real-time system (Bio-Rad Laboratories Inc., Hercules, CA, USA). Each DNA amplification was repeated in triplicates. Cycling parameters were the same as described by Parker et al. (2014). Reaction efficiencies of 90 to 105% were confirmed for each qPCR run. The number of CLas genome equivalents in each sample was calculated by coamplifying a four-point standard curve (**Fig. S3-2**) made from 10-fold serial dilutions of the pLas16S plasmid (Parker et al. 2014). Aliquots of the standard curve were used once before discarding. Samples with a value of threshold cycle (C_T) below 40 were considered CLas-positive (considering that our cycling parameters had a total of 44 amplification cycles), which corresponded to at least twelve genome equivalents of CLas according to the standard curve (**Fig. S3-2**). DNA extracted from noninoculated sterile grapefruit juice (or the corresponding used medium formulation) was included as negative control in our qPCR runs. If amplification was observed in these samples, their C_T values were considered as cutoff value for positive samples, meaning that any sample with a C_T value close (with less than 1 cycle difference) or above to that of the noninoculated grapefruit juice was considered negative and treated as no detection of CLas.

L. crescens qPCR analysis was performed using the Lcr-F/Lcr-R/Lcr-P pair of primers and TaqMan probe set as described elsewhere (Naranjo et al. 2020). In summary, DNA amplifications were carried out in 20 µl reactions containing 1× PerfeCTa qPCR FastMix II Low ROX (QuantaBio, Beverly, MA, USA), 250 nM of each primer, 150 nM of the probe (labeled 5′-6FAM, 3′-BHQ1), and 1 µL of DNA template. Each DNA amplification was repeated in triplicates and cycling parameters were 95 ºC for 2 min, followed by 39 cycles of 95 ºC for 5 s and 60 ºC for 30 s. Reaction efficiencies of 90 to 105% were confirmed for each qPCR run. The number of Lcr genome equivalents in each sample was calculated by coamplifying a five-point standard curve made from 10-fold serial dilutions of the Lcr genomic DNA. Aliquots of standard curves were used once before discarding.

Data analysis

The overall trend of CLas cell population in the different experimental conditions evaluated in this study was analyzed by two-tailed Student's *t*-test, except when incubating cells using the flow system. The CLas population obtained after the incubation period, calculated as genome equivalents, was always compared to the population in the initial inoculum to evaluate if there was significant growth or death of cells. The growth ratio was also determined, when possible. This was calculated as the ratio of genome equivalents obtained after the incubation period by the number of genome equivalents in the initial inoculum of each sample. For assays performed in flow conditions and for the CLas growth ex vivo using the periwinkle callus system, the CLas population in the different time points of evaluation and in the different analyzed media was compared by one-way analysis of variance (ANOVA) followed by Tukey’s

HSD multiple comparisons of means in R 4.0.0 under the package multcomp (Ihaka and Gentleman 1996).

Due to the variable nature of CLas growth observed in the assays described here and the variation in CLas population in the initial inocula -that was influenced by the source material and time of the year collected-, representative results from independent experiments are shown. In other words, all results included here are from a single experiment selected from at least two independent experiments (**Table S3-1**) that showed the same trend. Variation in population numbers among experiments precluded the consideration of data from multiple experiments for statistical analysis.

Results

CLas reaches higher growth ratios in grapefruit juice when starting from low cell numbers, a behavior repeated among subcultures

To reproduce our previous findings and establish transient cultures of CLas (Parker et al. 2014), samples were inoculated into GJ and incubated at 28 ºC, and CLas growth was monitored by qPCR. However, instead of growing cells in Erlenmeyer flasks and evaluating growth every other day as done in the past (Parker et al. 2014), in this study samples were diluted by 10-fold serial dilutions, incubated in 24-well plates and growth was assessed after 21 days of inoculation. As described above, different sources of CLas inoculum were used throughout this study (citrus seeds, periwinkle leaves and ACP guts), but no clear differences in CLas growth behavior were observed among these sources (data not shown). Thus, the source of inoculum used in each assay will not be mentioned here. Nonetheless, the number of CLas cells in citrus seeds used as

inoculum source to perform the assays described in this study was quantified to assess the distribution of its population throughout the years. No obvious annual trend was observed for the CLas population within citrus seeds, however, its concentration was higher during the year of 2018 (**Fig. S3-3**), although not statistically significant. When periwinkle leaves and ACP guts were used as inoculum source, the CLas concentration was more uniform (usually $\approx 10^6$ cells/ml), possibly because these samples were produced under controlled conditions (data not shown).

Curiously, when CLas was grown in GJ, results showed that decreasing the initial inoculum by 10-fold serial dilution was associated with a significant increase of CLas growth (**Fig. 3-1**). In other words, CLas did not grow in GJ when its titer was high in the initial inoculum (above 10^5 genome equivalents/ml), while decreasing the initial number of cells by performing 10-fold serial dilutions allowed samples to grow. This association was observed consistently in the vast majority of the various experiments (**Table S3-1**) performed in this study (≈88% out of 17 independent experiments that were performed, including different medium formulations) and suggests that the ability of CLas to grow is affected by its initial population, at least in GJ and related media tested here.

Next, to evaluate if CLas could survive passages in fresh culture medium and to determine its growth behavior, samples were incubated as described above, but three subcultures at 21 day-intervals each were performed (**Fig. 3-2**). In this assay, mGJ, which contains compounds selected for their potential aid for the in vitro growth of CLas (as described above), was used as broth medium. In the first inoculated plate, similarly to the previous result, CLas

numbers increased only when the initial inoculum was diluted until 10^{-4} ($\approx 10^3$ genome equivalents/ml) (**Fig. 3-2A**), although not significantly ($P = 0.15$).

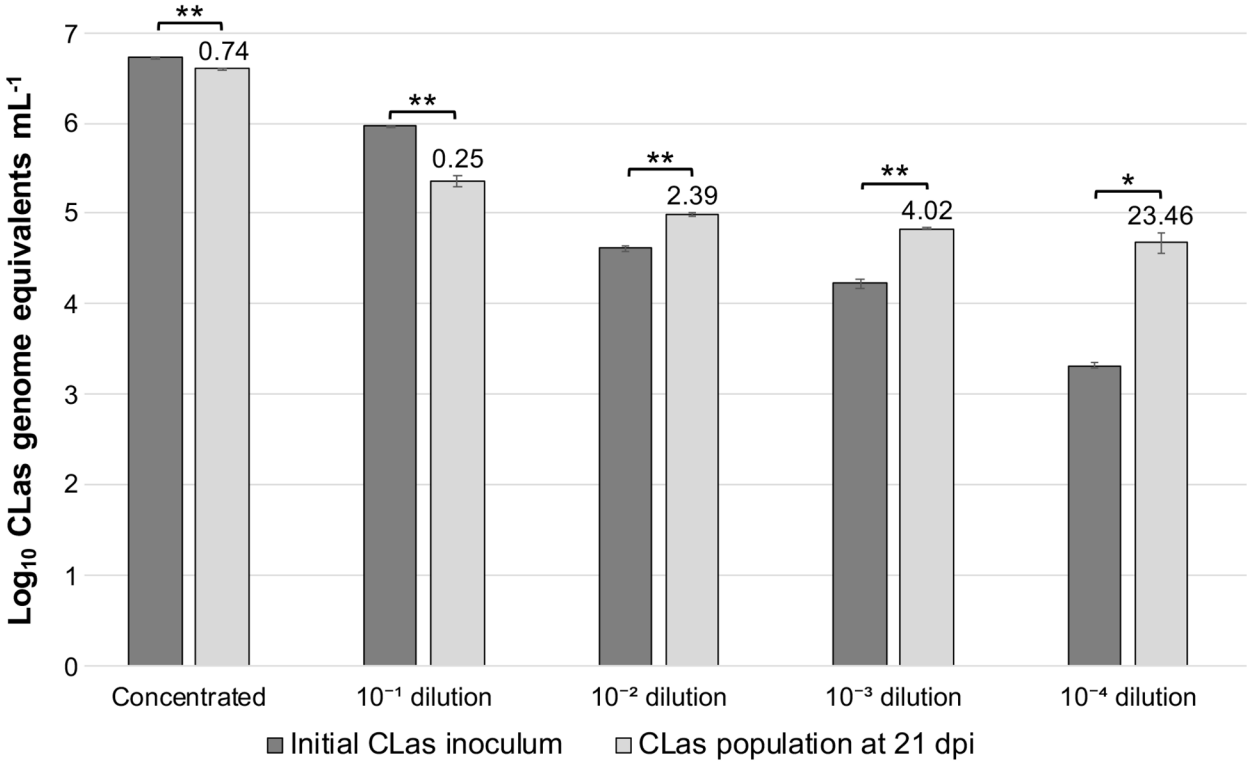

Fig. 3-1. Growth of CLas inoculated into grapefruit juice in 24-well plates. CLas samples were grown in GJ for 21 days at 28 ºC and the number of cells in the initial inoculum and after incubation was determined by qPCR. Data represent means and standard errors. Numbers above light gray columns indicate growth ratio of CLas. Statistical significance was determined using Student's *t*-test (* indicates $P \leq 0.05$ and ** indicates $P \leq 0.005$ in comparison to the initial inoculum; n = 3 technical replicates). "dpi" means days post inoculation. The experiment was repeated twice with similar results.

However, when samples were diluted for the first subculture, all presented significant growth after the three weeks incubation period (**Fig. 3-2B**), while an additional subculture led to a significant decrease in CLas population in almost every sample (**Fig. 3-2C**). Finally, no CLas was detected at the final time point of the last subculture (**Fig. 3-2D**). This result was also consistent among independent replicates and indicates a highly repeatable transient growth behavior of CLas in which cells grow better starting from a low inoculum concentration; and

while the first subculture seems to support CLas growth, further subculturing attempts do not improve or even impair the in vitro viability of this bacterium over time. Interestingly, some samples presented CLas growth even though bacterial titers were too low to be detected in the initial inoculum by qPCR (**Fig. 3-2B**). We stress that this finding was a common trend among independent replicates. It is worth noting that in both results presented above (**Figs. 3-1** and **3-2**) there was no visible growth of fast-growing cocultured bacteria with CLas, as analyzed by turbidity. Nonetheless, a few of the replicates with similar CLas growth trend results did show contamination with fast-growing bacteria (data not shown).

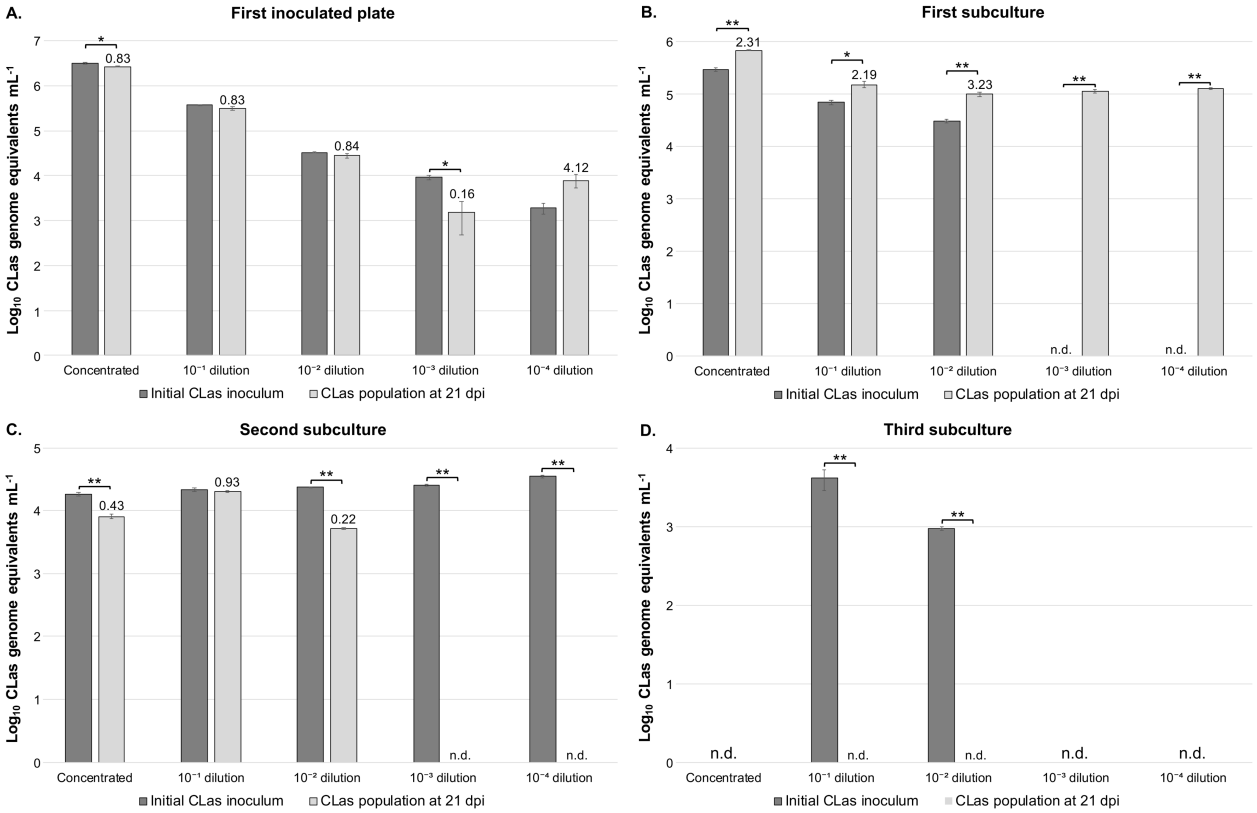

Fig. 3-2. Growth of CLas among subcultures in modified grapefruit juice in 24-well plates. CLas samples grown in mGJ in 24-well plates were subcultured three times at the final time points of incubation to assess growth behaviors. **A.** Results from first inoculated plate. **B, C, D.** Results from first, second and third subculture, respectively. Data represent means and standard errors. Numbers above light gray columns indicate growth ratio of CLas. Statistical significance was determined using Student's *t*-test (* indicates $P \leq 0.05$ and ** indicates $P \leq 0.005$ in comparison to the initial inoculum; n = 3 technical replicates). "dpi" means days post

inoculation. “n.d.” indicates no detection signal of CLas by qPCR. A representative result of at least three independent experiments is shown here.

CLas shows quick but limited growth when incubated in a flow system

Since a consistent growth behavior of CLas was obtained by diluting samples between subcultures, attempts to grow this bacterium in flow conditions with a constant increase of culture volume were performed. We designed a system that allows constant broth culture medium replenishment in CLas cultures for 12 days by introducing inocula to a reservoir that is continually supplied with medium by using a syringe pump (**Fig. S3-1**). This experiment was carried out to minimize the density of CLas while seeking to maximize its growth. Although results were somewhat variable, in most assays, CLas presented significant increase in bacterial cell numbers as soon as 3- and 9-days post inoculation (dpi) in mGJ (**Fig. 3-3**). On the other hand, this bacterium usually reached non-detectable levels after 12 days of incubation, evidencing that this quick increase in CLas population is not sustainable for prolonged periods in this system.

Noteworthy is that an oscillating behavior of growth was evidenced here as well, similar to our results in 24-well plates subcultures and our previous study (Parker et al. 2014). Likewise, as in our previous results in 24-well plates, there was no visual presence of fast-growing cocultured bacteria with CLas in the flow system results shown here (**Fig. 3-3**). When cocultured bacteria were present in this system, they were mostly harmful to CLas and decreased its population (data not shown).

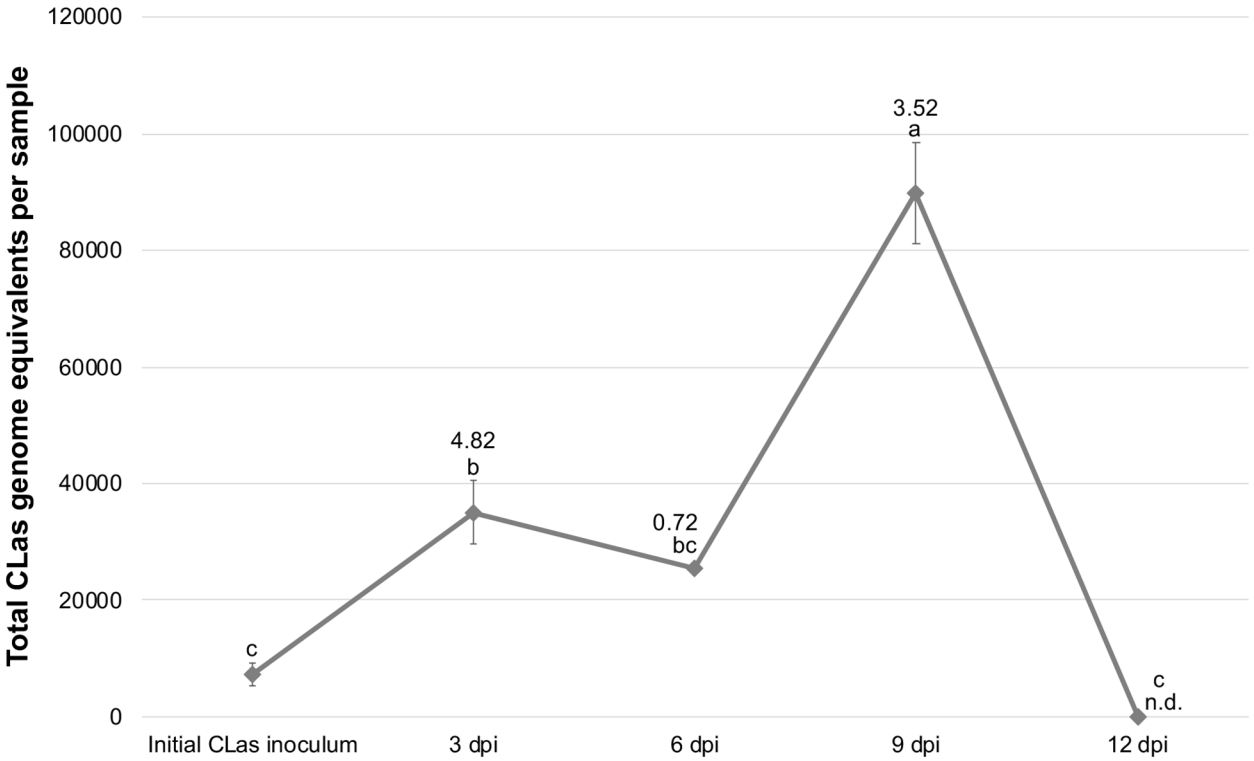

Fig. 3-3. Growth of CLas when incubated using the flow system. CLas was grown in flow conditions in which the broth medium is constantly replenished using a syringe pump (**Fig. S3-1**). Samples were incubated for 12 days in mGJ and collected at every 3 days to assess CLas population by qPCR. Data represent means and standard errors. Numbers above markers in each time point of evaluation indicate growth ratio of CLas in comparison to the previous time point. Different letters in each marker indicate significant difference of CLas population as analyzed by one-way ANOVA followed by Tukey's HSD multiple comparisons of means ($P \leq 0.05$; n = 3 technical replicates). Because the culture medium volume is continuously increasing in the flow system, the total CLas population present in the entire culture volume in each time point of evaluation is shown. "dpi" means days post inoculation. "n.d." indicates no detection signal of CLas by qPCR. A representative result of at least three independent experiments is shown here.

CLas also presents a rapid, but limited growth when subcultured at a shorter period

Due to the growth behavior of CLas in 24-well plates and in flow conditions that indicated a quick, limited growth when cultures had initially a low density of cells, CLas was inoculated into mGJ and grown in 24-well plates as previously described; however, subcultures were performed at 3-day intervals, instead of 21 days. Similar to what was observed when growing CLas in flow conditions, not all results were constant among replicates. However, CLas

presented an overall significant increase in cell numbers in the first subculture of most assays (**Fig. 3-4**).

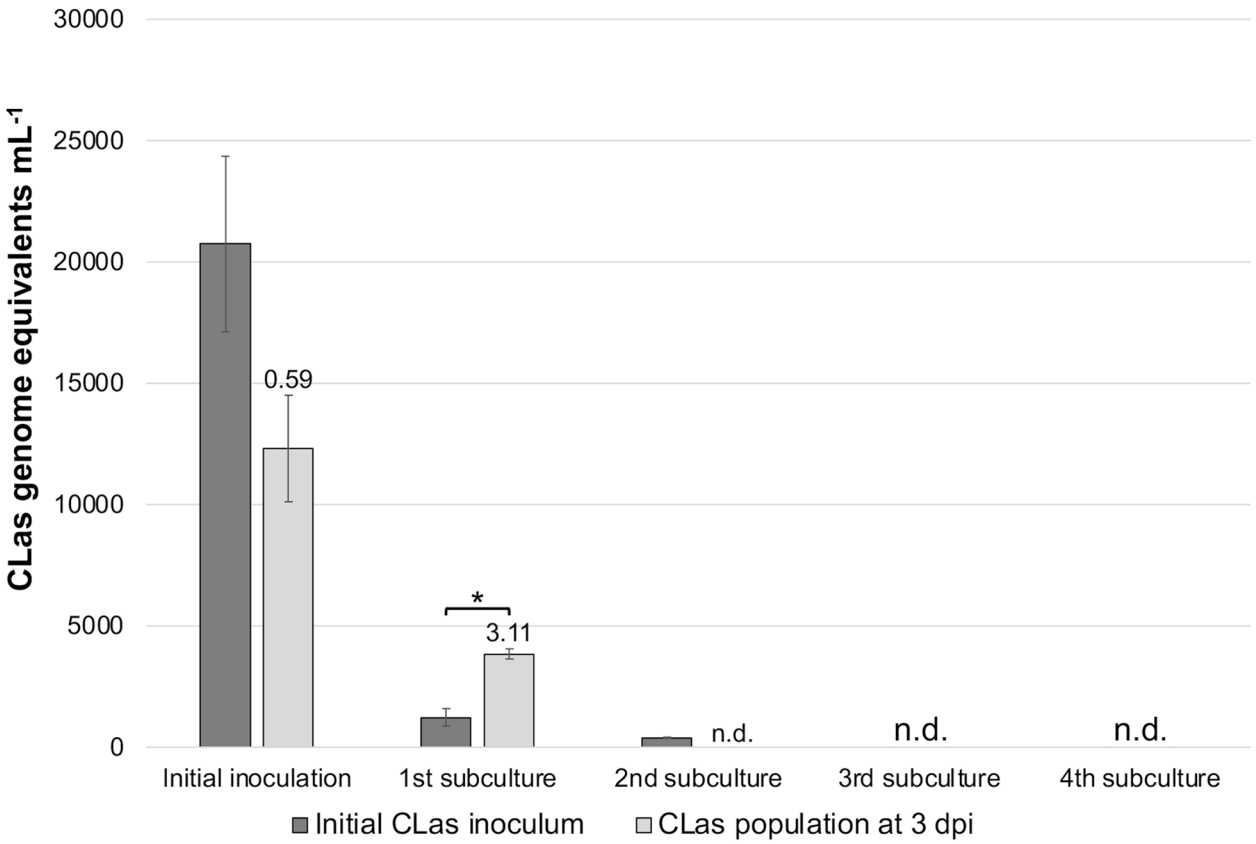

Fig. 3-4. Growth of CLas when subcultured at 3-day intervals. CLas samples inoculated into mGJ in 24-well plates were subcultured four times at every 3 days to assess if this bacterium could grow in a shorter period. Data represent means and standard errors. Numbers above light gray columns indicate growth ratio of CLas. Statistical significance was determined using Student's *t*-test (* indicates $P \leq 0.05$ in comparison to the initial inoculum; n = 3 technical replicates). "dpi" means days post inoculation. "n.d." indicates no detection signal of CLas by qPCR. A representative result of at least three independent experiments is shown here.

This demonstrates an ability to grow quickly within this system. Notwithstanding, CLas usually could not be detected in further subcultures beyond the first subculture (**Fig. 3-4**). Possibly, subcultures beyond this point dilute the CLas inoculum to a level that it is no more detectable by qPCR since subcultures were done as 1/10 inoculations. The rapid increase of CLas population within 3 days was similar to what was observed when samples were incubated

under flow conditions. It is worth noting that no visual presence of fast-growing cocultured bacteria was detected in any of the experiments conducted.

CLas does not grow on solid grapefruit juice culture medium

CLas inocula were plated on solid GJ plates to evaluate the formation of colonies or microcolonies, either with or without cocultured bacteria. Culture medium was composed of 50% GJ + 50% autoclaved Gelrite aqueous solution. The concentration of GJ was chosen based on our previous results showing that CLas establishes transient cultures in 50% GJ broth (Parker et al. 2014). Plates were incubated at 28 ºC and the total CLas population was determined weekly at 14, 21 and 28 dpi by qPCR. CLas presented neither an increase in genome equivalents nor formation of colonies or microcolonies in inoculated plates (**Fig. 3-5**).

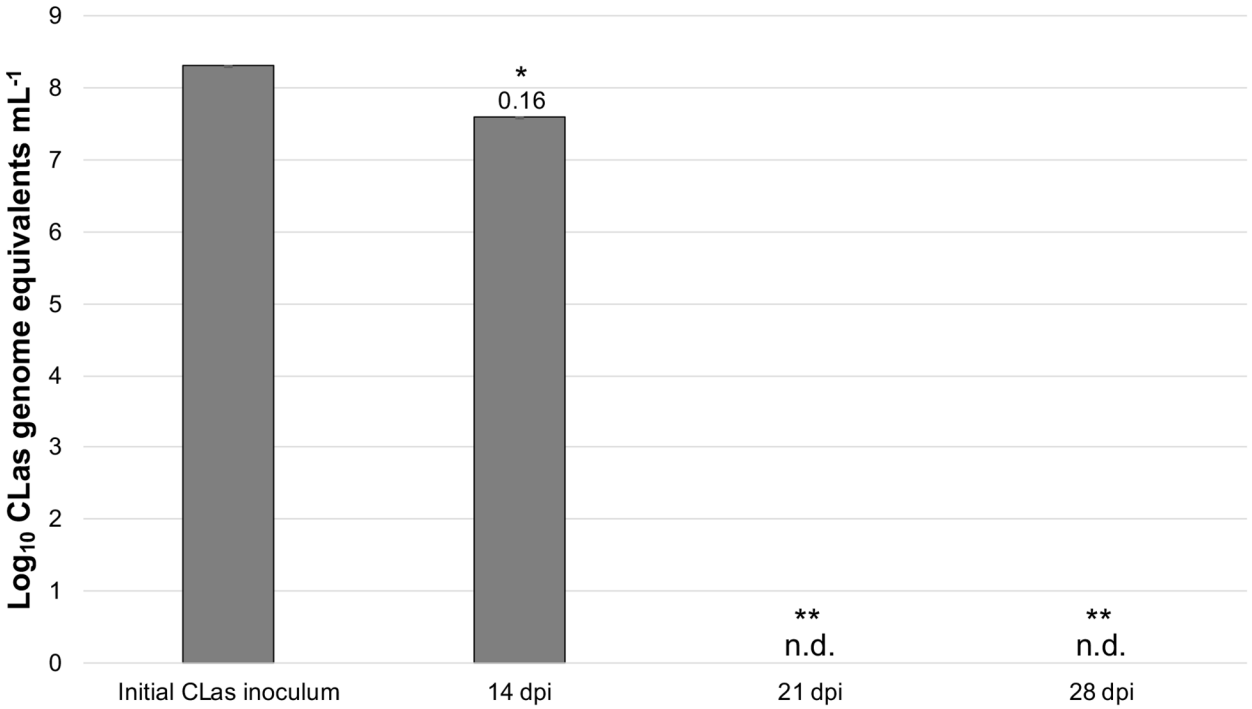

Fig. 3-5. Assessment of CLas growth on solid grapefruit juice plates. CLas was inoculated into GJ Gelrite plates and incubated at 28 ºC for a total of 28 days. The total CLas population was determined weekly at 14, 21 and 28 dpi by qPCR to assess growth. Data represent means

and standard errors. Numbers above columns indicate growth ratio of CLas. Statistical significance was determined using Student's *t*-test (* indicates $P \leq 0.05$ and ** indicates $P \leq 0.005$ in comparison to the initial inoculum; n = 3 technical replicates). "dpi" means days post inoculation. "n.d." indicates no detection signal of CLas by qPCR. A representative result of at least three independent experiments is shown here.

Instead, the CLas population declined progressively over the time course of the experiment, with no detection at the final two points of evaluation (21 and 28 dpi). This demonstrates an inability of CLas to grow when incubated in solid medium by using GJ Gelrite plates. Moreover, no growth of cocultured fast-growing bacteria was observed in the analyzed plates.

Assessing the contribution of other compounds and incubation conditions to CLas growth

A wide range of additional compounds and incubation conditions, in addition to the results already presented here, were assessed to determine their contribution to CLas growth in our GJ system. These additional CLas culturing assays were performed in attempts to overcome the growth limitations we observed in our experiments. Changes to GJ and rationale to choose compounds and incubation conditions, as well as our main findings, are summarized in **Table 3-1**.

Overall, adjusting the pH of GJ to 5.85, incubating cells in a non-shaking condition and growing CLas at a constant temperature of 28 ºC in flow conditions contributed positively to CLas growth. Conversely, amending GJ or mGJ with ATP, *Wolbachia* repressor protein, TNM-FH insect medium, among other compounds, as well as co-culturing CLas with *L. crescens* or *P. acnes* did not show a contribution to its growth, while incubating CLas at 37 ºC and co-culturing

it with SF9 insect cell line were harmful to its growth by decreasing the population of CLas to non-detectable levels by qPCR.

Table 3-1. Contribution of different compounds and incubation conditions to CLas growth.

Compound and/or incubation condition [a]	Rationale	Culture medium formulation and/or growth conditions	Results	References
Compounds				
Adjusting the pH of GJ to 5.85	The pH of GJ is ≈3.5, while the pH of the phloem sap of plant hosts of CLas is ≈5.85. In addition, the surrogate bacterium Lcr has optimal growth in a pH range of 5.8 to 6.8	GJ pH 5.85	Adjusting the pH of GJ significantly contributed to CLas growth by increasing its growth ratio (**Fig. S3-4**)	(Cruz-Munoz et al. 2019; Hijaz and Killiny 2014; Killiny 2016; Parker et al. 2014; Sena-Vélez et al. 2019)
Addition of ATP to GJ	CLas is possibly an energy scavenger that circumvents its deficient glycolysis pathway by directly importing ATP from its host cells through a functional ATP/ADP transporter	GJ + ATP [b] (0.5 mM)	Adding ATP to GJ did not contribute to CLas growth (**Fig. S3-5**)	(Jain et al. 2017a; Vahling et al. 2010)
Addition of *Wolbachia* repressor protein (Wrp) to GJ	A small protein produced by *Wolbachia*, an endosymbiont of ACP, represses phage lytic cycle genes in CLas	GJ + Wrp (1.43 mg/l)	Adding *Wolbachia* repressor protein to GJ did not significantly contribute to CLas growth (**Fig. S3-6**)	(Jain et al. 2017b)
Addition of TNM-FH insect medium to mGJ	TNM-FH is a component of BM7, which is used to culture Lcr, and contains compounds that may benefit CLas growth. In addition, other compounds were added to assess if their combination could improve CLas culturability. Among these, sodium bicarbonate is required by TNM-FH, while BSA was added to mitigate oxidative stress	To 976 ml of mGJ, add: • TNM-FH [c] – 52.4 g • Sodium bicarbonate – 0.35 g • BSA Fraction V (7.5%) [d] – 24 ml • ATP – 0.28 g (0.5 mM)	Addition of TNM-FH insect medium and other compounds to mGJ did not contribute significantly to CLas growth (**Fig. S3-7**)	(Fagen et al. 2014a)

Amendment of mGJ with additional compounds	Additional compounds were added to mGJ to further assess if they could promote CLas growth in vitro. FBS, another component of BM7, was added, in addition to choline chloride (phospholipid precursor) and reduced glutathione (reduces oxidative stress)	To 821 ml of mGJ, add: • TNM-FH – 16 g • Sodium bicarbonate – 0.1 g • BSA Fraction V (7.5%) – 24 ml • ATP – 0.28 g • Fetal bovine serum (FBS) [e] – 150 mL • Choline chloride [f] – 1 g • Reduced glutathione [g] (100 mM) – 5 ml	Amendments did not contribute to CLas growth (**Fig. S3-8**)	(Cruz-Munoz et al. 2018; Fagen et al. 2014a)
Addition of extracellular DNA to mGJ	Studies with the surrogate Lcr suggest that CLas may be naturally competent to acquire exogenous DNA and use it as food source, since this bacterium lacks enzymes for purine and pyrimidine metabolism	CLas was grown in mGJ in flow conditions with addition of the pAX1-Cm [h] plasmid to a total amount of 2 µg	Addition of exogenous DNA did not contribute to CLas growth (**Fig. S3-9**)	(Hartung et al. 2011; Jain et al. 2019)
Incubation conditions				
Incubation at shaking vs. non-shaking conditions	CLas incubation in aeration (shaking) and non-aeration (non-shaking) conditions were compared because this bacterium likely has limited ability to perform aerobic respiration	CLas was inoculated into GJ and incubated at 28 ºC (nonshaking) and at 28º C and 150 rpm (shaking)	CLas presented higher growth ratios in non-shaking conditions (data not shown)	(Duan et al. 2009; Wang and Trivedi 2013)
Incubation at 37 ºC	Citrus groves are affected by high temperatures in some regions of the world, while CLas has been demonstrated to be heat tolerant	Inoculation into mGJ with incubation at 37 ºC	Incubation at 37 ºC was harmful to CLas growth, since it continuously decreased the population to non-detectable levels (data not shown) [i]	(Lopes et al. 2009)
Incubation at 28 ºC under flow conditions	Incubation of CLas in flow conditions was commonly done at room temperature. Thus, incubation in a controlled temperature (28 ºC) was assessed by using an aquarium heater (described in **Fig. S3-1**)	Inoculation into mGJ and incubation in flow conditions at room temperature and at 28ºC	CLas reached a higher growth ratio at room temperature, but incubation at 28 ºC allowed it to grow for a longer period (**Fig. S3-10**)	-

Resuspension of cells in fresh broth medium between subcultures	Samples were pelleted by centrifugation and resuspended into fresh broth medium between subcultures to remove any quorum sensing and/or other signaling molecules that could modulate CLas growth, as found with other bacteria	Centrifugation of CLas cells (4,000 rpm at 4 ºC for 5 minutes) and resuspension in fresh broth medium between subcultures	Method was not suitable because CLas cells were lost in the centrifugation and resuspension step, leading to non-detection by qPCR (data not shown)	(López et al. 2009; Prozorov and Danilenko 2011)
Coculture systems				
CLas coculture with Lcr	Lcr is the only culturable species of the genus *Liberibacter*, in addition to being a surrogate for CLas due to sharing high genome synteny and context with CLas. Thus, the ability of Lcr to improve CLas culturability by sharing metabolic goods was assessed through coculturing	CLas and Lcr were cultured in mGJ and BM7, respectively, using tissue culture plate inserts with 0.1-µm polycarbonate membranes [j] that allow cells of different species to exchange metabolic compounds while being spatially separated, to conduce coculture	Coculture with Lcr did not contribute to CLas growth (**Fig. S3-11**)	(Fagen et al. 2014b; Jain et al. 2019)
CLas coculture with *P. acnes*	CLas has previously been established in transient cocultures with *P. acnes* in a likely mutualistic relationship	CLas and *P. acnes* were cultured in mGJ and Reinforced Clostridial broth, respectively, using tissue culture plate inserts with 0.1-µm polycarbonate membranes to allow coculture	Coculture with *P. acnes* did not contribute to CLas growth (data not shown)	(Davis et al. 2008)
CLas coculture with SF9 insect cell line (*Spodoptera frugiperda*)	The ability of CLas to grow within cells of an insect cell line was evaluated due to the insect-transmitted nature of this bacterium by the ACP, which includes intracellular stages [k]	SF9 cells were grown in SF-900 III SFM broth and were inoculated with CLas to assess if a coculture could be established [l]	CLas did not establish a coculture with SF9 insect cell line (**Fig. S3-12**)	(Bové 2006; Marutani-Hert et al. 2009)
Addition of cell-free spent broth medium used to culture SF9 insect cell line to mGJ	Although CLas did not grow in coculture with SF9 insect cell line, spent SF-900 III SFM broth was added to mGJ to assess if possible secreted compounds could improve CLas culturability	mGJ + spent SF-900 III SFM (1:1) [m]	Addition of cell-free spent SF-900 III SFM broth to mGJ was harmful to CLas growth, since it persistently decreased the population to non-detectable levels (data not shown) [n]	-

[a] Unless otherwise noted, assays were conducted in 24-well plates at 28 ºC and 21 days of growth.
[b] Adenosine 5'-Triphosphate disodium salt hydrate (TCI, Portland, OR, USA).
[c] TNM-FH insect medium (HIMEDIA, Mumbai, India).

[d] BSA Fraction V (7.5%) (Life Technologies Corporation, Grand Island, NY, USA).
[e] HyClone Fetal Bovine Serum (GE Healthcare Life Sciences, Logan, UT, USA).
[f] Choline chloride (ACROS Organics, Geel, Belgium).
[g] Reduced Glutathione, 98%, for analysis (ACROS Organics, Geel, Belgium). Reduced glutathione is added to broth medium only at the time of assay. Aliquots of this compound are stored at -20 ºC at a stock concentration of 100 mM.
[h] pAX1-Cm plasmid was chosen as exogenous DNA because it has already been successfully used in natural competence assays by our group with the plant pathogenic bacterium *Xylella fastidiosa* (Kandel et al. 2017).
[i] At least three independent experiments were performed with similar results.
[j] Tissue culture plate inserts with 0.1-µm polycarbonate membrane (VWR, Radnor, PA, USA).
[k] Although primary cultures of *Diaphorina citri* have been reported, we used SF9 due to readiness of culture and availability of widely known protocols.
[l] A monolayer culture of SF9 insect cell line was performed in a 25 cm^2 cell culture flask using 5 ml of SF-900 III SFM broth culture medium (Life Technologies Corporation, Grand Island, NY, USA). Approximately 10^7 SF9 cells were inoculated with 100 µl of a CLas suspension containing a total of $\approx 10^6$ cells, as previously determined by qPCR. Culture flasks were incubated at 28 ºC in a non-humidified, air-regulated non-CO_2 atmosphere, with loosened caps for gas exchange. Samples were grown for 7 days and collected to quantify CLas population by qPCR.
[m] The mixing concentration of both media was chosen based on previous results that CLas establishes transient cultures in 50% GJ broth (Parker et al. 2014).
[n] Two independent experiments were performed with similar results in flow conditions. One experiment in 24-well plates also yielded similar results.

CLas presents substantial growth within periwinkle calli

Looking to obtain an alternative approach to propagate inoculum of CLas in laboratory conditions, we developed a system to grow this bacterium ex vivo within calli from infected periwinkle leaves. In this experiment, explants from CLas-infected periwinkle leaves were inoculated into different culture media (Nitsch & Nitsch, Murashige & Skoog and Gamborg's media) to assess callus formation and propagation (**Fig. 3-6A**) as well as CLas growth.

Analyses with 5-week-old calli demonstrated that CLas presented significant growth in periwinkle calli cultured in Murashige & Skoog and Gamborg's media, with a growth ratio as high as 3,416-fold when calli were grown in Gamborg's medium (**Fig. 3-6B**). Moreover, CLas also presented growth in 6-week-old calli that were subcultured from a previous assay (**Fig. 3-6C**). In this assay, significant growth was only observed in samples inoculated into Nitsch & Nitsch and Gamborg's medium (**Fig. 3-6C**).

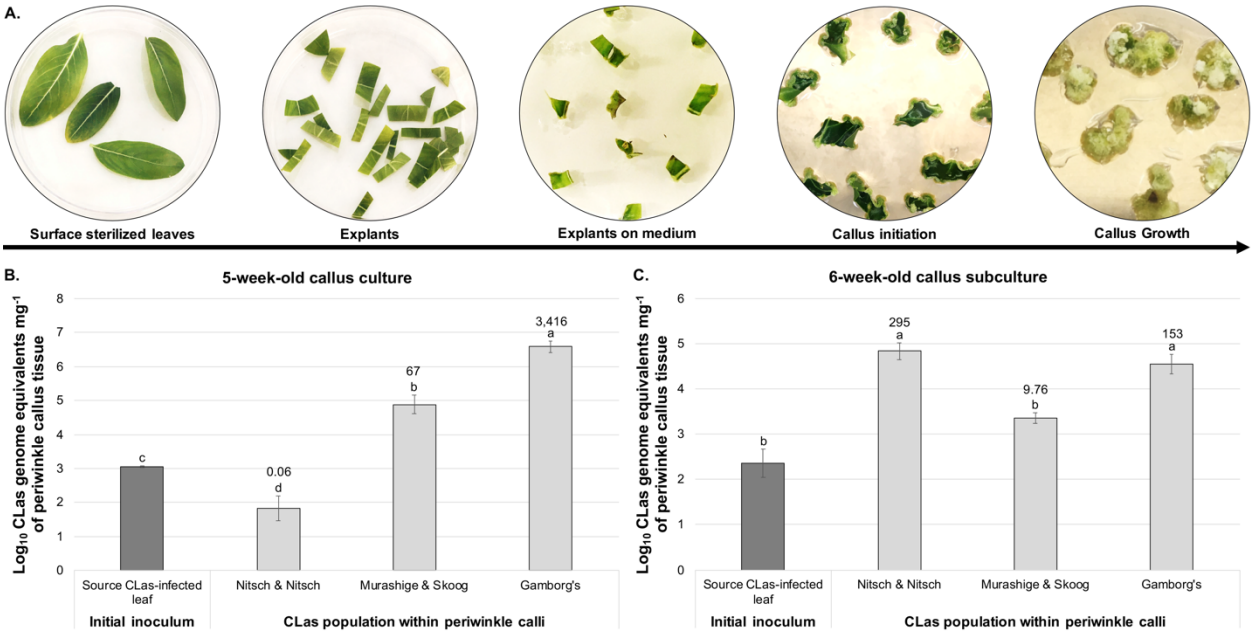

Fig. 3-6. Growth of CLas within periwinkle callus culture. CLas-infected periwinkle leaves were used as explants to establish callus cultures using different culture media (Nitsch & Nitsch, Murashige & Skoog and Gamborg's) amended with Gamborg's B5 vitamins, IAA, BAP, sucrose and phytagel as solidifying agent and assess CLas growth ex vivo by qPCR. **A.** Pictures representing steps involved in callus formation and propagation using CLas-infected periwinkle leaves as explant source. **B.** Total CLas population within 5-week-old periwinkle calli cultured in the different analyzed media. **C.** Total CLas population within 6-week-old subcultured periwinkle calli grown in the different analyzed media. Data represent means and standard errors. Numbers above light gray columns indicate growth ratio of CLas. Different letters in each column indicate significant difference of CLas population as analyzed by one-way ANOVA followed by Tukey's HSD multiple comparisons of means ($P \leq 0.05$; n = 3 to 5 technical replicates). A representative result from two independent experiments is shown here.

Presence of CLas within periwinkle calli was also analyzed by immune tissue printing (**Fig. 3-7**), which confirmed its detection within infected calli (**Fig. 3-7A**) and absence in healthy calli (**Fig. 3-7B**).

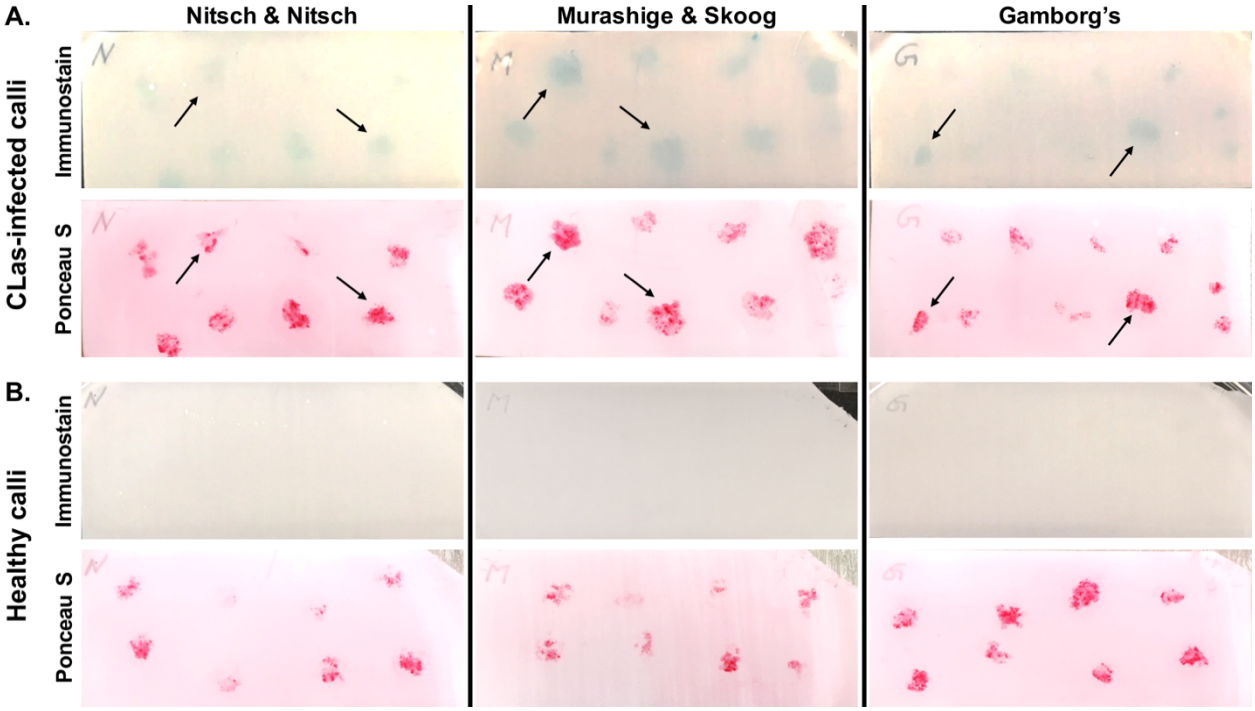

Fig. 3-7. Detection of CLas within periwinkle calli by immune tissue printing. CLas-infected periwinkle calli, as well as healthy calli cultured in the different analyzed media were imprinted onto PVDF membranes for CLas immunodetection using anti-OmpA primary antibody. **A.** Immune tissue prints of CLas-infected periwinkle calli cultured in Nitsch & Nitsch, Murashige & Skoog and Gamborg's media. Arrows indicate detection of CLas by immunostain with their correspondent total proteins visualized by Ponceau S staining. **B.** Immune tissue prints of healthy periwinkle calli cultured in Nitsch & Nitsch, Murashige & Skoog and Gamborg's media. In both **A** and **B**, the immunostain as well as the staining of total proteins by Ponceau S are shown. Blue-purple color development on immune tissue prints indicates presence of CLas within calli.

Discussion

Strategies to culture bacteria depend on the unique characteristics of each species (Overmann et al. 2017). This is even more relevant when considering intracellular fastidious bacteria. Approaches to grow such organisms in axenic conditions may include mimicking their habitats and determining specific growth conditions by analyzing required nutrients, temperature, oxygen levels, period of incubation, use of reducing agents, need for signaling molecules and coculture with one or more bacterial species that may provide metabolic goods to the community (Lagier et al. 2015; Overmann et al. 2017). CLas is an obligate intracellular pathogen of citrus

plants with a reduced genome, lacking several enzymes and biosynthetic pathways (Duan et al. 2009; Merfa et al. 2019; Wang and Trivedi 2013). Thus, it likely depends on nutrients found in phloem sieve tubes, ACP cells and hemolymph, as well as the coinhabiting microbial community to support its metabolic and physiological needs to grow (Killiny et al. 2017).

CLas has previously been obtained from citrus seeds and established in transient cultures using commercially available natural grapefruit juice as culture medium (Parker et al. 2014). This was our first step in producing a host plant-based culture medium to grow CLas. A similar approach has also been performed by Sechler and collaborators (2009), which obtained limited success by using citrus vein extract as carbon source in a medium formulation developed for CLas (for a recent comprehensive review of CLas culturing attempts, refer to Merfa et al. 2019). In the current study, we aimed at analyzing different compounds, molecules and growth conditions to further understand the growth needs of CLas. In our system, CLas survived a series of subcultures in GJ or mGJ, demonstrating that cell multiplication is due to acquisition of nutrients from these media and not because of nutrients remaining from the inoculum source, as suggested elsewhere (Ha et al. 2019). However, growth was mostly dependent on the culture density. Significant growth ratios were only obtained when the initial inoculum had low number of cells ($\approx 10^3$ to 10^4 genome equivalents/ml), while its increase (above $\approx 10^5$ genome equivalents/ml) led to subsequent decrease in the CLas population in subsequent subcultures, which sometimes resumed growth once again with follow-up subcultures. Even though CLas ultimately lost viability with the performance of subcultures, this intriguing oscillating growth behavior was observed in the vast majority of assays. Curiously, it has been demonstrated that bacterial insect endosymbionts may restrict their growth and adapt their replication to coordinate

with the development of their hosts (Baumann and Baumann 1994; Gil et al. 2004). However, since CLas is grown in the absence of host cells in our system, we hypothesize that this oscillating behavior, which was also previously observed by Parker and collaborators (2014), can be due to either (or a combination of) i. fast consumption of essential nutrients that are present in low quantities; ii. production of toxic byproducts; or iii. regulation by cell density-dependent mechanisms, such as quorum sensing or other signaling pathway; all of which are briefly discussed below.

Determining which nutrient(s) are potentially limiting and impairing CLas growth in GJ is challenging. However, in an effort to overcome this limitation, GJ and mGJ were amended with different compounds that are predicted to be required by CLas and incubated in different conditions. This approach is akin to the method used to culture the obligate intracellular bacterial human pathogen *Coxiella burnetii*, the causative agent of Q (Query) fever (Omsland et al. 2009). For *C. burnetii*, a systematic evaluation of its metabolic requirements was performed using expression microarrays, genomic reconstruction and metabolite typing, which led to the development of an optimal culture medium and defined the microaerophilic requirement of this bacterium (Omsland et al. 2009). These analyses were only possible due to the previous development of a culture medium that allowed *C. burnetii* to remain metabolically active in axenic conditions for at least 24 hours (Omsland et al. 2008). In our study, on the other hand, the choice of compounds and conditions was based on studies performed by other research groups (Cruz-Munoz et al. 2019; Fagen et al. 2014a; Jain et al. 2019; Jain et al. 2017a; Killiny 2016; Parker et al. 2014; Sena-Vélez et al. 2019; Vahling et al. 2010), since a culturing condition that allows axenic metabolic activity of CLas is yet to be developed. However, even with this

limitation, a large variety of compounds and conditions were screened and their contribution to CLas growth in GJ was established in the current study. Nonetheless, the recent development of a method to grow CLas ex vivo within hairy roots has allowed to validate prediction of nutrient requirements obtained from metabolic models and analyze changes in growth phenotypes of this bacterium (Zuñiga et al. 2020), constituting a powerful tool to advance our efforts to grow CLas in pure culture.

In relation to toxic byproducts, there are few candidates predicted to be harmful to CLas. Because of its deficient glyoxalase system, it is believed that CLas is not able to detoxify methylglyoxal (MG), a cytotoxic byproduct of glycolysis that causes carbonyl stress (Jain et al. 2017a). In addition to its defective glycolysis pathway, CLas possibly overcome these hurdles by directly importing ATP from its host cells through a functional ATP/ADP translocase (Jain et al. 2017a; Vahling et al. 2010). This structure is present in plastids and few other obligatory intracellular prokaryotes related to Chlamydiae and Rickettsiae, and catalyzes import of ATP from the host in exchange of bacterial ADP (Schmitz-Esser et al. 2004). Thus, to fulfill the energetic needs of CLas, as well as circumvent a possible MG toxicity originated from an insufficient ATP production, since CLas encodes ATP synthase nevertheless (Duan et al. 2009), ATP was added to culture medium. However, no improvement in CLas growth was observed, which may possibly be due to ATP being highly unstable in solution and readily degraded to ADP.

Another possible toxic effect of growing CLas is the expression of phage lytic cycle genes that may be activated when attempting to culture this bacterium axenically, due to lack of

a repressor (Fleites et al. 2014; Jain et al. 2017b). Hence, GJ was amended with a protein encoded by *Wolbachia* strain wDi (a bacterial endosymbiont of *D. citri*) termed *Wolbachia* repressor protein (Wrp), which has been demonstrated to repress expression of a phage lytic cycle gene from CLas (Jain et al. 2017b). Yet, no increase in CLas growth was observed. It is difficult to determine if this result was due to a lack of protein activity in our culture medium, although Wrp has been successfully used in studies with the surrogate Lcr (Jain et al. 2017b), deficiency of other essential nutrients, or a combination of both. An alternative to bypass this hindrance is to use a prophage-free CLas strain in culturing studies, as recently performed by Fujiwara and collaborators (2018). However, these strains seem to be the minority and are not readily available everywhere.

Finally, there has been some reports on cell density-dependent signaling mechanisms that may partially reduce specific bacterial populations. Allolysis is one of these mechanisms and refers to the phenomenon of cell lysis of a subpopulation of bacteria, which is induced by other cells of the same species or of closely related species of the same phylotype (Prozorov and Danilenko 2011). This quorum-sensing regulated mechanism, sometimes termed cannibalism, is associated with the onset of biofilm formation and natural competence in some bacterial species, as well as temporarily helping overcome nutrient limitation (López et al. 2009; Prozorov and Danilenko 2011). Another quorum-sensing dependent mechanism is the production of extracellular DNA, which may involve autolysis of a subpopulation of cells and other non-lethal mechanisms (Ibáñez de Aldecoa et al. 2017). In both cases, CLas could benefit on the availability of nutrients and DNA from lysed cells to use in its own metabolism, and that may even help explain its oscillating growth behavior previously observed by our group (Parker et al.

2014), which at the time was referred to as cryptic growth. Although we cannot ascertain if the obtained cell density-dependent growth behavior of CLas in this study is due to allolysis or other mechanism, the observed behavior may possibly be signaling-dependent. Unfortunately, attempts to "wash" our cultures with fresh medium to remove any signaling molecule that could impair CLas growth, and thus allow cells to grow to higher densities, failed. Nevertheless, CLas encodes a quorum sensing LuxR transcriptional activator protein in its genome (Duan et al. 2009; Fujiwara et al. 2018), which is activated in a density-dependent manner upon interaction with a cognate N-acyl homoserine lactone (AHL) (Tsai and Winans 2010). However, since CLas lacks a *luxI* gene that encodes an AHL synthase, the mechanism behind the coordination of the gene expression of CLas through LuxR is still unknown (Duan et al. 2009; Fujiwara et al. 2018; Yan et al. 2013).

Other approaches to keep cell culture density low and thus promote growth involved incubating CLas in flow conditions and subculturing samples at 3-day intervals. Both had limited success, because although bacterial growth was rapid, with significant growth ratios as fast as 3 dpi, cell viability was also quickly lost. A similar result was observed in an ex vivo system designed to grow CLas within citrus leaf discs, in which bacterial multiplication was observed 3 days after incubating infected leaf discs in test conditions (Attaran et al. 2020). The CLas population in that study was not evaluated for longer periods, but this result, together with ours, demonstrate that CLas may present a rapid increase in its in vitro population when incubated in optimized conditions.

Attempts to grow CLas in solid GJ plates were unsuccessful. It has been demonstrated that autoclaving agar together with phosphate may be harmful to microbes by producing reactive oxygen species (Tanaka et al. 2014). However, our solid GJ medium preparation used Gelrite instead of agar, which is not known to have any toxic effect and is solely autoclaved in deionized water before mixing with GJ. Thus, we hypothesize that availability of some compounds and/or leakiness of metabolic goods produced by cocultured bacteria, which may help survival of organisms with loss of function (Morris 2015), is likely compromised in solid medium. This may possibly be due to microbial interactions being restricted in the medium surface and suggests that all, or at least most physiological and nutrient requirements must be fulfilled for fastidious bacteria to grow in solid plates. Nonetheless, a recent report indicates that CLas was able to form microcolonies with associated microbiota when grown in solid plates of other medium formulation (Fujiwara et al. 2018). Curiously, our group has grown the bacterial plant pathogen *Xylella fastidiosa* in PD3 broth amended with grapevine sap (1:1) (Kandel et al. 2016). However, as similarly observed for CLas in this study, agar plates of this same medium formulation do not support growth of *X. fastidiosa* (*unpublished data*).

To take advantage of that possible leakiness of metabolic goods, which may include even ATP (Mempin et al. 2013), we tried to establish a coculture protocol that allow CLas to grow with other specific bacteria and share metabolic compounds but remain spatially separated by using plate inserts. Although the system we designed did not improve CLas culturability, the use of cocultures is a valuable method to isolate and grow bacteria deemed recalcitrant to axenic culturing (Stewart 2012). Many coculture methods have been used to isolate various fastidious and previous unculturable bacteria from distinct habitats (Ding et al. 2017b; Tanaka and Benno

2015; Vartoukian et al. 2016). For CLas specifically, different studies have established the importance of mutualistic relationships with coinhabiting bacteria for its survival and even determined which microbial taxa may be beneficial or harmful to its growth (Davis et al. 2008; Fujiwara et al. 2018; Ha et al. 2019; Molki et al. 2020; Parker et al. 2014). It is important to note that in our cultures growth of other bacteria was not visible in most assays. However, this phenomenon cannot be ruled out since it has a possible substantial role in aiding CLas growth.

Finally, we developed an ex vivo system to grow CLas within periwinkle calli. As mentioned above, approaches to grow CLas ex vivo within infected tissues of plant hosts are valuable tools that allowed the analyses of CLas growth in different conditions and validation of metabolic models (Attaran et al. 2020; Zuñiga et al. 2020). In our assays, three different culture media were assessed for periwinkle callus formation and CLas growth. All three media possess ammonium and phosphate in their composition, which have been demonstrated to be essential molecules in the *Liberibacter*-plant host interface by using the surrogate bacterium Lcr (Cruz-Munoz et al. 2019). However, Gamborg's medium was the most suitable for both callus formation and CLas growth overall because samples inoculated into this medium consistently presented growth of this bacterium. It has been shown that a high concentration of ammonium may induce oxidative stress, ionic imbalances and pH disturbances across cell membranes (Cruz-Munoz et al. 2019; Liu and von Wirén 2017), and that the alkalinization of the medium is harmful for the surrogate Lcr (Sena-Vélez et al. 2019). Thus, Gamborg's medium possibly performed better than the other tested media due to its low concentration of ammonium (in comparison to Murashige & Skoog medium). This shows that Gamborg's medium has a great potential to be explored in ex vivo assays to assess growth requirements of CLas and plant-

pathogen interactions and may constitute an important alternative tool to study this bacterium until axenic cultures are obtained.

In summary, this study has extended our knowledge on the suitability of using commercial grapefruit juice as a culture medium to grow CLas, as well as determined the contribution of a wide range of compounds and conditions to CLas growth. Nevertheless, sustained exponential growth in vitro, or development of colonies in solid media was not achieved with any of the conditions tested here. In addition, a highly conserved oscillating behavior of CLas growth was established, which is likely dependent on cell density levels. Many compounds and conditions analyzed here did not improve CLas growth. However, they still have the potential to enhance CLas culturability if an optimal condition is achieved. We hope that this information is considered when designing culture media for CLas, as well as establishing optimal incubation conditions for this bacterium.

Acknowledgments

We would like to thank Dr. Dean W. Gabriel and Dr. Mukesh Jain (Department of Plant Pathology, University of Florida, Gainesville, FL, USA) for providing CLas-infected citrus fruits and the *Wolbachia* repressor protein, as well as helpful suggestions; Dr. Amit Levy and Dr. Nabil Killiny (Citrus Research and Education Center, University of Florida, Lake Alfred, FL, USA) for providing CLas-infected psyllids; and Dr. Yongping Duan (USDA, Fort Pierce, FL, USA) for providing CLas-infected periwinkle plants. We thank Dr. Michael J. Davis (Citrus Research and Education Center, University of Florida, Lake Alfred, FL, USA) for providing training to dissect ACP guts. We thank Dr. Laura M. Gomez (Auburn University, Auburn, AL,

USA) for helping with periwinkle grafting. We thank Dr. Paul Cobine (Auburn University, Auburn, AL, USA), Dr. John Beckmann (Auburn University, Auburn, AL, USA) and Dr. Gwyn A. Beattie (Iowa State University, Ames, IA, USA) for helpful suggestions. We thank Dr. Adriana-Avila Flores (Auburn University, Auburn, AL, USA) for providing cell-free spent media used to culture SF9 insect cell line, and Dr. Kathleen Martin (Auburn University, Auburn, AL, USA) for providing SF9 insect cell line and SF-900 III SFM culture medium. Agriculture and Food Research Initiative competitive grant no. 2016-70016-24844 from the USDA National Institute of Food and Agriculture, Citrus Disease Research and Extension. Alabama Agricultural Experiment Station (AAES) Hatch Program (L.D.).

References

Achor, D., Welker, S., Ben-Mahmoud, S., Wang, C., Folimonova, S. Y., Dutt, M., Gowda, S., and Levy, A. 2020. Dynamics of *Candidatus* Liberibacter asiaticus movement and sieve-pore plugging in citrus sink cells. Plant Physiol 182:882-891.

Attaran, E., Berim, A., Killiny, N., Beyenal, H., Gang, D. R., and Omsland, A. 2020. Controlled replication of '*Candidatus* Liberibacter asiaticus' DNA in citrus leaf discs. Microb Biotechnol 13:747-759.

Austin, B. 2017. The value of cultures to modern microbiology. Antonie Van Leeuwenhoek 110:1247-1256.

Baumann, L., and Baumann, P. 1994. Growth kinetics of the endosymbiont *Buchnera aphidicola* in the aphid *Schizaphis graminum*. Appl Environ Microbiol 60:3340-3343.

Bové, J. 2014a. Heat-tolerant Asian HLB meets heat-sensitive African HLB in the Arabian Peninsula! Why? Journal of Citrus Pathology 1:1-78.

Bové, J. M. 2006. Huanglongbing: A destructive, newly-emerging, century-old disease of citrus. Journal of Plant Pathology 88:7-37.

Bové, J. M. 2014b. Huanglongbing or yellow shoot, a disease of Gondwanan origin: Will it destroy citrus worldwide? Phytoparasitica 42:579-583.

Braswell, W. E., Park, J. W., Stansly, P. A., Kostyk, B. C., Louzada, E. S., da Graça, J. V., and Kunta, M. 2020. Root samples provide early and improved detection of *Candidatus* Liberibacter asiaticus in *Citrus*. Sci Rep 10:16982.

Cruz-Munoz, M., Munoz-Beristain, A., Petrone, J. R., Robinson, M. A., and Triplett, E. W. 2019. Growth parameters of *Liberibacter crescens* suggest ammonium and phosphate as essential molecules in the *Liberibacter*-plant host interface. BMC Microbiol 19:222.

Cruz-Munoz, M., Petrone, J. R., Cohn, A. R., Munoz-Beristain, A., Killiny, N., Drew, J. C., and Triplett, E. W. 2018. Development of chemically defined media reveals citrate as preferred carbon source for *Liberibacter* growth. Front Microbiol 9:668.

Davis, M. J., Mondal, S. N., Chen, H., Rogers, M. E., and Brlansky, R. H. 2008. Co-cultivation of '*Candidatus* Liberibacter asiaticus' with Actinobacteria from citrus with Huanglongbing. Plant Dis 92:1547-1550.

Ding, F., Paul, C., Brlansky, R., and Hartung, J. S. 2017a. Immune tissue print and immune capture-PCR for diagnosis and detection of *Candidatus* Liberibacter asiaticus. Sci Rep 7:46467.

Ding, F., Duan, Y., Paul, C., Brlansky, R. H., and Hartung, J. S. 2015. Localization and distribution of '*Candidatus* Liberibacter asiaticus' in citrus and periwinkle by direct tissue blot immuno assay with an anti-OmpA polyclonal antibody. PLoS One 10:e0123939.

Ding, Z. W., Lu, Y. Z., Fu, L., Ding, J., and Zeng, R. J. 2017b. Simultaneous enrichment of denitrifying anaerobic methane-oxidizing microorganisms and anammox bacteria in a hollow-fiber membrane biofilm reactor. Appl Microbiol Biotechnol 101:437-446.

Doyle, J., and Doyle, J. L. 1987. Genomic plant DNA preparation from fresh tissue—CTAB method. Phytochem. Bull. 19:11-15.

Duan, Y., Zhou, L., Hall, D. G., Li, W., Doddapaneni, H., Lin, H., Liu, L., Vahling, C. M., Gabriel, D. W., Williams, K. P., Dickerman, A., Sun, Y., and Gottwald, T. 2009. Complete genome sequence of citrus Huanglongbing bacterium, '*Candidatus* Liberibacter asiaticus' obtained through metagenomics. Mol Plant Microbe Interact 22:1011-1020.

Fagen, J. R., Leonard, M. T., McCullough, C. M., Edirisinghe, J. N., Henry, C. S., Davis, M. J., and Triplett, E. W. 2014a. Comparative genomics of cultured and uncultured strains suggests genes essential for free-living growth of *Liberibacter*. PLoS One 9:e84469.

Fagen, J. R., Leonard, M. T., Coyle, J. F., McCullough, C. M., Davis-Richardson, A. G., Davis, M. J., and Triplett, E. W. 2014b. *Liberibacter crescens* gen. nov., sp. nov., the first cultured member of the genus *Liberibacter*. Int J Syst Evol Microbiol 64:2461-2466.

Fleites, L. A., Jain, M., Zhang, S., and Gabriel, D. W. 2014. "*Candidatus* Liberibacter asiaticus" prophage late genes may limit host range and culturability. Appl Environ Microbiol 80:6023-6030.

Fujiwara, K., Iwanami, T., and Fujikawa, T. 2018. Alterations of *Candidatus* Liberibacter asiaticus-associated microbiota decrease survival of *Ca.* L. asiaticus in in vitro assays. Front Microbiol 9:3089.

Gamborg, O. L., Miller, R. A., and Ojima, K. 1968. Nutrient requirements of suspension cultures of soybean root cells. Exp. Cell Res. 50:151-158.

Gil, R., Latorre, A., and Moya, A. 2004. Bacterial endosymbionts of insects: insights from comparative genomics. Environ Microbiol 6:1109-1122.

Gottwald, T., Poole, G., McCollum, T., Hall, D., Hartung, J., Bai, J., Luo, W., Posny, D., Duan, Y. P., Taylor, E., da Graça, J., Polek, M., Louws, F., and Schneider, W. 2020. Canine olfactory detection of a vectored phytobacterial pathogen, Liberibacter asiaticus, and integration with disease control. Proc Natl Acad Sci U S A 117:3492-3501.

Gottwald, T. R. 2010. Current epidemiological understanding of citrus Huanglongbing. Annu Rev Phytopathol 48:119-139.

Ha, P. T., He, R., Killiny, N., Brown, J. K., Omsland, A., Gang, D. R., and Beyenal, H. 2019. Host-free biofilm culture of "*Candidatus* Liberibacter asiaticus," the bacterium associated with Huanglongbing. Biofilm 1:100005.

Hartung, J. S., Shao, J., and Kuykendall, L. D. 2011. Comparison of the '*Ca.* Liberibacter asiaticus' genome adapted for an intracellular lifestyle with other members of the Rhizobiales. PLoS One 6:e23289.

Hijaz, F., and Killiny, N. 2014. Collection and chemical composition of phloem sap from *Citrus sinensis* L. Osbeck (sweet orange). PLoS One 9:e101830.

Hilf, M. E. 2011. Colonization of citrus seed coats by '*Candidatus* Liberibacter asiaticus': implications for seed transmission of the bacterium. Phytopathology 101:1242-1250.

Huang, C.-Y., Araujo, K., Sanchez, J. N., Kund, G., Trumble, J., Roper, C., Godfrey, K. E., and Jin, H. 2021. A stable antimicrobial peptide with dual functions of treating and preventing citrus Huanglongbing. Proc Natl Acad Sci U S A 118:e2019628118.

Ibáñez de Aldecoa, A. L., Zafra, O., and González-Pastor, J. E. 2017. Mechanisms and regulation of extracellular DNA release and its biological roles in microbial communities. Front Microbiol 8:1390.

Ihaka, R., and Gentleman, R. 1996. R: A language for data analysis and graphics. J. Comput. Graph. Stat. 5:299-314.

Irigoyen, S., Ramasamy, M., Pant, S., Niraula, P., Bedre, R., Gurung, M., Rossi, D., Laughlin, C., Gorman, Z., Achor, D., Levy, A., Kolomiets, M. V., Sétamou, M., Badillo-Vargas, I. E., Avila, C. A., Irey, M. S., and Mandadi, K. K. 2020. Plant hairy roots enable high throughput identification of antimicrobials against *Candidatus* Liberibacter spp. Nat Commun 11:5802.

Jagoueix, S., Bové, J. M., and Garnier, M. 1994. The phloem-limited bacterium of greening disease of citrus is a member of the alpha subdivision of the Proteobacteria. Int. J. Syst. Bacteriol. 44:379-386.

Jain, M., Munoz-Bodnar, A., and Gabriel, D. W. 2017a. Concomitant loss of the glyoxalase system and glycolysis makes the uncultured pathogen "*Candidatus* Liberibacter asiaticus" an energy scavenger. Appl Environ Microbiol 83:e01670-01617.

Jain, M., Fleites, L. A., and Gabriel, D. W. 2017b. A small *Wolbachia* protein directly represses phage lytic cycle genes in "*Candidatus* Liberibacter asiaticus" within psyllids. mSphere 2:e00171-00117.

Jain, M., Cai, L., Fleites, L. A., Munoz-Bodnar, A., Davis, M. J., and Gabriel, D. W. 2019. *Liberibacter crescens* is a cultured surrogate for functional genomics of uncultured pathogenic '*Candidatus* Liberibacter' spp. and is naturally competent for transformation. Phytopathology 109:1811-1819.

Kandel, P. P., Lopez, S. M., Almeida, R. P. P., and De La Fuente, L. 2016. Natural competence of *Xylella fastidiosa* occurs at a high frequency inside microfluidic chambers mimicking the bacterium's natural habitats. Appl Environ Microbiol 82:5269-5277.

Kandel, P. P., Almeida, R. P. P., Cobine, P. A., and De La Fuente, L. 2017. Natural competence rates are variable among *Xylella fastidiosa* strains and homologous recombination occurs in vitro between subspecies *fastidiosa* and *multiplex*. Mol Plant Microbe Interact 30:589-600.

Killiny, N. 2016. Generous hosts: What makes Madagascar periwinkle (*Catharanthus roseus*) the perfect experimental host plant for fastidious bacteria? Plant Physiol Biochem 109:28-35.

Killiny, N. 2021. Made for each other: Vector-pathogen interfaces in the Huanglongbing pathosystem. Phytopathology:1-68.

Killiny, N., Hijaz, F., El-Shesheny, I., Alfaress, S., Jones, S. E., and Rogers, M. E. 2017. Metabolomic analyses of the haemolymph of the Asian citrus psyllid *Diaphorina citri*, the vector of huanglongbing. Physiological Entomology 42:134-145.

Lagier, J. C., Edouard, S., Pagnier, I., Mediannikov, O., Drancourt, M., and Raoult, D. 2015. Current and past strategies for bacterial culture in clinical microbiology. Clin Microbiol Rev 28:208-236.

Li, J., Kolbasov, V. G., Lee, D., Pang, Z., Huang, Y., Collins, N., and Wang, N. 2020. Residue dynamics of streptomycin in citrus delivered by foliar spray and trunk injection and effect on '*Candidatus* Liberibacter asiaticus' titer. Phytopathology:1-41.

Li, W., Hartung, J. S., and Levy, L. 2006. Quantitative real-time PCR for detection and identification of *Candidatus Liberibacter* species associated with citrus huanglongbing. J Microbiol Methods 66:104-115.

Li, Y., Xu, M. R., Dai, L. P., and Xeng, X. R. 2018. Distribution pattern and titer of *Candidatus* Liberibacter asiaticus in periwinkle (*Catharanthus roseus*). Journal of Integrative Agriculture 17:2501-2508.

Liu, X., Zheng, Y., Wang-Pruski, G., Gan, Y., Zhang, B., Hu, Q., Du, Y., Zhao, J., and Liu, L. 2019. Transcriptome profiling of periwinkle infected with Huanglongbing ('*Candidatus* Liberibacter asiaticus'). European Journal of Plant Pathology 153:891-906.

Liu, Y., and von Wirén, N. 2017. Ammonium as a signal for physiological and morphological responses in plants. J Exp Bot 68:2581-2592.

Lopes, S. A., Frare, G. F., Bertolini, E., Cambra, M., Fernandes, N. G., Ayres, A. J., Marin, D. R., and Bové, J. M. 2009. Liberibacters associated with citrus Huanglongbing in Brazil: '*Candidatus* Liberibacter asiaticus' is heat tolerant, '*Ca.* L. americanus' is heat sensitive. Plant Dis 93:257-262.

López, D., Vlamakis, H., Losick, R., and Kolter, R. 2009. Cannibalism enhances biofilm development in *Bacillus subtilis*. Mol Microbiol 74:609-618.

Marutani-Hert, M., Hunter, W. B., and Hall, D. G. 2009. Establishment of Asian citrus psyllid (*Diaphorina citri*) primary cultures. In Vitro Cell Dev Biol Anim 45:317-320.

Mempin, R., Tran, H., Chen, C., Gong, H., Ho, K. K., and Lu, S. 2013. Release of extracellular ATP by bacteria during growth. BMC Microbiol 13:301.

Merfa, M. V., Pérez-López, E., Naranjo, E., Jain, M., Gabriel, D. W., and De La Fuente, L. 2019. Progress and obstacles in culturing '*Candidatus* Liberibacter asiaticus', the bacterium associated with Huanglongbing. Phytopathology 109:1092-1101.

Molki, B., Call, D. R., Ha, P. T., Omsland, A., Gang, D. R., Lindemann, S. R., Killiny, N., and Beyenal, H. 2020. Growth of '*Candidatus* Liberibacter asiaticus' in a host-free microbial culture is associated with microbial community composition. Enzyme Microb Technol 142:109691.

Morris, J. J. 2015. Black Queen evolution: the role of leakiness in structuring microbial communities. Trends Genet 31:475-482.

Murashige, T., and Skoog, F. 1962. A revised medium for rapid growth and bio assays with tobacco tissue cultures. Physiol. Plant. 15:473-497.

Naranjo, E., Merfa, M. V., Santra, S., Ozcan, A., Johnson, E., Cobine, P. A., and De La Fuente, L. 2020. Zinkicide is a ZnO-based nanoformulation with bactericidal activity against *Liberibacter crescens* in batch cultures and in microfluidic chambers simulating plant vascular systems. Appl Environ Microbiol 86:e00788-00720.

Nelson, W. R., Sengoda, V. G., Alfaro-Fernandez, A. O., Font, M. I., Crosslin, J. M., and Munyaneza, J. E. 2012. A new haplotype of "*Candidatus* Liberibacter solanacearum" identified in the Mediterranean region. European Journal of Plant Pathology 135:633-639.

Nitsch, J. P., and Nitsch, C. 1969. Haploid plants from pollen grains. Science 163:85-87.

Omsland, A., Cockrell, D. C., Fischer, E. R., and Heinzen, R. A. 2008. Sustained axenic metabolic activity by the obligate intracellular bacterium *Coxiella burnetii*. J Bacteriol 190:3203-3212.

Omsland, A., Cockrell, D. C., Howe, D., Fischer, E. R., Virtaneva, K., Sturdevant, D. E., Porcella, S. F., and Heinzen, R. A. 2009. Host cell-free growth of the Q fever bacterium *Coxiella burnetii*. Proc Natl Acad Sci U S A 106:4430-4434.

Overmann, J., Abt, B., and Sikorski, J. 2017. Present and future of culturing bacteria. Annu Rev Microbiol 71:711-730.

Pandey, S. S., and Wang, N. 2019. Targeted early detection of citrus Huanglongbing causal agent '*Candidatus* Liberibacter asiaticus' before symptom expression. Phytopathology 109:952-959.

Parker, J. K., Wisotsky, S. R., Johnson, E. G., Hijaz, F. M., Killiny, N., Hilf, M. E., and De La Fuente, L. 2014. Viability of '*Candidatus* Liberibacter asiaticus' prolonged by addition of citrus juice to culture medium. Phytopathology 104:15-26.

Pietrosiuk, A., Furmanowa, M., and Łata, B. 2007. *Catharanthus roseus*: micropropagation and in vitro techniques. Phytochemistry Reviews 6:459-473.

Prozorov, A. A., and Danilenko, V. N. 2011. Allolysis in bacteria. Microbiology 80:1-9.
Schmitz-Esser, S., Linka, N., Collingro, A., Beier, C. L., Neuhaus, H. E., Wagner, M., and Horn, M. 2004. ATP/ADP translocases: a common feature of obligate intracellular amoebal symbionts related to Chlamydiae and Rickettsiae. J Bacteriol 186:683-691.
Sechler, A., Schuenzel, E. L., Cooke, P., Donnua, S., Thaveechai, N., Postnikova, E., Stone, A. L., Schneider, W. L., Damsteegt, V. D., and Schaad, N. W. 2009. Cultivation of '*Candidatus* Liberibacter asiaticus', '*Ca.* L. africanus', and '*Ca.* L. americanus' associated with Huanglongbing. Phytopathology 99:480-486.
Sena-Vélez, M., Holland, S. D., Aggarwal, M., Cogan, N. G., Jain, M., Gabriel, D. W., and Jones, K. M. 2019. Growth dynamics and survival of *Liberibacter crescens* BT-1, an important model organism for the citrus Huanglongbing pathogen "*Candidatus* Liberibacter asiaticus". Appl Environ Microbiol 85:e01656-01619.
Singh, R. 2011. Fast in-vitro callus induction in *Catharanthus roseus* - A medicinally important plant used in cancer therapy. Research Journal of Pharmaceutical, Biological and Chemical Sciences 2:597-603.
Stewart, E. J. 2012. Growing unculturable bacteria. J Bacteriol 194:4151-4160.
Tanaka, T., Kawasaki, K., Daimon, S., Kitagawa, W., Yamamoto, K., Tamaki, H., Tanaka, M., Nakatsu, C. H., and Kamagata, Y. 2014. A hidden pitfall in the preparation of agar media undermines microorganism cultivability. Appl Environ Microbiol 80:7659-7666.
Tanaka, Y., and Benno, Y. 2015. Application of a single-colony coculture technique to the isolation of hitherto unculturable gut bacteria. Microbiol Immunol 59:63-70.
Thapa, N., Danyluk, M. D., Gerberich, K. M., Johnson, E. G., and Dewdney, M. M. 2021. Assessment of the effect of thermotherapy on '*Candidatu*s Liberibacter asiaticus' viability in woody tissue of citrus via graft-based assays and RNA assays. Phytopathology:1-11.
Thompson, S., Fletcher, J. D., Ziebell, H., Beard, S., Panda, P., Jorgensen, N., Fowler, S. V., Liefting, L. W., Berry, N., and Pitman, A. R. 2013. First report of '*Candidatus* Liberibacter europaeus' associated with psyllid infested Scotch broom. New Dis. Rep. 27:6.
Tsai, C. S., and Winans, S. C. 2010. LuxR-type quorum-sensing regulators that are detached from common scents. Mol Microbiol 77:1072-1082.
Vahling, C. M., Duan, Y., and Lin, H. 2010. Characterization of an ATP translocase identified in the destructive plant pathogen "*Candidatus* Liberibacter asiaticus". J Bacteriol 192:834-840.
Vartoukian, S. R., Adamowska, A., Lawlor, M., Moazzez, R., Dewhirst, F. E., and Wade, W. G. 2016. In vitro cultivation of 'unculturable' oral bacteria, facilitated by community culture and media supplementation with siderophores. PLoS One 11:e0146926.
Wang, N., and Trivedi, P. 2013. Citrus Huanglongbing: a newly relevant disease presents unprecedented challenges. Phytopathology 103:652-665.
Wheatley, M. S., Duan, Y.-P., and Yang, Y. 2021. Highly sensitive and rapid detection of citrus Huanglongbing pathogen (*Candidatus* Liberibacter asiaticus) using Cas12a-based methods. Phytopathology:1-27.
Yan, Q., Sreedharan, A., Wei, S., Wang, J., Pelz-Stelinski, K., Folimonova, S., and Wang, N. 2013. Global gene expression changes in *Candidatus* Liberibacter asiaticus during the transmission in distinct hosts between plant and insect. Mol Plant Pathol 14:391-404.
Yuan, X., Chen, C., Bassanezi, R. B., Wu, F., Feng, Z., Shi, D., Li, J., Du, Y., Zhong, L., Zhong, B., Lu, Z., Song, X., Hu, Y., Ouyang, Z., Liu, X., Xie, J., Rao, X., Wang, X., Wu, D. O.,

Guan, Z., and Wang, N. 2020. Region-wide comprehensive implementation of roguing infected trees, tree replacement, and insecticide applications successfully controls citrus HLB. Phytopathology:1-29.

Zengler, K., Toledo, G., Rappé, M., Elkins, J., Mathur, E. J., Short, J. M., and Keller, M. 2002. Cultivating the uncultured. Proc Natl Acad Sci U S A 99:15681-15686.

Zhang, M., Duan, Y., Zhou, L., Turechek, W. W., Stover, E., and Powell, C. A. 2010. Screening molecules for control of citrus Huanglongbing using an optimized regeneration system for '*Candidatus* Liberibacter asiaticus'-infected periwinkle (*Catharanthus roseus*) cuttings. Phytopathology 100:239-245.

Zhang, S., Flores-Cruz, Z., Zhou, L., Kang, B. H., Fleites, L. A., Gooch, M. D., Wulff, N. A., Davis, M. J., Duan, Y. P., and Gabriel, D. W. 2011. '*Ca.* Liberibacter asiaticus' carries an excision plasmid prophage and a chromosomally integrated prophage that becomes lytic in plant infections. Mol Plant Microbe Interact 24:458-468.

Zuñiga, C., Peacock, B., Liang, B., McCollum, G., Irigoyen, S. C., Tec-Campos, D., Marotz, C., Weng, N. C., Zepeda, A., Vidalakis, G., Mandadi, K. K., Borneman, J., and Zengler, K. 2020. Linking metabolic phenotypes to pathogenic traits among "*Candidatus* Liberibacter asiaticus" and its hosts. NPJ Syst Biol Appl 6:24.

Supplementary material for chapter 3

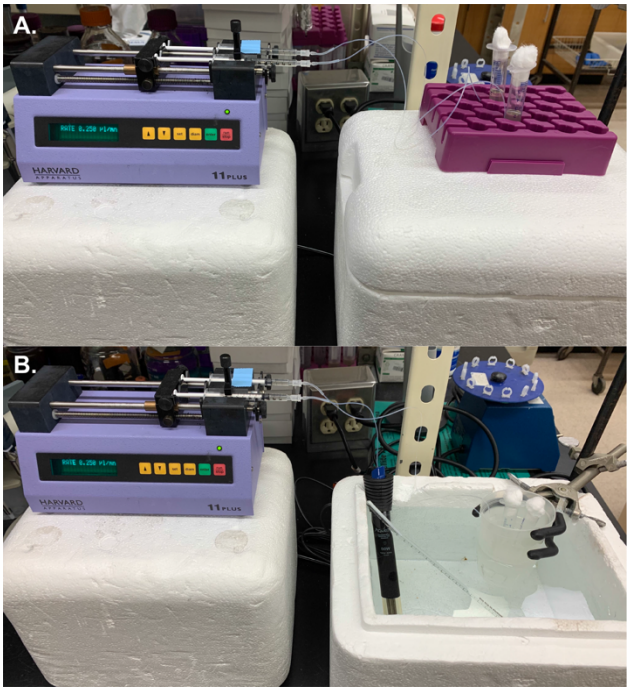

Fig. S3-1. System used to assess CLas growth under flow conditions. A. Broth culture medium was constantly pumped through tubing (flow rate = 0.25 µl/min), while CLas was deposited in a 5-ml syringe barrel, which is used as collection tube. Samples were collected at every 3 days to assess CLas population by qPCR. Cells were incubated for a total of 12 days at room temperature, while broth culture medium was replenished in 1-ml syringes as needed. **B.** When necessary, samples were incubated in temperature-controlled conditions by placing collection tubes inside a Styrofoam box filled with deionized water heated to 28 ºC using an aquarium heater.

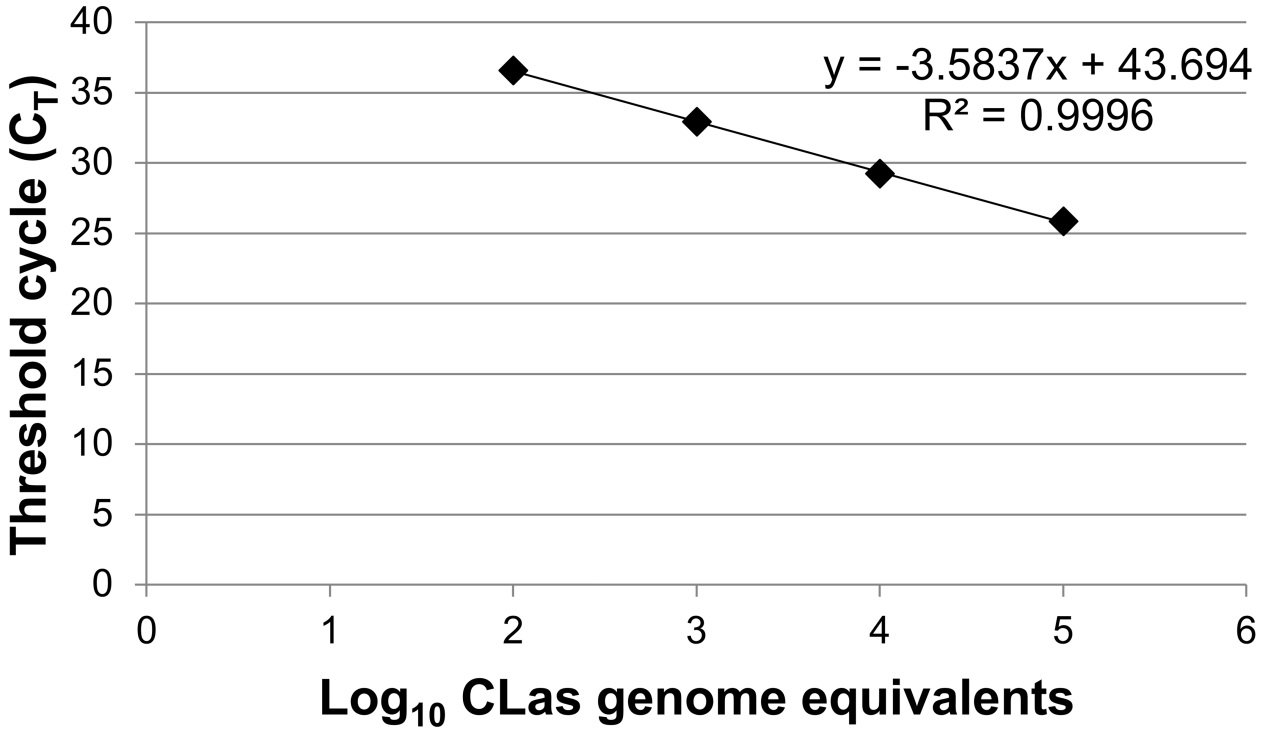

Fig. S3-2. qPCR standard curve used to quantify '*Ca.* Liberibacter asiaticus' in each sample as genome equivalents. The target DNA sequence ranged from 10^5 to 10^2 copies. In addition, the standard curve presented a 0.9013 amplification efficiency and 0.9996 correlation coefficient.

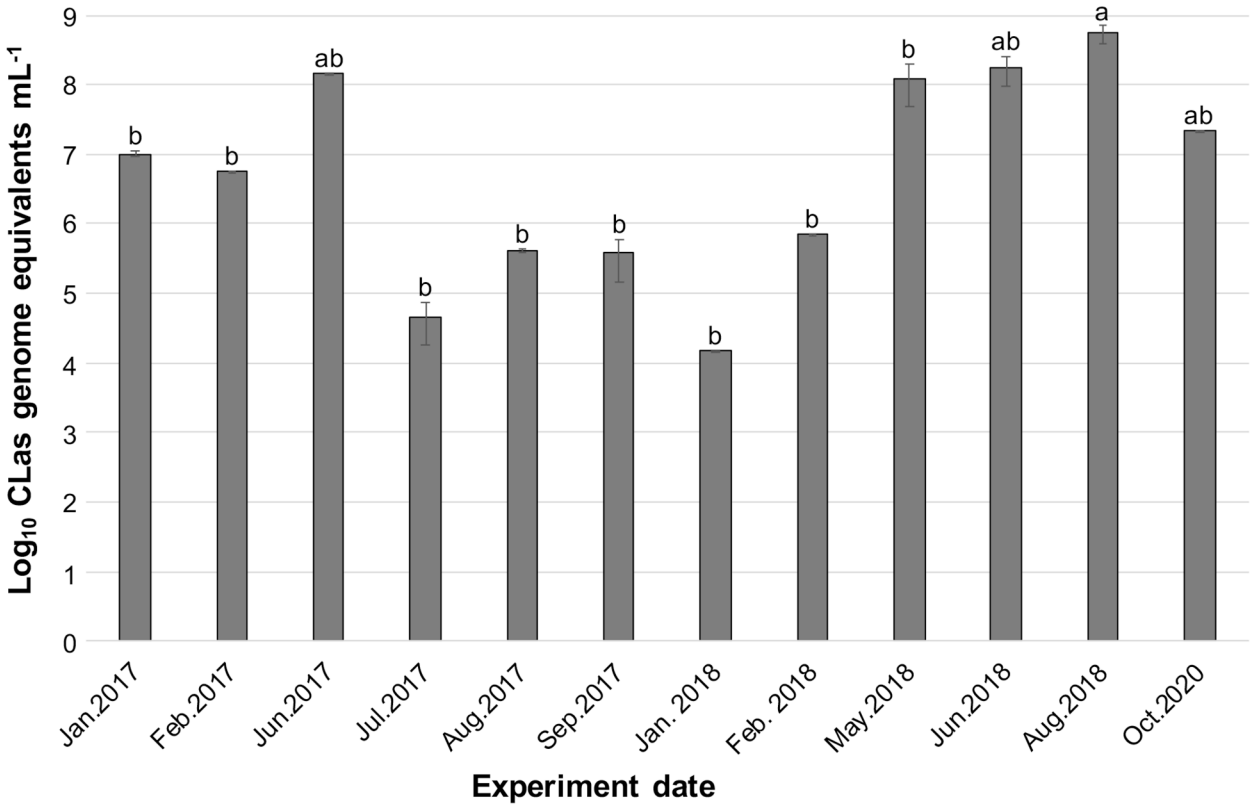

Fig. S3-3. CLas population in citrus seeds used as inoculum source throughout this study. Data represent means and standard errors. The CLas population in seeds used in each assay was standardized to genome equivalents/ml to facilitate comparisons among samples. Different letters above columns indicate significant difference of CLas population among samples as analyzed by one-way ANOVA followed by Tukey's HSD multiple comparisons of means ($P \leq 0.05$; n = 3 technical replicates in each sample). The apparent no significant difference among samples even when the CLas population seems to differ by more than 2-$\log_{10}$ fold is due to the variable number of CLas cells in seeds from different fruits analyzed in each date, leading to high standard deviations.

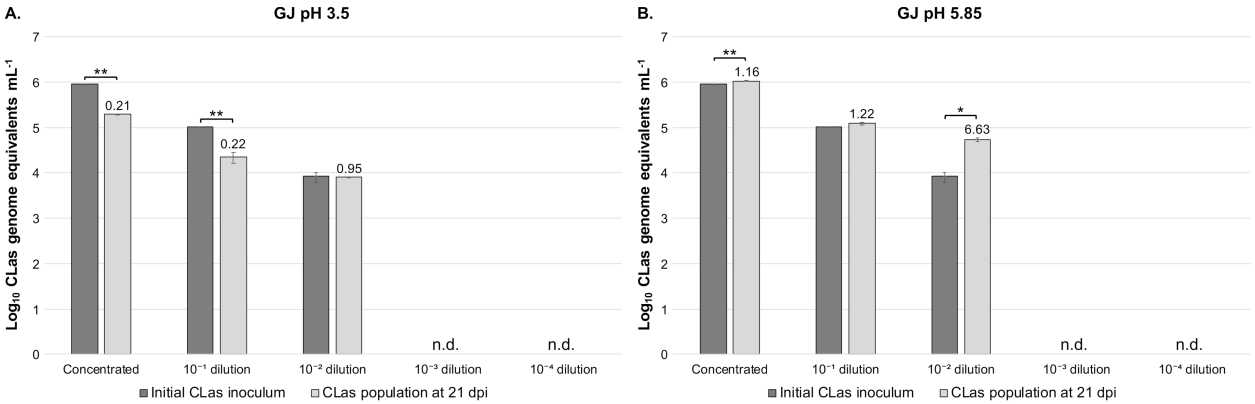

Fig. S3-4. Comparison of CLas growth in different pH of grapefruit juice. The pH of GJ, which is normally 3.5, was adjusted to 5.85 to mimic conditions of the phloem sap of plant hosts of CLas. Samples were inoculated into 24-well plates and incubated at 28 ºC for 21 days before assessing total population of CLas by qPCR. Adjusting the pH of GJ to 5.85 significantly contributed to CLas growth, since significant increases in genome equivalents were only observed in GJ pH 5.85. **A.** CLas growth in GJ pH 3.5. **B.** CLas growth in GJ pH 5.85. Data represent means and standard errors. Numbers above light gray columns indicate growth ratio of CLas. Statistical significance was determined using Student's *t*-test (* indicates $P \leq 0.05$ and ** indicates $P \leq 0.005$ in comparison to the initial inoculum; n = 3 technical replicates). "dpi" means days post inoculation. "n.d." indicates no detection signal of CLas by qPCR. A representative result of two independent experiments is shown here.

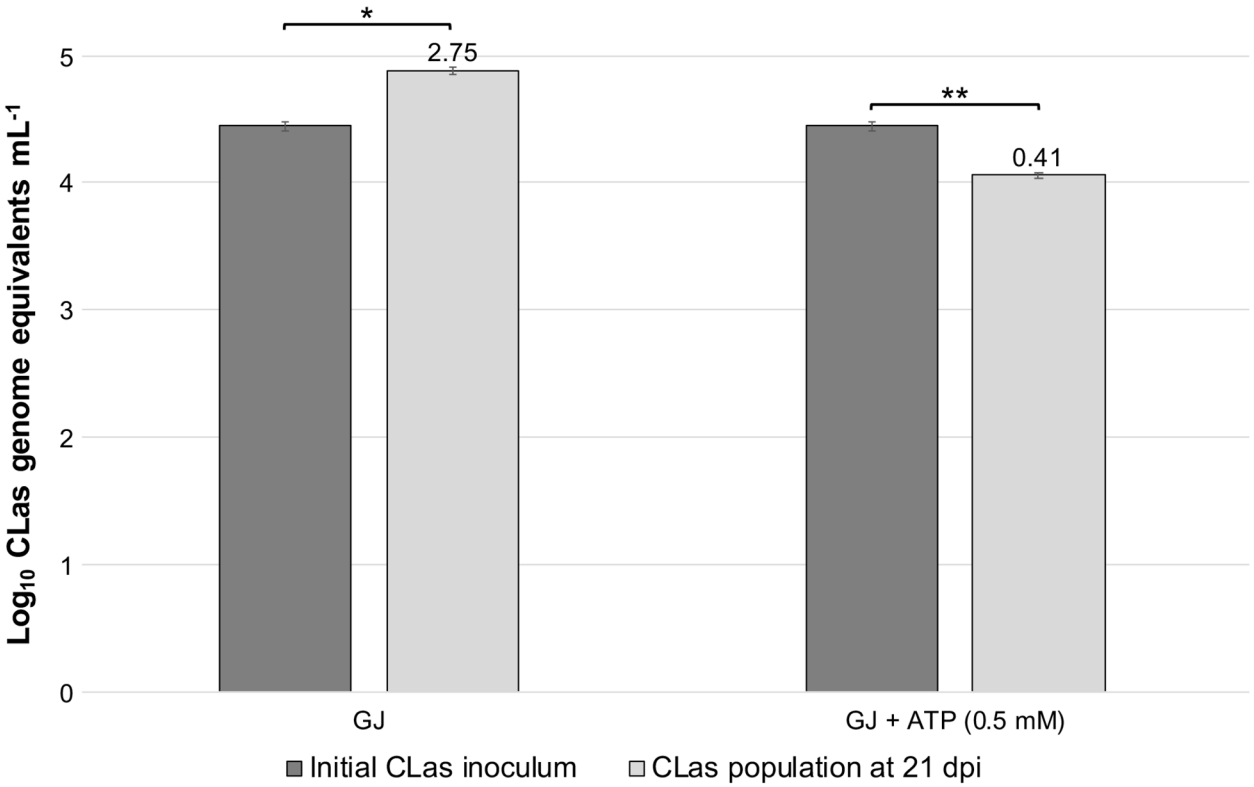

Fig. S3-5. Effect of adding ATP to GJ on CLas growth. ATP was added to GJ at a final concentration of 0.5 mM because CLas is likely an energy scavenger that obtains ATP from its host cells through an ATP/ADP translocase. Assays were conducted in 24-well plates with incubation at 28 ºC for 21 days. Total population of CLas was determined by qPCR. Addition of ATP to GJ did not contribute to CLas growth. A significant increase in CLas genome equivalents was only observed in nonamended GJ, while adding ATP to GJ significantly decreased the CLas population. Data represent means and standard errors. Numbers above light gray columns indicate growth ratio of CLas. Statistical significance was determined using Student's *t*-test (* indicates $P \leq 0.05$ and ** indicates $P \leq 0.005$ in comparison to the initial inoculum; n = 3 technical replicates). "dpi" means days post inoculation. A representative result of at least three independent experiments is shown here.

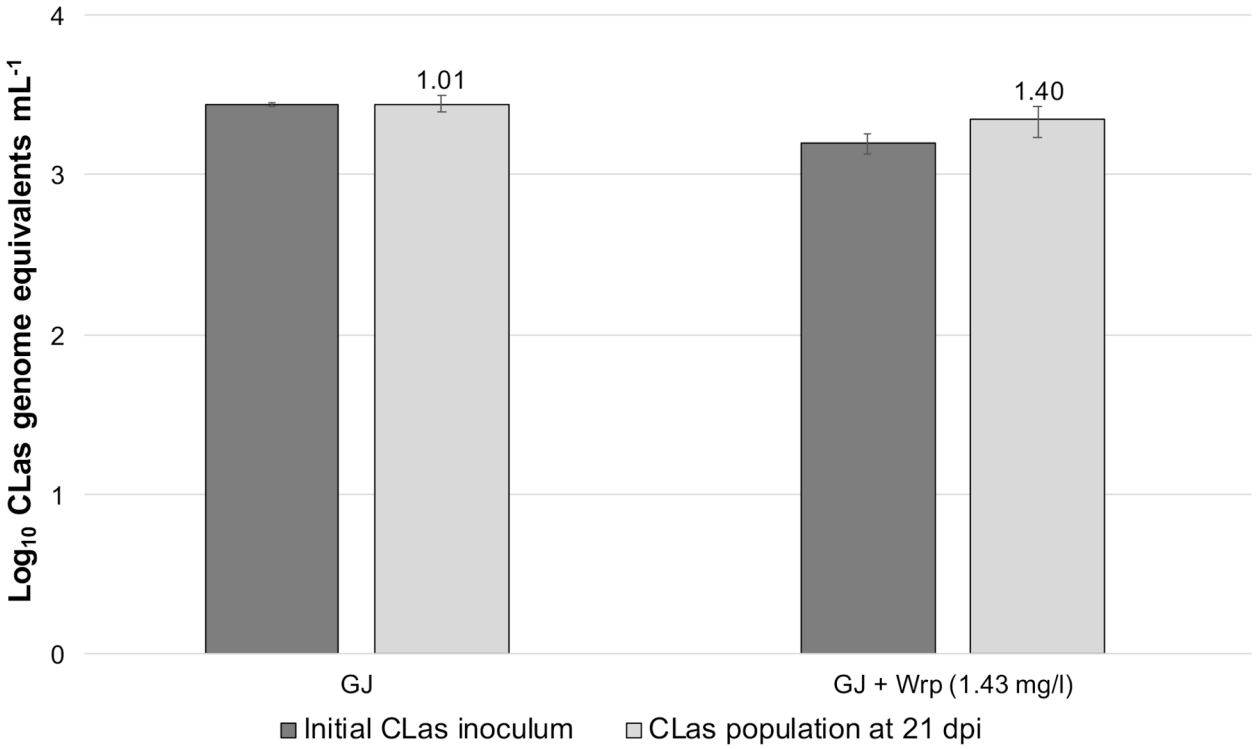

Fig. S3-6. Assessing the contribution of *Wolbachia* repressor protein (Wrp) to CLas growth. To verify if Wrp could promote CLas growth by repressing phage lytic cycle genes that possibly kill this bacterium in vitro, this protein was added to GJ at a concentration of 1.43 mg/l. CLas was inoculated into 24-well plates and grown at 28 ºC for 21 days, while its total population was assessed by qPCR. Adding Wrp to GJ did not contribute to CLas growth, since there was no significant increase of the CLas population. Data represent means and standard errors. Numbers above light gray columns indicate growth ratio of CLas. There was no statistical significance of the CLas population after the growth period in comparison to the initial inoculum in any of the samples, as determined by Student's *t*-test ($P \leq 0.05$; n = 3 technical replicates). "dpi" means days post inoculation. A representative result of at least three independent experiments is shown here.

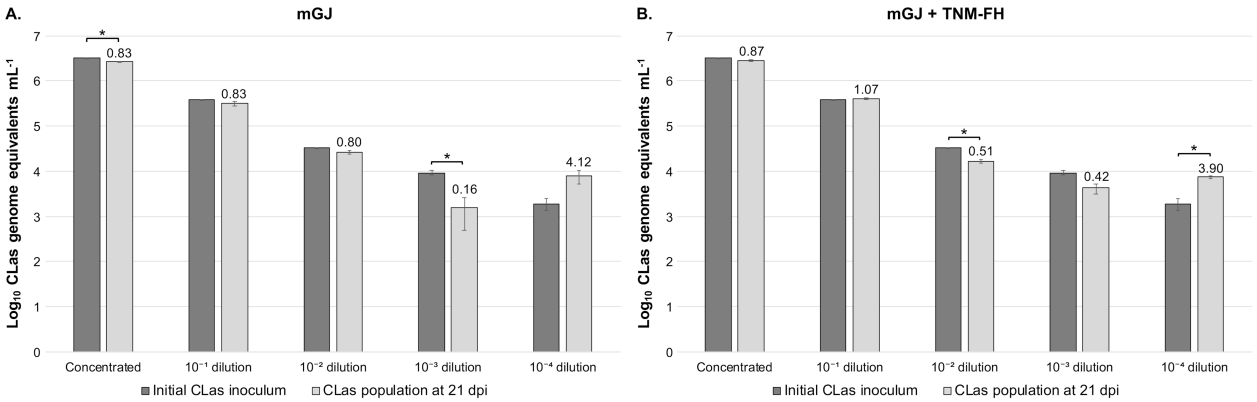

Fig. S3-7. CLas growth in mGJ amended with TNM-FH insect medium, BSA and ATP. The culture medium mGJ was amended with TNM-FH insect medium (52.4 g/l), sodium bicarbonate (0.35 g/l), BSA Fraction V (7.5%; 24 ml/l) and ATP (final concentration of 0.5 mM), and CLas was inoculated into it in 24-well plates to compare its growth when inoculated into nonamended mGJ. Samples were incubated at 28 ºC for 21 days and the total population of CLas was determined by qPCR. The addition of the selected compounds did not significantly contribute to CLas growth. The growth behavior in mGJ and mGJ + TNM-FH was similar, although levels of significance varied. **A.** CLas growth in mGJ. **B.** CLas growth in mGJ + TNM-FH. Data represent means and standard errors. Numbers above light gray columns indicate growth ratio of CLas. Statistical significance was determined using Student's *t*-test (* indicates $P \leq 0.05$ in comparison to the initial inoculum; n = 3 technical replicates). "dpi" means days post inoculation. A representative result of at least three independent experiments is shown here.

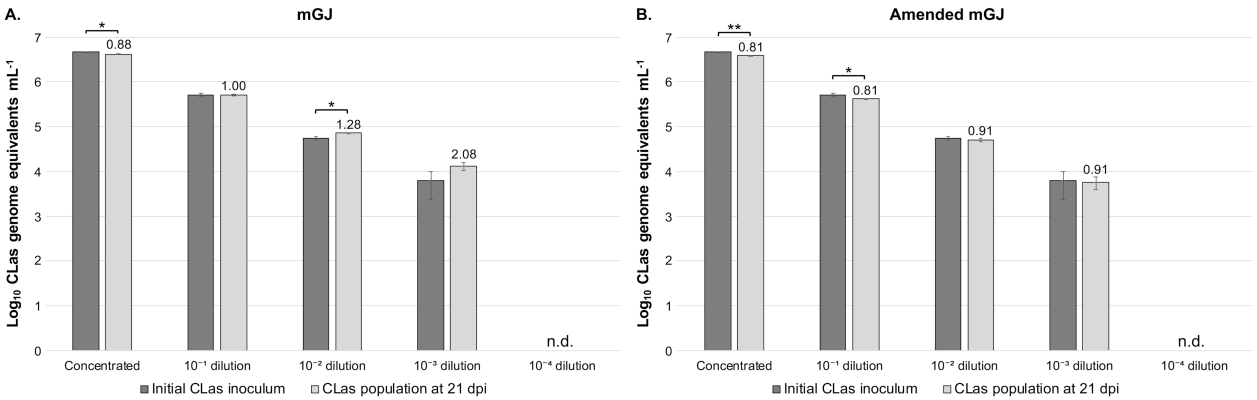

Fig. S3-8. Comparison of CLas growth in mGJ and amended mGJ. In addition to TNM-FH, sodium bicarbonate, BSA and ATP, mGJ was amended with FBS (150 ml/l), choline chloride (1 g/l) and reduced glutathione (5 ml of a 100 mM stock solution). Samples were inoculated into 24-well plates, grown at 28 ºC for 21 days and total CLas population was assessed by qPCR. Amendment of mGJ did not contribute to CLas growth, as a better growth performance was observed in mGJ alone. **A.** CLas growth in mGJ. **B.** CLas growth in amended mGJ. Data represent means and standard errors. Numbers above light gray columns indicate growth ratio of CLas. Statistical significance was determined using Student's *t*-test (* indicates $P \leq 0.05$ and ** indicates $P \leq 0.005$ in comparison to the initial inoculum; n = 3 technical replicates). "dpi" means days post inoculation. "n.d." indicates no detection signal of CLas by qPCR. A representative result of at least three independent experiments is shown here.

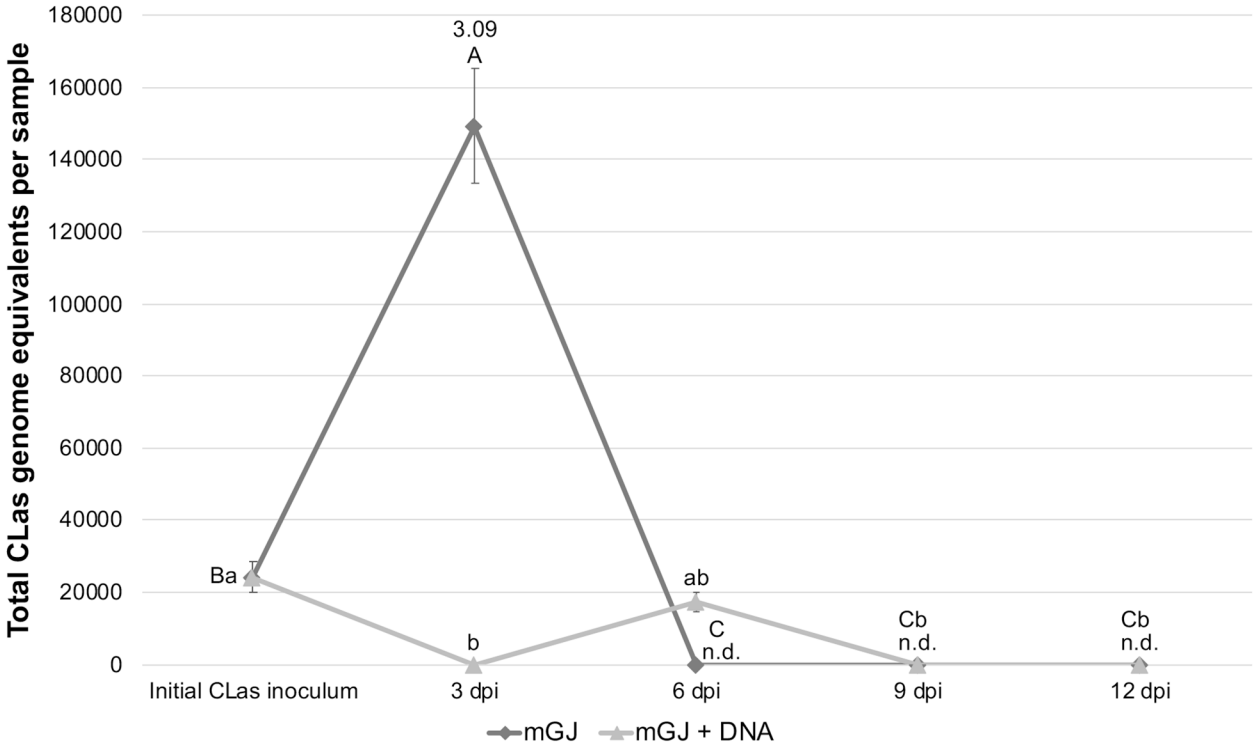

Fig. S3-9. Determining the contribution of adding exogenous DNA to CLas growth. To assess if addition of exogenous DNA could contribute to CLas growth, this bacterium was grown in flow conditions in mGJ and mGJ + DNA, which contains 2 µg of the pAX1-Cm plasmid in total. Samples were incubated at room temperature for a total of 12 days and aliquots were taken at 3-day intervals to determine CLas population by qPCR. Addition of exogenous DNA did not contribute to CLas growth since no significant increase of the population above levels of the initial inoculum was observed. One experiment in 24-well plates was also performed with similar results. Data represent means and standard errors. Numbers above markers in each time point of evaluation indicate growth ratio of CLas in comparison to the previous time point. Different capital letters in each dark gray marker indicate significant difference of CLas population in mGJ, while different letters in each light gray marker indicate significant difference of CLas population in mGJ + DNA, as analyzed by one-way ANOVA followed by Tukey's HSD multiple comparisons of means ($P \leq 0.05$; n = 3 technical replicates). Because the culture medium volume is continuously increasing in the flow system, the total CLas population present in the entire culture volume in each time point of evaluation is shown. "dpi" means days post inoculation. "n.d." indicates no detection signal of CLas by qPCR. A representative result of two independent experiments is shown here.

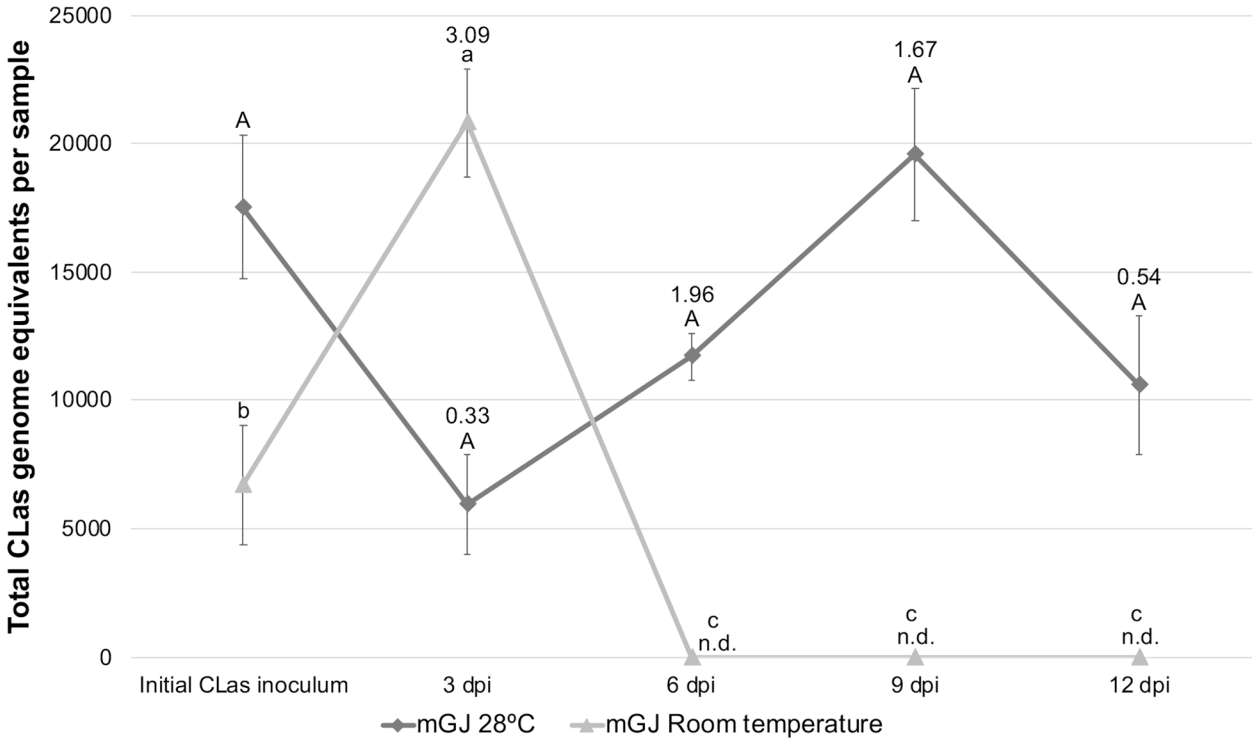

Fig. S3-10. Comparison of CLas growth in flow conditions at 28 ºC and room temperature. CLas was inoculated into mGJ in flow conditions and grown at room temperature and at 28 ºC to determine if incubation at a constant temperature of 28 ºC could contribute to its growth. The assay was conducted for 12 days with sampling at 3-day intervals to quantify CLas population by qPCR. Growth at room temperature allowed CLas to reach a higher growth ratio. However, CLas presented growth for a longer period when incubated at 28 ºC, although not significantly. Data represent means and standard errors. Numbers above markers in each time point of evaluation indicate growth ratio of CLas in comparison to the previous time point. Different capital letters in each dark gray marker indicate significant difference of CLas population in mGJ at 28 ºC, while different letters in each light gray marker indicate significant difference of CLas population in mGJ at room temperature, as analyzed by one-way ANOVA followed by Tukey's HSD multiple comparisons of means ($P \leq 0.05$; n = 3 technical replicates in one independent experiment). Because the culture medium volume is continuously increasing in the flow system, the total CLas population present in the entire culture volume in each time point of evaluation is shown. "dpi" means days post inoculation. "n.d." indicates no detection signal of CLas by qPCR.

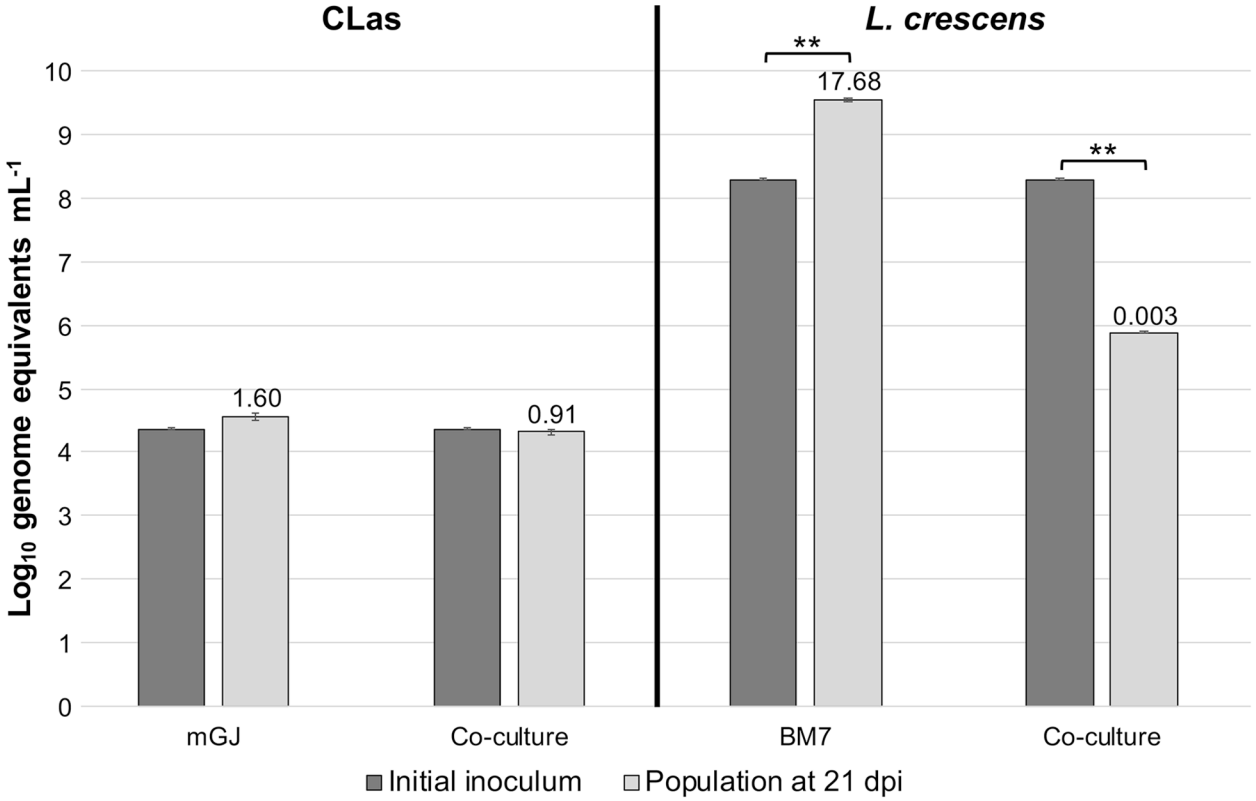

Fig. S3-11. CLas and Lcr growth in coculture. CLas and Lcr were cocultured in 24-well plates using plate inserts with 0.1-µm polycarbonate membranes that allow exchange of metabolic compounds, while keeping cells of both species spatially separated. Both bacteria were inoculated into their own medium (mGJ for CLas and BM7 for Lcr) either in coculture and separated to assess the contribution of coculture to CLas growth. Samples were incubated at 28 ºC for 21 days and total population of CLas and Lcr was determined by qPCR. The coculture of CLas and Lcr did not contribute to CLas growth. Growing CLas together with Lcr decreased the population of both, while they presented growth when inoculated into their own medium separately (although there was no significance for CLas). Data represent means and standard errors. Numbers above light gray columns indicate growth ratio of CLas or Lcr. Statistical significance was determined using Student's *t*-test (** indicates $P \leq 0.005$ in comparison to the initial inoculum; n = 3 technical replicates). "dpi" means days post inoculation. A representative result of two independent experiments is shown here.

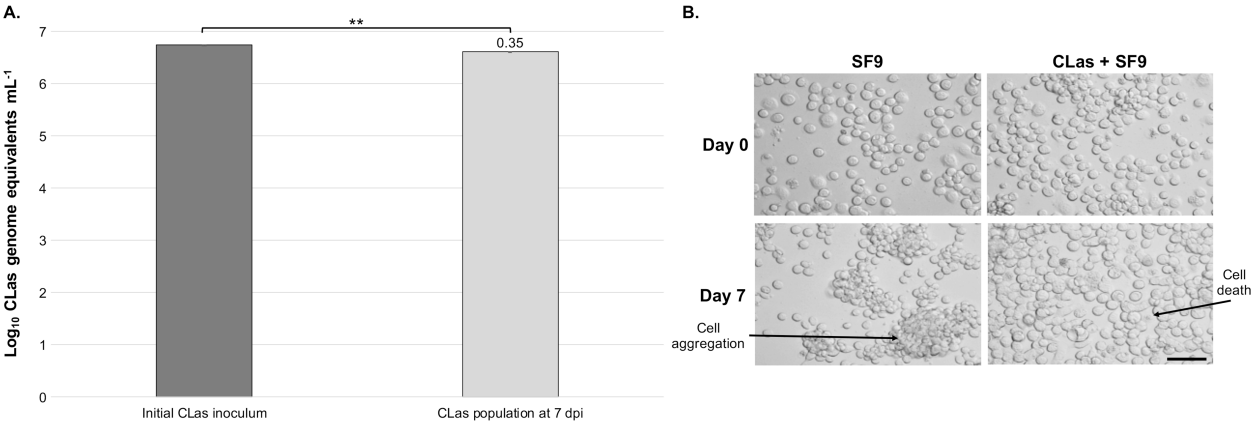

Fig. S3-12. CLas growth in coculture with SF9 insect cell line. SF9 cells grown in broth medium in culture flasks were inoculated with CLas and incubated for 7 days at 28 ºC in an attempt to establish an intracellular coculture of CLas. The total population of CLas was quantified by qPCR. CLas did not establish a coculture with SF9. The population of CLas consistently decreased when grown together with SF9, which also presented cell death as observed by microscopy. **A.** CLas growth in coculture with SF9. Data represent means and standard errors. Number above light gray column indicates growth ratio of CLas. Statistical significance was determined using Student's *t*-test (** indicates $P \leq 0.005$ in comparison to the initial inoculum; n = 3 technical replicates). "dpi" means days post inoculation. A representative result of three independent experiments is shown here. **B.** Microscopy analysis of SF9 cells in coculture with CLas. SF9 cells were observed at the initial time point of assays and after 7 days of growth. Cell death was only observed in coculture with CLas, in which SF9 cells also did not form aggregates. Each phenotype is highlighted in the figure by arrows. Samples were observed in a Nikon Eclipse Ti inverted microscope (Nikon, Melville, NY, USA) with a Nikon DS-Q1 digital camera (Nikon, Melville, NY, USA), and controlled by NIS-Elements software 3.2 (Nikon, Melville, NY, USA). Scale bar = 20 μm.

Table S3-1. Experiments conducted from 2017 to 2021.

Date [x]	CLas inoculum source	Treatment	N [y]
June, 2017	Citrus seeds	Inoculation into GJ in 24-well plates	2
June, 2017	Citrus seeds and periwinkle leaves	Inoculation into solid GJ	4
August, 2017	Citrus seeds, periwinkle leaves and ACP guts	Inoculation into GJ or mGJ in 24-well plates with subsequent subcultures	17
August, 2017	Citrus seeds	Inoculation into GJ and incubation in shaking and non-shaking conditions	2
October, 2017	Citrus seeds	Addition of Wrp to GJ	4
October, 2017	Citrus seeds	Addition of ATP to GJ	3
November, 2017	Citrus seeds	Coculture with *P. acnes*	2
January, 2018	Citrus seeds	Coculture with *L. crescens*	2
March, 2018	Citrus seeds	Adjusting the pH of GJ to 5.85	2
July, 2019	ACP guts	Addition of TNM-FH insect medium to mGJ	3
August, 2019	ACP guts	Resuspension of cells in fresh broth medium between subcultures	2
August, 2019	ACP guts	Incubation at 37 ºC	3
September, 2019	Periwinkle leaves and ACP guts	Incubation in flow conditions	10
October, 2019	ACP guts	Amendment of mGJ with additional compounds	3
April, 2020	Periwinkle leaves	Subculturing at 3-day intervals	4
April, 2020	Periwinkle leaves	Addition of cell-free spent broth medium used to culture SF9 insect cell line to mGJ	2
July, 2020	Periwinkle leaves	Incubation at 28 ºC under flow conditions	1
September, 2020	Periwinkle leaves and ACP guts	Coculture with SF9 insect cell line	3
October, 2020	ACP guts	Addition of extracellular DNA to mGJ	2

[x] Refers to the date of the first experiment that was conducted for each treatment.
[y] Number of independent experiments performed in total for each treatment.

Chapter 4

Overview of *Xylella fastidiosa*: main features, adaptation to the xylem, type IV pili, and natural competence

Xylella fastidiosa

The plant pathogen *Xylella fastidiosa* is a Gram-negative, fastidious bacterium member of the Xanthomonadaceae (Gammaproteobacteria) that, in natural environments, is limited to the xylem of infected plants and to the foregut of sharpshooter and spittlebug insect vectors, which transmit the bacteria directly to the xylem of plant hosts (Almeida et al. 2014; Chatterjee et al. 2008a). Cells of this bacterium are slow-growing, mesophilic (with optimum growth at 26-28 ºC), neutrophilic (optimal pH ranging from 6.5 to 6.9), rod shaped and with 0.9 to 3.5 μm in length and 0.25 to 0.35 μm of radius (Wells et al. 1987). In addition, they are non-flagellated, but possess both short type I pili (0.4 to 1.0 μm) and long type IV pili (1.0 to 5.8 μm) at one of their poles (Meng et al. 2005).

Type I pili are involved in cell attachment to surfaces and cell-to-cell adhesion, whereas type IV pili mediate twitching motility, as described below (De La Fuente et al. 2007; Li et al. 2007; Meng et al. 2005). This bacterium is the causal agent of many diseases in economically important crop plants worldwide, including grapevine, citrus, coffee, plum, almond, peach, blueberry, and olives (Chang et al. 2009; Hopkins and Purcell 2002; Saponari et al. 2013). In addition, *X. fastidiosa* colonizes many grasses and weeds without causing disease (EFSA 2021).

Pathogen transmission and disease development

The main insect vectors of *X. fastidiosa* are xylem-sap-feeding sharpshooter leafhoppers (Hemiptera, Cicadellidae) and spittlebugs (Hemiptera, Cercopidae) (Almeida et al. 2014). However, xylem-feeding members of the Machaerotidae and Cicadae families can also vector this bacterium (Almeida et al. 2005). Once acquired by insect vectors when feeding on infected plants, *X. fastidiosa* cells attach to the precibarium and colonize the cuticular lining of the foregut, from where they are inoculated into healthy plant hosts by detaching during insect feeding (Almeida and Purcell 2006). In the Americas, sharpshooter leafhopper species are the most important group of vectors for the pathogen, and they play a great role in disease epidemiology (Almeida et al. 2014). On the other hand, Europe has few species of these insects, but it has various endemic spittlebug species (froghoppers), which are potential vectors of *X. fastidiosa* (Almeida 2016). Among them, the hemipteran species *Philaenus spumarius* (meadow spittlebug) is possibly the main vector of *X. fastidiosa* in the heavily affected Apulia region in Italy, since this insect is widespread in that area, thrives well in olive plants by reaching high populations, and successfully acquires and transmits *X. fastidiosa* to periwinkle and olive plants (Cornara et al. 2017; Martelli et al. 2016; Saponari et al. 2014).

Strains of *X. fastidiosa* have caused severe plant disease outbreaks throughout the world, with great economic losses. Among the diseases caused by this bacterium, Pierce's Disease of grapevine (PD), found mainly in California, and Citrus Variegated Chlorosis (CVC), which primarily affects sweet orange plants in Brazil, have been the most economically important, and thus are the most well studied so far (Chatterjee et al. 2008a). PD is caused by strains of subsp. *fastidiosa* and is characterized by stunted growth of grapevines and leaf scorch, followed by vine

death in 1-5 years (Goodwin and Purcell 1992; Hewit et al. 1942; Nunney et al. 2010). It is estimated that PD causes approximately $104 million losses every year to the wine industry in California alone (Tumber et al. 2014).

On the other hand, CVC is caused by *X. fastidiosa* strains belonging to subsp. *pauca* (Almeida et al. 2008), and citrus plants affected by this disease do not die, but become economically nonproductive when severely affected (Almeida et al. 2014). Typically, CVC symptoms include leaves displaying irregular chlorosis symptoms on the upper side of the leaf, with corresponding brownish gum-like material over the side, and fruits are reduced in size and hardened, becoming unsuitable for both juice production and fresh fruit market (Almeida et al. 2014). Because of CVC, losses to the Brazilian citriculture are estimated to be around $120 million per year (Bové and Ayres 2007). Due to its importance, the 9a5c strain of *X. fastidiosa* subsp. *pauca* causing CVC was the first bacterial plant pathogen to have its genome entirely sequenced (Simpson et al. 2000). Consequently, much knowledge on the bacterium was gained, and several studies of functional genomics were enabled, significantly increasing our knowledge about the pathogen's biology and interaction with plant hosts (Almeida and Nunney 2015; Chatterjee et al. 2008a).

The main symptoms of plants infected with *X. fastidiosa* include leaf chlorosis, marginal scorching and/or dwarfing, depending on the host (Hopkins and Purcell 2002). Although not fully understood, systemic colonization of vessels in infected plants by multiplication and movement of bacteria, followed by biofilm formation, which blocks xylem vessels and impairs movement of water and nutrients within plants, are considered to be the main pathogenicity

mechanism of *X. fastidiosa* (Chatterjee et al. 2008a). However, there is some controversy, as discussed below. Nevertheless, insect vectors only acquire bacteria in biofilm, which is thus a necessary condition to spread the pathogen in the environment (Chatterjee et al. 2008a). Additionally, the lateral movement of *X. fastidiosa* within infected plants from one neighboring vessel to the other is achieved by dissolving pit membranes (PM) using cell wall-degrading enzymes such as polygalacturonase and endo-1,4-β-glucanase (Pérez-Donoso et al. 2010; Roper et al. 2007). PM is a primary cell wall that separate neighboring vessels, which primarily functions to limit the spread of vascular pathogens and embolism (Choat et al. 2008). Moreover, the production of tyloses, pectin-rich gels and crystals in the vessels by the immune system of the plant host also contribute to occlude the xylem of plants infected with this bacterium (Sun et al. 2013). However, even with the advance of our understanding about the pathogen, *X. fastidiosa* continues to spread and cause different and novel plant diseases around the world. For instance, this pathogen was identified as the causal agent of a novel bacterial leaf scorch disease of blueberry in the U.S. (Chang et al. 2009), and a new species in the *Xylella* genus, *X. taiwanensis*, has been found in Taiwan causing pear leaf scorch (Su et al. 2016).

In addition, *X. fastidiosa* has recently reached the European continent, where it infects different plants and causes great damage on many levels in different countries (Almeida 2016; EFSA 2015; Olmo et al. 2017; Rapicavoli et al. 2018; Stokstad 2015). Among diseases caused by *X. fastidiosa* in Europe, the olive quick decline syndrome has been the most devastating. This disease severely impacts centuries-old olive trees, and it is not only a threat to the Italian olive industry but is also a cultural disaster by harming the Apulian society beyond qualification, since these trees represent their cultural history (Almeida 2016; Colella et al. 2019). Currently, there is

no cure or effective control for diseases caused by *X. fastidiosa*, and disease management relies on controlling the insect vector and using tolerant or resistant varieties (Hopkins and Purcell 2002).

Adaptation of *X. fastidiosa* to the xylem environment

Bacterial plant pathogens, including *X. fastidiosa*, rely on specialized structures and features to cope within the xylem environment of plants hosts and colonize it. These most well-studied structures include type IV pili, biofilm formation, attachment structures, and outer membrane vesicles, and are described below.

Type IV pili. Type IV pili (TFP) are proteinaceous cell appendages with a hair-like appearance and a diameter of 5 to 8 nm that are mainly encoded by *pil* genes. They are mostly located at one or both poles of bacterial cells and extend to many micrometers in length and also retract (Mattick 2002). TFP mediate twitching motility, an efficient type of bacterial movement that is flagellar-independent. During twitching motility, TFP extend and attach to a surface through the distal end of the pilus, which pulls the cell towards the attached surface when it is retracted (Jarrell and McBride 2008; Mattick 2002). In *X. fastidiosa*, which moves exclusively through twitching motility (Chatterjee et al. 2008a), deletion of the TFP genes *pilB* and *pilQ* leads to abrogation of motility and reduces the basipetal movement within infected plants (Meng et al. 2005). Likewise, deletion of the TFP regulatory genes *pilG* and *pilL* within this bacterium also abolishes twitching motility and leads to avirulence and development of delayed, less severe symptoms in grapevines, respectively (Cursino et al. 2011; Shi and Lin 2016, 2018). Curiously, knockout strains of *rpfF* in *X. fastidiosa*, which encodes the diffusible signable factor (DSF;

quorum sensing molecule of this organism) synthase (Newman et al. 2004), have increased twitching motility and display hypervirulence in planta (Chatterjee et al. 2008c; Cruz et al. 2014; Ionescu et al. 2013; Newman et al. 2004). Since DSF positively regulates biofilm formation in *X. fastidiosa* while negatively modulates movement (Newman et al. 2004), absence of its production in Δ*rpfF* mutants leads to hypervirulence by likely increasing the movement of this pathogen within infected plants, thus expanding its ability to systemically colonize plant hosts (Chatterjee et al. 2008c; Ionescu et al. 2013). Strikingly, preliminary results demonstrate that deletion of specific *pil* genes within *X. fastidiosa* that leads to increased movement results in reduced virulence in tobacco plants (M. V. Merfa & L. De La Fuente, unpublished information; described in chapter 5). Therefore, since deletion of TFP genes leading to both reduced and increased twitching motility results in reduced virulence in planta, indicates that this structure is needed for full symptom development by *X. fastidiosa*, whereas disruption of its individual components suppresses virulence.

Twitching motility mediated by TFP is also required by other xylem-colonizing pathogens to move within plant hosts, including *Ralstonia solanacearum* (wilt diseases) (Liu et al. 2001). This pathogen also moves through flagellar motility. However, this type of movement is used together with chemotaxis to locate the root system of plant hosts in the early stages of host invasion, being repressed in the xylem (Lowe-Power et al. 2018; Tans-Kersten et al. 2001). In fact, the velocity of the xylem sap flow is much higher than that of the flagellar movement, rendering this type of movement ineffective within xylem vessels (Atsumi et al. 1996; Lowe-Power et al. 2018; Windt et al. 2006). Although cells moving through twitching motility have an even lower speed of translocation, the ability of TFP to move cells by attaching to a surface

allows them to move against the flow of xylem sap, thereby facilitating the systemic colonization of plant hosts (Meng et al. 2005). However, contrary to what has been described, flagellar movement is important for the host colonization of another plant pathogen, *Pantoea stewartii* (Stewart's wilt of corn) (Herrera et al. 2008). Similar to *X. fastidiosa*, TFP mutant strains of *R. solanacearum* are impaired in twitching motility and present decreased virulence in tomato plants (Corral et al. 2020; Kang et al. 2002; Liu et al. 2001).

In *Erwinia amylovora* (fire blight of apple and pear), deletion of a gene involved in polysaccharide biosynthesis reduces twitching motility as well as virulence of this pathogen (Berry et al. 2009). Other bacterial plant pathogens in which TFP are important for xylem colonization and full symptom development include *Acidovorax citrulli*, which infects plants belonging to the Cucurbitaceae family (Bahar et al. 2010; Bahar et al. 2009); few vascular xanthomonads, such as *Xanthomonas oryzae* pv. *oryzae* (bacterial leaf blight of rice) (Das et al. 2009; Lim et al. 2008; Wang et al. 2008) and *X. campestris* pv. *campestris* (black rot disease of cruciferous plants) (McCarthy et al. 2008), and surprisingly the non-vascular *X. oryzae* pv. *oryzicola* (bacterial leaf strike of rice) (Wang et al. 2007); and some pathovars of *Pseudomonas syringae*, in which TFP interestingly seem to play a role in the initial adhesion and colonization of leaves, with no assessment of their contribution to the xylem colonization (Nguyen et al. 2012; Roine et al. 1998; Romantschuk and Bamford 1986; Suoniemi et al. 1995; Taguchi and Ichinose 2011). Nevertheless, together, these data demonstrate that twitching motility mediated by TFP is a specific virulence mechanism that pathogens use to colonize the xylem of plant hosts. However, some gaps remain, including whether there is a specific interaction between components of TFP with the xylem constituents, which xylem molecules and conditions may

regulate the activity of TFP, and if the role of TFP on virulence is primarily motility, considering that cells may move much faster along the xylem sap flow (Lowe-Power et al. 2018; Windt et al. 2006).

Biofilm formation. Biofilms consist of aggregates of microbial cells that adhere to each other and/or to a surface and are enclosed in a matrix of extracellular polymers (Morris and Monier 2003). Because of this structure, cells in biofilm have a series of adaptive advantages in the environment in comparison to planktonic cells, including increased resistance to antimicrobial compounds (Mah and O'Toole 2001), protection from desiccation, UV and predation, increase of genetic exchange (Costerton et al. 1995; Davey and O'Toole 2000), facilitation of nutrient acquisition (Rooney et al. 2020), among others. Biofilm formation within xylem vessels by plant pathogenic bacteria such as *R. solanacearum* (Caldwell et al. 2017; Tran et al. 2016), *X. fastidiosa* (Chatterjee et al. 2008a; Stevenson et al. 2004), *E. amylovora* (Kharadi and Sundin 2020) and *P. stewartii* (Koutsoudis et al. 2006) has been implicated in disease development by occluding the xylem, which leads to the development of symptoms including wilting and others that occur from nutrient imbalances and water stress due to vascular malfunction. However, there is some controversy about the role of biofilms in disease development.

In *E. amylovora*, deletion of the amylovoran and levan exopolysaccharides that compose its biofilm matrix leads to nonvirulence and reduced virulence phenotypes, respectively (Koczan et al. 2009). Similarly, biofilm formation plays a key role on virulence of *R. solanacearum* (Mori et al. 2016), but the disruption of xylem vessels that leads to wilt diseases may also be caused by

tyloses produced by the plant host immune system or by gas embolism (Lowe-Power et al. 2018). Additionally, biofilm formation is a tightly regulated process and some *R. solanacearum* cells need to escape this structure at some point to systemically colonize plant hosts (Tran et al. 2016). On the other hand, deletion of *rpfC*, which encodes a two-component regulatory protein that is a negative regulator of DSF, leads to increased biofilm formation and reduced virulence in *X. fastidiosa* (Chatterjee et al. 2008b), whereas embolism and tyloses formation within xylem vessels have been suggested to play a pivotal role in diseases caused by this pathogen (Ingel et al. 2021; McElrone et al. 2008; Pérez-Donoso et al. 2007; Petit et al. 2021; Sabella et al. 2019; Sun et al. 2013). Mutant cells of *rpfC* present a hyperattachment phenotype and are severely affected in their ability to move away from the point of inoculation within infected plants (Chatterjee et al. 2008b), suggesting that biofilm is a secondary trait for the virulence of this bacterium. Biofilm formation within the xylem, however, is a key phenotype of *X. fastidiosa* that allows its acquisition from infected plants and dispersion by insect vectors, thus allowing the maintenance of its life cycle (Chatterjee et al. 2008a; Chatterjee et al. 2008b; Newman et al. 2004). Moreover, biofilms possibly facilitate the accumulation of molecules such as cell wall-degrading enzymes and quorum sensing signals, protecting cells of different pathogens from quorum quenching mediated by the flow of xylem sap (Emge et al. 2016; Kim et al. 2016; Lowe-Power et al. 2018). Therefore, biofilm formation contributes for the successful colonization of the xylem vessels of plant hosts by bacterial pathogens, although its role in virulence remains elusive, especially in *X. fastidiosa*. More studies are needed to fully elucidate the function of biofilm formation in the colonization and pathogenesis mechanism of xylem-colonizing plant pathogenic bacteria.

Attachment structures. Different structures that mediate bacterial attachment are important for the interaction of plant pathogens with xylem vessels. These include fimbrial and afimbrial adhesins, pili, hemagglutinins, and lectins (proteins that bind to carbohydrates). *R. solanacearum*, for example, encodes few thousands outer membrane proteins that share homology to afimbrial adhesins of other bacterial pathogens, but which have not been characterized within this bacterium (Lowe-Power et al. 2018). Investigating their interaction to the xylem of plant hosts at different steps during colonization and disease development could elucidate their individual contributions to virulence. Nevertheless, few have been characterized in *R. solanacearum*, including *lecM*, which encodes the lectin RS-IIL. Deletion of this gene reduces biofilm formation and leads to a nonvirulent phenotype on tomato plants (Mori et al. 2016). Moreover, a *pilA* (TFP major subunit) mutant could not attach to tobacco cells or tomato roots and was nonvirulent, as mentioned above (Kang et al. 2002). Likewise, the afimbrial adhesins XadA, XadB and XadM are required for attachment and optimal virulence of the vascular xanthomonad *X. oryzae* pv. *oryzae* (Das et al. 2009; Pradhan et al. 2012; Ray et al. 2002), whereas the filamentous hemagglutinin HecA contributes to the virulence of *Dickeya dadantii* (bacterial wilt and soft rot diseases; formerly known as *Erwinia chrysanthemi*) (Rojas et al. 2002). However, it is not clear whether these adhesins of *X. oryzae* pv. *oryzae* and *D. dadantii* have a role within the xylem vessels or only in initial epiphytic attachment.

Similarly, in the xylem-limited plant pathogen *X. fastidiosa*, there are conflicting results regarding the role of adhesins on xylem colonization and virulence. An initial report demonstrated that the hemagglutinins HxfA and HxfB are avirulence factors of this pathogen, since their deletion increases virulence likely due to a resulting hypermotile phenotype and less

efficient attachment to xylem vessels, which allows for a more efficient systemic colonization of plant hosts (Guilhabert and Kirkpatrick 2005). However, another study demonstrated that deletion of the hemagglutinin HxfB, as well as of the afimbrial adhesin XadA, reduces virulence in grapevines, with similar results being observed for the type I pili components FimA and FimF responsible for cell-to-cell attachment (Feil et al. 2007). The presence of afimbrial adhesins, however, is important for the efficient acquisition and subsequent transmission of *X. fastidiosa* by insect vectors (Killiny and Almeida 2009), thus completing its life cycle as similarly discussed above for biofilm formation. In addition, the O-antigen of the lipopolysaccharide of *X. fastidiosa* also mediates the adhesiveness of cells, biofilm formation and virulence in grapevines (Clifford et al. 2013). As mentioned for *R. solanacearum* (Lowe-Power et al. 2018), *X. fastidiosa* encodes several other fimbrial and afimbrial adhesins (Chatterjee et al. 2008a; Van Sluys et al. 2003), in which it would be interesting to assess their roles on the virulence and lifestyle of these pathogens to fully understand their contribution for host colonization.

Outer membrane vesicles. The production of outer membrane vesicles (OMVs) is an ubiquitous feature of all investigated Gram-negative bacteria (Kuehn and Kesty 2005). OMVs are spherical particles formed by the blebbing or pinching off of sections of the outer membranes of such bacteria and their sizes vary from 20 to 250 nm in diameter. These structures contain periplasmic soluble proteins in their lumen, which are entrapped by the lipopolysaccharide-phospholipid double layer together with outer membrane lipoproteins (Schwechheimer et al. 2013; Toyofuku et al. 2019). OMVs perform many functions, including delivery of virulence factors and antigens, resistance to antimicrobial compounds, protection against bacteriophages by serving as decoys, modulation of the host's immune response, among others (Schwechheimer

and Kuehn 2015). In *X. fastidiosa*, OMVs have been described to play a curious role in its pathogenicity mechanism. They function as antiadhesives by attaching to the walls of xylem vessels, presumably through the afimbrial adhesin XadA1, and blocking the interaction of *X. fastidiosa* cells to these plant structures. In turn, this pathogen colonizes the plant more efficiently and OMVs thus adjust the attachment of *X. fastidiosa* to surfaces, mediating its interchange from an adhesive state required for insect acquisition and transmission to a motile, virulent condition in which cells systemically colonize plant hosts (Ionescu et al. 2014). Additionally, OMVs are negatively regulated by quorum sensing, as described above for twitching motility (Ionescu et al. 2014; Newman et al. 2004). This further demonstrates that attachment of *X. fastidiosa* to xylem vessels impairs its ability to colonize plant hosts and that a tight regulation between biofilm formation/adhesiveness and motile lifestyles is required for this pathogen to successfully infect plants and be spread by insect vectors. Such function of OMVs is yet to be characterized in other xylem-colonizing plant pathogenic bacteria.

X. fastidiosa taxonomy and distribution

Based on DNA relatedness and multilocus sequence typing (MLST), five subspecies were classified within the *X. fastidiosa* species: subsp. *fastidiosa*, *pauca*, *multiplex* and *sandyi*/*morus* (2, 76–78) (Almeida et al. 2014; Nunney et al. 2014b; Scally et al. 2005; Schaad et al. 2004; Schuenzel et al. 2005). Between these subspecies there are some biological differences, and recent MLST studies have also shown that they have evolved in geographic isolation (Almeida et al. 2014; Almeida and Nunney 2015). Subsp. *fastidiosa* is found in North America and Costa Rica, being much more diverse within Central America, which is its presumed center of origin (Nunney et al. 2010). Subsp. *pauca* is native to South America (Almeida et al. 2008;

Nunney et al. 2012), while subsp. *multiplex* occurs in temperate and subtropical North America, and subsp. *sandyi*/*morus* has been found in southern regions of the U.S. (Nunney et al. 2014a; Nunney et al. 2014b; Nunney et al. 2012; Yuan et al. 2010). In addition, all subspecies have been found in Europe (Denancé et al. 2017; Giampetruzzi et al. 2017; Olmo et al. 2017). Curiously, these findings suggest that the emergence of *X. fastidiosa* in Europe is linked to several introduction events of diverse strains from different subspecies (Denancé et al. 2017; Landa et al. 2020).

In addition to each subspecies being related to specific geographic regions, they also show host specificity to some extent. Subsp. *fastidiosa* comprises strains from grape, alfalfa, almond and maple; subsp. *multiplex* includes strains from plum, peach, elm, almond and sycamore; subsp. *pauca* contains strains from citrus, coffee and olive; in subsp. *sandyi* are included strains from oleander, daylily, magnolia and jacaranda; and subsp. *morus* infects mulberry (Giampetruzzi et al. 2017; Hernandez-Martinez et al. 2007; Janse and Obradovic 2010; Nunney et al. 2014b). This is important because intersubspecific homologous recombination (IHR) among *X. fastidiosa* strains, including strains from different subspecies, is implicated in host shift and emergence of diseases caused by this pathogen and is rapidly changing the host specificity of its different subspecies (Almeida and Nunney 2015; Nunney et al. 2014a; Nunney et al. 2014b; Nunney et al. 2012). It is also worth noting that a recent study proposed that only *fastidiosa*, *multiplex* and *pauca* are clearly defined subspecies of *X. fastidiosa* (Marcelletti and Scortichini 2016).

Intersubspecific homologous recombination in *X. fastidiosa*

Homologous recombination (HR) is a mechanism by which two similar DNA molecules exchange genetic information, and it fosters rapid evolution by generating genetic diversity in almost every known organism (Dorer et al. 2011; Johnston et al. 2014; Wiedenbeck and Cohan 2011). HR has a pivotal role in maintaining the integrity of the bacterial genome since it is involved in repairing breaks of double stranded DNA when this molecule is exposed to mutagens such as UV or reactive oxygen species, or when there is an interruption of the replication fork (Dorer et al. 2011; Lenhart et al. 2012). The source of DNA for HR occurs naturally in bacteria via three different types of horizontal gene transfer, including conjugation, transduction, and natural transformation. Conjugation involves physical contact of cells and transfer of the genetic material as plasmids; transduction is the delivery of the incoming DNA via bacteriophages; and natural transformation is the uptake of exogenous DNA from the environment and incorporation into the genome of the recipient cell via homologous recombination (Soucy et al. 2015).

In *X. fastidiosa*, MLST and whole genome analyses of strains collected from diverse geographic regions and plant hosts have determined that widespread IHR and intrasubspecific HR events contribute to its genetic diversity (Almeida et al. 2008; Castillo et al. 2020; Coletta-Filho et al. 2017; Jacques et al. 2016; Nunney et al. 2014a; Nunney et al. 2010; Nunney et al. 2012; Potnis et al. 2019; Scally et al. 2005; Vanhove et al. 2019). Interestingly, HR has a greater role in generating allelic variation than point mutation in this pathogen (Scally et al. 2005; Vanhove et al. 2019). In addition, IHR has been predicted to be involved in plant host expansion in *X. fastidiosa* by causing host shifts (Nunney et al. 2014a; Nunney et al. 2014b; Nunney et al. 2012). The fact that *X. fastidiosa* was recently described to be naturally competent for

transformation (Kung and Almeida 2011) suggests that this mechanism has a key role in driving HR within this pathogen to generate genetic diversity.

Natural competence: from discovery to current knowledge

As mentioned above, natural transformation or natural competence is the acquisition of free DNA fragments from the environment and incorporation into the bacterial genome of recipient cells by HR (Johnston et al. 2014; Soucy et al. 2015). This trait was first discovered in 1928 by Frederick Griffith (Griffith 1928), but it was only decades later that natural competence was better studied and described (Dubnau 1999). Griffith studied two strains of *Streptococcus pneumoniae*: type III-S (smooth) that is covered by a polysaccharide capsule that allows cells to evade the host's immune system and is thus lethal; and type II-R (rough), in which the capsule is absent, and cells are then recognized and killed by immune responses of the host. When heat-killed cells of the smooth strain were mixed with live rough cells, the latter converted into smooth, lethal cells. Griffith concluded that an unknown 'transforming principle' was transferred from dead to live cells, converting them into lethal strains (Griffith 1928). Further studies demonstrated that the transforming agent was DNA, which is the genetic material of organisms (Lorenz and Wackernagel 1994).

Initially, natural competence was thought to be a mechanism for nutrient acquisition, considering that this phenotypical state developed under starvation conditions (Seitz and Blokesch 2013a). However, although the precise role of this mechanism is not fully understood, it is also involved in repair of damaged DNA, and adaptation to new habitats, spread of antibiotic resistance and emergence of pathogens by generating genetic diversity (Johnsborg et al. 2007;

Johnston et al. 2014; Seitz and Blokesch 2013a; Wiedenbeck and Cohan 2011). To date, more than 80 bacterial species have been described to be naturally competent, with many presenting specific aspects regarding this mechanism, as described below (Johnsborg et al. 2007; Johnston et al. 2014).

Haemophilus influenzae and *Neisseria* spp., for example, preferentially uptake homotypic self-DNA, which is mediated by DNA uptake sequences (DUS) that are conserved sequence motifs widely distributed in the genome of each of these bacteria (Elkins et al. 1991; Smith et al. 1999). On the other hand, *Acinetobacter calcoaceticus* does not discriminate between self or foreign DNA, and its competence phenotype during different growth phases is dependent upon the availability of different nutrients (Palmen et al. 1994). Additionally, *Neisseria meningitidis* (Catlin 1960), *N. gonorrhoeae* (Biswas et al. 1977), and *Helicobacter pylori* (Israel et al. 2000) present constitutive competence at all growth phases, whereas *H. influenzae* is competent at the stationary phase (Macfadyen et al. 2001) and *S. pneumoniae* at mid-log phase (Håvarstein et al. 1995). *H pylori* also limits the acquisition of distantly related DNA sequences, but through the use of a restriction modification system (Humbert and Salama 2008).

The regulation of competence also differs among bacterial species. In *H. influenzae*, natural competence is induced under starvation conditions (Herriott et al. 1970), which involves the accumulation of the secondary messenger cyclic AMP (Wise et al. 1973). CRP (the cAMP receptor protein) (Chandler 1992) and adenylate cyclase (CyaA) (Dorocicz et al. 1993) are also required in this process, as well as the central regulator for natural competence *sxy*, a cAMP-dependent gene (Cameron et al. 2008; Redfield 1991; Redfield et al. 2005). This suggests that a

signal transduction mechanism mediates natural competence induction in *H. influenzae*, although an actual link among these regulatory proteins is yet to be described. Similarly, competence induction in *Vibrio cholerae* is mediated by the chitin-induced transcription regulator TfoX, which is a homologue of Sxy, and by the quorum-sensing regulator HapR (Meibom et al. 2005; Scrudato and Blokesch 2012, 2013). DNA damage also induces competence in some bacterial species. This process has been shown to regulate competence in *H. pylori* (Dorer et al. 2010), *S. pneumonia* (Prudhomme et al. 2006), and *Legionella pneumophila* (Charpentier et al. 2011). These distantly related species have in common the absence of an efficient SOS system for DNA damage repair, suggesting that competence is thus induced during DNA damage so that the incoming DNA may be used as a repair template (Seitz and Blokesch 2013a).

Natural competence mechanisms: the role of type IV pili

Because of the differences between the cell membranes of Gram-positive and Gram-negative bacteria, the mechanisms of natural competence among these bacteria somewhat vary. Specifically, the initial interaction of DNA with the cell components is different since Gram-negative bacteria have an outer cell wall that is absent in Gram-positive bacteria. However, translocation through the inner membrane occurs by a similar process, being carried out by orthologous proteins (Dubnau 1999). The overall mechanism of natural competence shared by both Gram-positive and Gram-negative bacteria involves i. binding of extracellular DNA by cell surface proteins; ii. degradation of the 3' strand of the DNA by a hitherto unknown exonuclease; iii. transfer of the 5' strand to the cytoplasm; iv. SSB proteins such as DprA and RecA bind the single-stranded DNA (ssDNA); and v. RecA scans for homology and performs homologous recombination with the recipient chromosome (Bakkali 2013).

In Gram-positive bacteria, competence is regulated by quorum sensing signals such as competence stimulating proteins (CSP) (Håvarstein et al. 1995). These signaling proteins activate a two-component regulatory system comprised by ComD (histidine-kinase sensor) and ComE (response regulator), which in turn activates the alternative sigma factor SigX. This sigma factor then modulates the expression of competence genes to allow natural transformation (Håvarstein et al. 1995). Additionally, DNA binding occurs non-specifically at defined sites on the cell surface of Gram-positive bacteria (Dubnau 1999). On the other hand, natural competence in Gram-negative bacteria is mediated by TFP, as well as competence and recombination proteins. Initially, the extracellular DNA is bound by TFP through their tip (Ellison et al. 2018), while the competence protein ComEA performs the translocation of DNA to the periplasm through the PilQ secretin (Seitz et al. 2014). In the periplasms, the DNA is concomitantly degraded to a single strand by an unidentified exonuclease and transferred to the cytoplasm through the ComEC channel (Dubnau and Blokesch 2019). At last, the ssDNA is bound by DprA, which recruits RecA that will perform recombination with the recipient chromosome if homology is found (Dubnau and Blokesch 2019; Seitz and Blokesch 2013a).

TFP are involved in the initial step of the natural competence process. As mentioned, they mediate the binding of the exogenous DNA, which upon TFP retraction is presented to the cell surface, where entry into the cytoplasm is performed by ComEA (Ellison et al. 2018; Seitz et al. 2014). TFP are mainly encoded and regulated by *pil* genes, which are required for their proper assembly and functioning (Burdman et al. 2011; Mattick 2002). The core structure of TFP includes the major pilin subunit PilA (Mattick 2002), as well as minor pilins that prime the assembly of the structure and promote the positioning of the pilY1 adhesin at the tip of the pilus

(Nguyen et al. 2015); the pilQ secretin required for TFP extrusion (Mattick 2002); an inner membrane motor subcomplex that includes the prepilin peptidase PilD (Giltner et al. 2010; Strom et al. 1993), the platform protein PilC (Takhar et al. 2013) and dedicated extension (PilB) and retraction (PilT and PilU) ATPases (Mattick 2002); the alignment subcomplex PilMNOP that is needed for TFP stabilization and assembly (Tammam et al. 2013); as well as regulatory proteins such as the two-component regulatory system PilR/S, the chemosensory system comprised by PilGHIJL and ChpB/C, and the signal transduction protein PilZ (Alm et al. 1996; Cursino et al. 2011; Darzins 1994; Guzzo et al. 2009; Ishimoto and Lory 1992; Jin et al. 1994; Kilmury and Burrows 2016). In addition, some species-specific minor pilins may dictate additional functions of TFP, such as aggregation and adherence, according to sequence differences in their C-terminal regions (Giltner et al. 2012; Jacobsen et al. 2020). The structure and mechanism of TFP involved in both natural competence and twitching motility of bacterial species is shown in **Fig. 4-1**.

Functional studies of TFP components in *Pseudomonas aeruginosa* and *V. cholerae* demonstrated that individual *pil* genes have a role in the natural competence of these bacteria but are not essential for this trait (Nolan et al. 2020; Seitz and Blokesch 2013b). Conversely, deletion of the major pilin PilA, as well as of the secretin PilQ and the retraction ATPase PilT abrogates natural competence in both *Acinetobacter baylyi* and *A. baumannii*. Additional *pil* genes that are essential for the natural competence of some of these bacteria include *pilC*, *pilF*, *pilG*, *pilM*, *pilR*, *pilS*, *pilU*, *pilW*, and *pilX* (Leong et al. 2017; Vesel and Blokesch 2021). Moreover, TFP genes have been demonstrated to be important for the natural competence of other bacteria, including *N. gonorrhoeae* (Drake et al. 1997), *N. meningitidis* (Brown et al. 2010), and *L.*

pneumophila (Hardy et al. 2021). Curiously, it was recently demonstrated that the ComP minor pilin is the DNA receptor of the *Neisseria* pilus (Berry et al. 2013; Berry et al. 2016; Cehovin et al. 2013), whereas another minor pilin, ComZ, is the DNA receptor for the TFP of *Thermus thermophilus* (Salleh et al. 2019). However, these minor pilins are specific to each of these groups of bacteria, and it is currently not known which TFP components of other bacteria are responsible for binding extracellular DNA to initiate natural competence.

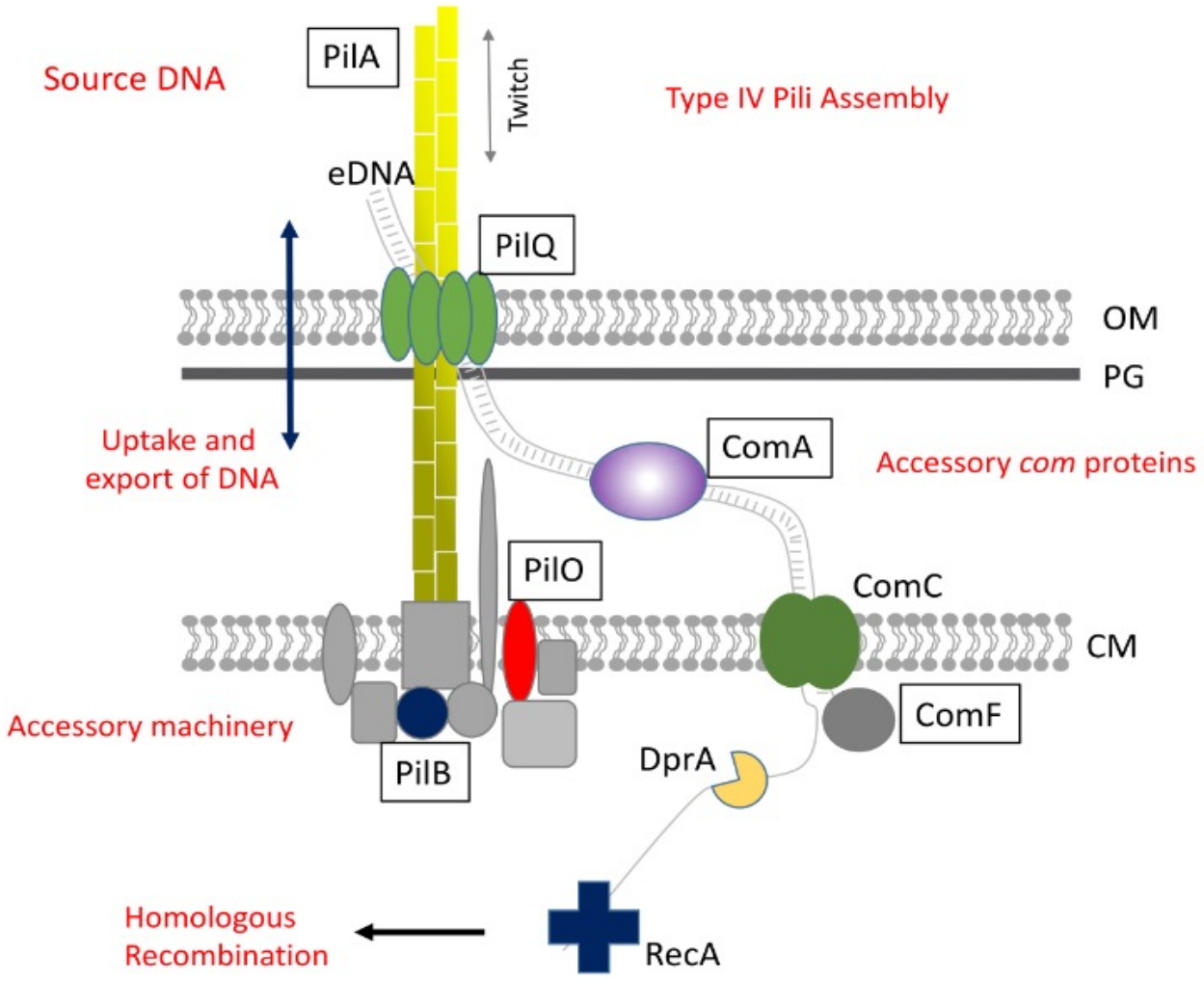

Fig. 4-1. General TFP structure and mechanism required for twitching motility and natural competence in Gram-negative bacteria. See text for details. eDNA – exogenous DNA; OM – outer membrane; PG – peptidoglycan layer; CM – cytoplasmic membrane.

The role of natural competence in evolution and adaptation

It has been suggested that natural competence confers adaptive advantages to recipient cells by increasing their genetic diversity (Johnsborg et al. 2007; Johnston et al. 2014; Seitz and Blokesch 2013a; Wiedenbeck and Cohan 2011). However, actual experimental demonstrations of this phenomenon are scarce. The first experiment by Griffith brilliantly illustrated the transfer of virulence from a pathogenic strain to a non-pathogenic strain by natural competence (Griffith 1928). More recently, natural competence was demonstrated to increase the rate of adaptation in the human pathogen *H. pylori* by increasing its fitness (Baltrus et al. 2008). Similar results have also been observed in *Bacillus subtilis* (Power et al. 2021) and *R. solanacearum* (Coupat-Goutaland et al. 2011). In addition, DNA uptake by itself increases the fitness of *A. baylyi*, regardless of UV stress, but with recombination reducing survival of cells (Hülter et al. 2017). Therefore, there is still much room for investigation of whether and how natural competence may shape bacterial evolution and adaption.

Naturally competent plant pathogenic bacteria

Only two plant pathogens have been described as naturally competent to date: *R. solanacearum* (Bertolla et al. 1997) and *X. fastidiosa* (Kung and Almeida 2011). *R. solanacearum* is competent during the exponential growth phase, with the highest transformation frequency being obtained when cells are grown in minimal medium (Bertolla et al. 1997). Additionally, DNA from closely related species is preferred, whereas the transformation frequency is affected by the concentration of DNA in medium. Together, these data suggest that starvation may induce competence in *R. solanacearum*, and that the preference for self-DNA may indicate the role of competence for DNA repair (Bertolla et al. 1997). Other study has

demonstrated that *R. solanacearum* cells can exchange large fragments of DNA (39.4 to 78.9 kb) through natural competence, which increased the virulence of one of the recipient strains to tomato plants (Coupat-Goutaland et al. 2011). This suggests that DNA exchange through natural competence increases the adaptability of this plant pathogen, but more investigation is needed. Remarkably, the natural competence of *R. solanacearum* has been observed to indeed develop in planta (Bertolla et al. 1999).

The natural competence of *X. fastidiosa*

As similarly described for *R. solanacearum*, natural competence in *X. fastidiosa* is highest at the exponential phase of growth and when cells are cultured in a minimal medium (Kung and Almeida 2011). Curiously, the use of donor DNA methylated with a methyl transferase from *X. fastidiosa* resulted in higher transformation frequencies than non-methylated DNA, indicating a preference for self-DNA (Kung and Almeida 2011). The use of solid agar media also increases the recombination frequency in comparison to liquid medium (Kung and Almeida 2011, 2014). *X. fastidiosa* cells required homologous flanking sequences of at least 96 bp for natural competence to occur, with maximum recombination frequency observed when using 1 kb of flanking homology. Besides, the length of non-homologous insert negatively correlates with recombination frequency, supporting the preference for self-DNA uptake (Kung et al. 2013).

Further studies also demonstrated that natural competence readily occurs when growing *X. fastidiosa* under conditions mimicking its natural habitats, by using grapevine sap as culture medium (Kandel et al. 2016), suggesting that natural competence may occur in planta. Moreover,

strains belonging to different subspecies were demonstrated to recombine in vitro. Specifically, the occurrence of recombination when using heat-killed donor cells suggest that natural competence is a major force driving HR in *X. fastidiosa* to generate genetic diversity (Kandel et al. 2017). In addition, different strains of this pathogen present different natural competence rates, which positively and significantly correlates with their twitching motility ability (Kandel et al. 2017).

However, there is limited information regarding the molecular mechanism of natural competence in *X. fastidiosa* and to what extent homologous recombination events shape its evolution. TFP genes have been demonstrated to participate in the natural competence of the pathogen (Kung and Almeida 2014), but only few genes were analyzed. TFP mediate both natural competence and twitching motility in many bacterial species (Dubnau and Blokesch 2019; Jarrell and McBride 2008), which is indeed observed in *X. fastidiosa* (Kandel et al. 2017). Therefore, additional studies are needed to understand the mechanism of natural competence in *X. fastidiosa* and how the molecular components of an important structure such as TFP mediate the interplay between its natural competence and twitching motility traits. Furthermore, the ability of homologous recombination to contribute to the genetic diversity of *X. fastidiosa* and its probable role in disease emergence also need to be investigated.

Long-term goal

Characterize mechanisms of DNA uptake and recombination in *X. fastidiosa*, as well as define the importance of intersubspecific recombination in its evolution, virulence, and host adaptation. Understanding the mechanisms by which *X. fastidiosa* may spread and emerge as a

plant pathogen in different hosts and parts of the world may contribute to the development of new management approaches, mediating the transfer of knowledge to agricultural practices.

Specific objectives

B.1. Determine the role of TFP molecular components in both natural transformation and twitching motility of *X. fastidiosa*.

B.2. Investigate the role of intersubspecific recombination in the virulence and host adaptation of *X. fastidiosa*.

Hypotheses

B.1. Individual components of the TFP machinery have different roles in natural transformation and twitching motility.

B.2. Whole genome analyses will allow the identification of defined regions that underwent intersubspecific homologous recombination events in *X. fastidiosa*.

References

Alm, R. A., Bodero, A. J., Free, P. D., and Mattick, J. S. 1996. Identification of a novel gene, *pilZ*, essential for type 4 fimbrial biogenesis in *Pseudomonas aeruginosa*. J Bacteriol 178:46-53.

Almeida, R. P. P. 2016. Can Apulia's olive trees be saved? Science 356:346-348.

Almeida, R. P. P., and Purcell, A. H. 2006. Patterns of *Xylella fastidiosa* colonization on the precibarium of sharpshooter vectors relative to transmission to plants. Ann Entomol Soc Am 99:884-890.

Almeida, R. P. P., and Nunney, L. 2015. How do plant diseases caused by *Xylella fastidiosa* emerge? Plant Dis 99:1457-1467.

Almeida, R. P. P., Coletta-Filho, H. D., and Lopes, J. R. S. 2014. *Xylella fastidiosa*. Pages 841-850 in: Manual of Security Sensitive Microbes and Toxins. D. Liu, ed. CRC Press, Boca Raton, FL.

Almeida, R. P. P., Blua, M. J., Lopes, J. R. S., and Purcell, A. H. 2005. Vector transmission of *Xylella fastidiosa*: applying fundamental knowledge to generate disease management strategies. Ann Entomol Soc Am 98:775-786.

Almeida, R. P. P., Nascimento, F. E., Chau, J., Prado, S. S., Tsai, C. W., Lopes, S. A., and Lopes, J. R. S. 2008. Genetic structure and biology of *Xylella fastidiosa* strains causing disease in citrus and coffee in Brazil. Appl Environ Microbiol 74:3690-3701.

Atsumi, T., Maekawa, Y., Yamada, T., Kawagishi, I., Imae, Y., and Homma, M. 1996. Effect of viscosity on swimming by the lateral and polar flagella of *Vibrio alginolyticus*. J Bacteriol 178:5024-5026.

Bahar, O., Goffer, T., and Burdman, S. 2009. Type IV pili are required for virulence, twitching motility, and biofilm formation of *Acidovorax avenae* subsp. *citrulli*. Mol Plant Microbe Interact 22:909-920.

Bahar, O., De La Fuente, L., and Burdman, S. 2010. Assessing adhesion, biofilm formation and motility of *Acidovorax citrulli* using microfluidic flow chambers. FEMS Microbiol Lett 312:33-39.

Bakkali, M. 2013. Could DNA uptake be a side effect of bacterial adhesion and twitching motility? Arch Microbiol 195:279-289.

Baltrus, D. A., Guillemin, K., and Phillips, P. C. 2008. Natural transformation increases the rate of adaptation in the human pathogen *Helicobacter pylori*. Evolution 62:39-49.

Berry, J. L., Cehovin, A., McDowell, M. A., Lea, S. M., and Pelicic, V. 2013. Functional analysis of the interdependence between DNA uptake sequence and its cognate ComP receptor during natural transformation in *Neisseria* species. PLoS Genet 9:e1004014.

Berry, J. L., Xu, Y., Ward, P. N., Lea, S. M., Matthews, S. J., and Pelicic, V. 2016. A comparative structure/function analysis of two type IV pilin DNA receptors defines a novel mode of DNA binding. Structure 24:926-934.

Berry, M. C., McGhee, G. C., Zhao, Y., and Sundin, G. W. 2009. Effect of a *waaL* mutation on lipopolysaccharide composition, oxidative stress survival, and virulence in *Erwinia amylovora*. FEMS Microbiol Lett 291:80-87.

Bertolla, F., Van Gijsegem, F., Nesme, X., and Simonet, P. 1997. Conditions for natural transformation of *Ralstonia solanacearum*. Appl Environ Microbiol 63:4965-4968.

Bertolla, F., Frostegård, Å., Brito, B., Nesme, X., and Simonet, P. 1999. During infection of its host, the plant pathogen *Ralstonia solanacearum* naturally develops a state of competence and exchanges genetic material. Mol Plant Microbe Interact 12:467-472.
Biswas, G. D., Sox, T., Blackman, E., and Sparling, P. F. 1977. Factors affecting genetic transformation of *Neisseria gonorrhoeae*. J Bacteriol 129:983-992.
Bové, J. M., and Ayres, A. J. 2007. Etiology of three recent diseases of citrus in São Paulo State: sudden death, variegated chlorosis and Huanglongbing. IUBMB Life 59:346-354.
Brown, D. R., Helaine, S., Carbonnelle, E., and Pelicic, V. 2010. Systematic functional analysis reveals that a set of seven genes is involved in fine-tuning of the multiple functions mediated by type IV pili in *Neisseria meningitidis*. Infect Immun 78:3053–3063.
Burdman, S., Bahar, O., Parker, J. K., and De La Fuente, L. 2011. Involvement of type IV pili in pathogenicity of plant pathogenic bacteria. Genes 2:706-735.
Caldwell, D., Kim, B. S., and Iyer-Pascuzzi, A. S. 2017. *Ralstonia solanacearum* differentially colonizes roots of resistant and susceptible tomato plants. Phytopathology 107:528-536.
Cameron, A. D. S., Volar, M., Bannister, L. A., and Redfield, R. J. 2008. RNA secondary structure regulates the translation of *sxy* and competence development in *Haemophilus influenzae*. Nucleic Acids Res 36:10-20.
Castillo, A. I., Chacón-Díaz, C., Rodríguez-Murillo, N., Coletta-Filho, H. D., and Almeida, R. P. P. 2020. Impacts of local population history and ecology on the evolution of a globally dispersed pathogen. BMC Genomics 21:369.
Catlin, B. W. 1960. Transformation of *Neisseria meningitidis* by deoxyribonucleates from cells and from culture slime. J Bacteriol 79:579-590.
Cehovin, A., Simpson, P. J., McDowell, M. A., Brown, D. R., Noschese, R., Pallett, M., Brady, J., Baldwin, G. S., Lea, S. M., Matthews, S. J., and Pelicic, V. 2013. Specific DNA recognition mediated by a type IV pilin. Proc Natl Acad Sci U S A 110:3065-3070.
Chandler, M. S. 1992. The gene encoding cAMP receptor protein is required for competence development in *Haemophilus influenzae* Rd. Proc Natl Acad Sci USA 89:1626-1630.
Chang, C. J., Donaldson, R., Brannen, P., Krewer, G., and Boland, R. 2009. Bacterial leaf scorch, a new blueberry disease caused by *Xylella fastidiosa*. HortScience 44:413-417.
Charpentier, X., Kay, E., Schneider, D., and Shuman, H. A. 2011. Antibiotics and UV radiation induce competence for natural transformation in *Legionella pneumophila*. J Bacteriol 193:1114-1121.
Chatterjee, S., Almeida, R. P. P., and Lindow, S. 2008a. Living in two worlds: the plant and insect lifestyles of *Xylella fastidiosa*. Annu Rev Phytopathol 46:243-271.
Chatterjee, S., Wistrom, C., and Lindow, S. E. 2008b. A cell-cell signaling sensor is required for virulence and insect transmission of *Xylella fastidiosa*. Proc Natl Acad Sci U S A 105:2670-2675.
Chatterjee, S., Newman, K. L., and Lindow, S. E. 2008c. Cell-to-Cell signaling in *Xylella fastidiosa* suppresses movement and xylem vessel colonization in grape. Mol Plant Microbe Interact 21:1309-1315.
Choat, B., Cobb, A. R., and Jansen, S. 2008. Structure and function of bordered pits: new discoveries and impacts on whole-plant hydraulic function. New Phytol 177:608-626.
Clifford, J. C., Rapicavoli, J. N., and Roper, M. C. 2013. A rhamnose-rich O-antigen mediates adhesion, virulence, and host colonization for the xylem-limited phytopathogen *Xylella fastidiosa*. Mol Plant Microbe Interact 26:676-685.

Colella, C., Carradore, R., and Cerroni, A. 2019. Problem setting and problem solving in the case of olive quick decline syndrome in Apulia, Italy: a sociological approach. Phytopathology 109:187-199.
Coletta-Filho, H. D., Francisco, C. S., Lopes, J. R. S., Muller, C., and Almeida, R. P. P. 2017. Homologous recombination and *Xylella fastidiosa* host-pathogen associations in South America. Phytopathology 107:305-312.
Cornara, D., Saponari, M., Zeilinger, A. R., de Stradis, A., Boscia, D., Loconsole, G., Bosco, D., Martelli, G. P., Almeida, R. P. P., and Porcelli, F. 2017. Spittlebugs as vectors of *Xylella fastidiosa* in olive orchards in Italy. J Pest Sci (2004) 90:521-530.
Corral, J., Sebastià, P., Coll, N. S., Barbé, J., Aranda, J., and Valls, M. 2020. Twitching and swimming motility play a role in *Ralstonia solanacearum* pathogenicity. mSphere 5:e00740-00719.
Costerton, J. W., Lewandowski, Z., Caldwell, D. E., Korber, D. R., and Lappin-Scott, H. M. 1995. Microbial biofilms. Annu Rev Microbiol 49:711-745.
Coupat-Goutaland, B., Bernillon, D., Guidot, A., Prior, P., Nesme, X., and Bertolla, F. 2011. *Ralstonia solanacearum* virulence increased following large interstrain gene transfers by natural transformation. Mol Plant Microbe Interact 24:497-505.
Cruz, L. F., Parker, J. K., Cobine, P. A., and De La Fuente, L. 2014. Calcium-enhanced twitching motility in *Xylella fastidiosa* is linked to a single PilY1 homolog. Appl Environ Microbiol 80:7176-7185.
Cursino, L., Galvani, C. D., Athinuwat, D., Zaini, P. A., Li, Y., De La Fuente, L., Hoch, H. C., Burr, T. J., and Mowery, P. 2011. Identification of an operon, Pil-Chp, that controls twitching motility and virulence in *Xylella fastidiosa*. Mol Plant Microbe Interact 24:1198-1206.
Darzins, A. 1994. Characterization of a *Pseudomonas aeruginosa* gene cluster involved in pilus biosynthesis and twitching motility: sequence similarity to the chemotaxis proteins of enterics and the gliding bacterium *Myxococcus xanthus*. Mol Microbiol 11:137-153.
Das, A., Rangaraj, N., and Sonti, R. V. 2009. Multiple adhesin-like functions of *Xanthomonas oryzae* pv. *oryzae* are involved in promoting leaf attachment, entry, and virulence on rice. Mol Plant Microbe Interact 22:73-85.
Davey, M. E., and O'Toole, G. A. 2000. Microbial biofilms: from ecology to molecular genetics. Microbiol Mol Biol Rev 64:847-867.
De La Fuente, L., Burr, T. J., and Hoch, H. C. 2007. Mutations in type I and type IV pilus biosynthetic genes affect twitching motility rates in Xylella fastidiosa. J Bacteriol 189:7507-7510.
Denancé, N., Legendre, B., Briand, M., Olivier, V., de Boisseson, C., Poliakoff, F., and Jacques, M. A. 2017. Several subspecies and sequence types are associated with the emergence of *Xylella fastidiosa* in natural settings in France. Plant Pathology 66:1054-1064.
Dorer, M. S., Fero, J., and Salama, N. R. 2010. DNA damage triggers genetic exchange in *Helicobacter pylori*. PLoS Pathog 6:e1001026.
Dorer, M. S., Sessler, T. H., and Salama, N. R. 2011. Recombination and DNA repair in *Helicobacter pylori*. Annu Rev Microbiol 65:329-348.
Dorocicz, I., Williams, P. M., and Redfield, R. J. 1993. The *Haemophilus influenzae* adenylate cyclase gene: cloning, sequence, and essential role in competence. J Bacteriol 175:7142-7149.

Drake, S. L., Sandstedt, S. A., and Koomey, M. 1997. PilP, a pilus biogenesis lipoprotein in *Neisseria gonorrhoeae*, affects expression of PilQ as a high-molecular-mass multimer. Mol Microbiol 23:657-668.
Dubnau, D. 1999. DNA uptake in bacteria. Annu Rev Microbiol 53:217-244.
Dubnau, D., and Blokesch, M. 2019. Mechanisms of DNA uptake by naturally competent bacteria. Annu Rev Genet 53:217-237.
EFSA. 2015. Scientific Opinion on the risks to plant health posed by *Xylella fastidiosa* in the EU territory, with the identification and evaluation of risk reduction options. EFSA J 13:3989.
EFSA. 2021. Update of the *Xylella* spp. host plant database – systematic literature search up to 31 December 2020. EFSA J 19:6674.
Elkins, C., Thomas, C., Seifert, H., and Sparling, P. 1991. Species-specific uptake of DNA by gonococci is mediated by a 10-base-pair sequence. J Bacteriol 173:3911-3913.
Ellison, C. K., Dalia, T. N., Vidal Ceballos, A., Wang, J. C., Biais, N., Brun, Y. V., and Dalia, A. B. 2018. Retraction of DNA-bound type IV competence pili initiates DNA uptake during natural transformation in *Vibrio cholerae*. Nat Microbiol 3:773-780.
Emge, P., Moeller, J., Jang, H., Rusconi, R., Yawata, Y., Stocker, R., and Vogel, V. 2016. Resilience of bacterial quorum sensing against fluid flow. Sci Rep 6:33115.
Feil, H., Feil, W. S., and Lindow, S. E. 2007. Contribution of fimbrial and afimbrial adhesins of *Xylella fastidiosa* to attachment to surfaces and virulence to grape. Phytopathology 97:318-324.
Giampetruzzi, A., Saponari, M., Almeida, R. P. P., Essakhi, S., Boscia, D., Loconsole, G., and Saldarelli, P. 2017. Complete genome sequence of the olive-infecting strain *Xylella fastidiosa* subsp. *pauca* De Donno. Genome Announc 5.
Giltner, C. L., Habash, M., and Burrows, L. L. 2010. *Pseudomonas aeruginosa* minor pilins are incorporated into type IV pili. J Mol Biol 398:444-461.
Giltner, C. L., Nguyen, Y., and Burrows, L. L. 2012. Type IV pilin proteins: versatile molecular modules. Microbiol Mol Biol Rev 76:740-772.
Goodwin, P., and Purcell, A. H. 1992. Pierce's Disease. Pages 76-84 in: Grape Pest Management. University of California, Divison of Agriculture and Natural Resources, Oakland, USA.
Griffith, F. 1928. The significance of pneumococcal types. J Hyg 27:113-159.
Guilhabert, M. R., and Kirkpatrick, B. C. 2005. Identification of *Xylella fastidiosa* antivirulence genes: hemagglutinin adhesins contribute to *X. fastidiosa* biofilm maturation and colonization and attenuate virulence. Mol Plant Microbe Interact 18:856-868.
Guzzo, C. R., Salinas, R. K., Andrade, M. O., and Farah, C. S. 2009. PILZ protein structure and interactions with PILB and the FIMX EAL domain: implications for control of type IV pilus biogenesis. J Mol Biol 393:848-866.
Hardy, L., Juan, P. A., Coupat-Goutaland, B., and Charpentier, X. 2021. Transposon insertion sequencing in a clinical isolate of *Legionella pneumophila* identifies essential genes and determinants of natural transformation. J Bacteriol 203:e00548-00520.
Håvarstein, L. S., Coomaraswamy, G., and Morrison, D. A. 1995. An unmodified heptadecapeptide pheromone induces competence for genetic transformation in *Streptococcus pneumoniae*. Proc Natl Acad Sci USA 92:11140-11144.

Hernandez-Martinez, R., de la Cerda, K. A., Costa, H. S., Cooksey, D. A., and Wong, F. P. 2007. Phylogenetic relationships of *Xylella fastidiosa* strains isolated from landscape ornamentals in southern California. Phytopathology 97:857-864.

Herrera, C. M., Koutsoudis, M. D., Wang, X., and von Bodman, S. B. 2008. *Pantoea stewartii* subsp. *stewartii* exhibits surface motility, which is a critical aspect of Stewart's wilt disease development on maize. Mol Plant Microbe Interact 21:1359-1370.

Herriott, R. M., Meyer, E. M., and Vogt, M. 1970. Defined nongrowth media for stage II development of competence in *Haemophilus influenzae*. J Bacteriol 101:517-524.

Hewit, W., Frazier, N., Jacob, H., and Freitag, J. 1942. Pierce's disease of grapevines. Calif Agric Exp Stn Circ 353:1-32.

Hopkins, D. L., and Purcell, A. H. 2002. *Xylella fastidiosa*: Cause of Pierce's Disease of grapevine and other emergent diseases. Plant Dis 86:1056-1066.

Hülter, N., Sørum, V., Borch-Pedersen, K., Liljegren, M. M., Utnes, A. L. G., Primicerio, R., Harms, K., and Johnsen, P. J. 2017. Costs and benefits of natural transformation in *Acinetobacter baylyi*. BMC Microbiol 17:34.

Humbert, O., and Salama, N. R. 2008. The *Helicobacter pylori* HpyAXII restriction–modification system limits exogenous DNA uptake by targeting GTAC sites but shows asymmetric conservation of the DNA methyltransferase and restriction endonuclease components. Nucleic Acids Res 36:6893-6906.

Ingel, B., Reyes, C., Massonnet, M., Boudreau, B., Sun, Y., Sun, Q., McElrone, A. J., Cantu, D., and Roper, M. C. 2021. *Xylella fastidiosa* causes transcriptional shifts that precede tylose formation and starch depletion in xylem. Mol Plant Pathol 22:175-188.

Ionescu, M., Baccari, C., Da Silva, A. M., Garcia, A., Yokota, K., and Lindow, S. E. 2013. Diffusible signal factor (DSF) synthase RpfF of *Xylella fastidiosa* is a multifunction protein also required for response to DSF. J Bacteriol 195:5273-5284.

Ionescu, M., Zaini, P. A., Baccari, C., Tran, S., da Silva, A. M., and Lindow, S. E. 2014. *Xylella fastidiosa* outer membrane vesicles modulate plant colonization by blocking attachment to surfaces. Proc Natl Acad Sci U S A 111:E3910-3918.

Ishimoto, K. Y., and Lory, S. 1992. Identification of pilR, which encodes a transcriptional activator of the *Pseudomonas aeruginosa* pilin gene. J Bacteriol 174:3514-3521.

Israel, D. A., Lou, A. S., and Blaser, M. J. 2000. Characteristics of *Helicobacter pylori* natural transformation. FEMS Microbiol Lett 186:275-280.

Jacobsen, T., Bardiaux, B., Francetic, O., Izadi-Pruneyre, N., and Nilges, M. 2020. Structure and function of minor pilins of type IV pili. Med Microbiol Immunol 209:301-308.

Jacques, M. A., Denancé, N., Legendre, B., Morel, E., Briand, M., Mississipi, S., Durand, K., Olivier, V., Portier, P., Poliakoff, F., and Crouzillat, D. 2016. New coffee plant-infecting *Xylella fastidiosa* variants derived via homologous recombination. Appl Environ Microbiol 82:1556-1568.

Janse, J. D., and Obradovic, A. 2010. *Xylella fastidiosa*: its biology, diagnosis, control and risks. J Plant Pathol 92:S1.35-48.

Jarrell, K. F., and McBride, M. J. 2008. The surprisingly diverse ways that prokaryotes move. Nat Rev Microbiol 6:466-476.

Jin, S., Ishimoto, K. Y., and Lory, S. 1994. PilR, a transcriptional regulator of piliation in *Pseudomonas aeruginosa*, binds to a *cis*-acting sequence upstream of the pilin gene promoter. Mol Microbiol 14:1049-1057.

Johnsborg, O., Eldholm, V., and Håvarstein, L. S. 2007. Natural genetic transformation: prevalence, mechanisms and function. Res Microbiol 158:767-778.
Johnston, C., Martin, B., Fichant, G., Polard, P., and Claverys, J. P. 2014. Bacterial transformation: distribution, shared mechanisms and divergent control. Nat Rev Microbiol 12:181-196.
Kandel, P. P., Lopez, S. M., Almeida, R. P. P., and De La Fuente, L. 2016. Natural competence of *Xylella fastidiosa* occurs at a high frequency inside microfluidic chambers mimicking the bacterium's natural habitats. Appl Environ Microbiol 82:5269-5277.
Kandel, P. P., Almeida, R. P. P., Cobine, P. A., and De La Fuente, L. 2017. Natural competence rates are variable among *Xylella fastidiosa* strains and homologous recombination occurs in vitro between subspecies *fastidiosa* and *multiplex*. Mol Plant Microbe Interact 30:589-600.
Kang, Y., Liu, H., Genin, S., Schell, M. A., and Denny, T. P. 2002. *Ralstonia solanacearum* requires type 4 pili to adhere to multiple surfaces and for natural transformation and virulence. Mol Microbiol 2:427-437.
Kharadi, R. R., and Sundin, G. W. 2020. Dissecting the process of xylem colonization through biofilm formation in *Erwinia amylovora*. J Plant Pathol 103:41-49.
Killiny, N., and Almeida, R. P. P. 2009. *Xylella fastidiosa* afimbrial adhesins mediate cell transmission to plants by leafhopper vectors. Appl Environ Microbiol 75:521-528.
Kilmury, S. L., and Burrows, L. L. 2016. Type IV pilins regulate their own expression via direct intramembrane interactions with the sensor kinase PilS. Proc Natl Acad Sci U S A 113:6017-6022.
Kim, M. K., Ingremeau, F., Zhao, A., Bassler, B. L., and Stone, H. A. 2016. Local and global consequences of flow on bacterial quorum sensing. Nat Microbiol 1:15005.
Koczan, J. M., McGrath, M. J., Zhao, Y., and Sundin, G. W. 2009. Contribution of *Erwinia amylovora* exopolysaccharides amylovoran and levan to biofilm formation: implications in pathogenicity. Phytopathology 99:1237-1244.
Koutsoudis, M. D., Tsaltas, D., Minogue, T. D., and von Bodman, S. B. 2006. Quorum-sensing regulation governs bacterial adhesion, biofilm development, and host colonization in *Pantoea stewartii* subspecies *stewartii*. Proc Natl Acad Sci U S A 103:5983-5988.
Kuehn, M. J., and Kesty, N. C. 2005. Bacterial outer membrane vesicles and the host-pathogen interaction. Genes Dev 19:2645-2655.
Kung, S. H., and Almeida, R. P. P. 2011. Natural competence and recombination in the plant pathogen *Xylella fastidiosa*. Appl Environ Microbiol 77:5278-5284.
Kung, S. H., and Almeida, R. P. P. 2014. Biological and genetic factors regulating natural competence in a bacterial plant pathogen. Microbiology 160:37-46.
Kung, S. H., Retchless, A. C., Kwan, J. Y., and Almeida, R. P. P. 2013. Effects of DNA size on transformation and recombination efficiencies in *Xylella fastidiosa*. Appl Environ Microbiol 79:1712-1717.
Landa, B. B., Castillo, A. I., Giampetruzzi, A., Kahn, A., Roman-Ecija, M., Velasco-Amo, M. P., Navas-Cortés, J. A., Marco-Noales, E., Barbé, S., Moralejo, E., Coletta-Filho, H. D., Saldarelli, P., Saponari, M., and Almeida, R. P. P. 2020. Emergence of a plant pathogen in Europe associated with multiple intercontinental introductions. Appl Environ Microbiol 86:e01521-01519.
Lenhart, J. S., Schroeder, J. W., Walsh, B. W., and Simmons, L. A. 2012. DNA repair and genome maintenance in *Bacillus subtilis*. Microbiol Mol Biol Rev 76:530-564.

Leong, C. G., Bloomfield, R. A., Boyd, C. A., Dornbusch, A. J., Lieber, L., Liu, F., Owen, A., Slay, E., Lang, K. M., and Lostroh, C. P. 2017. The role of core and accessory type IV pilus genes in natural transformation and twitching motility in the bacterium *Acinetobacter baylyi*. PLoS One 12:e0182139.

Li, Y., Hao, G., Galvani, C. D., Meng, Y., De La Fuente, L., Hoch, H. C., and Burr, T. J. 2007. Type I and type IV pili of *Xylella fastidiosa* affect twitching motility, biofilm formation and cell-cell aggregation. Microbiology 153:719-726.

Lim, S. H., So, B. H., Wang, J. C., Song, E. S., Park, Y. J., Lee, B. M., and Kang, H. W. 2008. Functional analysis of *pilQ* gene in *Xanthomonas oryzae* pv. *oryzae*, bacterial blight pathogen of rice. J Microbiol 46:214-220.

Liu, H., Kang, Y., Genin, S., Schell, M. A., and Denny, T. P. 2001. Twitching motility of *Ralstonia solanacearum* requires a type IV pilus system. Microbiology 147:3215-3229.

Lorenz, M. G., and Wackernagel, W. 1994. Bacterial gene transfer by natural genetic transformation in the environment. Microbiol Rev 58:563-602.

Lowe-Power, T. M., Khokhani, D., and Allen, C. 2018. How *Ralstonia solanacearum* exploits and thrives in the flowing plant xylem environment. Trends Microbiol 26:929-942.

Macfadyen, L. P., Chen, D., Vo, H. C., Liao, D., Sinotte, R., and Redfield, R. J. 2001. Competence development by *Haemophilus influenzae* is regulated by the availability of nucleic acid precursors. Mol Microbiol 40:700-707.

Mah, T. F. C., and O'Toole, G. A. 2001. Mechanisms of biofilm resistance to antimicrobial agents. Trends Microbiol 9:34-39.

Marcelletti, S., and Scortichini, M. 2016. *Xylella fastidiosa* CoDiRO strain associated with the olive quick decline syndrome in southern Italy belongs to a clonal complex of the subspecies *pauca* that evolved in Central America. Microbiology 162:2087-2098.

Martelli, G. P., Boscia, D., Porcelli, F., and Saponari, M. 2016. The olive quick decline syndrome in south-east Italy: a threatening phytosanitary emergency. Eur J Plant Pathol 144:235-243.

Mattick, J. S. 2002. Type IV pili and twitching motility. Annu Rev Microbiol 56:289-314.

McCarthy, Y., Ryan, R. P., O'Donovan, K., He, Y. Q., Jiang, B. L., Feng, J. X., Tang, J. L., and Dow, J. M. 2008. The role of PilZ domain proteins in the virulence of *Xanthomonas campestris* pv. *campestris*. Mol Plant Pathol 9:819-824.

McElrone, A. J., Jackson, S., and Habdas, P. 2008. Hydraulic disruption and passive migration by a bacterial pathogen in oak tree xylem. J Exp Bot 59:2649-2657.

Meibom, K. L., Blokesch, M., Dolganov, N. A., Wu, C. Y., and Schoolnik, G. K. 2005. Chitin induces natural competence in *Vibrio cholerae*. Science 310:1824-1827.

Meng, Y., Li, Y., Galvani, C. D., Hao, G., Turner, J. N., Burr, T. J., and Hoch, H. C. 2005. Upstream migration of *Xylella fastidiosa* via pilus-driven twitching motility. J Bacteriol 187:5560-5567.

Mori, Y., Inoue, K., Ikeda, K., Nakayashiki, H., Higashimoto, C., Ohnishi, K., Kiba, A., and Hikichi, Y. 2016. The vascular plant-pathogenic bacterium *Ralstonia solanacearum* produces biofilms required for its virulence on the surfaces of tomato cells adjacent to intercellular spaces. Mol Plant Pathol 17:890-902.

Morris, C. E., and Monier, J. M. 2003. The ecological significance of biofilm formation by plant-associated bacteria. Annu Rev Phytopathol 41:429-453.

Newman, K. L., Almeida, R. P. P., Purcell, A. H., and Lindow, S. E. 2004. Cell-cell signaling controls *Xylella fastidiosa* interactions with both insects and plants. Proc Natl Acad Sci U S A 101:1737-1742.

Nguyen, L. C., Taguchi, F., Tran, Q. M., Naito, K., Yamamoto, M., Ohnishi-Kameyama, M., Ono, H., Yoshida, M., Chiku, K., Ishii, T., Inagaki, Y., Toyoda, K., Shiraishi, T., and Ichinose, Y. 2012. Type IV pilin is glycosylated in *Pseudomonas syringae* pv. *tabaci* 6605 and is required for surface motility and virulence. Mol Plant Pathol 13:764-774.

Nguyen, Y., Sugiman-Marangos, S., Harvey, H., Bell, S. D., Charlton, C. L., Junop, M. S., and Burrows, L. L. 2015. *Pseudomonas aeruginosa* minor pilins prime type IVa pilus assembly and promote surface display of the PilY1 adhesin. J Biol Chem 290:601-611.

Nolan, L. M., Turnbull, L., Katrib, M., Osvath, S. R., Losa, D., Lazenby, J. J., and Whitchurch, C. B. 2020. *Pseudomonas aeruginosa* is capable of natural transformation in biofilms. Microbiology 166:995-1003.

Nunney, L., Yuan, X., Bromley, R. E., and Stouthamer, R. 2012. Detecting genetic introgression: high levels of intersubspecific recombination found in *Xylella fastidiosa* in Brazil. Appl Environ Microbiol 78:4702-4714.

Nunney, L., Hopkins, D. L., Morano, L. D., Russell, S. E., and Stouthamer, R. 2014a. Intersubspecific recombination in *Xylella fastidiosa* strains native to the United States: infection of novel hosts associated with an unsuccessful invasion. Appl Environ Microbiol 80:1159-1169.

Nunney, L., Schuenzel, E. L., Scally, M., Bromley, R. E., and Stouthamer, R. 2014b. Large-scale intersubspecific recombination in the plant-pathogenic bacterium *Xylella fastidiosa* is associated with the host shift to mulberry. Appl Environ Microbiol 80:3025-3033.

Nunney, L., Yuan, X., Bromley, R., Hartung, J., Montero-Astúa, M., Moreira, L., Ortiz, B., and Stouthamer, R. 2010. Population genomic analysis of a bacterial plant pathogen: novel insight into the origin of Pierce's disease of grapevine in the U.S. PLoS One 5:e15488.

Olmo, D., Nieto, A., Adrover, F., Urbano, A., Beidas, O., Juan, A., Marco-Noales, E., López, M. M., Navarro, I., Monterde, A., Montes-Borrego, M., Navas-Cortés, J. A., and Landa, B. B. 2017. First detection of *Xylella fastidiosa* infecting cherry (*Prunus avium*) and *Polygala myrtifolia* plants, in Mallorca island, Spain. Plant Dis 101:1820.

Palmen, R., Buijsman, P., and Hellingwerf, K. J. 1994. Physiological regulation of competence induction for natural transformation in *Acinetobacter calcoaceticus*. Arch Microbiol 162:344-351.

Pérez-Donoso, A. G., Greve, L. C., Walton, J. H., Shackel, K. A., and Labavitch, J. M. 2007. Xylella fastidiosa infection and ethylene exposure result in xylem and water movement disruption in grapevine shoots. Plant Physiol 143:1024-1036.

Pérez-Donoso, A. G., Sun, Q., Roper, M. C., Greve, L. C., Kirkpatrick, B., and Labavitch, J. M. 2010. Cell wall-degrading enzymes enlarge the pore size of intervessel pit membranes in healthy and *Xylella fastidiosa*-infected grapevines. Plant Physiol 152:1748-1759.

Petit, G., Bleve, G., Gallo, A., Mita, G., Montanaro, G., Nuzzo, V., Zambonini, D., and Pitacco, A. 2021. Susceptibility to *Xylella fastidiosa* and functional xylem anatomy in *Olea europaea*: revisiting a tale of plant-pathogen interaction. AoB Plants 13:plab027.

Potnis, N., Kandel, P. P., Merfa, M. V., Retchless, A. C., Parker, J. K., Stenger, D. C., Almeida, R. P. P., Bergsma-Vlami, M., Westenberg, M., Cobine, P. A., and De La Fuente, L. 2019. Patterns of inter- and intrasubspecific homologous recombination inform eco-evolutionary dynamics of *Xylella fastidiosa*. ISME J 13:2319-2333.

Power, J. J., Pinheiro, F., Pompei, S., Kovacova, V., Yuksel, M., Rathmann, I., Förster, M., Lässig, M., and Maier, B. 2021. Adaptive evolution of hybrid bacteria by horizontal gene transfer. Proc Natl Acad Sci U S A 118:e2007873118.

Pradhan, B. B., Ranjan, M., and Chatterjee, S. 2012. XadM, a novel adhesin of *Xanthomonas oryzae* pv. *oryzae*, exhibits similarity to Rhs family proteins and is required for optimum attachment, biofilm formation, and virulence. Mol Plant Microbe Interact 25:1157-1170.

Prudhomme, M., Attaiech, L., Sanchez, G., Martin, B., and Claverys, J. P. 2006. Antibiotic stress induces genetic transformability in the human pathogen *Streptococcus pneumoniae*. Science 313:89-92.

Rapicavoli, J., Ingel, B., Blanco-Ulate, B., Cantu, D., and Roper, C. 2018. *Xylella fastidiosa*: an examination of a re-emerging plant pathogen. Mol Plant Pathol 19:786-800.

Ray, S. K., Rajeshwari, R., Sharma, Y., and Sonti, R. V. 2002. A high-molecular-weight outer membrane protein of *Xanthomonas oryzae* pv. *oryzae* exhibits similarity to non-fimbrial adhesins of animal pathogenic bacteria and is required for optimum virulence. Mol Microbiol 46:637-647.

Redfield, R. J. 1991. *sxy-1*, a *Haemophilus influenzae* mutation causing greatly enhanced spontaneous competence. J Bacteriol 173:5612-5618.

Redfield, R. J., Cameron, A. D. S., Qian, Q., Hinds, J., Ali, T. R., Kroll, J. S., and Langford, P. R. 2005. A novel CRP-dependent regulon controls expression of competence genes in *Haemophilus influenzae*. J Mol Biol 347:735-747.

Roine, E., Raineri, D. M., Romantschuk, M., Wilson, M., and Nunn, D. N. 1998. Characterization of type IV pilus genes in *Pseudomonas syringae* pv. *tomato* DC3000. Mol Plant Microbe Interact 11:1048-1056.

Rojas, C. M., Ham, J. H., Deng, W. L., Doyle, J. J., and Collmer, A. 2002. HecA, a member of a class of adhesins produced by diverse pathogenic bacteria, contributes to the attachment, aggregation, epidermal cell killing, and virulence phenotypes of *Erwinia chrysanthemi* EC16 on *Nicotiana clevelandii* seedlings. Proc Natl Acad Sci U S A 99:13142-13147.

Romantschuk, M., and Bamford, D. H. 1986. The causal agent of halo blight in bean, *Pseudomonas syringae* pv. *phaseolicola*, attaches to stomata via its pili. Microb Pathog 1:139-148.

Rooney, L. M., Amos, W. B., Hoskisson, P. A., and McConnell, G. 2020. Intra-colony channels in *E. coli* function as a nutrient uptake system. ISME J 14:2461-2473.

Roper, M. C., Greve, L. C., Warren, J. G., Labavitch, J. M., and Kirkpatrick, B. C. 2007. *Xylella fastidiosa* requires polygalacturonase for colonization and pathogenicity in *Vitis vinifera* grapevines. Mol Plant Microbe Interact 20:411-419.

Sabella, E., Aprile, A., Genga, A., Siciliano, T., Nutricati, E., Nicolì, F., Vergine, M., Negro, C., De Bellis, L., and Luvisi, A. 2019. Xylem cavitation susceptibility and refilling mechanisms in olive trees infected by Xylella fastidiosa. Sci Rep 9:9602.

Salleh, M. Z., Karuppiah, V., Snee, M., Thistlethwaite, A., Levy, C. W., Knight, D., and Derrick, J. P. 2019. Structure and properties of a natural competence-associated pilin suggest a unique pilus tip-associated DNA receptor. mBio 10:e00614-00619.

Saponari, M., Boscia, D., Nigro, F., and Martelli, G. P. 2013. Identification of DNA sequences related to *Xylella fastidiosa* in oleander, almond and olive trees exhibiting leaf scorch symptoms in Apulia (Southern Italy). J. Plant Pathol. 95:668.

Saponari, M., Loconsole, G., Cornara, D., Yokomi, R. K., De Stradis, A., Boscia, D., Bosco, D., Martelli, G. P., Krugner, R., and Porcelli, F. 2014. Infectivity and transmission of *Xylella*

fastidiosa by *Philaenus spumarius* (Hemiptera: Aphrophoridae) in Apulia, Italy. J Econ Entomol 107:1316-1319.
Scally, M., Schuenzel, E. L., Stouthamer, R., and Nunney, L. 2005. Multilocus sequence type system for the plant pathogen *Xylella fastidiosa* and relative contributions of recombination and point mutation to clonal diversity. Appl Environ Microbiol 71:8491-8499.
Schaad, N. W., Postnikova, E., Lacy, G., Fatmi, M., and Chang, C. J. 2004. *Xylella fastidiosa* subspecies: *X. fastidiosa* subsp. [correction] *fastidiosa* [correction] subsp. nov., *X. fastidiosa* subsp. *multiplex* subsp. nov., and *X. fastidiosa* subsp. *pauca* subsp. nov. Syst Appl Microbiol 27:290-300.
Schuenzel, E. L., Scally, M., Stouthamer, R., and Nunney, L. 2005. A multigene phylogenetic study of clonal diversity and divergence in North American strains of the plant pathogen *Xylella fastidiosa*. Appl Environ Microbiol 71:3832-3839.
Schwechheimer, C., and Kuehn, M. J. 2015. Outer-membrane vesicles from Gram-negative bacteria: biogenesis and functions. Nat Rev Microbiol 13:605-619.
Schwechheimer, C., Sullivan, C. J., and Kuehn, M. J. 2013. Envelope control of outer membrane vesicle production in Gram-negative bacteria. Biochemistry 52:3031-3040.
Scrudato, M. L., and Blokesch, M. 2012. The regulatory network of natural competence and transformation of *Vibrio cholerae*. PLoS Genet 8:e1002778.
Scrudato, M. L., and Blokesch, M. 2013. A transcriptional regulator linking quorum sensing and chitin induction to render *Vibrio cholerae* naturally transformable. Nucleic Acids Res 41:3644-3658.
Seitz, P., and Blokesch, M. 2013a. Cues and regulatory pathways involved in natural competence and transformation in pathogenic and environmental Gram-negative bacteria. FEMS Microbiol Rev 37:336-363.
Seitz, P., and Blokesch, M. 2013b. DNA-uptake machinery of naturally competent *Vibrio cholerae*. Proc Natl Acad Sci U S A 110:17987-17992.
Seitz, P., Pezeshgi Modarres, H., Borgeaud, S., Bulushev, R. D., Steinbock, L. J., Radenovic, A., Dal Peraro, M., and Blokesch, M. 2014. ComEA is essential for the transfer of external DNA into the periplasm in naturally transformable *Vibrio cholerae* cells. PLoS Genet 10:e1004066.
Shi, X., and Lin, H. 2016. Visualization of twitching motility and characterization of the role of the *PilG* in *Xylella fastidiosa*. J Vis Exp:e53816.
Shi, X., and Lin, H. 2018. The chemotaxis regulator *pilG* of *Xylella fastidiosa* is required for virulence in *Vitis vinifera* grapevines. Eur J Plant Pathol 150:351-362.
Simpson, A. J. G., Reinach, F. C., Arruda, P., Abreu, F. A., Acencio, M., Alvarenga, R., Alves, L. M. C., Araya, J. E., Baia, G. S., Baptista, C. S., Barros, M. H., Bonaccorsi, E. D., Bordin, S., Bové, J. M., Briones, M. R. S., Bueno, M. R. P., Camargo, A. A., Camargo, L. E. A., Carraro, D. M., Carrer, H., Colauto, N. B., Colombo, C., Costa, F. F., Costa, M. C. R., Costa-Neto, C. M., Coutinho, L. L., Cristofani, M., Dias-Neto, E., Docena, C., El-Dorry, H., Facincani, A. P., Ferreira, A. J. S., Ferreira, V. C. A., Ferro, J. A., Fraga, J. S., França, S. C., Franco, M. C., Frohme, M., Furlan, L. R., Garnier, M., Goldman, G. H., Goldman, M. H. S., Gomes, S. L., Gruber, A., Ho, P. L., Hoheisel, J. D., Junqueira, M. L., Kemper, E. L., Kitajima, J. P., Krieger, J. E., Kuramae, E. E., Laigret, F., Lambais, M. R., Leite, L. C. C., Lemos, E. G. M., Lemos, M. V. F., Lopes, S. A., Lopes, C. R., Machado, J. A., Machado, M. A., Madeira, A. M. B. N., Madeira, H. M. F., Marino, C.

L., Marques, M. V., Martins, E. A. L., Martins, E. M. F., Matsukuma, A. Y., Menck, C. F. M., Miracca, E. C., Miyaki, C. Y., Monteiro-Vitorello, C. B., Moon, D. H., Nagai, M. A., Nascimento, A. L. T. O., Netto, L. E. S., Nhani, A., Nobrega, F. G., Nunes, L. R., Oliveira, M. A., de Oliveira, M. C., de Oliveira, R. C., Palmieri, D. A., Paris, A., Peixoto, B. R., Pereira, G. A. G., Pereira, H. A., Pesquero, J. B., Quaggio, R. B., Roberto, P. G., Rodrigues, V., de M. Rosa, A. J., de Rosa, V. E., de Sá, R. G., Santelli, R. V., Sawasaki, H. E., da Silva, A. C. R., da Silva, A. M., da Silva, F. R., Silva, W. A., da Silveira, J. F., Silvestri, M. L. Z., Siqueira, W. J., de Souza, A. A., de Souza, A. P., Terenzi, M. F., Truffi, D., Tsai, S. M., Tsuhako, M. H., Vallada, H., Van Sluys, M. A., Verjovski-Almeida, S., Vettore, A. L., Zago, M. A., Zatz, M., Meidanis, J., and Setubal, J. C. 2000. The genome sequence of the plant pathogen *Xylella fastidiosa*. Nature 406:151-157.

Smith, H. O., Gwinn, M. L., and Salzberg, S. L. 1999. DNA uptake signal sequences in naturally transformable bacteria. Res Microbiol 150:603-616.

Soucy, S. M., Huang, J., and Gogarten, J. P. 2015. Horizontal gene transfer: building the web of life. Nat Rev Genet 16:472-482.

Stevenson, J. F., Matthews, M. A., and Rost, T. L. 2004. Grapevine susceptibility to Pierce's disease I: relevance to hydraulic architecture. Am J Enol Vitic 55:228-237.

Stokstad, E. 2015. Italy's olives under siege. Science 348:620.

Strom, M. S., Nunn, D. N., and Lory, S. 1993. A single bifunctional enzyme, PilD, catalyzes cleavage and N-methylation of proteins belonging to the type IV pilin family. Proc Natl Acad Sci U S A 90:2404-2408.

Su, C. C., Deng, W. L., Jan, F. J., Chang, C. J., Huang, H., Shih, H. T., and Chen, J. 2016. *Xylella taiwanensis* sp. nov., causing pear leaf scorch disease. Int J Syst Evol Microbiol 66:4766-4771.

Sun, Q., Sun, Y., Walker, M. A., and Labavitch, J. M. 2013. Vascular occlusions in grapevines with Pierce's disease make disease symptom development worse. Plant Physiol 161:1529-1541.

Suoniemi, A., Björklöf, K., Haahtela, K., and Romantschuk, M. 1995. Pili of *Pseudomonas syringae* pathovar *syringae* enhance initiation of bacterial epiphytic colonization of bean. Microbiology 141:497-503.

Taguchi, F., and Ichinose, Y. 2011. Role of type IV pili in virulence of *Pseudomonas syringae* pv. *tabaci* 6605: correlation of motility, multidrug resistance, and HR-inducing activity on a nonhost plant. Mol Plant Microbe Interact 24:1001-1011.

Takhar, H. K., Kemp, K., Kim, M., Howell, P. L., and Burrows, L. L. 2013. The platform protein is essential for type IV pilus biogenesis. J Biol Chem 288:9721-9728.

Tammam, S., Sampaleanu, L. M., Koo, J., Manoharan, K., Daubaras, M., Burrows, L. L., and Howell, P. L. 2013. PilMNOPQ from the *Pseudomonas aeruginosa* type IV pilus system form a transenvelope protein interaction network that interacts with PilA. J Bacteriol 195:2126-2135.

Tans-Kersten, J., Huang, H., and Allen, C. 2001. *Ralstonia solanacearum* needs motility for invasive virulence on tomato. J Bacteriol 183:3597-3605.

Toyofuku, M., Nomura, N., and Eberl, L. 2019. Types and origins of bacterial membrane vesicles. Nat Rev Microbiol 17:13-24.

Tran, T. M., MacIntyre, A., Khokhani, D., Hawes, M., and Allen, C. 2016. Extracellular DNases of *Ralstonia solanacearum* modulate biofilms and facilitate bacterial wilt virulence. Environ Microbiol 18:4103-4117.

Tumber, K., Alston, J., and Fuller, K. 2014. Pierce's disease costs California $104 million per year. Calif Agric 68:20-29.

Van Sluys, M. A., de Oliveira, M. C., Monteiro-Vitorello, C. B., Miyaki, C. Y., Furlan, L. R., Camargo, L. E., da Silva, A. C., Moon, D. H., Takita, M. A., Lemos, E. G., Machado, M. A., Ferro, M. I., da Silva, F. R., Goldman, M. H., Goldman, G. H., Lemos, M. V., El-Dorry, H., Tsai, S. M., Carrer, H., Carraro, D. M., de Oliveira, R. C., Nunes, L. R., Siqueira, W. J., Coutinho, L. L., Kimura, E. T., Ferro, E. S., Harakava, R., Kuramae, E. E., Marino, C. L., Giglioti, E., Abreu, I. L., Alves, L. M., do Amaral, A. M., Baia, G. S., Blanco, S. R., Brito, M. S., Cannavan, F. S., Celestino, A. V., da Cunha, A. F., Fenille, R. C., Ferro, J. A., Formighieri, E. F., Kishi, L. T., Leoni, S. G., Oliveira, A. R., Rosa, V. E., Jr., Sassaki, F. T., Sena, J. A., de Souza, A. A., Truffi, D., Tsukumo, F., Yanai, G. M., Zaros, L. G., Civerolo, E. L., Simpson, A. J., Almeida, N. F., Jr., Setubal, J. C., and Kitajima, J. P. 2003. Comparative analyses of the complete genome sequences of Pierce's disease and citrus variegated chlorosis strains of *Xylella fastidiosa*. J Bacteriol 185:1018-1026.

Vanhove, M., Retchless, A. C., Sicard, A., Rieux, A., Coletta-Filho, H. D., De La Fuente, L., Stenger, D. C., and Almeida, R. P. P. 2019. Genomic diversity and recombination among *Xylella fastidiosa* subspecies. Appl Environ Microbiol 85:e02972-02918.

Vesel, N., and Blokesch, M. 2021. Pilus production in *Acinetobacter baumannii* is growth phase dependent and essential for natural transformation. J Bacteriol 203:e00034- 00021.

Wang, J. C., So, B. H., Kim, J. H., Park, Y. J., Lee, B. M., and Kang, H. W. 2008. Genome-wide identification of pathogenicity genes in *Xanthomonas oryzae* pv. *oryzae* by transposon mutagenesis. Plant Pathology 57:1136-1145.

Wang, L., Makino, S., Subedee, A., and Bogdanove, A. J. 2007. Novel candidate virulence factors in rice pathogen *Xanthomonas oryzae* pv. *oryzicola* as revealed by mutational analysis. Appl Environ Microbiol 73:8023-8027.

Wells, J. M., Raju, B. C., Hung, H. Y., Weisburg, W. G., Mandelco-Paul, L., and Brenner, D. J. 1987. *Xylella fastidiosa* gen. nov., sp. nov.: Gram-negative, xylem-limited, fastidious plant bacteria related to *Xanthomonas* spp. Int J Syst Bacteriol 37:136-143.

Wiedenbeck, J., and Cohan, F. M. 2011. Origins of bacterial diversity through horizontal genetic transfer and adaptation to new ecological niches. FEMS Microbiol Rev 35:957-976.

Windt, C. W., Vergeldt, F. J., de Jager, P. A., and van As, H. 2006. MRI of long-distance water transport: a comparison of the phloem and xylem flow characteristics and dynamics in poplar, castor bean, tomato and tobacco. Plant Cell Environ 29:1715-1729.

Wise, E. M., Alexander, S. P., and Powers, M. 1973. Adenosine 3′: 5′-cyclic monophosphate as a regulator of bacterial transformation. Proc Natl Acad Sci USA 70:471-474.

Yuan, X., Morano, L., Bromley, R., Spring-Pearson, S., Stouthamer, R., and Nunney, L. 2010. Multilocus sequence typing of *Xylella fastidiosa* causing Pierce's disease and oleander leaf scorch in the United States. Phytopathology 100:601-611.

Chapter 5

Movement and evolution: complete functional analysis of type IV pilus of a re-emergent plant pathogen reveals a unique DNA receptor

Abstract

Natural competence for transformation is a mechanism of horizontal gene transfer that drives evolution by generating genetic diversity. The naturally competent, fastidious prokaryote, plant pathogen *Xylella fastidiosa* impacts hundreds of economically important crops worldwide and causes re-emergent diseases, notably in Europe and the Americas. Widespread intersubspecific homologous recombination (HR) events likely mediated by natural competence have been suggested to influence plant host expansion of *X. fastidiosa* by generating novel pathogenic variants. Thus, in this study we have assessed the functional role of a comprehensive set of 38 genes of *X. fastidiosa* involved in the regulation, assembly and functioning of type IV pili (TFP), which compose a central DNA-uptake machinery required for natural competence and twitching motility, a key virulence mechanism of this plant pathogen. We have identified ten core genes that were essential for both features of this bacterium as well as components that were specific to each trait or presented unique functions in comparison to other bacterial species. By combining approaches of molecular microbiology, structural biology, and biochemistry, we determined that the minor pilin FimT3 is the DNA receptor of the *X. fastidiosa* TFP. FimT3 binds DNA non-specifically via a surface-exposed electropositive stripe and has an exclusive role in natural competence of *X. fastidiosa*. This minor pilin is found only in few plant pathogens and structurally differ from two proteins with similar function identified in human pathogens.

This study identified a critical mechanism required for exogenous DNA acquisition and thus expansion of genetic diversity in this devastating plant pathogen.

Significance Statement

Xylella fastidiosa, a re-emergent bacterial pathogen that damages economically important crops worldwide, is naturally competent, which allows it to take up and incorporate exogenous DNA into its genome via homologous recombination. This leads to emergence of novel pathogenic variants, potentially capable of host range expansion. Our study investigated the function of each molecular component of the type IV pilus structure, which mediates DNA-uptake, twitching motility and virulence. We teased apart the functional role of 38 genes in both natural competence and movement of *X. fastidiosa* and identified its DNA receptor component, which is exclusive to a small subgroup of plant pathogens. Conclusively, our study described a key protein behind generation of genetic diversity in this devastating plant pathogen.

Introduction

Natural competence for transformation is a mechanism of horizontal gene transfer in which physiologically competent cells take up free DNA present in the environment through a specialized DNA import apparatus and incorporate it into their own genomes via homologous recombination (Dubnau and Blokesch 2019; Johnston et al. 2014). This mechanism can support rapid evolution by generating genetic diversity and may be involved in spread of antibiotic resistance, adaptation to new environments and emergence of pathogens (Johnsborg et al. 2007; Johnston et al. 2014; Seitz and Blokesch 2013b; Wiedenbeck and Cohan 2011). In addition, natural competence has been observed in many bacterial species (Johnsborg et al. 2007; Johnston

et al. 2014), including two plant pathogens, *Ralstonia solanacearum* (Bertolla et al. 1999) and *Xylella fastidiosa* (Kung and Almeida 2011), both of which possess a very broad plant host range. *X. fastidiosa* is a Gram-negative fastidious prokaryote that infects and causes disease in many economically important crops worldwide, such as grapevine, citrus, almond, peach, coffee, blueberry, and olive (Chang et al. 2009; Hopkins and Purcell 2002; Saponari et al. 2013). This bacterium is limited to the xylem of infected plants and the foregut of insect vectors that transmit *X. fastidiosa* directly to the xylem of plant hosts (Almeida et al. 2014). Within the xylem, this organism multiplies, moves systemically through twitching motility and forms biofilm that blocks the xylem sap flow. Thus, although the disease process caused by *X. fastidiosa* is not completely understood, twitching motility and biofilm formation are currently considered its main mechanisms of virulence (Chatterjee et al. 2008).

X. fastidiosa undergoes natural competence in all the media sustaining growth of this bacterium (Kandel et al. 2016; Kung and Almeida 2011); and occurs under flow conditions even when cells were grown on grapevine xylem sap from tolerant and susceptible varieties (Kandel et al. 2016). Recombination frequency is higher when cells are growing exponentially in solid agar plates, and minimal medium was initially described to support higher natural competence than rich medium (Kung and Almeida 2014). However, additional studies determined the rich undefined PD3 medium as the most conducive for natural competence of this pathogen (Kandel et al. 2016). Only four type IV pili (TFP) and competence genes were assessed and shown to be involved in natural competence as predicted (Kung and Almeida 2014). *X. fastidiosa* strains are classified into five subspecies based on DNA-DNA relatedness and multilocus sequence typing (MLST) studies (Nunney et al. 2014b; Scally et al. 2005; Schaad et al. 2004), and widespread

intersubspecific and intrasubspecific homologous recombination events have been identified based on MLST and whole-genome sequence analyses (Almeida et al. 2008; Castillo et al. 2020; Coletta-Filho et al. 2017; Jacques et al. 2016; Nunney et al. 2014a; Nunney et al. 2010; Nunney et al. 2012; Potnis et al. 2019; Scally et al. 2005; Vanhove et al. 2019). Moreover, intersubspecific HR has been implicated in plant host expansion by generating strains that infect mulberry (Nunney et al. 2014b), citrus and coffee (Nunney et al. 2012), and blueberry and blackberry (Nunney et al. 2014a). In fact, HR has a greater impact in generating genetic diversity in *X. fastidiosa* than point mutations (Scally et al. 2005; Vanhove et al. 2019). The finding that *X. fastidiosa* strains belonging to different subspecies recombine in vitro during coculture, and even when using heat-killed donor cells, indicates that natural competence is a key mechanism that possibly drives HR within this bacterium and generates genetic diversity (Kandel et al. 2017).

Both natural competence and twitching motility are mediated by TFP (Dubnau and Blokesch 2019; Ellison et al. 2018; Jarrell and McBride 2008), which are hair-like proteinaceous cell appendages with a diameter of 5-8 nm that extend up to many micrometers in length and can also be retracted, and are usually located at one or both poles of a bacterial cell (Mattick 2002). During twitching motility, which is an efficient flagellar-independent type of bacterial movement, TFP extend, attach to surfaces through the distal end of the pilus and then retract, pulling cells towards the point of attachment (Jarrell and McBride 2008; Mattick 2002). On the other hand, TFP compose a central part of the DNA-uptake machinery that enables natural transformation (Dubnau and Blokesch 2019; Seitz and Blokesch 2013a). Although knowledge of some steps involved in this process is still fragmented, the currently accepted model of natural transformation in Gram-negative bacteria involves binding of double-stranded DNA to the tip of

TFP, which upon retraction brings this molecule to the outer-membrane surface of the cell (Ellison et al. 2018). The competence protein ComEA then mediates the entry of the incoming DNA to the periplasm through the PilQ secretin in a likely Brownian ratchet mechanism (Ellison et al. 2018; Seitz et al. 2014). Once in the periplasm, the DNA is converted to a single strand by an unidentified nuclease and translocated to the cytosol through the ComEC channel, where recombination will then be performed by RecA if the incoming DNA shares homology with the genome of the recipient cell (Dubnau and Blokesch 2019). Alternatively, the incoming DNA can also be used as a source of food or as template for the repair of DNA damage (Seitz and Blokesch 2013b).

In both processes, shared TFP molecular components are required for the proper assembly, functioning and regulation of such structures. Notably, minor pilins, which are present in much lower quantities than the major pilin, prime the assembly of TFP (Nguyen et al. 2015). However, some species-specific minor pilins may promote additional functions of TFP, such as aggregation and adherence (Giltner et al. 2012; Jacobsen et al. 2020). This is dictated by differences in the C-terminal region of these proteins, since all pilins (including major and minor pilins) share a highly conserved N-terminal region (Giltner et al. 2012). Due to the evident importance of natural competence in *X. fastidiosa* that promotes HR and thus generates large genetic diversity (Kandel et al. 2017; Potnis et al. 2019; Vanhove et al. 2019), and the exclusive mechanism of movement through twitching motility of this bacterium (Chatterjee et al. 2008), which is fundamental for a xylem-limited bacterium living under flow conditions, in this study we individually assessed the functional role of a comprehensive set of 38 TFP-related genes on both of these features by performing site-directed mutagenesis. Previously, only few TFP-related

genes have been evaluated for their role on movement of *X. fastidiosa* (Cruz et al. 2014; Cursino et al. 2011; De La Fuente et al. 2007; Li et al. 2007; Meng et al. 2005), and even a smaller number of genes were assessed for their contribution to natural competence (Kung and Almeida 2014). Here, we identified ten core genes that were essential for both natural competence and movement of this plant pathogen. However, some components, including mainly minor pilins, were only essential to one feature or the other. This analysis allowed the identification of the FimT3 minor pilin as the DNA receptor of the *X. fastidiosa* pilus, which is only the third minor pilin demonstrated to effectively bind DNA. Moreover, FimT3 was only identified in bacterial species belonging to the Xanthomonadaceae family and two *Pseudomona*s spp. strains, which indicates specificity to this group of plant pathogenic microorganisms. Together, our data provide insight into how different bacterial species use unique minor pilins to acquire exogenous DNA for recombination through natural competence.

Materials and Methods

Methods that are only cited here are described in detail in supplementary materials and methods.

Bacterial strains, plasmids, and culture conditions

All strains and plasmids used in this study are listed in **Table S5-1**. All *X. fastidiosa* mutant strains used here are derivatives of the TemeculaL strain (Potnis et al. 2019), with site-directed mutagenesis of each gene of interest (GOI) being performed as described elsewhere (Kandel et al. 2018). Primers used in this process are listed in **Table S5-2**. *X. fastidiosa* was recovered from -80 ºC glycerol stocks and routinely cultured for seven days at 28 ºC on

periwinkle wilt (PW) agar plates (Davis et al. 1981), modified by removing phenol red and using bovine serum albumin (1.8 g/l) (BSA; Gibco Life Sciences Technology), and sub-cultured onto fresh PW agar plates for another seven days at 28 ºC before use. *X. fastidiosa* mutant strains were grown similarly but using PW plates amended with Km. All assays were performed using the subcultured *X. fastidiosa* strains. Cells were suspended and cultured in PD3 broth (Davis et al. 1981) to perform phenotypic assays, while phosphate-buffered saline (PBS) was used to suspend cells in liquid for in planta assays. Whenever needed, the antibiotics kanamycin (Km) and chloramphenicol (Cm) were used at concentrations of 50 and 10 µg/ml, respectively. When used together with Cm, the Km concentration was reduced to 30 µg/ml. Luria-Bertani (LB) medium (BD Difco) was used to culture *E. coli* cells. When needed, Km, Cm and ampicillin (Amp) were added to LB at concentrations of 50, 35 and 100 µg/ml, respectively.

Phenotypic analyses of *X. fastidiosa* WT and mutant strains

Analyses of natural competence among strains (Kandel et al. 2017), twitching motility (Kandel et al. 2016), growth curve and growth rate (Kandel et al. 2017), biofilm formation and planktonic growth (Cruz et al. 2012; Kandel et al. 2017), settling rate (Kandel et al. 2017), piliation observation by TEM (Kandel et al. 2018), and virulence in planta using tobacco as model system (Gluck-Thaler et al. 2020) were performed as described elsewhere. All experiments had at least three biological replicates, unless otherwise stated.

DNA uptake assays

DNA uptake assays were performed as similarly described for the analysis of natural competence among *X. fastidiosa* strains (see supplementary materials and methods). Briefly,

recipient cells were suspended in PD3 broth to OD_{600nm} of 0.6, spotted onto PD3 agar plates and grown for three days at 28 ºC. Then, 1 µg of fluorescently labeled pAX1-Cm plasmid (10-µl volume), labeled using the *Label* IT Nucleic Acid Labeling kit, Cy3 (Mirus Bio LLC), was added on top of cells, air-dried, and incubated at 28 ºC for another 24 hours. After, cells were harvested in 150 µl of PD3 broth, and a 50 µl aliquot was treated with 10 units of DNase I (New England Biolabs) for 10 minutes at 37 ºC to degrade the remaining extracellular DNA, and cells were observed using a ×100 oil immersion objective in a Nikon Eclipse Ti inverted microscope (Nikon). Image acquisition was performed using a Nikon DS-Q1 digital camera (Nikon) controlled by the NIS-Elements software version 3.0 (Nikon), which was also used to create merged fluorescent images. To detect Cy3, an excitation wavelength of 590 nm was used (tetramethyl rhodamine isothiocyanate; TRITC filter). The proportion of cells that acquired extracellular DNA was calculated as the percentage of cells with fluorescent DNA foci to cells without fluorescent DNA foci. Experiments were performed at least three times independently.

Protein cloning, expression, and purification

Cloning, expression, and purification of FimT1s, FimT2s and FimT3s were performed similarly as described elsewhere using the pHIS-Parallel1 plasmid (**Table S5-1**) (Sheffield et al. 1999; Zhu et al. 2021). Amino acid exchanges in FimT3s were performed by designing a pair of primers (**Table S5-2**) that exchanged the arginine residues at positions 160 and 162 by alanine residues. This pair of primers was designed using the QuickChange Primer Design tool (Agilent Technologies, Inc.; https://www.agilent.com/store/primerDesignProgram.jsp). For amino acid exchanges, the whole pHIS-Parallel1-*fimT3s* construct was amplified via *Pfu* DNA polymerase (G-Biosciences) using a standard protocol from the manufacturer and this pair of primers in a

S1000 thermal cycler (Bio-Rad). Expression and purification of FimT3s-R160AR162A was performed as described in supplementary materials and methods (Zhu et al. 2021). PCR products were purified using the Gel/PCR DNA Fragments Extraction kit (IBI Scientific). Correct cloning and amino acid exchanges in all constructs were confirmed by Sanger sequencing (Sequetech Corporation) using the T7 promoter forward primer (**Table S5-2**).

DNA binding assays

Agarose EMSAs were mainly performed to assess the DNA-binding ability of purified FimT1s, FimT2s and FimT3s. Briefly, 200 ng of DNA (usually pAX1-Cm plasmid) were incubated for 30 minutes at 28 ºC with increasing concentrations of purified proteins in 20 µL EMSA reaction buffer (50 mM Tris-HCl, pH 7.5; 50 mM NaCl; 200 mM KCl; 5 mM $MgCl_2$; 5 mM EDTA, pH 8.0; 5 mM DTT; 0.25 mg/ml BSA). Lysis buffer containing 250 µM imidazole, in which proteins were suspended, was included as blank control. After the incubation period, DNA was separated by electrophoresis on a 0.8% agarose gel containing GelRed nucleic acid gel stain (Biotium) in Tris-acetate-EDTA buffer (120 V for 40 minutes). Experiments were performed at least three times independently. On the other hand, native acrylamide EMSAs were used to perform titration of the DNA binding activity of FimT3s and FimT3s-R160AR162A. In summary, 60 ng of Cy-3 labeled Km resistance cassette were incubated for 30 minutes at 28 ºC with increasing concentrations of purified proteins in 20 µL EMSA reaction buffer and separated by electrophoresis on a 3.5% native acrylamide gel in Tris-borate-EDTA buffer (40 V for 4 hours). Native acrylamide gels were pre-run at 40 V for 30 minutes before being used. DNA samples were directly visualized using the ImageQuant LAS 4010 Imaging System (GE Healthcare), since the used DNA was fluorescently labeled with Cy3. Experiments were

performed two times independently. A densitometry analysis of the shifted bands of Cy-3 labeled DNA in native acrylamide gels was performed by measuring the fluorescent intensity of these bands when treated with 1, 2, 5, and 10 μM of each protein using ImageJ (Schneider et al. 2012). Then, these values were used to calculate the area under the fluorescent curves, as performed to obtain the AUDPC (see supplementary materials and methods) (Simko and Piepho 2012), to quantify the DNA-binding affinity of FimT3s and FimT3s-R160AR162A by determining the progress of shifted bands in relation to each protein concentration.

Bioinformatic analyses

The FimT3 modeling was performed using the Phyre2 web portal (Kelley et al. 2015) and visualized via PyMOL version 2.4.0 (Schrödinger, LLC). The surface electrostatics of FimT3 was predicted using the APBS Electrostatics plugin from PyMOL. Sequence alignments of FimT3 with ComP and VC0858 were performed by retrieving the respective sequences from NCBI, aligning through the T-Coffee Multiple Sequence Alignment Server (Di Tommaso et al. 2011) and visualizing using the BoxShade webserver (https://embnet.vital-it.ch/software/BOX_form.html). For FimT3 analyses within the Xanthomonadaceae family, the total number of whole-genome sequences from this family was downloaded from NCBI, searched for the presence of FimT3 by tblastn using 30% coverage and 50% identity cutoff, and extracted sequences were aligned using MAFFT (Katoh et al. 2002). Then, the alignment was assembled into a maximum-likelihood tree with 1000 bootstraps using RAxML version 8.0.24 (Stamatakis 2014) and visualized using FigTree version 1.4.4 (http://tree.bio.ed.ac.uk/). The alignment was also submitted to Clustal Omega (Clustal 12.1) to determine percentage of identical amino acids (Madeira et al. 2019). The visualization of the alignment of representative

FimT3 sequences among *X. fastidiosa* strains and bacterial species belonging to the Xanthomonadaceae family was performed using the BoxShade webserver.

Data analysis

Data from natural competence assays (recombination frequency) and the area under the fluorescent curve were compared by two-tailed Student's *t*-test. Data from twitching motility, growth rate, viable *X. fastidiosa* CFU/ml obtained during natural competence assays, biofilm formation, planktonic growth, settling rate, AUDPC, *X. fastidiosa* population in planta and percentage of cells acquiring DNA from the extracellular environment were individually analyzed by one-way analysis of variance (ANOVA) followed by Tukey's HSD multiple comparisons of means in R 4.0.0 under the package multcomp (Ihaka and Gentleman 1996). Correlation among analyzed phenotypes was determined by Pearson's correlation using the SigmaPlot software version 11.0 (Systat Software Inc.).

Results

Deletion of TFP-related genes differentially affected natural competence and movement of *X. fastidiosa*

To investigate the functional role of the TFP machinery and its regulatory components on both natural competence and twitching motility of *X. fastidiosa*, we generated a set of individual deletion mutant strains in 38 TFP-related genes (**Table S5-3**) within *X. fastidiosa* subsp. *fastidiosa* strain TemeculaL (Potnis et al. 2019). Genes were chosen according to *X. fastidiosa* genome annotation and by searches based on homology to counterparts encoded by *Pseudomonas aeruginosa*, a well-studied model for TFP and twitching motility that was recently

found to be naturally competent (Burrows 2012; Nolan et al. 2020). To the best of our knowledge, these genes represent the entire set of TFP genes encoded by *X. fastidiosa* strain TemeculaL. Assessment of natural competence was conducted using the pAX1-Cm plasmid, which recombines into the neutral site 1 of the *X. fastidiosa* genome and inserts a Cm resistance cassette (Kandel et al. 2017; Matsumoto et al. 2009), whereas twitching motility was determined by measuring colony fringe widths in solid agar plates (Galvani et al. 2007). Upon deletion, a set of ten genes abrogated both natural competence and movement of *X. fastidiosa* and were thus considered core TFP genes for these two traits (**Fig. 5-1** and **Figs. S5-1**, **S5-2** and **S5-3**). They include the ATPases *pilB* and *pilT*, the prepilin peptidase *pilD*, the TFP assembly platform *pilC*, the whole alignment subcomplex *pilMNOP*, the secretin *pilQ* and the regulatory gene *pilZ*. Conversely, fewer genes were essential to each of these phenotypes by abolishing them upon deletion. The minor pilin *fimT3* was the only gene demonstrated to be essential specifically for natural competence (**Fig. 5-1** and **Fig. S5-1**), while its mutant strain showed significant higher twitching motility than the wild-type (WT) (**Fig. 5-1** and **Figs. S5-2** and **S5-3**). Regarding twitching motility, the minor pilins *pilE1V1W1X1*, which are encoded in the same operon (**Table S5-4**), as well as the regulatory gene *pilR* of the PilRS two-component regulatory system, were essential exclusively for this phenotype (**Fig. 5-1** and **Figs. S5-2** and **S5-3**). Moreover, mutants of all these genes showed significant lower recombination frequencies by natural competence in comparison to the WT (**Fig. 5-1** and **Fig. S5-1**). In addition, individual deletions in each paralog of the major pilin *pilA* encoded by *X. fastidiosa* abrogated neither natural competence nor twitching motility. Knockout of *pilA1* significantly increased both phenotypes, whereas deletion of *pilA2* and *pilA3* significantly reduced twitching motility and did not alter natural competence (**Fig. 5-1** and **Figs. S5-1**, **S5-2** and **S5-3**). On the other hand, concomitant deletion of both *pilA1*

and *pilA2* abolished twitching motility (**Fig. 5-1** and **Figs. S5-2** and **S5-3**), as described elsewhere (Kandel et al. 2018). The only other gene to significantly increase both traits upon deletion, besides *pilA1*, was the sensor gene *pilS* of the PilRS two-component regulatory system mentioned above (**Fig. 5-1** and **Figs. S5-1**, **S5-2** and **S5-3**).

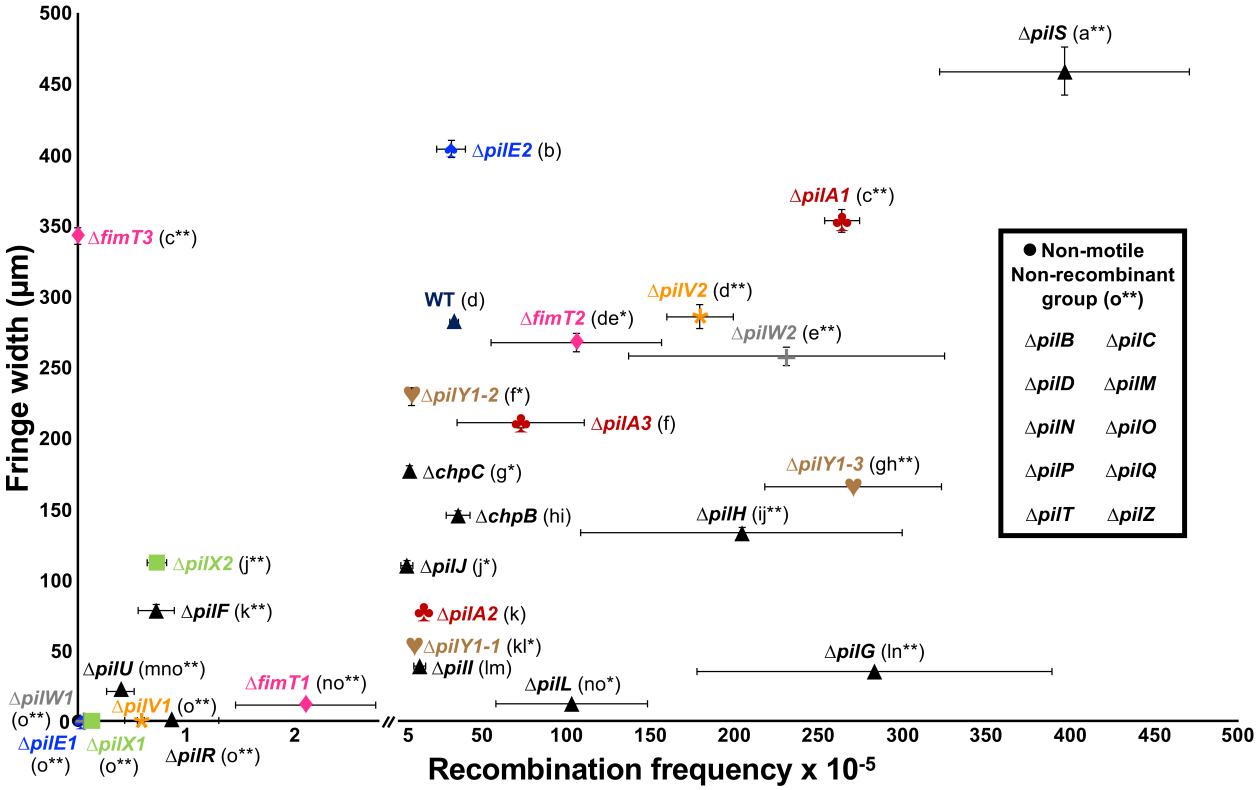

Fig. 5-1. Natural competence and twitching motility phenotypes of *X. fastidiosa* mutant strains used in this study. Quantification of natural competence was performed by enumerating total viable cells and recombinants and results are expressed as the ratio of recipient cells transformed (recombination frequency; values shown in the x-axis of the chart). Twitching motility was determined by spotting cells of each strain in PW without BSA plates and measuring the movement fringe width after 4 days of growth at 28 ºC (values shown in the y-axis of the chart). Results of mutant strains for paralogous genes are shown using the same color and symbol. The non-motile and non-recombinant mutants are shown as a black dot. The WT is represented as a dark blue triangle and all other mutants are represented as black triangles. Data represent means and standard errors. Statistics are shown in parenthesis. Different letters indicate significant difference in fringe width as analyzed by ANOVA followed by Tukey's HSD multiple comparisons of means ($P<0.05$; n = three to 14 independent replicates with eight to 48 internal replicates each). * and ** indicate significant difference ($P<0.05$ and $P<0.005$, respectively) of recombination frequency through natural competence in comparison to the WT as determined using Student's *t*-test (n = three to 21 independent replicates with two internal

replicates each). The detection limit for recombination frequency was 10^{-7} and for twitching motility was 10 μm. Mutants below the detection limit are shown in the non-motile and non-recombinant group.

Intriguingly, the knockout of paralogs usually presented opposite phenotypes, as described for *pilA1*, *pilA2* and *pilA3*. Within minor pilins, Δ*pilE1*, Δ*pilV1*, Δ*pilW1* and Δ*pilX1* all presented significant lower natural competence than the WT and were non-motile, as mentioned above; however, in comparison to the WT, Δ*pilE2* presented significant higher twitching motility and no changes in natural competence, Δ*pilV2* had significant higher natural competence with no altered movement, Δ*pilW2* showed significant higher natural competence and significant lower movement, and Δ*pilX2* possessed both significant lower natural competence and twitching motility (**Fig. 5-1** and **Figs. S5-1**, **S5-2** and **S5-3**). Additionally, deletion of the minor pilin *fimT1* significantly decreased both natural competence and movement, while knockout of *fimT2* significantly increased natural competence and did not change twitching motility, and Δ*fimT3* lost natural competence and presented significant higher movement than the WT (**Fig. 5-1** and **Figs. S5-1**, **S5-2** and **S5-3**).

As for the *pilY1-1*, *pilY1-2* and *pilY1-3* tip adhesins, deletion of all significantly reduced twitching motility, however Δ*pilY1-1* and Δ*pilY1-2* presented significant lower natural competence whilst Δ*pilY1-3* had significant higher natural competence than the WT (**Fig. 5-1** and **Figs. S5-1**, **S5-2** and **S5-3**). Lastly, deletion of the pilotin *pilF* and of the retraction ATPase *pilU* significantly reduced natural competence and movement, and knockout of the chemotaxis genes *pilGHIJL* and *chpBC* significantly reduced twitching, but with Δ*pilG*, Δ*pilH* and Δ*pilL* presenting significant higher natural competence, Δ*pilJ* and Δ*chpC* having significant lower natural competence, and Δ*pilI* and Δ*chpB* showing no change in this phenotype in comparison to

the WT (**Fig. 5-1** and **Figs. S5-1**, **S5-2** and **S5-3**). Although the knockout of genes studied here did not always modulate natural competence and twitching motility in the same manner, the correlation between these two traits among mutant strains was positive (R^2 = 0.56, P<0.001; **Table S5-5**), indicating that they were usually increased or reduced in a similar manner upon deletion of TFP genes.

TFP-related genes also affect other key phenotypes of *X. fastidiosa*

We also evaluated the ability of TFP genes to modulate other important phenotypes of *X. fastidiosa*, such as growth, biofilm formation, cell aggregation (measured by settling rate) and virulence in planta. Growth curves are shown in **Fig. S5-4**. Mutant strains Δ*pilD*, Δ*pilP* and Δ*pilT* presented significant lower growth rates than the WT, while Δ*pilA1*, Δ*pilA2*, Δ*pilA1pilA2*, Δ*pilC*, Δ*pilE1*, Δ*pilY1-3*, Δ*fimT1* and Δ*fimT2* did not show significant differences in comparison to the WT (**Fig. S5-5**). All other mutant strains had significant higher growth rates than the WT (**Fig. S5-5**). Since this growth analysis considered only OD_{600nm} values, the number of viable *X. fastidiosa* cells (measured as colony forming units – CFU – per ml) counted during natural competence assays was also evaluated. Only the non-recombinant and non-motile Δ*pilC* and Δ*pilP* mutants presented significant changes in the number of cells in comparison to the WT, with both having significant higher CFU/ml (**Fig. S5-6**). Concerning biofilm formation, individual deletion of *pilB*, *pilD*, *pilH*, *pilI*, *pilM*, *pilN*, *pilO*, *pilQ*, *pilR*, *pilT*, *pilX1* and *fimT1* significantly increased this phenotype, whereas only Δ*pilA3* and Δ*fimT3* formed significant lower biofilm than the WT (**Fig. S5-7**). Furthermore, the planktonic growth significantly increased upon individual deletion of *pilA1*, *pilC*, *pilE1*, *pilF*, *pilM*, *pilN*, *pilO*, *pilP*, *pilQ*, *pilR*, *pilV1*, *pilW1*, *pilW2*, *pilX1*, *pilA1pilA2*, *pilY1-1*, *fimT3* and *chpC*, while individual knockout of *pilD*,

pilT and *pilY1-3* significantly decreased this phenotype (**Fig. S5-8**). Moreover, only Δ*pilD*, Δ*pilT* and Δ*pilX2* showed significant higher settling rates, with other mutants not differing significantly from the WT (**Fig. S5-9**). Besides, biofilm formation and settling rate, and planktonic growth and growth rate had significant positive correlations (**Table S5-5**). Meanwhile, biofilm formation and twitching motility/growth rate, settling rate and planktonic growth/growth rate, and growth rate and total viable *X. fastidiosa* presented significant negative correlations (**Table S5-5**). No other phenotype presented a significant correlation to natural competence (recombination frequency) apart from twitching motility.

Ultimately, the virulence in planta of some *X. fastidiosa* mutant strains was assessed by inoculating *Nicotiana tabacum* L. cv. Petite SR1 plants and scoring disease incidence and severity. Mutant strains chosen for analysis had different twitching motility phenotypes, such as higher movement (Δ*pilA1* and Δ*pilS*), lower movement (Δ*pilA2*) and non-motility (Δ*pilA1pilA2*, Δ*pilQ* and Δ*pilR*). All inoculated plants reached 100% disease incidence at the end of assays, except plants inoculated with Δ*pilA1*, which presented 88.88% disease incidence (±11.11%, standard error). Notably, WT-inoculated plants presented the highest disease severity over the time course of assays (**Fig. S5-10A**), with all plants inoculated with the mutant strains having significant lower AUDPC (Area Under the Disease Progress Curve) values, except plants inoculated with Δ*pilA2* (**Fig. S5-10B**).

However, only WT-inoculated plants consistently presented severe symptoms of leaf scorch, while plants inoculated with the mutant strains mostly presented mild symptoms (**Fig. S5-10D**). In addition, when evaluating the population of *X. fastidiosa* in planta by qPCR, only

the Δ*pilA1pilA2* double mutant showed a defect in colonizing the top leaf of the plant host, although not significantly, and the Δ*pilQ* and Δ*pilR* mutants presented a significant higher population in the basal leaf of plant hosts (**Fig. S5-10C**). Together, results demonstrate that the deletion of analyzed genes significantly reduced symptoms development in infected tobacco plants (except for deletion of *pilA2*), which was not explained by bacterial distribution, since most strains could effectively colonize the entirety of plants (except Δ*pilA1pilA2*).

The minor pilin FimT3 is the DNA receptor of the *X. fastidiosa* type IV pilus

The fact that the minor pilin FimT3 was the only component of TFP found to be essential exclusively for natural competence of *X. fastidiosa*, while its deletion still maintained twitching motility (**Fig. 5-1** and **Figs. S5-1**, **S5-2** and **S5-3**), led us to hypothesize that this minor pilin is the DNA receptor of the TFP of this bacterium. Before testing our hypothesis, we first analyzed the piliation phenotype of Δ*fimT3* in comparison to WT by transmission electron microscopy (TEM). Both presented long TFP as well as short type I pili, with no apparent changes in the piliation of *X. fastidiosa* cells upon deletion of *fimT3* (**Fig. 5-2A**). Next, the ability of these cells to take up DNA from the extracellular environment was evaluated by exposing them to Cy-3-labeled pAX1-Cm plasmid and observing under a fluorescent microscope. After exposure to the fluorescently labeled DNA fragment, only WT cells imported DNA to their periplasm that was thus into a DNaseI resistant state, with no fluorescent DNA foci being present in Δ*fimT3* cells (**Fig. 5-2B**). Besides, DNA foci were mostly observed at one pole of cells, which coincides to the described phenotype of *X. fastidiosa* that forms TFP at only one of its poles (Meng et al. 2005). The DNA-uptake ability of the mutant strains of other minor pilins that decreased the natural competence ability of *X. fastidiosa* upon deletion was also evaluated for comparison. These

included Δ*pilE1*, Δ*pilV1*, Δ*pilW1*, Δ*pilX1*, Δ*pilX2*, Δ*fimT1* and Δ*fimT2* (**Fig. 5-1** and **Fig. S5-1**). The Δ*fimT2* mutant strain was included because this gene is a paralog of *fimT3*, even though its deletion increased the natural competence of *X. fastidiosa* (**Fig. 5-1** and **Fig. S5-1**). Cells of all analyzed strains maintained the DNA-uptake phenotype upon deletion of genes (**Fig. S5-11**), but at different scales (**Fig. S5-12**). WT cells presented the highest percentage of cells with DNA foci, with Δ*pilE1* having the lowest proportion of cells with DNA acquisition (**Fig. S5-12**).

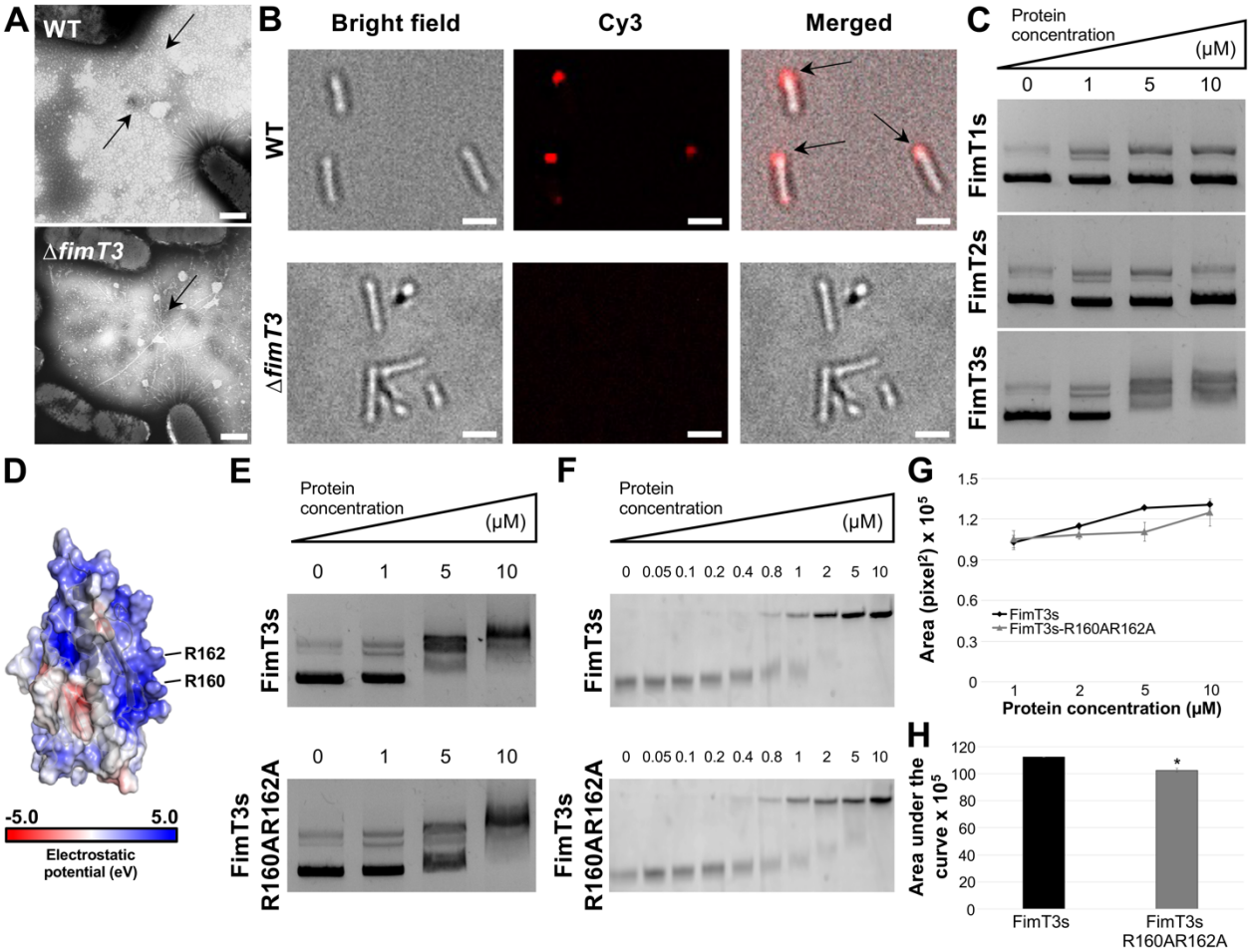

Fig. 5-2. FimT3 DNA binding activity. A. Transmission electron microscopy micrographs of pilus formation by *X. fastidiosa* WT and Δ*fimT3* cells. Cells were negatively stained by phosphotungstic acid. Arrows are pointing to TFP. Similar events were captured in two independent experiments. Images were captured at 31,500× magnification. Scale bars, 500 nm. **B.** Uptake of Cy-3-labeled pAX1-Cm plasmid into a DNaseI resistant state by *X. fastidiosa* cells. WT (upper row) and Δ*fimT3* (lower row) cells were exposed to Cy-3-labeled pAX1-Cm plasmid (1 µg) for 24 hours, treated with DNase I and DNA foci were observed using a fluorescent

microscope. The images shown correspond to the bright field (left), Cy-3 channel (center) and merged fluorescent images (right). In merged fluorescent images, arrows are pointing to fluorescent DNA foci at the poles of cells. Similar events were captured in three independent experiments. Images were captured at 100× magnification. Scale bars, 1.5 μm. **C.** DNA-binding ability of purified FimT1s, FimT2s and FimT3s assessed by agarose EMSA. A standard amount (200 ng) of DNA (pAX1-Cm plasmid) was incubated for 30 min at 28 ºC with increasing concentrations of each protein and resolved by electrophoresis on a 0.8% agarose gel. Lysis buffer containing 250 μM imidazole, in which proteins were suspended, was included as blank control (0 μM). Similar events were captured in three independent experiments. **D.** Surface electrostatics representation of FimT3. The image shows the surface electrostatics of FimT3 merged with its ribbon representation. The arginine amino acid residues (R160 and R162) that were mutated for functional studies are highlighted in the figure. Positive charges are shown in blue, while negative charges are shown in red. The electrostatic potential (eV) scale is shown in the figure. **E.** DNA-binding ability of purified FimT3s and FimT3s-R160AR162A assessed by agarose EMSA. The assay was performed as described in **C**. Similar events were captured in three independent experiments. **F.** Titration of the DNA binding activity of FimT3s and FimT3s-R160AR162A by native acrylamide EMSA. Increasing concentrations of FimT3s and FimT3s-R160AR162A were incubated with Cy-3 labeled Km resistance cassette (60 ng) for 30 min at 28 ºC and resolved by electrophoresis on a 3.5% native acrylamide gel. Samples were visualized using the ImageQuant LAS 4010 Imaging System (GE Healthcare). Similar events were captured in two independent experiments. **G.** Densitometry analysis of the DNA binding activity of FimT3s and FimT3s-R160AR162A in acrylamide EMSA. The fluorescent intensity of the shifted DNA bands of Cy-3-labeled Km resistance cassette presented in **F** was measured using ImageJ. The fluorescent intensity of shifted bands when treated only with 1, 2, 5, and 10 μM of each protein was measured. This was performed because DNA bands presented higher shifts in electrophoretic mobility within this protein concentration range. **H.** Area under the fluorescent curve. The area under the fluorescent curves in **G** was calculated to quantify the DNA-binding affinity of FimT3s and FimT3s-R160AR162A. Statistical significance was determined using Student's *t*-test (* indicates $P<0.05$ in comparison to the wild-type protein; n = two independent replicates).

Then, to define whether FimT3 indeed binds to DNA, the soluble portion of this protein (named FimT3s) and of its paralogs FimT1 and FimT2 (named FimT1s and FimT2s, respectively), without the conserved N-terminal hydrophobic α-helices of pilins (Giltner et al. 2012), were purified and their ability to interact with DNA was determined by agarose EMSAs (Electrophoretic Mobility Shit Assay). The pAX1-Cm plasmid was used as target DNA. Only FimT3s was able to bind DNA, since no shift was observed with FimT1s and FimT2s when using as much as 10 μM of each protein (**Fig. 5-2C**). Moreover, FimT3s was able to bind to

different DNA sequences, which shared or not homology to the *X. fastidiosa* TemeculaL genome, indicating that binding is not sequence-specific (**Fig. S5-13**). Collectively, *fimT3* being the only gene essential exclusively for natural competence, the ability of FimT3 to bind to DNA and the loss of DNA acquisition from the extracellular environment by cells upon its deletion demonstrate that this minor pilin is the DNA receptor of the *X. fastidiosa* type IV pilus.

To further characterize the DNA-binding ability of FimT3, we searched for specific amino acid residues that possibly foster DNA-binding activity. The binding of DNA to TFP by a minor pilin was recently demonstrated through the finding that the ComP minor pilin is the specific DNA receptor of the *Neisseria* pilus (Berry et al. 2013; Berry et al. 2016; Cehovin et al. 2013). Additionally, the ComZ minor pilin of *Thermus thermophilus* was the second minor pilin described as a TFP-associated DNA receptor (Salleh et al. 2019). However, FimT3 shares no homology with either of these proteins. Amino acids alignments revealed that FimT3 and ComP share a 28.21% percentage identity over a 20% query cover, while FimT3 and ComZ have no significant similarities. However, in search of DNA-binding amino acid residues, we visualized the FimT3 alignment with ComP of *Neisseria meningitidis*, and the minor pilin VC0858 of *Vibrio cholerae* (35.14% percentage identity with FimT3 over a 18% query cover), which was described as important for the DNA-binding ability of this bacterium's type IV pilus, although no direct binding to DNA was assayed (Ellison et al. 2018). Alignments showed that the arginine residue at position 162 of FimT3 aligned with a lysine of ComP (K108) demonstrated to be essential for its DNA-binding ability (Cehovin et al. 2013) (**Fig. S5-14**). Additionally, the arginine residue at position 160 of FimT3 aligned with an arginine of VC0858 (R168) that was important for the DNA-binding activity of the *V. cholerae* pilus (Ellison et al. 2018) (**Fig. S5-**

14). These two arginine residues of FimT3 (R160 and R162) were also predicted in silico to have the highest probabilities of binding DNA among the residues of this protein (**Table S5-6**). Besides, analysis of the surface electrostatics of FimT3 revealed that the residues R160 and R162 are located within an electropositive stripe and form a shaft that can possibly harbor DNA (**Fig. 5-2D**). Thus, to assess the importance of these arginine residues and of the electropositive stripe in the DNA-binding ability of FimT3, we generated a FimT3s variant by site-directed mutagenesis in which both arginine residues were replaced by hydrophobic alanine residues (FimT3s-R160AR162A). Agarose EMSAs revealed a decrease in DNA binding affinity with the arginine residue exchanges (**Fig. 5-2E**). A higher shift was observed for FimT3s when using 5 μM of each protein, while a comparable shift was only present when using 10 μM of FimT3s-R160AR162A (**Fig. 5-2E**). Similar results were also obtained when using the more sensitive acrylamide EMSA and the Km resistance cassette sequence as target DNA (previously determined to be bound by FimT3s in **Fig. S5-13**). An abrupt shift was detected when using concentrations of FimT3s ranging between 1 and 5 μM, whereas a much more subtle and gradual shift was observed for samples treated with FimT3s-R160AR162A within the same concentration range (**Fig. 5-2F**). We then performed a densitometry analysis of the shifted bands treated with concentrations ranging between 1 and 10 μM of each protein (**Fig. 5-2G**) and calculated the area under the curve to quantify the DNA-binding affinity of FimT3s and FimT3s-R160AR162A (similarly as performed to obtain the AUDPC described above). The DNA-binding affinity of FimT3s-R160AR162A was significantly lower than that of FimT3s (**Fig. 5-2H**), however, the performed amino acid exchanges did not abolish the DNA-binding ability of the latter. These results show that R160 and R162 residing within the electropositive stripe are

important for the DNA-binding activity of FimT3, but other residues of the stripe also likely play a role in DNA-binding.

FimT3 is widely conversed within *X. fastidiosa* strains and is present in some other members of the Xanthomonadaceae family

We performed searches using the Basic Local Alignment Search Tool for proteins (blastp) (Johnson et al. 2008) to explore the distribution of FimT3 and found that this protein is only encoded by some members of the Xanthomonadaceae family besides *X. fastidiosa*, and two *Pseudomonas* spp. strains (**Table S5-7**). Thus, to further investigate the distribution of FimT3 within the Xanthomonadaceae, the total number of whole-genome sequences from this family was downloaded from NCBI (National Center for Biotechnology Information), screened for the presence of FimT3 by tblastn, and a phylogenetic tree based on FimT3 amino acid sequences was constructed using the maximum-likelihood method. FimT3 was found to be encoded by 270 out of 2,699 genomes of the Xanthomonadaceae (~10%) with amino acid identities ranging from 95.60% to 100% within *X. fastidiosa*, and from 33.33% to 53.99% among the other species, including *Pseudomonas* spp. (**Table S5-7**). In the phylogenetic tree, *Pseudoxanthomonas* spp. strains grouped into different clades, while *X. fastidiosa* strains grouped together, with the same trend being observed for *Xanthomonas* spp. strains, except for *Xanthomonas* sp. AmX2, which grouped with *X. fastidiosa* (**Fig. 5-3**). Furthermore, the alignment of the different FimT3 sequences encoded by *X. fastidiosa* strains demonstrated that this minor pilin is nearly identical within this bacterial species, with a maximum of six nonconservative substitutions within strains belonging to the subspecies *pauca*, which also presented FimT3 sequences that were 13 amino acids shorter in comparison to the other strains (**Fig. S5-15A**). At last, alignment of all different

FimT3 sequences among strains belonging to the Xanthomonadaceae family revealed that the arginine residues at positions 160 and 162 of FimT3 from *X. fastidiosa* strain TemeculaL were conserved in most orthologous sequences of this protein (46 out of 50 different FimT3 sequences) (**Fig. S5-15B**). Additionally, R160 was always preceded by a glycine residue. Overall, results indicate that FimT3 is mostly encoded by the Xanthomonadaceae (primarily *X. fastidiosa*) and that R160 and R162 are highly conserved within FimT3 sequences.

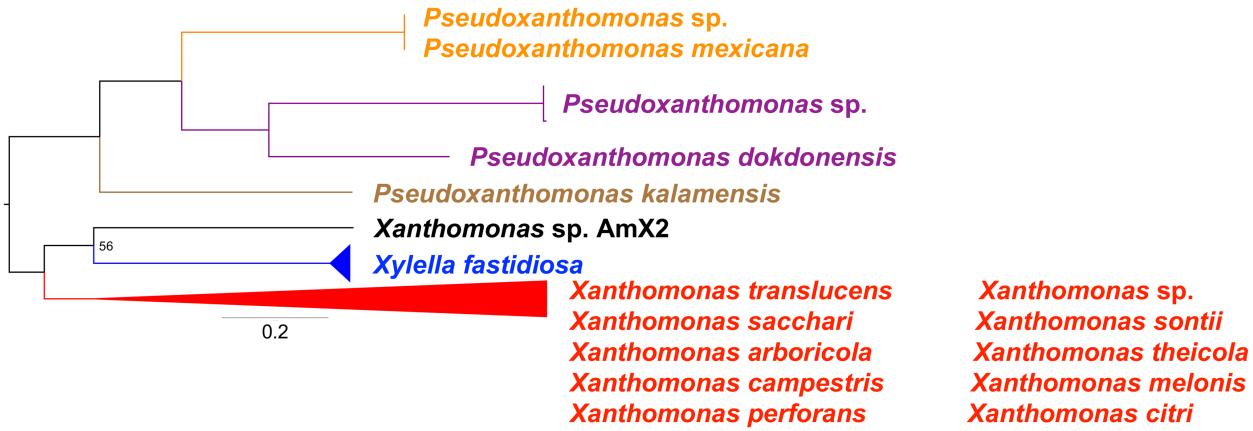

Fig. 5-3. Phylogenetic tree based on FimT3 amino acid sequences from Xanthomonadaceae bacterial strains with whole-genome sequences. The phylogenetic tree was built using the Maximum-likelihood method and visualized using FigTree. Branches with bootstrap values below 70% were collapsed, except where indicated. The bootstrap value for the branch with *Xanthomonas* sp. AmX2 was below that threshold but was included to show the only non-*X. fastidiosa* member of that cluster. For representation purposes, branches in the tree are color-coded according to groupings of bacterial species.

Discussion

In this study, we sought to explore how the molecular components responsible for the regulation, assembly, and proper functioning of the *X. fastidiosa* TFP contribute to its natural competence and twitching motility phenotypes (summarized in **Fig. 5-4**). By performing site-directed mutagenesis and functional studies in all genes directly related to the TFP of this bacterium, we defined a set of ten core genes (*pilBCDMNOPQTZ*) that were essential for both

traits. Interestingly, studies with one or a few these genes in other bacterial species have also produced similar results, including *Acinetobacter baumannii* (Vesel and Blokesch 2021), *A. baylyi* (Leong et al. 2017), *Thermus thermophilus* (Rumszauer et al. 2006), *Haemophilus influenzae* (Carruthers et al. 2012), *P. aeruginosa* (Alm et al. 1996; Ayers et al. 2009; Marko et al. 2018; Tammam et al. 2013), besides *X. fastidiosa* itself (Kung and Almeida 2014; Li et al. 2007; Meng et al. 2005). The exceptions were *pilP* and *pilZ* in which previous deletion of both greatly reduced natural competence, but did not abolish it (Drake et al. 1997; Hardy et al. 2021). However, very few of these genes have been simultaneously assayed for their role in both natural competence and movement mediated by TFP.

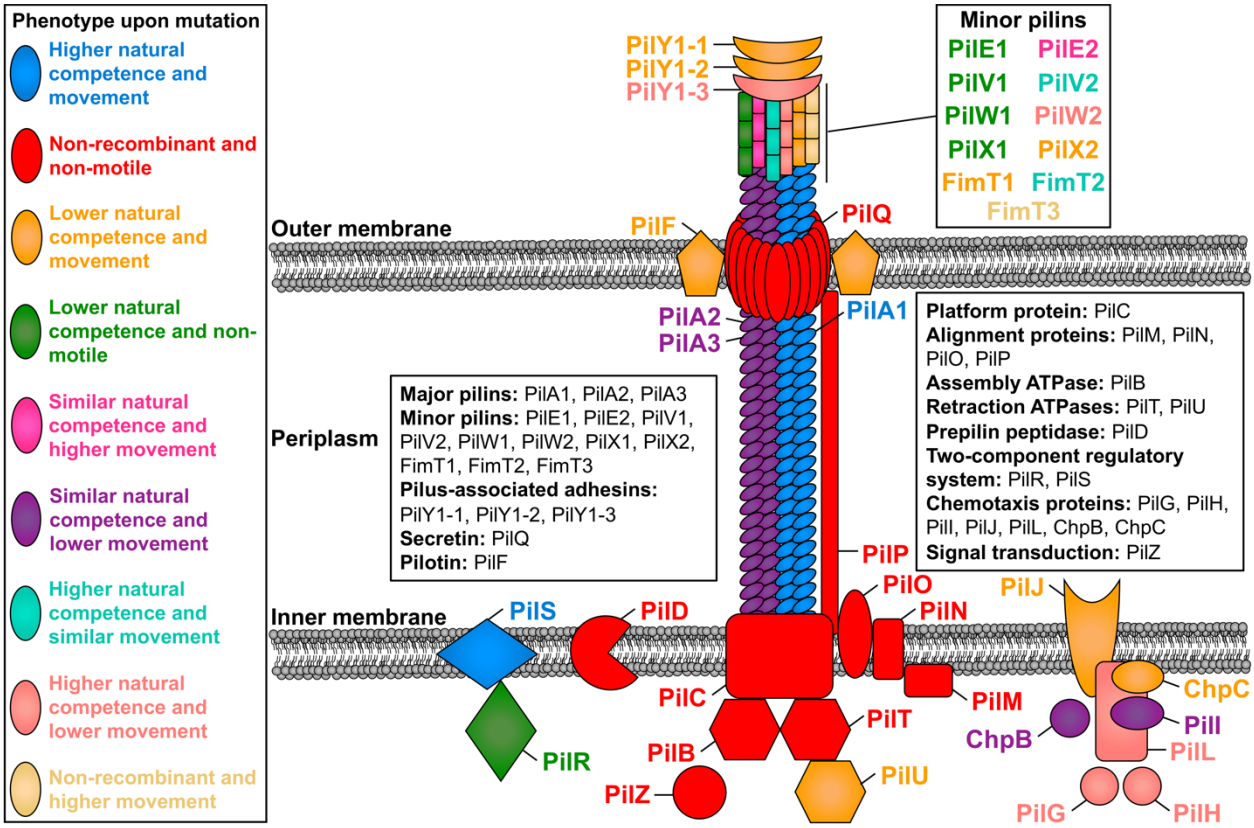

Fig. 5-4. Schematic representation of the functional role of TFP molecular components in natural competence and twitching motility of *X. fastidiosa*. The figure shows the structure of a type IV pilus (PilA1, PilA2 and PilA3), the alignment subcomplex (PilM, PilN, PilO and PilP), the inner membrane motor subcomplex (PilB, PilC, PilD, PilT and PilU), the pore subcomplex

(PilF and PilQ), minor pilins (PilE1, PilE2, PilV1, PilV2, PilW1, PilW2, PilX1, PilX2, FimT1, FimT2 and FimT3), TFP tip adhesins (PilY1-1, PilY1-2 and PilY1-3), as well as regulatory proteins (PilG, PilH, PilI, PilJ, PilL, PilR, PilS, PilZ, ChpB and ChpC). Proteins in the figure are color-coded according to their phenotype upon knockout mutation and thus functional role. More information about the role of each protein is described in **Table S5-3**, throughout the manuscript and in supplementary discussion.

To our knowledge, our study comprises the largest simultaneous functional description of a comprehensive set of TFP-related genes on natural competence and twitching motility of a bacterium. An extensive discussion including all genes analyzed in this study and their functional roles in natural competence and twitching motility of *X. fastidiosa*, in addition to unique behaviors and other phenotypes such as biofilm formation and virulence in planta, is included in supplementary discussion.

Mostly remarkably, however, is the finding that the unique minor pilin FimT3 is the DNA receptor of the *X. fastidiosa* TFP. The interaction of DNA molecules to an extracellular specific receptor is a key initial step in the DNA uptake and thus natural competence of bacterial species. DNA binding by TFP has been observed in *P. aeruginosa* (van Schaik et al. 2005), *Streptococcus pneumoniae* (Laurenceau et al. 2013), and *V. cholerae* (Ellison et al. 2018), in which pilus retraction drives DNA uptake in the latter by transporting these molecules to the cell surface, which are then imported to the periplasm by the competence protein ComEA (Ellison et al. 2018; Seitz et al. 2014). Although these studies provide evidence that the specialized DNA receptor resides within type IV competence pilus fibers, no direct binding of DNA by individual purified major and/or minor pilins has been reported by them. In *V. cholerae*, targeted mutations of positively charged amino acid residues within the minor pilins VC0858 and VC0859 reduced the DNA-binding affinity of its TFP (Ellison et al. 2018), but the ability of these minor pilins to

directly bind DNA was not assayed. In this scenario, ComP from *N. meningitidis* was the first pilin demonstrated to bind DNA, which occurs through an electropositive stripe exposed in the surface of this minor pilin (Cehovin et al. 2013). Moreover, ComP has an exclusive role in competence within this organism, since mutant cells have piliation levels similar to the WT (Wolfgang et al. 1999). In addition, its orthologs are found mostly within the Neisseriaceae family, where they mediate DNA uptake by binding to specific DNA uptake sequences (DUS) as *Neisseria* spp. preferentially take up homotypic DNA (Berry et al. 2013; Cehovin et al. 2013).

Likewise, the FimT3 minor pilin of *X. fastidiosa* described here affects exclusively the natural competence of this plant pathogen, since mutant cells maintain piliation and twitching motility, while it binds to DNA via a surface-exposed electropositive stripe, in which positively charged arginine residues contribute to the DNA binding ability of this protein. FimT3, however, seems to bind to DNA non-specifically, in contrast to ComP (Cehovin et al. 2013). Additionally, FimT3 is a nearly exclusive minor pilin of the Xanthomonadaceae family, being encoded by all *X. fastidiosa* strains as well as few other bacterial species belonging to this family and two strains classified as *Pseudomonas* spp.. However, one of these two *Pseudomonas* spp. strains, *P. boreopolis*, has been shown to belong to the *Xanthomonas*-*Xylella* lineage based on 16S rRNA phylogenetic analyses (Anzai et al. 2000). This further supports the exclusivity of FimT3 to the Xanthomonadaceae family. Thus, our results, together with previous studies, demonstrate that DNA binding by TFP occurs among bacterial species through a similar component such as minor pilins, which themselves are not widely distributed or conserved, but are rather specific to different bacterial groups. For instance, the ability of strain-specific subsets of minor pilins to modulate TFP dynamics has already been described in *P. aeruginosa* (see supplementary

discussion) (Giltner et al. 2011). Curiously, a FimT homolog was also demonstrated to be specialized in natural competence in *A. baylyi* (Leong et al. 2017). However, this FimT from *A. baylyi* shares no homology with FimT3 of *X. fastidiosa*, and no analysis has been performed to determine whether it can bind to DNA.

Therefore, FimT3 is only the third minor pilin demonstrated to bind DNA. ComZ, encoded by *T. thermophilus*, was the second minor pilin described as a TFP DNA receptor (Salleh et al. 2019). However, ComZ is an unusual minor pilin that possesses an additional large β-solenoid domain inserted into the common β-sheet structure of pilins. Furthermore, ComZ binds to another minor pilin, PilA2 (PilV in *X. fastidiosa*), and its DNA binding ability does not appear to require positive charges in its surface (Salleh et al. 2019). Nonetheless, the binding of ComZ to another minor pilin suggests that specific interactions within the pilus structure may occur to compose the competence pilus fiber. Here, the deletion of individual paralogs of the major pilin PilA abrogated neither natural competence nor twitching motility, suggesting functional overlapping among them (see supplementary discussion). However, we were able to determine that the minor pilin FimT3 confers DNA-binding specificity to TFP. Therefore, it is important to investigate whether FimT3 interacts with different minor and major pilins of *X. fastidiosa* to establish the basic structure of its competence pilus. Moreover, FimT3 by itself may not be enough to dictate natural competence, because competence and recombination proteins located downstream in the natural competence process are as essential to this phenotype as DNA uptake (Dubnau and Blokesch 2019; Ellison et al. 2018; Seitz et al. 2014). Besides, it is not known whether the other bacterial species encoding FimT3 described in this study are also naturally competent. At last, *X. fastidiosa* strains belonging to the *pauca* subspecies presented a

shorter FimT3 and the biggest sequence divergence in comparison to our model FimT3 from *X. fastidiosa* subsp. *fastidiosa* strain TemeculaL. Intriguingly, the only reported attempt to transform a *X. fastidiosa* strain belonging to the subspecies *pauca* by natural competence in vitro has failed (D'Attoma et al. 2020). Thus, it may be worth investigating if the changes in the FimT3 sequence among *pauca* strains may alter the DNA binding ability of this minor pilin.

Collectively, our data demonstrate that some individual components of the TFP machinery of *X. fastidiosa* provide unique behaviors to this bacterium (see supplementary discussion). Among them, the newly described minor pilin FimT3 acts as its TFP DNA receptor and plays an essential role in natural competence by mediating extracellular DNA uptake. Ultimately, the acquired DNA may be integrated into the genome, thereby conferring new phenotypic traits that may carry host expansion within this bacterium. Due to the worldwide threat that *X. fastidiosa* presents to many economically important crops and to its increasing list of plant hosts, it is imperative to investigate how this plant pathogen acquires foreign DNA and expands its genetic diversity to help researchers understand its eco-evolutionary history and re-emergence in many geographic areas.

Acknowledgments

We thank Dr. Michelle Mendonça Pena for helping with phylogenetic analyses. We thank the Alabama Supercomputing Authority for granting access to their high-performance computing platform. We acknowledge funding from Alabama Agricultural Experiment Station (AAES) Hatch Program (L.D., P.V., N.P) and Auburn Internal Grant Program.

References

Alm, R. A., Bodero, A. J., Free, P. D., and Mattick, J. S. 1996. Identification of a novel gene, *pilZ*, essential for type 4 fimbrial biogenesis in *Pseudomonas aeruginosa*. J Bacteriol 178:46-53.

Almeida, R. P. P., Coletta-Filho, H. D., and Lopes, J. R. S. 2014. *Xylella fastidiosa*. Pages 841-850 in: Manual of Security Sensitive Microbes and Toxins. D. Liu, ed. CRC Press, Boca Raton, FL.

Almeida, R. P. P., Nascimento, F. E., Chau, J., Prado, S. S., Tsai, C. W., Lopes, S. A., and Lopes, J. R. S. 2008. Genetic structure and biology of *Xylella fastidiosa* strains causing disease in citrus and coffee in Brazil. Appl Environ Microbiol 74:3690-3701.

Anzai, Y., Kim, H., Park, J. Y., Wakabayashi, H., and Oyaizu, H. 2000. Phylogenetic affiliation of the pseudomonads based on 16S rRNA sequence. Int J Syst Evol Microbiol 50:1563-1589.

Ayers, M., Sampaleanu, L. M., Tammam, S., Koo, J., Harvey, H., Howell, P. L., and Burrows, L. L. 2009. PilM/N/O/P proteins form an inner membrane complex that affects the stability of the *Pseudomonas aeruginosa* type IV pilus secretin. J Mol Biol 394:128-142.

Berry, J. L., Cehovin, A., McDowell, M. A., Lea, S. M., and Pelicic, V. 2013. Functional analysis of the interdependence between DNA uptake sequence and its cognate ComP receptor during natural transformation in *Neisseria* species. PLoS Genet 9:e1004014.

Berry, J. L., Xu, Y., Ward, P. N., Lea, S. M., Matthews, S. J., and Pelicic, V. 2016. A comparative structure/function analysis of two type IV pilin DNA receptors defines a novel mode of DNA binding. Structure 24:926-934.

Bertolla, F., Frostegård, Å., Brito, B., Nesme, X., and Simonet, P. 1999. During infection of its host, the plant pathogen *Ralstonia solanacearum* naturally develops a state of competence and exchanges genetic material. Mol Plant Microbe Interact 12:467-472.

Burrows, L. L. 2012. *Pseudomonas aeruginosa* twitching motility: type IV pili in action. Annu Rev Microbiol 66:493-520.

Carruthers, M. D., Tracy, E. N., Dickson, A. C., Ganser, K. B., Munson, R. S., Jr., and Bakaletz, L. O. 2012. Biological roles of nontypeable *Haemophilus influenzae* type IV pilus proteins encoded by the *pil* and *com* operons. J Bacteriol 194:1927-1933.

Castillo, A. I., Chacón-Díaz, C., Rodríguez-Murillo, N., Coletta-Filho, H. D., and Almeida, R. P. P. 2020. Impacts of local population history and ecology on the evolution of a globally dispersed pathogen. BMC Genomics 21:369.

Cehovin, A., Simpson, P. J., McDowell, M. A., Brown, D. R., Noschese, R., Pallett, M., Brady, J., Baldwin, G. S., Lea, S. M., Matthews, S. J., and Pelicic, V. 2013. Specific DNA recognition mediated by a type IV pilin. Proc Natl Acad Sci U S A 110:3065-3070.

Chang, C. J., Donaldson, R., Brannen, P., Krewer, G., and Boland, R. 2009. Bacterial leaf scorch, a new blueberry disease caused by *Xylella fastidiosa*. HortScience 44:413-417.

Chatterjee, S., Almeida, R. P. P., and Lindow, S. 2008. Living in two worlds: the plant and insect lifestyles of *Xylella fastidiosa*. Annu Rev Phytopathol 46:243-271.

Coletta-Filho, H. D., Francisco, C. S., Lopes, J. R. S., Muller, C., and Almeida, R. P. P. 2017. Homologous recombination and *Xylella fastidiosa* host-pathogen associations in South America. Phytopathology 107:305-312.

Cruz, L. F., Cobine, P. A., and De La Fuente, L. 2012. Calcium increases *Xylella fastidiosa* surface attachment, biofilm formation, and twitching motility. Appl Environ Microbiol 78:1321-1331.

Cruz, L. F., Parker, J. K., Cobine, P. A., and De La Fuente, L. 2014. Calcium-enhanced twitching motility in *Xylella fastidiosa* is linked to a single PilY1 homolog. Appl Environ Microbiol 80:7176-7185.

Cursino, L., Galvani, C. D., Athinuwat, D., Zaini, P. A., Li, Y., De La Fuente, L., Hoch, H. C., Burr, T. J., and Mowery, P. 2011. Identification of an operon, Pil-Chp, that controls twitching motility and virulence in *Xylella fastidiosa*. Mol Plant Microbe Interact 24:1198-1206.

D'Attoma, G., Morelli, M., De La Fuente, L., Cobine, P. A., Saponari, M., de Souza, A. A., De Stradis, A., and Saldarelli, P. 2020. Phenotypic characterization and transformation attempts reveal peculiar traits of *Xylella fastidiosa* subspecies *pauca* strain De Donno. Microorganisms 8:1832.

Davis, M. J., French, W. J., and Schaad, N. W. 1981. Axenic culture of the bacteria associated with phony disease of peach and plum leaf scald. Curr Microbiol 6:309-314.

De La Fuente, L., Burr, T. J., and Hoch, H. C. 2007. Mutations in type I and type IV pilus biosynthetic genes affect twitching motility rates in Xylella fastidiosa. J Bacteriol 189:7507-7510.

Di Tommaso, P., Moretti, S., Xenarios, I., Orobitg, M., Montanyola, A., Chang, J. M., Taly, J. F., and Notredame, C. 2011. T-Coffee: a web server for the multiple sequence alignment of protein and RNA sequences using structural information and homology extension. Nucleic Acids Res 39:W13-17.

Drake, S. L., Sandstedt, S. A., and Koomey, M. 1997. PilP, a pilus biogenesis lipoprotein in *Neisseria gonorrhoeae*, affects expression of PilQ as a high-molecular-mass multimer. Mol Microbiol 23:657-668.

Dubnau, D., and Blokesch, M. 2019. Mechanisms of DNA uptake by naturally competent bacteria. Annu Rev Genet 53:217-237.

Ellison, C. K., Dalia, T. N., Vidal Ceballos, A., Wang, J. C., Biais, N., Brun, Y. V., and Dalia, A. B. 2018. Retraction of DNA-bound type IV competence pili initiates DNA uptake during natural transformation in *Vibrio cholerae*. Nat Microbiol 3:773-780.

Galvani, C. D., Li, Y., Burr, T. J., and Hoch, H. C. 2007. Twitching motility among pathogenic *Xylella fastidiosa* isolates and the influence of bovine serum albumin on twitching-dependent colony fringe morphology. FEMS Microbiol Lett 268:202-208.

Giltner, C. L., Nguyen, Y., and Burrows, L. L. 2012. Type IV pilin proteins: versatile molecular modules. Microbiol Mol Biol Rev 76:740-772.

Giltner, C. L., Rana, N., Lunardo, M. N., Hussain, A. Q., and Burrows, L. L. 2011. Evolutionary and functional diversity of the *Pseudomonas* type IVa pilin island. Environ Microbiol 13:250-264.

Gluck-Thaler, E., Cerutti, A., Perez-Quintero, A. L., Butchacas, J., Roman-Reyna, V., Madhavan, V. N., Shantharaj, D., Merfa, M. V., Pesce, C., Jauneau, A., Vancheva, T., Lang, J. M., Allen, C., Verdier, V., Gagnevin, L., Szurek, B., Beckham, G. T., De La Fuente, L., Patel, H. K., Sonti, R. V., Bragard, C., Leach, J. E., Noël, L. D., Slot, J. C., Koebnik, R., and Jacobs, J. M. 2020. Repeated gain and loss of a single gene modulates the evolution of vascular plant pathogen lifestyles. Sci Adv 6:eabc4516.

Hardy, L., Juan, P. A., Coupat-Goutaland, B., and Charpentier, X. 2021. Transposon insertion sequencing in a clinical isolate of *Legionella pneumophila* identifies essential genes and determinants of natural transformation. J Bacteriol 203:e00548-00520.

Hopkins, D. L., and Purcell, A. H. 2002. *Xylella fastidiosa*: Cause of Pierce's Disease of grapevine and other emergent diseases. Plant Dis 86:1056-1066.

Ihaka, R., and Gentleman, R. 1996. R: A language for data analysis and graphics. J. Comput. Graph. Stat. 5:299-314.

Jacobsen, T., Bardiaux, B., Francetic, O., Izadi-Pruneyre, N., and Nilges, M. 2020. Structure and function of minor pilins of type IV pili. Med Microbiol Immunol 209:301-308.

Jacques, M. A., Denancé, N., Legendre, B., Morel, E., Briand, M., Mississipi, S., Durand, K., Olivier, V., Portier, P., Poliakoff, F., and Crouzillat, D. 2016. New coffee plant-infecting *Xylella fastidiosa* variants derived via homologous recombination. Appl Environ Microbiol 82:1556-1568.

Jarrell, K. F., and McBride, M. J. 2008. The surprisingly diverse ways that prokaryotes move. Nat Rev Microbiol 6:466-476.

Johnsborg, O., Eldholm, V., and Håvarstein, L. S. 2007. Natural genetic transformation: prevalence, mechanisms and function. Res Microbiol 158:767-778.

Johnson, M., Zaretskaya, I., Raytselis, Y., Merezhuk, Y., McGinnis, S., and Madden, T. L. 2008. NCBI BLAST: a better web interface. Nucleic Acids Res 36:W5-9.

Johnston, C., Martin, B., Fichant, G., Polard, P., and Claverys, J. P. 2014. Bacterial transformation: distribution, shared mechanisms and divergent control. Nat Rev Microbiol 12:181-196.

Kandel, P. P., Chen, H., and De La Fuente, L. 2018. A short protocol for gene knockout and complementation in *Xylella fastidiosa* shows that one of the type IV pilin paralogs (PD1926) is needed for twitching while another (PD1924) affects pilus number and location. Appl Environ Microbiol 84:e01167-01118.

Kandel, P. P., Lopez, S. M., Almeida, R. P. P., and De La Fuente, L. 2016. Natural competence of *Xylella fastidiosa* occurs at a high frequency inside microfluidic chambers mimicking the bacterium's natural habitats. Appl Environ Microbiol 82:5269-5277.

Kandel, P. P., Almeida, R. P. P., Cobine, P. A., and De La Fuente, L. 2017. Natural competence rates are variable among *Xylella fastidiosa* strains and homologous recombination occurs in vitro between subspecies *fastidiosa* and *multiplex*. Mol Plant Microbe Interact 30:589-600.

Katoh, K., Misawa, K., Kuma, K., and Miyata, T. 2002. MAFFT: a novel method for rapid multiple sequence alignment based on fast Fourier transform. Nucleic Acids Res 30:3059-3066.

Kelley, L. A., Mezulis, S., Yates, C. M., Wass, M. N., and Sternberg, M. J. E. 2015. The Phyre2 web portal for protein modeling, prediction and analysis. Nat Protoc 10:845-858.

Kung, S. H., and Almeida, R. P. P. 2011. Natural competence and recombination in the plant pathogen *Xylella fastidiosa*. Appl Environ Microbiol 77:5278-5284.

Kung, S. H., and Almeida, R. P. P. 2014. Biological and genetic factors regulating natural competence in a bacterial plant pathogen. Microbiology 160:37-46.

Laurenceau, R., Péhau-Arnaudet, G., Baconnais, S., Gault, J., Malosse, C., Dujeancourt, A., Campo, N., Chamot-Rooke, J., Le Cam, E., Claverys, J. P., and Fronzes, R. 2013. A type IV pilus mediates DNA binding during natural transformation in *Streptococcus pneumoniae*. PLoS Pathog 9:e1003473.

Leong, C. G., Bloomfield, R. A., Boyd, C. A., Dornbusch, A. J., Lieber, L., Liu, F., Owen, A., Slay, E., Lang, K. M., and Lostroh, C. P. 2017. The role of core and accessory type IV pilus genes in natural transformation and twitching motility in the bacterium *Acinetobacter baylyi*. PLoS One 12:e0182139.

Li, Y., Hao, G., Galvani, C. D., Meng, Y., De La Fuente, L., Hoch, H. C., and Burr, T. J. 2007. Type I and type IV pili of *Xylella fastidiosa* affect twitching motility, biofilm formation and cell-cell aggregation. Microbiology 153:719-726.

Madeira, F., Park, Y. M., Lee, J., Buso, N., Gur, T., Madhusoodanan, N., Basutkar, P., Tivey, A. R. N., Potter, S. C., Finn, R. D., and Lopez, R. 2019. The EMBL-EBI search and sequence analysis tools APIs in 2019. Nucleic Acids Res 47:W636-W641.

Marko, V. A., Kilmury, S. L. N., MacNeil, L. T., and Burrows, L. L. 2018. *Pseudomonas aeruginosa* type IV minor pilins and PilY1 regulate virulence by modulating FimS-AlgR activity. PLoS Pathog 14:e1007074.

Matsumoto, A., Young, G. M., and Igo, M. M. 2009. Chromosome-based genetic complementation system for *Xylella fastidiosa*. Appl Environ Microbiol 75:1679-1687.

Mattick, J. S. 2002. Type IV pili and twitching motility. Annu Rev Microbiol 56:289-314.

Meng, Y., Li, Y., Galvani, C. D., Hao, G., Turner, J. N., Burr, T. J., and Hoch, H. C. 2005. Upstream migration of *Xylella fastidiosa* via pilus-driven twitching motility. J Bacteriol 187:5560-5567.

Nguyen, Y., Sugiman-Marangos, S., Harvey, H., Bell, S. D., Charlton, C. L., Junop, M. S., and Burrows, L. L. 2015. *Pseudomonas aeruginosa* minor pilins prime type IVa pilus assembly and promote surface display of the PilY1 adhesin. J Biol Chem 290:601-611.

Nolan, L. M., Turnbull, L., Katrib, M., Osvath, S. R., Losa, D., Lazenby, J. J., and Whitchurch, C. B. 2020. *Pseudomonas aeruginosa* is capable of natural transformation in biofilms. Microbiology 166:995-1003.

Nunney, L., Yuan, X., Bromley, R. E., and Stouthamer, R. 2012. Detecting genetic introgression: high levels of intersubspecific recombination found in *Xylella fastidiosa* in Brazil. Appl Environ Microbiol 78:4702-4714.

Nunney, L., Hopkins, D. L., Morano, L. D., Russell, S. E., and Stouthamer, R. 2014a. Intersubspecific recombination in *Xylella fastidiosa* strains native to the United States: infection of novel hosts associated with an unsuccessful invasion. Appl Environ Microbiol 80:1159-1169.

Nunney, L., Schuenzel, E. L., Scally, M., Bromley, R. E., and Stouthamer, R. 2014b. Large-scale intersubspecific recombination in the plant-pathogenic bacterium *Xylella fastidiosa* is associated with the host shift to mulberry. Appl Environ Microbiol 80:3025-3033.

Nunney, L., Yuan, X., Bromley, R., Hartung, J., Montero-Astúa, M., Moreira, L., Ortiz, B., and Stouthamer, R. 2010. Population genomic analysis of a bacterial plant pathogen: novel insight into the origin of Pierce's disease of grapevine in the U.S. PLoS One 5:e15488.

Potnis, N., Kandel, P. P., Merfa, M. V., Retchless, A. C., Parker, J. K., Stenger, D. C., Almeida, R. P. P., Bergsma-Vlami, M., Westenberg, M., Cobine, P. A., and De La Fuente, L. 2019. Patterns of inter- and intrasubspecific homologous recombination inform eco-evolutionary dynamics of *Xylella fastidiosa*. ISME J 13:2319-2333.

Rumszauer, J., Schwarzenlander, C., and Averhoff, B. 2006. Identification, subcellular localization and functional interactions of PilMNOWQ and PilA4 involved in transformation competency and pilus biogenesis in the thermophilic bacterium *Thermus thermophilus* HB27. FEBS J 273:3261-3272.

Salleh, M. Z., Karuppiah, V., Snee, M., Thistlethwaite, A., Levy, C. W., Knight, D., and Derrick, J. P. 2019. Structure and properties of a natural competence-associated pilin suggest a unique pilus tip-associated DNA receptor. mBio 10:e00614-00619.

Saponari, M., Boscia, D., Nigro, F., and Martelli, G. P. 2013. Identification of DNA sequences related to *Xylella fastidiosa* in oleander, almond and olive trees exhibiting leaf scorch symptoms in Apulia (Southern Italy). J. Plant Pathol. 95:668.

Scally, M., Schuenzel, E. L., Stouthamer, R., and Nunney, L. 2005. Multilocus sequence type system for the plant pathogen *Xylella fastidiosa* and relative contributions of recombination and point mutation to clonal diversity. Appl Environ Microbiol 71:8491-8499.

Schaad, N. W., Postnikova, E., Lacy, G., Fatmi, M., and Chang, C. J. 2004. *Xylella fastidiosa* subspecies: *X. fastidiosa* subsp. [correction] *fastidiosa* [correction] subsp. nov., *X. fastidiosa* subsp. *multiplex* subsp. nov., and *X. fastidiosa* subsp. *pauca* subsp. nov. Syst Appl Microbiol 27:290-300.

Schneider, C. A., Rasband, W. S., and Eliceiri, K. W. 2012. NIH Image to ImageJ: 25 years of image analysis. Nat Methods 9:671-675.

Seitz, P., and Blokesch, M. 2013a. DNA-uptake machinery of naturally competent *Vibrio cholerae*. Proc Natl Acad Sci U S A 110:17987-17992.

Seitz, P., and Blokesch, M. 2013b. Cues and regulatory pathways involved in natural competence and transformation in pathogenic and environmental Gram-negative bacteria. FEMS Microbiol Rev 37:336-363.

Seitz, P., Pezeshgi Modarres, H., Borgeaud, S., Bulushev, R. D., Steinbock, L. J., Radenovic, A., Dal Peraro, M., and Blokesch, M. 2014. ComEA is essential for the transfer of external DNA into the periplasm in naturally transformable *Vibrio cholerae* cells. PLoS Genet 10:e1004066.

Sheffield, P., Garrard, S., and Derewenda, Z. 1999. Overcoming expression and purification problems of RhoGDI using a family of "Parallel" expression vectors. Protein Expr. Purif. 15:34-39.

Simko, I., and Piepho, H.-P. 2012. The area under the disease progress stairs: Calculation, advantage, and application. Phytopathology 102:381-389.

Stamatakis, A. 2014. RAxML version 8: a tool for phylogenetic analysis and post-analysis of large phylogenies. Bioinformatics 30:1312-1313.

Tammam, S., Sampaleanu, L. M., Koo, J., Manoharan, K., Daubaras, M., Burrows, L. L., and Howell, P. L. 2013. PilMNOPQ from the *Pseudomonas aeruginosa* type IV pilus system form a transenvelope protein interaction network that interacts with PilA. J Bacteriol 195:2126-2135.

van Schaik, E. J., Giltner, C. L., Audette, G. F., Keizer, D. W., Bautista, D. L., Slupsky, C. M., Sykes, B. D., and Irvin, R. T. 2005. DNA binding: a novel function of *Pseudomonas aeruginosa* type IV pili. J Bacteriol 187:1455-1464.

Vanhove, M., Retchless, A. C., Sicard, A., Rieux, A., Coletta-Filho, H. D., De La Fuente, L., Stenger, D. C., and Almeida, R. P. P. 2019. Genomic diversity and recombination among *Xylella fastidiosa* subspecies. Appl Environ Microbiol 85:e02972-02918.

Vesel, N., and Blokesch, M. 2021. Pilus production in *Acinetobacter baumannii* is growth phase dependent and essential for natural transformation. J Bacteriol 203:e00034- 00021.

Wiedenbeck, J., and Cohan, F. M. 2011. Origins of bacterial diversity through horizontal genetic transfer and adaptation to new ecological niches. FEMS Microbiol Rev 35:957-976.

Wolfgang, M., van Putten, J. P. M., Hayes, S. F., and Koomey, M. 1999. The *comP* locus of *Neisseria gonorrhoeae* encodes a type IV prepilin that is dispensable for pilus biogenesis but essential for natural transformation. Mol Microbiol 31:1345-1357.

Zhu, X., Boulet, A., Buckley, K. M., Phillips, C. B., Gammon, M. G., Oldfather, L. E., Moore, S. A., Leary, S. C., and Cobine, P. A. 2021. Mitochondrial copper and phosphate transporter specificity was defined early in the evolution of eukaryotes. Elife 10:e64690.

Supplementary material for chapter 5

Supplementary information text

Supplementary materials and methods

Site-directed mutagenesis of genes of interest in *X. fastidiosa* strain TemeculaL

The deletion of each gene of interest (GOI) (**Table S5-3**) in *X. fastidiosa* strain TemeculaL (Potnis et al. 2019) was performed using a protocol developed by our research group (Kandel et al. 2018). Briefly, the upstream and downstream regions immediately flanking each GOI were amplified from the *X. fastidiosa* TemeculaL genome using pairs of primers (**Table S5-2**) containing overlapping nucleotides with the Km resistance cassette encoded by the pUC4K plasmid (**Table S5-1**). When deleting genes in operons that share overlapping nucleotides with flanking genes, the corresponding nucleotides were maintained in the primer design to mitigate frameshift mutations.

To obtain the targeting construct, the amplified upstream and downstream regions of each GOI were fused to the Km resistance cassette via overlap-extension PCR, as detailed elsewhere (Kandel et al. 2018). The purified PCR product was then used to transform WT *X. fastidiosa* strain TemeculaL cells through natural competence directly. In summary, WT cells were suspended in PD3 broth to OD_{600nm} of 0.25 (~10^8 cells/ml), and 10 µL of this suspension was spotted on a PD3 agar plate, with 10 µL of the targeting construct being spotted on top of it. The resulting mix of cells and the targeting construct was air-dried and incubated at 28 ºC for five days. Then, cells were suspended into 1ml of PD3 broth and plated into PW agar plates amended with Km for the selection of mutant strains obtained through homologous recombination.

Deletion of each GOI was confirmed through PCR (**Table S5-2**), in which non-amplification of an internal sequence of each GOI, and amplification of an internal sequence of the upstream region of each GOI and the Km resistance cassette, confirmed deletion of each of these genes in *X. fastidiosa* strain TemeculaL (WT was included as control in each PCR reaction). The obtained mutant strains were stored as 25% glycerol stocks in PD3 broth at -80 ºC until use. PCR reactions were carried out using a standard protocol with the iProof High-Fidelity PCR kit (Bio-Rad) in a S1000 thermal cycler (Bio-Rad). PCR products and agarose gel fragments were purified using the Gel/PCR DNA Fragments Extraction kit (IBI Scientific). The pUC4K plasmid was prepared from an overnight culture of *E. coli* Dh5α using the extraction kit GeneJET Plasmid Miniprep kit (Thermo Scientific).

Analysis of natural competence among *X. fastidiosa* strains

The plasmid pAX1-Cm (Matsumoto et al. 2009), prepared from an overnight culture of *E. coli* EAM1 (**Table S5-1**) (Matsumoto and Igo 2010) using the extraction kit GeneJET Plasmid Miniprep kit (Thermo Scientific), was used in this assay. The plasmid concentration was adjusted to 100 ng/µl before using (Cytation 3 Image Reader spectrophotometer; BioTek Instruments Inc.) and aliquots were stored at -20 ºC until use. For natural competence assays, recipient cells were suspended in PD3 broth to OD_{600nm} of 0.25 and spotted onto PD3 agar plates similarly as described above for site-directed mutagenesis. Briefly, 10 µl of cells were spotted together with 1 µg of pAX1-Cm (10-µl volume), air-dried, and incubated at 28 ºC for five days. Then, cells were suspended in 1 ml of PD3 broth, diluted by 10-fold serial dilutions and plated in selective (PW+Cm agar plates for WT cells and PW+Km+Cm agar plates for mutant strains) and

non-selective (PW agar plates for WT cells and PW+Km agar plates for mutant strains) media for growth of recombinants and total viable cells (both counted as CFU/ml), respectively.

After 21 days of incubation at 28 ºC, CFUs were enumerated for recombinants and total viable cells and the recombination frequency was calculated as the ratio of the number of recombinants to total viable cells. At least three independent biological replicates with two internal replicates were performed for each *X. fastidiosa* strain. To confirm homologous recombination, five recombinant CFUs from each strain per biological replicate were randomly selected and plated onto new selective medium agar plates to observe growth, and colony PCR was performed using a pair of primers designed to amplify the Cm resistance cassette (Kandel et al. 2018) (**Table S5-2**). PCR reactions were carried out using a standard protocol with the *Taq* 5X Master Mix (New England Biolabs) in a S1000 thermal cycler (Bio-Rad).

Twitching motility assays

The twitching motility of *X. fastidiosa* strains was evaluated using PW agar plates without BSA, as previously described (Kandel et al. 2016). In short, 15 to 20 spots of each strain (six strains per plate) were made onto PW without BSA plates using the needle side of a sterile inoculation loop (Globe Scientific). Plates were incubated at 28 ºC for 4 days before analysis. Then, the colony peripheral fringes were visualized under ×10 magnification using a Nikon Eclipse Ti inverted microscope (Nikon). Image acquisition was performed using a Nikon DS-Q1 digital camera (Nikon) controlled by the NIS-Elements software version 3.0 (Nikon). Fringe widths were measured for six colonies per strain per plate, with four measurements per colony,

using the ImageJ software (Schneider et al. 2012). Twitching experiments were performed at least three times independently, with 48 internal replicates each.

Growth curve and growth rate, biofilm formation and planktonic growth, and settling rate measurements of *X. fastidiosa* strains

X. fastidiosa cells were suspended in PD3 broth to OD_{600nm} of 0.25 and inoculated into polystyrene 96-well plates (Corning Inc.) to generate growth curves (Kandel et al. 2017). Eight wells were used per strain, which were inoculated as 10 µl aliquots into 190 µl of PD3 broth. In addition, eight wells per plate were inoculated with 200 µl of PD3 broth to serve as controls. Plates were incubated at 28 ºC and 150 rpm for eight days and the OD_{600nm} value for each well was measured daily using the Cytation 3 Image Reader spectrophotometer (BioTek Instruments Inc.). OD_{600nm} values were adjusted by subtracting values from control wells. Growth rates were calculated as the slope of the line obtained by performing natural log-transformation of the growth values at the exponential growth phase (two to six days post inoculation) using the formula: rate = [ln (OD_{600nm} day 6) - ln (OD_{600nm} day 2)]/time (days) (Kandel et al. 2017). On the other hand, planktonic growth was evaluated by transferring a 150 µl aliquot of the supernatant of each suspension at the final day of evaluation (day 8) to a new 96-well plate and measuring the OD_{600nm}, while biofilm formation was quantified by staining cells that remained attached to each well using a 0.1% crystal violet solution, as previously described (Cruz et al. 2012).

Briefly, wells were gently rinsed three times with Milli-Q water and stained with 230 µl of 0.1% crystal violet solution for 20 minutes at room temperature. Then, the crystal violet solution was removed, the wells were gently rinsed once again three times with Milli-Q water,

and the crystal violet was solubilized by adding 230 µl of 95% ethanol and incubating under agitation (150 rpm) for 5 minutes. The OD_{600nm} values of wells was then measured using the Cytation 3 Image Reader spectrophotometer (BioTek Instruments Inc.). At last, settling rate (used as a measure of cell aggregation), was determined by suspending cells in PD3 broth to OD_{600nm} of 1.0 and measuring the OD_{600nm} values in a cuvette when cells settled exponentially (0 to 2 hours post inoculation; hpi) (Kandel et al. 2017). As used for growth rate, the settling rate was calculated using the formula: rate = [ln (OD_{600nm} 0 hpi) - ln (OD_{600nm} 2 hpi)]/time (hours). Experiments were performed at least three times independently.

Transmission electron microscopy

The piliation phenotype of cells was visualized under a transmission electron microscope, as described elsewhere (Kandel et al. 2018). Briefly, two-day old *X. fastidiosa* cultures were harvested from PW without BSA agar plates and suspended in 200 µl of sterile Milli-Q water. Then, 10 µl of each cell suspension were pipetted onto a Formvar-coated TEM grid (Electron Microscopy Sciences) and cells were allowed to settle for 10 minutes. After, the leftover liquid was blotted out using a filter paper and the grid was negatively stained with 10 µl of 2% phosphotungstic acid (PTA) for 10 seconds. The excess PTA was then removed using filter paper, and grids were air-dried and observed under a Zeiss EM10 transmission electron microscope (Carl Zeiss), with images being captured at 31,500× magnification using the MaxIm DL software (Diffraction LTD). Alternatively, grids were placed directly on top of *X. fastidiosa* cells growing in PW without BSA agar plates for few seconds and negatively stained with PTA, as described above, for observation in the transmission electron microscope. Two independent experiments were performed.

X. fastidiosa* in planta virulence assays using the model plant *Nicotiana tabacum

For in planta assays, *Nicotiana tabacum* L. cv. Petite Havana SR1 plants were propagated at the Plant Science Research Center at Auburn University (AL, USA) and inoculated with *X. fastidiosa* TemeculaL WT, Δ*pilA1*, Δ*pilA2*, Δ*pilA1pilA2*, Δ*pilQ*, Δ*pilR* and Δ*pilS* strains using a modified protocol from elsewhere (Francis et al. 2008). The experiment was conducted in a completely randomized design. Briefly, transplanted three-week-old tobacco plants were inoculated by pin pricking using 23-gauge needles with 20 µL of either PBS (mock control) or individual suspensions of each *X. fastidiosa* strain at an OD_{600nm} of 1.0 in PBS. Inoculation at the base of the second and third (counting from the bottom) leaf petioles was done twice with one week apart. In total, plants were individually inoculated with PBS (n=10) and *X. fastidiosa* strains (n=10). Disease incidence (percentage of symptomatic plants per total inoculated plants) and severity were recorded weekly for nine-time points after first symptom appearance (about 8 weeks post-inoculation). Disease severity was calculated for each plant by counting symptomatic leaves and total number of leaves [(symptomatic leaves/total leaves) × 100], whereas the Area Under the Disease Progress Curve (AUDPC) was calculated by the midpoint rule method (Simko and Piepho 2012) using disease severity data. Two independent experiments were performed.

On the other hand, the *X. fastidiosa* population in planta was determined by qPCR using leaf samples from the end time point of disease evaluation. To analyze the ability of *X. fastidiosa* strains to colonize infected plants, basal and top leaves were used in this analysis. DNA was extracted from 100 mg of the petiole of each leaf using a modified CTAB protocol (Doyle and Doyle 1987). qPCR reactions were performed using the HL5/HL6/HLp pair of primers and TaqMan probe labeled with FAM (**Table S5-2**) (Francis et al. 2006). DNA amplifications were

performed using a standard protocol with the PerfeCTa Multiplex qPCR ToughMix Low ROX kit (Quantabio) in a C1000 thermal cycler base with a CFX96 real-time system (Bio-Rad), using standard cycling parameters. DNA amplification of each sample was repeated in triplicates. Reaction efficiencies of 95 to 105% were confirmed for each qPCR run. The number of *X. fastidiosa* cells in each sample was calculated by comparing the obtained values with a standard curve made from 10-fold serial dilutions of the genomic DNA of *X. fastidiosa*. Two independent experiments were performed.

Cloning, expression, and purification of FimT1s, FimT2s and FimT3s

FimT1s, FimT2s and FimT3s from *X. fastidiosa* strain TemeculaL were cloned into pHIS-Parallel1 for *E. coli* expression (primers used in this process are listed in **Table S5-2**). PCR reactions were carried out using a standard protocol with the iProof High-Fidelity PCR kit (Bio-Rad) in a S1000 thermal cycler (Bio-Rad). PCR products and agarose gel fragments were purified using the Gel/PCR DNA Fragments Extraction kit (IBI Scientific). Restriction enzymes and T4 DNA ligase used in the cloning process were obtained from New England Biolabs and Promega, respectively. *E. coli* BL21(DE3) cells carrying each vector were grown in LB broth to OD_{600nm} 0.6-0.8, and protein expression was induced with 400 µM of isopropyl β-D-1-thiogalactopyranoside (IPTG) for 3 hours and 30 minutes. Then, cells were collected by centrifugation (4,000 rpm for 15 minutes at 4 ºC), suspended in lysis buffer (500 mM NaCl, 20 mM Tris, pH 8.0) and disrupted by sonication. The soluble fractions were collected by centrifugation (12,000 rpm for 30 minutes at 4 ºC) and the proteins were individually purified by affinity chromatography using Ni-NTA agarose resin columns (Thermo Scientific). Protein concentration in each sample was determined by Bradford assay (VWR) and, when needed,

samples were concentrated using the Spin-X UF Concentrator (Corning) and centrifugation (12,000 rpm for 1 hour at 4 ºC). Protein purifications were visualized by submitting samples to 10% SDS-PAGE (150 V for 1 hour) and staining with Coomassie Brilliant Blue.

Supplementary discussion

Our core genes that were essential for both natural competence and twitching motility of *X. fastidiosa* represent a central machinery required for the biogenesis and functioning of type IV pili (TFP) resembling that of *P. aeruginosa*, a well-studied model for TFP and twitching motility (Burrows 2012). This central machinery involves, in addition to the major pilin PilA, the retraction and extension ATPases PilB and PilT, respectively, the platform protein PilC, the prepilin peptidase PilD and the secretin PilQ (Mattick 2002). Moreover, the essential function of PilMNOP in *X. fastidiosa* was close to that found in *N. meningitidis*, in which the presence of this alignment subcomplex is essential for the piliation phenotype and functions performed by TFP (Carbonnelle et al. 2006; Goosens et al. 2017), with the opposite being described in *P. aeruginosa* (Takhar et al. 2013). Surprisingly, *pilZ* was essential not only for twitching motility, but also natural competence in our study. This seems to be the first observation of *pilZ* being essential for this phenotype. Many PilZ orthologs have been demonstrated to interact with the secondary messenger 3',5'-cyclic diguanylic acid (c-di-GMP) directly through its EAL, GGDEF and/or HD-GYP domains (Guzzo et al. 2009; Pratt et al. 2007; Ryjenkov et al. 2006) or by interacting with other c-di-GMP receptor protein (Yang et al. 2014). Although the *X. fastidiosa* PilZ does not appear to possess canonical EAL, GGDEF or HD-GYP domains, it could interact with c-di-GMP through degenerate domains, as already describe to one of its proteins (Cursino et al. 2015), or by interacting with an unidentified receptor. This would contribute to establish the

apparent link between high levels of c-di-GMP and induction of twitching motility in this bacterium (de Souza et al. 2013). However, this hypothesis needs further elucidation.

In contrast, although required for movement, TFP genes are not essential for natural competence in *P. aeruginosa* (Nolan et al. 2020). Likewise, deletion of TFP genes in *V. cholerae* does not abrogate its natural competence (Seitz and Blokesch 2013). This may be related to the lifestyle of each individual species, their specific needs and genome content. *X. fastidiosa* lives exclusively in the xylem of plant hosts and foregut of insect vectors (Chatterjee et al. 2008b) in addition to having a reduced genome in comparison to the closely related *Xanthomonas* spp. (Almeida et al. 2014). Besides, *X. fastidiosa* moves only through twitching motility (Chatterjee et al. 2008b). Together, these findings suggest that this bacterium relies heavily on TFP genes to perform essential functions.

Curiously, however, is the presence of many paralogs of TFP genes encoded by *X. fastidiosa*. Deletion of the major pilin *pilA* has been shown to abolish natural competence and movement in *Acinetobacter baylyi* (Leong et al. 2017) and *A. baumannii* (Vesel and Blokesch 2021), and only twitching motility in *P. aeruginosa* (Harvey et al. 2009). In our study, the individual deletion of *pilA* paralogs did not abrogate either phenotype, suggesting functional overlapping. *V. cholerae*, for example, encodes three different TFP, including the competence pilus (Seitz and Blokesch 2013), toxin-coregulated pili (TCP) (Taylor et al. 1987), and mannose-sensitive hemagglutination (MSHA) pili (Jouravleva et al. 1998). Although TCP and MSHA pili are encoded by their own set of genes, rather than being encoded by *pil* and associated genes, the existence of different TFP led us to hypothesize that PilA1, PilA2 and PilA3 could compose

different pilus with specific functions. We were particularly interested in defining whether these different paralogs could specialize in natural competence or twitching motility.

As mentioned above, our results instead suggested functional overlapping among PilA paralogs. Previously, TFP hyperpiliation was observed in a *X. fastidiosa* Δ*pilA1* mutant (Kandel et al. 2018), which could explain our observation that deletion of this gene increases both natural competence and twitching motility of this bacterium. In addition, the same study described that deletion of *pilA2* leads to loss of movement (Kandel et al. 2018), opposing our results. However, movement analysis of Δ*pilA2* was previously performed using PD3 agar plates, while in this study we used PW without BSA agar plates, which proved to be more conducive for twitching motility and thus yield more accurate results. Therefore, we determined that *pilA2* is not essential for the movement of *X. fastidiosa*, which was previously described (Kandel et al. 2018). Our Δ*pilA3* mutant produced similar phenotypic results as Δ*pilA2*, further supporting the overlapping of functions. However, we cannot discard that these *pilA* paralogs may play different roles according to different host conditions and/or environmental signals, which remains elusive. For instance, different *pilA* alleles among strains of other bacterial species have been implicated in kin recognition (Adams et al. 2019a) and susceptibility to a bacteriophage (Kim et al. 2018). Nonetheless, a study performed with a non-pathogenic strain of *X. fastidiosa* encoding five *pilA* paralogs demonstrated that deletion of the global σ^{54} regulator RpoN downregulated the expression of only one of these paralogs (da Silva Neto et al. 2008), suggesting some level of specificity.

In *P. aeruginosa*, the PilR regulatory protein of the PilRS two-component regulatory system is the transcription factor that binds to a *cis*-acting region upstream to the *pilA* promoter and enables its transcription by the RNA polymerase containing the alternative σ factor RpoN (Ishimoto and Lory 1992; Jin et al. 1994). On the other hand, the PilS sensor protein interacts directly with PilA for pilin autoregulation (Kilmury and Burrows 2016). When high levels of PilA are present in the inner membrane, PilS deactivates PilR by adopting a phosphatase-active conformation, whereas absence of PilA leads to phosphorylation of PilR by PilS that remains in a kinase state, which in turn increases transcription of *pilA* and of other coregulated genes presumably important for virulence and surface-associated behaviors of *P. aeruginosa* (Kilmury and Burrows 2016; Kilmury and Burrows 2018). Deletion of *pilR* abrogates *pilA* transcription (Boyd et al. 1994), with individual deletion of both *pilR* and *pilS* leading to significant reductions of twitching motility (or even abolition) in *P. aeruginosa* (Kilmury and Burrows 2018), *A. baumannii* (Vesel and Blokesch 2021), *A. baylyi* (Leong et al. 2017), *Dichelobacter nodosus* (Parker et al. 2006), *Xanthomonas oryzae* pv. *oryzae* (Yu et al. 2020), besides *X. fastidiosa* (Li et al. 2007). The twitching motility of the latter three was only evaluated in a Δ*pilR* background. Moreover, natural competence has been negatively impacted by the deletion of this two-component system in *A. baumannii* (Vesel and Blokesch 2021), but not in *A. baylyi* (Leong et al. 2017). Our phenotypic results upon deletion of *pilR* follows what have been mostly described, with abrogation of movement and significant reduction in natural competence. Conversely, deletion of *pilS* in *X. fastidiosa* significantly increased both phenotypes, generating the highest recombination frequencies and longest fringe widths of twitching motility recorded in this study. This is the first report of a Δ*pilS* mutant having increased TFP-related phenotypes and suggests novel regulatory mechanisms in *X. fastidiosa*. Notably, the well-studied PilS of *P. aeruginosa*

has six transmembrane segments and thus faces the cytoplasm of cells whilst interacting with PilA stored in their inner membrane (Boyd and Lory 1996; Kilmury and Burrows 2016). The PilS of *X. fastidiosa*, however, has only five transmembrane domains (predicted using the TMHMM Server, v. 2.0) (Krogh et al. 2001), which likely allows it to still interact with PilA in the inner membrane, but also suggests that it can interact with different or even additional signals for pilin regulation. This is supported by the fact that the vast majority of histidine kinase sensor proteins from two-component systems are membrane-bound with a C-terminal cytoplasmic kinase domain (West and Stock 2001), and not periplasmic as predicted for *X. fastidiosa*. However, this hypothesis needs to be further explored.

The motility of bacterial species can also be controlled by chemotaxis, a mechanism in which cells sense environmental stimuli and move either toward or away from the chemical signal. In *X. fastidiosa*, twitching motility is regulated by the Pil-Chp operon composed by *pilGIJL-chpBC* (Cursino et al. 2011). In addition, we found that this plant pathogen encodes the PilH chemosensory response regulator, previously thought to be absent in this bacterium (Cursino et al. 2011), in another area of the genome far from the Pil-Chp operon (**Table S5-4**). Similarly, the Pil-Chp chemosensory system that regulates TFP assembly and movement in *P. aeruginosa* is composed by *pilGHIJK-chpABC* (Darzins 1993, 1994, 1995; Whitchurch et al. 2004). *X. fastidiosa* lacks a *pilK* homolog, while PilL is likely this bacterium's counterpart to ChpA from *P. aeruginosa* (Cursino et al. 2011). Based on the *P. aeruginosa* and *Escherichia coli* (Gram-negative model system for chemotaxis involving flagellum) chemosensory systems, these are composed mainly by a transmembrane chemoreceptor (MCP/PilJ; located in the inner membrane) that interacts with histidine kinases (CheA/PilL) via adaptor proteins (CheW/PilI-

ChpC) (Darzins 1994; Hazelbauer et al. 2008). In *E. coli*, MCPs alter the kinase activity of CheA in the presence of ligand binding (chemical stimuli), which transfers a high-energy phosphoryl group to the response regulator CheY (PilG) that will then interact with the flagellar motor proteins to modulate the direction of rotation (Hazelbauer et al. 2008). The adaptation to ligand concentrations is performed through reversible methylation changes to the MCP adjusted by a methyltransferase (CheR) and a methylesterase (CheB/ChpB) (Hazelbauer et al. 2008). Likewise, the Pil-Chp system in *P. aeruginosa* controls TFP biogenesis by modulating the intracellular levels of the secondary messenger 3',5'-cyclic monophosphate (cAMP), whereas the response regulators PilG and PilH presumably control twitching motility in a cAMP-independent manner by modulating pilus extension and retraction mediated by the ATPases PilB and PilT, respectively, in a hitherto unidentified mechanism (Bertrand et al. 2010; Fulcher et al. 2010). Individual deletions of *pilGIJ* in *P. aeruginosa* leads to impaired twitching motility (Bertrand et al. 2010; Darzins 1993, 1994), whereas Δ*pilH* mutants either displayed reduced movement or an altered pattern of twitching motility depending on the strain background (Bertrand et al. 2010; Darzins 1994). Additionally, Δ*chpA* (PilL) mutants present significantly reduced twitching motility (Bertrand et al. 2010; Whitchurch et al. 2004), with individual deletions of *chpBC* not altering this phenotype (Whitchurch et al. 2004). In *A. baylyi*, *pilG* knockout significantly reduced twitching motility with no apparent effects on natural competence (Leong et al. 2017). On the contrary, deletion of *pilG* and *pilH* in *A. baumannii* significantly reduced twitching motility, but with deletion of *pilG* leading to abrogation of natural competence and deletion of *pilH* not affecting this phenotype (Vesel and Blokesch 2021). Lastly, deletion of both *pilG* and *pilL* in *X. fastidiosa* leads to a deficient phenotype of twitching motility (Cursino et al. 2011; Shi and Lin 2016).

Our results showed that deletion of any gene belonging to the Pil-Chp chemosensory system of *X. fastidiosa* strain TemeculaL significantly reduced its twitching motility, although no abrogation of this phenotype was observed among deletion mutants. The observed differences with previous studies of *X. fastidiosa* may be due to different strain genetic backgrounds, even though the genes analyzed in this study from strain TemeculaL share 100% homology with corresponding genes in strain Temecula1, and/or gene knockout methods. Here, we have deleted genes of interest by entirely replacing them by a kanamycin-resistance cassette in *X. fastidiosa* strain TemeculaL, while in the other mentioned studies, knockout of *pilG* and *pilL* was performed by transposon insertion in strain Temecula1. Regarding natural competence phenotypes, we obtained variable results upon deletion of Pil-Chp genes. Regardless of a reduced twitching motility, Δ*pilG*, Δ*pilH* and Δ*pilL* mutants presented significant higher natural competence phenotypes (contrarily to what was observed in *A. baylyi* and *A. baumannii*, described above), while deletion of *pilJ* and *chpC* reduced this trait and Δ*pilI* and Δ*chpB* did not present altered natural competence. Conclusively, we have completely assayed the Pil-Chp operon function on both natural competence and twitching motility of *X. fastidiosa* and determined that the individual components of this system were not essential for either of these traits in our study. Together, our findings with the PilRS two-component regulatory system and with the Pil-Chp chemosensory system suggest that TFP regulation in *X. fastidiosa* has its own specific characteristics, which may include alternate signaling pathways and/or environmental stimuli.

Returning to the analysis of paralogous genes in *X. fastidiosa*, next we have the minor pilins *pilEVWX* and *fimT*, as well as the TFP tip adhesin *pilY1*. The minor pilins *pilE1V1W1X1*

and *fimT1*, as well as the tip adhesin *pilY1-1* are encoded in the same operon (**Table S5-4**). A similar genomic arrangement has also been observed in *P. aeruginosa* (Alm et al. 1996b). On the other hand, paralogs of these genes are encoded in two sequential operons located in a different region of the *X. fastidiosa* genome (**Table S5-4**). One operon is composed by *pilE2* and *pilY1-2* and the other by *pilV2W2X2* and *fimT2* (**Table S5-4**). Additionally, a third tip adhesin, *pilY1-3*, is present but is not encoded in an operon, while we determined that FimT3, which is also not encoded in an operon, is the DNA receptor of the *X. fastidiosa* TFP (discussed in the main manuscript).

In *P. aeruginosa*, genetic analyses revealed the presence of the minor pilins *pilEVWX* and *fimTU* that are required for TFP assembly (except FimT, which is a substitute of FimU), twitching motility and infection by pilus-specific phage (Alm et al. 1996b; Alm and Mattick 1995, 1996; Mattick 2002; Russell and Darzins 1994). Moreover, it has been demonstrated that these minor pilins prime the assembly of TFP whilst promoting the display of the PilY1 adhesin at the cell surface and thus at the pilus tip (Nguyen et al. 2015). Briefly, PilVWX interact with PilY1 and form a complex that is bound by PilE, whereas FimU (substituted by FimT in *X. fastidiosa*) contacts PilA directly and promotes its connection to PilVWXY1E by interacting with PilV and PilE. Minor pilins are essential for TFP assembly since their deletion abrogates pilus assembly and twitching motility (Alm et al. 1996b; Alm and Mattick 1995, 1996; Giltner et al. 2010; Nguyen et al. 2015; Russell and Darzins 1994). However, *P. aeruginosa* mutant cells lacking the minor pilin operon still produce reduced amounts of TFP that are twitching motility-defective, which is mediated by the expression of minor pseudopilins from this bacterium's type II secretion system (TIISS) (Nguyen et al. 2015). The TFP assembly system and the TIISS are

evolutionary related and share many homologs (Craig et al. 2004; Nunn 1999). Ultimately, in a strain background lacking minor pseudopilins encoded by the TIISS, the minimal components required for TFP assembly included PilVWXY1 and either FimU or PilE (Nguyen et al. 2015). In *A. baylyi*, deletion of *pilW* abrogated both natural competence and twitching motility, while individual deletions of *pilV*, *pilY1* and *fimT* abolished natural competence and reduced twitching motility (Leong et al. 2017).

In *X. fastidiosa*, we observed that individual deletion of the genes belonging to the *pilE1V1W1X1*, *fimT1* and *pilY1-1* operon mostly abrogated twitching motility. The exceptions were Δ*fimT1* and Δ*pilY1-1*, which still presented movement, but significantly reduced. However, deletion mutants of all these genes were still naturally competent but displayed significantly reduced recombination frequencies. In *X. fastidiosa* strain Temecula1, deletion of *fimT1* abrogated twitching motility (Li et al. 2007), contrarily to our results. This may be due to different strain background and/or gene knockout method, as commented above. Our results demonstrated that *pilE1V1W1X1* are essential for twitching motility of *X. fastidiosa* strain TemeculaL, while no gene encoded within this operon is essential for natural competence. Curiously, the presence of mutants defective in movement indicates that paralogs of these minor pilins and tip adhesin did not compensate for the loss of their counterparts. In fact, deletion mutants within the operons *pilE2Y1-2* and *pilV2W2X2*/*fimT2* produced variable results. Deletion of *pilE2* significantly increased movement and did not alter natural competence; Δ*pilV2* and Δ*fimT2* presented significant increased natural competence and no change in twitching motility; Δ*pilW2* displayed significant higher natural competence and significant lower movement; and deletion of *pilX2* and *pilY1-2* significantly reduced both phenotypes. On the other hand, the

Δ*pilY1-3* mutant presented higher natural competence and lower twitching motility. Thus, no gene belonging to this operon was essential for either natural competence or twitching motility, suggesting a key role for the *pilE1V1W1X1*, *fimT1* and *pilY1-1* operon in comparison to their paralogs. Intriguingly, it has been demonstrated that *P. aeruginosa* strains encode major pilins associated with a specific set of minor pilins. This means that major pilins require their specific subset of minor pilins for both TFP assembly and twitching motility, since strains expressing the major pilin from another strain that has heterologous minor pilins do not assemble TFP nor perform twitching motility (Giltner et al. 2011). If this correlation also happens in *X. fastidiosa*, it may explain the lack of compensation by their paralogs when the *pilE1V1W1X1*, *fimT1* and *pilY1-1* operon was deleted. Moreover, the ability of minor pseudopilins from the TIISS in *P. aeruginosa* to assemble small amounts of TFP when minor pilins are deleted is suggested to occur at a lower affinity, leading to inefficient pilus extension that cannot compete with retraction (Nguyen et al. 2015). This is because of the specific interaction of major pilins to their minor pilin subsets described above (Giltner et al. 2011). Nevertheless, we suggest that the ability of the minor pilin mutants Δ*pilE1V1W1X1* and Δ*fimT1* of *X. fastidiosa* to remain naturally competent at low frequencies regardless of losing their motility may be due to TFP assemble by TIISS minor pseudopilins encoded by this bacterium (Jha et al. 2005). This would allow *X. fastidiosa* to assemble TFP that can still perform DNA uptake but are not able to carry out twitching motility. However, all our hypothesis raised here need to be further investigated.

It would be interesting to determine whether the different PilA paralogs encoded by *X. fastidiosa* require specific subsets of minor pilins. Strikingly, the strain we have analyzed in this study encodes three *pilA* paralogs, but only two subsets of minor pilins. Additionally, this strain

encodes a third *pilY1* paralog not encoded within the two subsets of minor pilins. PilY1 was initially described in *Neisseria* spp. (in which it is named PilC) as important for adherence to epithelial cells and thus acting as a pilus tip adhesin (Rudel et al. 1995). In *P. aeruginosa*, PilY1 was shown to bind calcium (Ca^{2+}) and oppose pilus retraction in a calcium-dependent manner (Orans et al. 2010). In *X. fastidiosa*, the paralog PilY1-2 is the only TFP tip adhesin that has a Ca-binding motif and likely contributes for this bacterium to cope within the xylem sap of plant hosts, which is an environment with high Ca concentrations (Cruz et al. 2014). Deletion of *pilY1* in *X. fastidiosa*, however, has generated antagonistic results. Deletion of *pilY1-1* in some studies have been shown to significantly reduce twitching motility (De La Fuente et al. 2007; Li et al. 2007). Conversely, analysis of the same mutant strain and of Δ*pilY1-2* in another study demonstrated that deletion of these genes does not alter the movement phenotype of *X. fastidiosa* (Cruz et al. 2014). As mentioned above, our study, however, demonstrated that deletion of all three *pilY1* paralogs significantly reduced twitching motility. Nonetheless, phenotypic results of natural competence and twitching motility from our study and others demonstrate that the presence of different *pilY1* paralogs with variable domains in *X. fastidiosa* may dictate function specificity.

At last, deletion of both *pilF* and *pilU* in *X. fastidiosa* led to significantly reduced natural competence and twitching motility phenotypes. PilF has been described in *P. aeruginosa* as a pilotin (outer membrane lipoprotein) required for the localization and assembly of the multimeric PilQ secretin, being essential for both TFP and twitching motility of this bacterium (Koo et al. 2008; Watson et al. 1996). In *A. baylyi*, both *pilF* and *pilU* are essential for natural competence and twitching motility. On the other hand, PilU is a secondary retraction ATPase homologous to

PilT essential for twitching motility of *P. aeruginosa* (Chiang et al. 2008). Our Δ*pilU* results, however, are close to those described for *A. baumannii* and *V. cholerae* in which PilU is not essential for natural competence (Seitz and Blokesch 2013; Vesel and Blokesch 2021). Thus, PilU does not work as an independent retraction ATPase, but it likely functions in conjunction with PilT to increase the retraction force of TFP (Adams et al. 2019b; Chlebek et al. 2019; Vesel and Blokesch 2021). Curiously, this mechanism was also suggested in *P. aeruginosa* despite previous phenotypic results upon deletion of *pilU* (Talà et al. 2019).

TFP have also been demonstrated to affect other bacterial phenotypes besides natural competence and twitching motility. These include aggregation and adherence, biofilm formation, conjugation, electron transfer, manipulation of host cells, virulence, and secretion of proteins (Giltner et al. 2012). Therefore, we analyzed whether deletion of TFP-related genes could also affect additional key phenotypes of *X. fastidiosa*, including growth, biofilm formation, cell aggregation and virulence in planta. Deletion of genes analyzed in this study greatly changed the growth curve and growth rate of *X. fastidiosa*. However, since these analyses are traditionally performed by only measuring the turbidity of bacterial cultures, we also investigated the ability of TFP genes to alter the growth of this bacterium by counting the number of viable cells (CFU/ml) grown during natural competence assays. This was performed because *X. fastidiosa* presents higher recombination frequency via natural competence when growing exponentially (Kung and Almeida 2014), thus changes in growth could indirectly reflect in its natural competence. However, only two non-recombinant mutant strains, Δ*pilC* and Δ*pilP*, had altered growth by presenting significant higher number of viable cells than the WT, thus indicating that our natural competence results were not affected by changes in the growth of *X. fastidiosa*.

Previously, deletion of *pilG* and *pilL* has been shown to significantly decrease biofilm formation by *X. fastidiosa* (Cursino et al. 2011; Shi and Lin 2018), while knockout of *pilB*, *pilQ* and *fimT1* significantly increases this phenotype (Li et al. 2007; Meng et al. 2005), and deletion of *pilY1-1* and *pilY1-2* does not affect it (Cruz et al. 2014). Our results mostly followed what has been described for *X. fastidiosa*, except for Δ*pilG* and Δ*pilL*, which presented similar biofilm formation to the WT. This may be due to different strain genetic backgrounds and/or knockout methods as discussed above. Nonetheless, we have established here that 14 TFP-related genes modulate biofilm formation, whereas 19 TFP genes modulate planktonic growth, an opposite phenotype to biofilm formation. In addition, only three genes have been found to modulate cell aggregation despite its known positive correlation to biofilm formation (Chatterjee et al. 2008b). We have indeed found a positive correlation between biofilm formation and settling rate (measurement of cell aggregation), while these two phenotypes were negatively correlated with planktonic growth (**Table S5-5**). Therefore, our results demonstrate that TFP may modulate other important phenotypes of *X. fastidiosa* besides natural competence and twitching motility. However, it is not known whether TFP genes directly regulate biofilm formation, planktonic growth and cell aggregation in *X. fastidiosa* by hitherto unknown mechanisms or if that is an indirect reflect of altered twitching motility phenotypes, which in turn modulate biofilm formation (Chatterjee et al. 2008b).

The functional role of some TFP genes in the virulence in planta of *X. fastidiosa* has also been previously investigated. Deletion of *pilG* and *pilL*, which abrogated twitching motility in previous studies (Cursino et al. 2011; Shi and Lin 2016), resulted in avirulence and delayed, less severe symptoms in infected grapevines, respectively (Cursino et al. 2011; Shi and Lin 2018).

Moreover, the non-motile Δ*pilB* and Δ*pilQ* mutants have significantly reduced basipetal translocation in planta, which occurs in a reverse direction away from the leaves and thus against the flow of xylem sap (Meng et al. 2005). Similarly, Δ*pilA*, Δ*pilQ* and Δ*pilT* mutants in *R. solanacearum*, which are all impaired in twitching motility, also presented reduced virulence in tomato plants (Kang et al. 2002; Liu et al. 2001). However, all these studies were performed with twitching motility-deficient mutant strains. Here, we have assayed the virulence of *X. fastidiosa* using mutant strains with variable phenotypes, including higher movement, lower movement, and non-motility. Regardless, all presented reduced virulence in planta, except for the Δ*pilA2* mutant, which promoted similar disease severity to WT-inoculated plants. Although the results obtained for movement-deficient strains were in accordance with their twitching motility phenotypes, we expected that mutant strains with higher twitching motility would be hypervirulent. Likewise, *X. fastidiosa* mutant strains lacking the *rpfF* gene, which encodes the diffusible signal factor (DSF; quorum sensing molecule of this bacterium) (Newman et al. 2004) synthase, have increased motility and are hypervirulent in planta (Chatterjee et al. 2008a; Cruz et al. 2014; Ionescu et al. 2013; Newman et al. 2004). DSF negatively regulates twitching motility in *X. fastidiosa* and positively modulates biofilm formation (Newman et al. 2004). Thus, the higher virulence of Δ*rpfF* is linked to increased movement of *X. fastidiosa* within infected plants and higher colonization of xylem vessels (Chatterjee et al. 2008a; Ionescu et al. 2013). In our study, however, we have mutated genes directly linked to TFP assembly and functioning, and not genes upstream of these processes. Also, we did not observe significant impairment in the colonization of infected plants by the analyzed mutant strains. This may be due to experimental bias, since we have inoculated basal leaves of young tobacco plants, which possibly allowed *X. fastidiosa* cells to colonize the plants by moving with the flow of xylem sap. Therefore, it would

be interesting to complement our study in the future by inoculating the canopy of full-grown plants and observing whether colonization will be impaired or enhanced due to the observed changes in twitching motility in vitro upon deletion of TFP-related genes, which may be reflected in their basipetal movement. Together, the fact that twitching motility-deficient strains, as well as mutant strains with higher movement, had reduced virulence in this study indicate that TFP genes are required for the proper functioning and regulation of this machinery, which is needed for full symptom development; whilst deletion of its individual components suppresses virulence.

Overall, our data demonstrate that *X. fastidiosa* has a central TFP machinery that is composed and functions similarly to other well-studied TFP systems, such as the ones from *P. aeruginosa* and *N. meningitidis*. However, *X. fastidiosa* also has many unique behaviors involving mainly its regulatory proteins and minor pilins, which are worth being investigated to better understand the TFP dynamics of this bacterium.

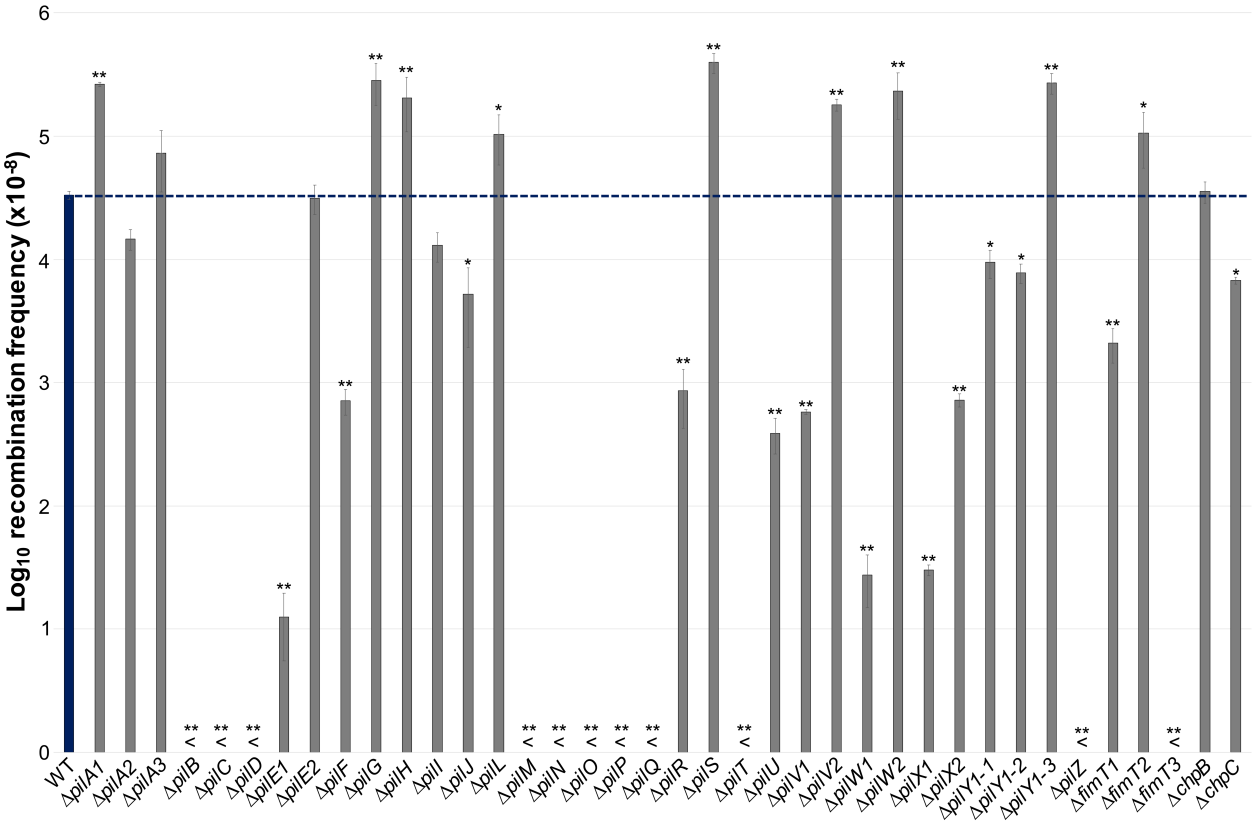

Fig. S5-1. Recombination frequencies obtained through natural competence of *X. fastidiosa* mutant strains used in this study. Quantification of natural competence was performed in PD3 plates by applying 1 µg of the pAX1-Cm plasmid to equivalent numbers of recipient cells of each *X. fastidiosa* strain to generate chloramphenicol-resistant (Cm^R) mutations. Total viable cells and transformants were counted and results are expressed as the ratio of recipient cells transformed. WT is highlighted in blue, and the dashed blue line indicates the mean value of recombination frequency for the WT. Data represent means and standard errors. * and ** indicate significant difference ($P<0.05$ and $P<0.005$, respectively) of recombination frequency through natural competence in comparison to the WT as determined using Student's *t*-test (n = three to 21 independent replicates with two internal replicates each). "<" indicates below detection limit, which was 10^{-7}. Mutant strains below the detection limit were considered non-recombinant.

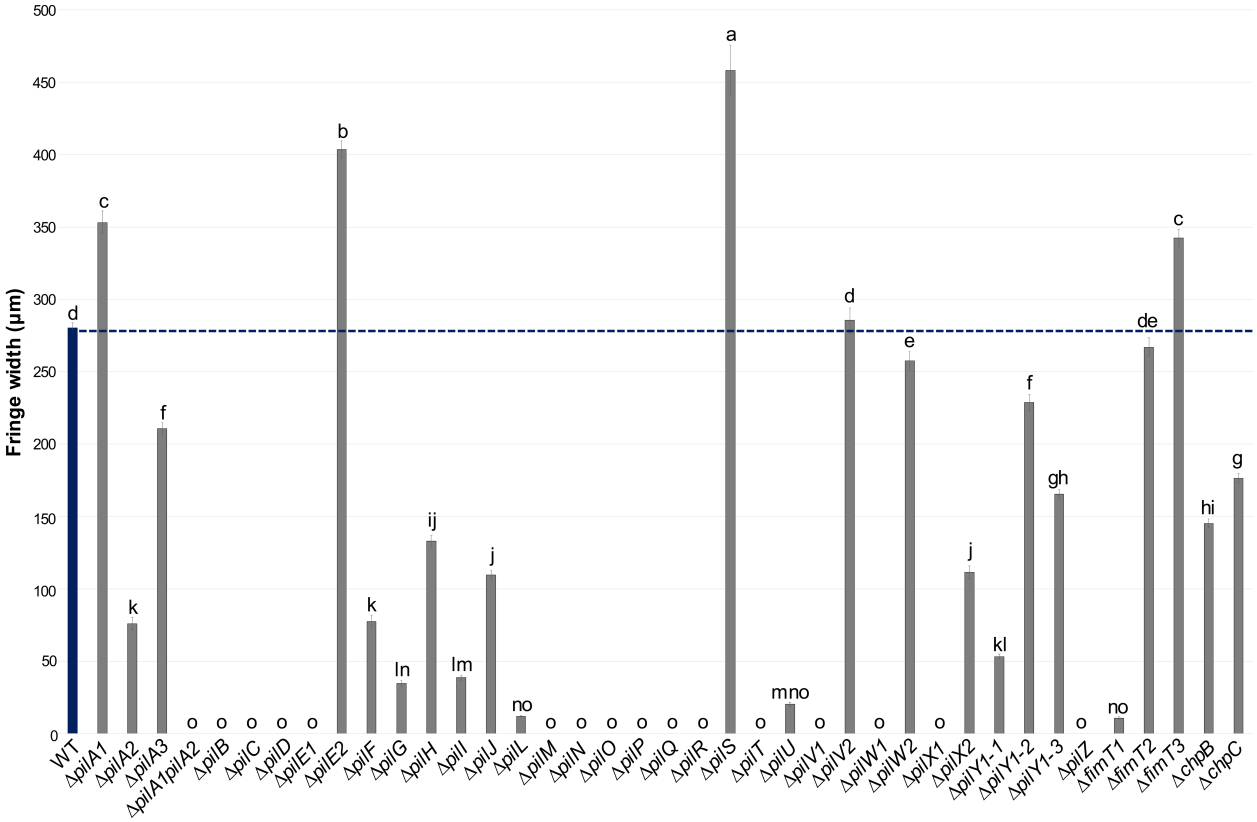

Fig. S5-2. Fringe width measurements of the twitching motility phenotypes of *X. fastidiosa* mutant strains used in this study. Twitching motility was determined by spotting cells of each strain in PW without BSA plates and measuring the movement fringe width after 4 days of growth at 28 ºC. WT is highlighted in blue, and the dashed blue line indicates the mean value of fringe width for the WT. Data represent means and standard errors. Different letters on top of bars indicate significant difference as analyzed by ANOVA followed by Tukey's HSD multiple comparisons of means (P<0.05; n = three to 14 independent replicates with eight to 48 internal replicates each). The detection limit was 10 µm. Mutant strains below the detection limit were considered non-motile.

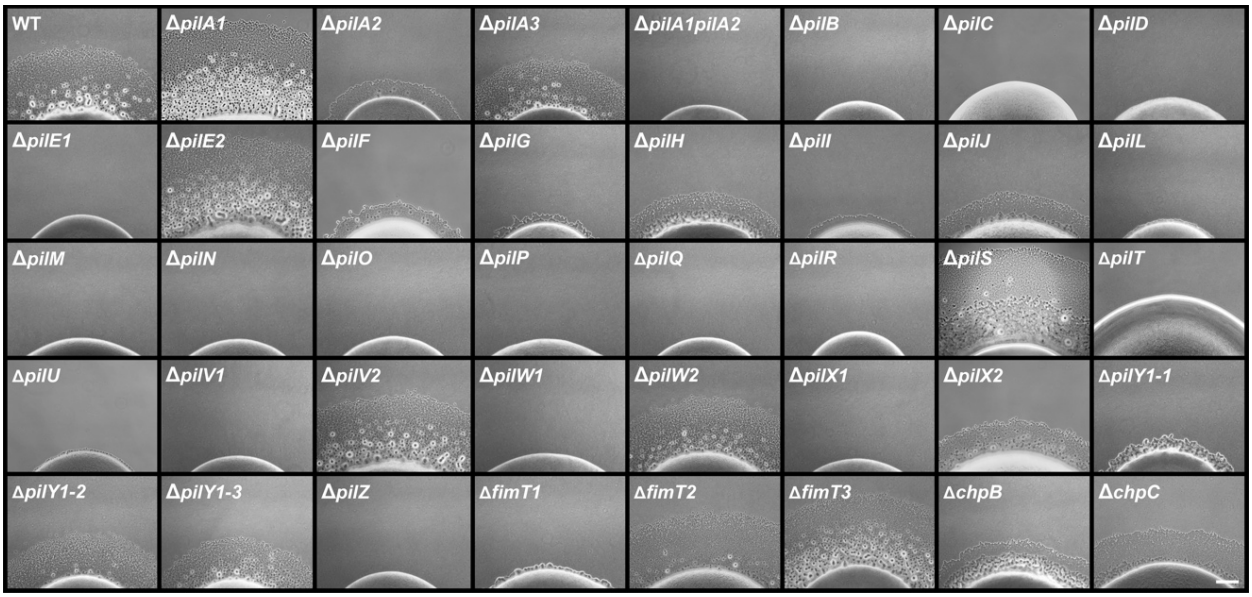

Fig. S5-3. Figure panel with representative pictures of the twitching motility phenotypes of *X. fastidiosa* mutant strains used in this study. The assay was performed as described in **Fig. S5-2**. Similar events were captured in three to 14 independent experiments. Images were captured at 10× magnification. Scale bar (right lower panel), 100 μm.

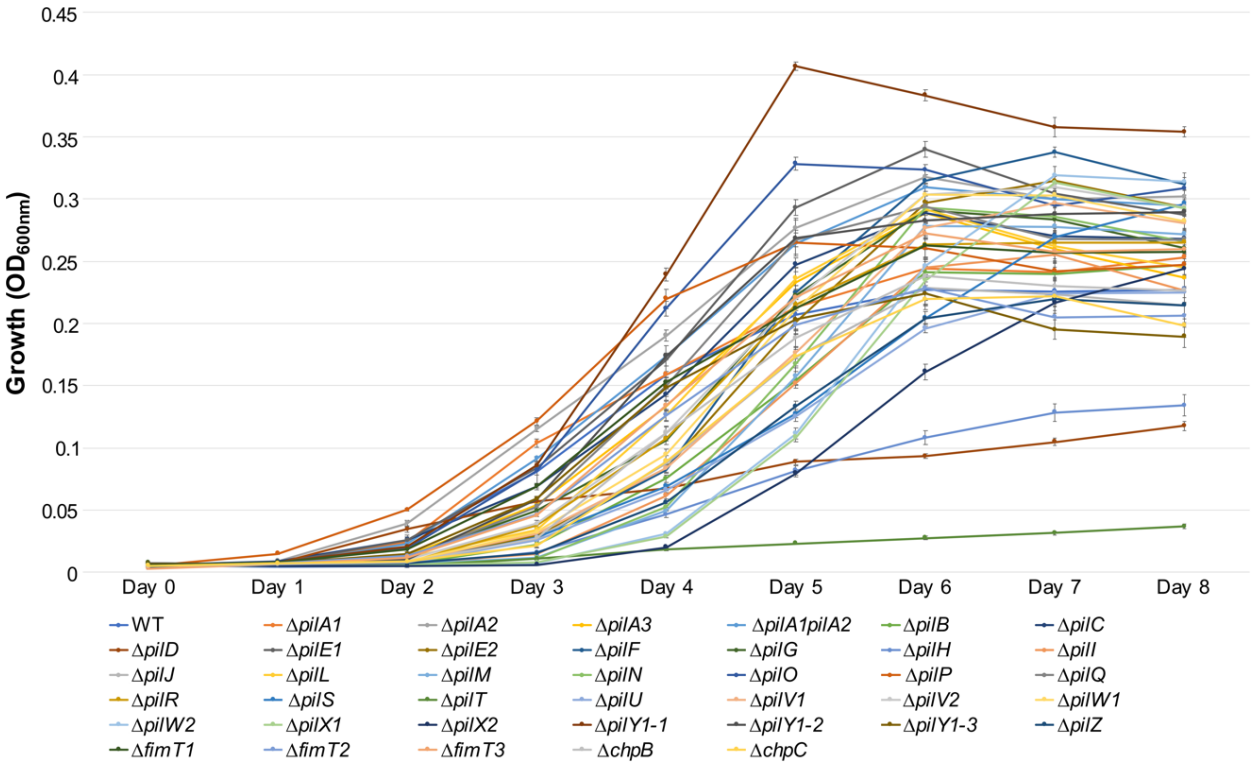

Fig. S5-4. Growth curves of *X. fastidiosa* mutant strains used in this study. Growth curves were generated by culturing bacteria in PD3 broth within 96-well plates and measuring the optical density at 600 nm (OD_{600nm}) values each day for 8 days. Data represent means and standard errors (n = three to 15 independent replicates, with eight internal replicates each).

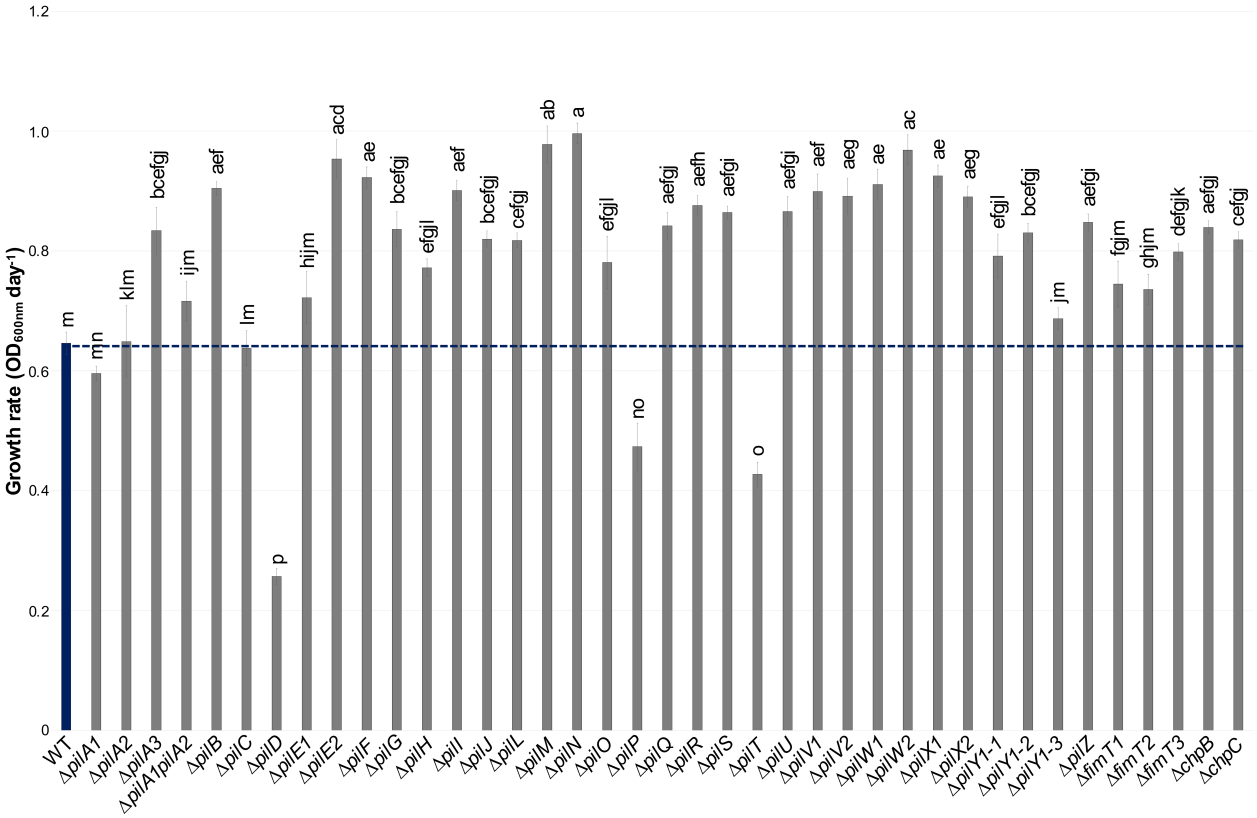

Fig. S5-5. Growth rates of *X. fastidiosa* mutant strains used in this study. Growth rate was calculated from the growth curve at the exponential growth phase (2 to 6 days post inoculation). WT is highlighted in blue, and the dashed blue line indicates the mean value of growth rate for the WT. Data represent means and standard errors. Different letters on top of bars indicate significant difference as analyzed by ANOVA followed by Tukey's HSD multiple comparisons of means (P<0.05; n = three to 15 independent replicates with eight internal replicates each).

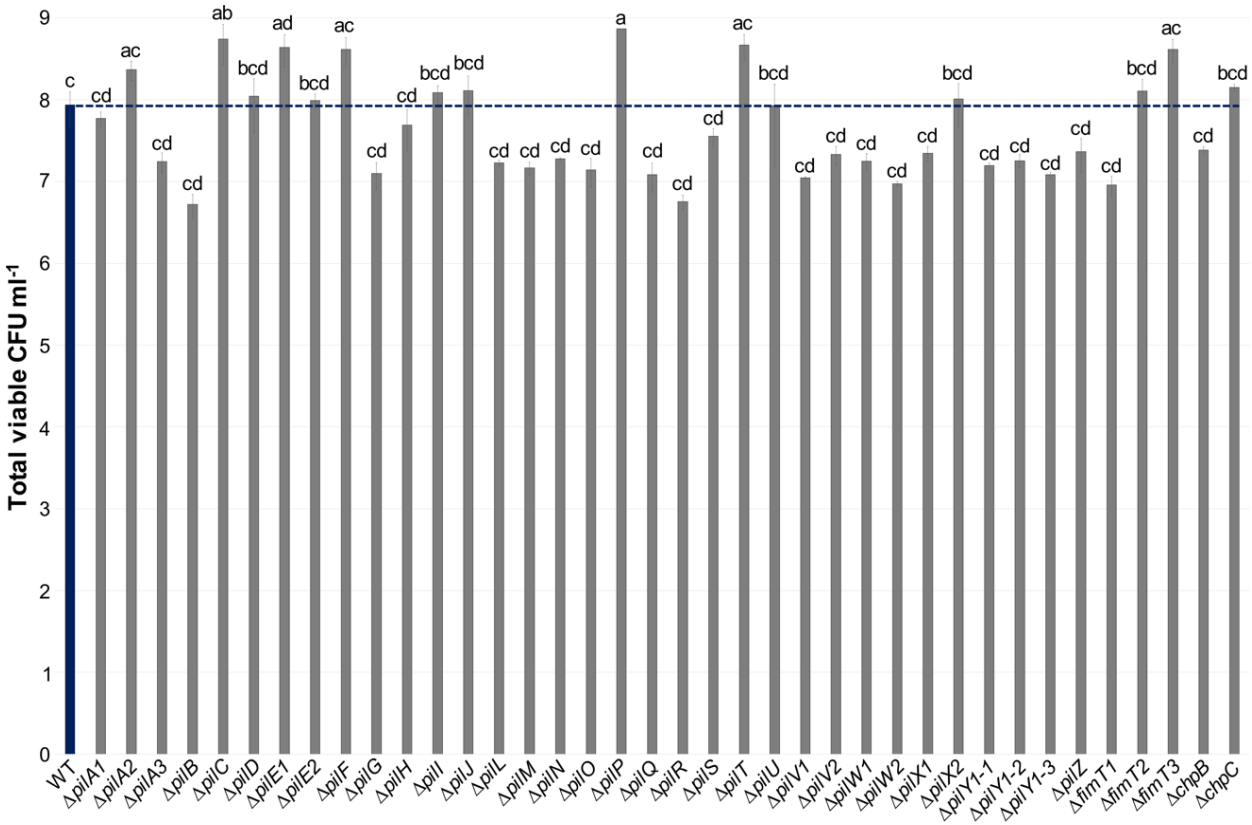

Fig. S5-6. Total number of viable CFU/ml of *X. fastidiosa* mutant strains used in this study after growth during natural competence assays. Total viable CFUs of each *X. fastidiosa* strain obtained during natural competence assays described in **Fig. S5-1** are shown here. WT is highlighted in blue, and the dashed blue line indicates the mean value of the total number of viable CFU/ml obtained during natural competence assays for the WT. Data represent means and standard errors. Different letters on top of bars indicate significant difference as analyzed by ANOVA followed by Tukey's HSD multiple comparisons of means (P<0.05; n = three to 21 independent replicates with two internal replicates each).

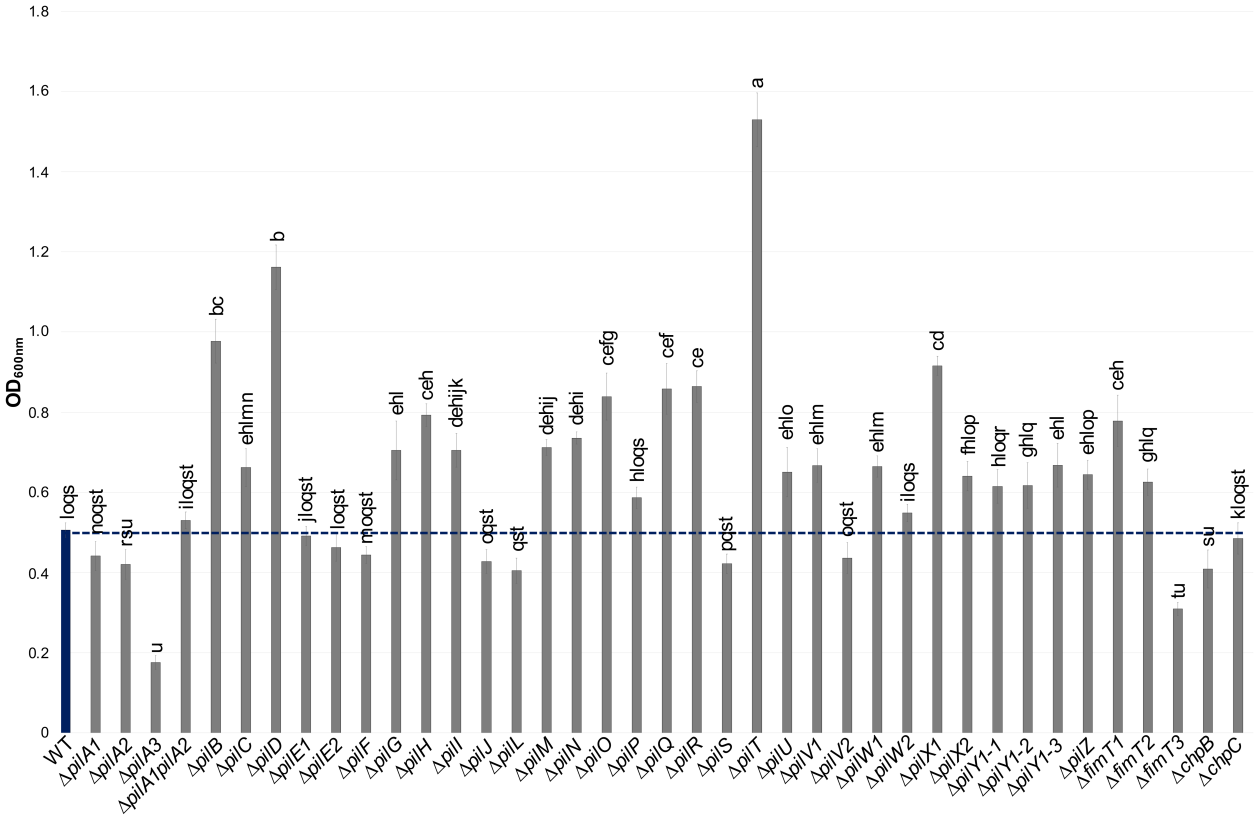

Fig. S5-7. Biofilm formation of *X. fastidiosa* mutant strains used in this study. Biofilm was measured by staining *X. fastidiosa* cells attached to the 96-well plates at the end of the growth curve experiment with crystal violet. WT is highlighted in blue, and the dashed blue line indicates the mean value of biofilm formation for the WT. Data represent means and standard errors. Different letters on top of bars indicate significant difference as analyzed by ANOVA followed by Tukey's HSD multiple comparisons of means (P<0.05; n = three to 14 independent replicates with six to eight internal replicates each).

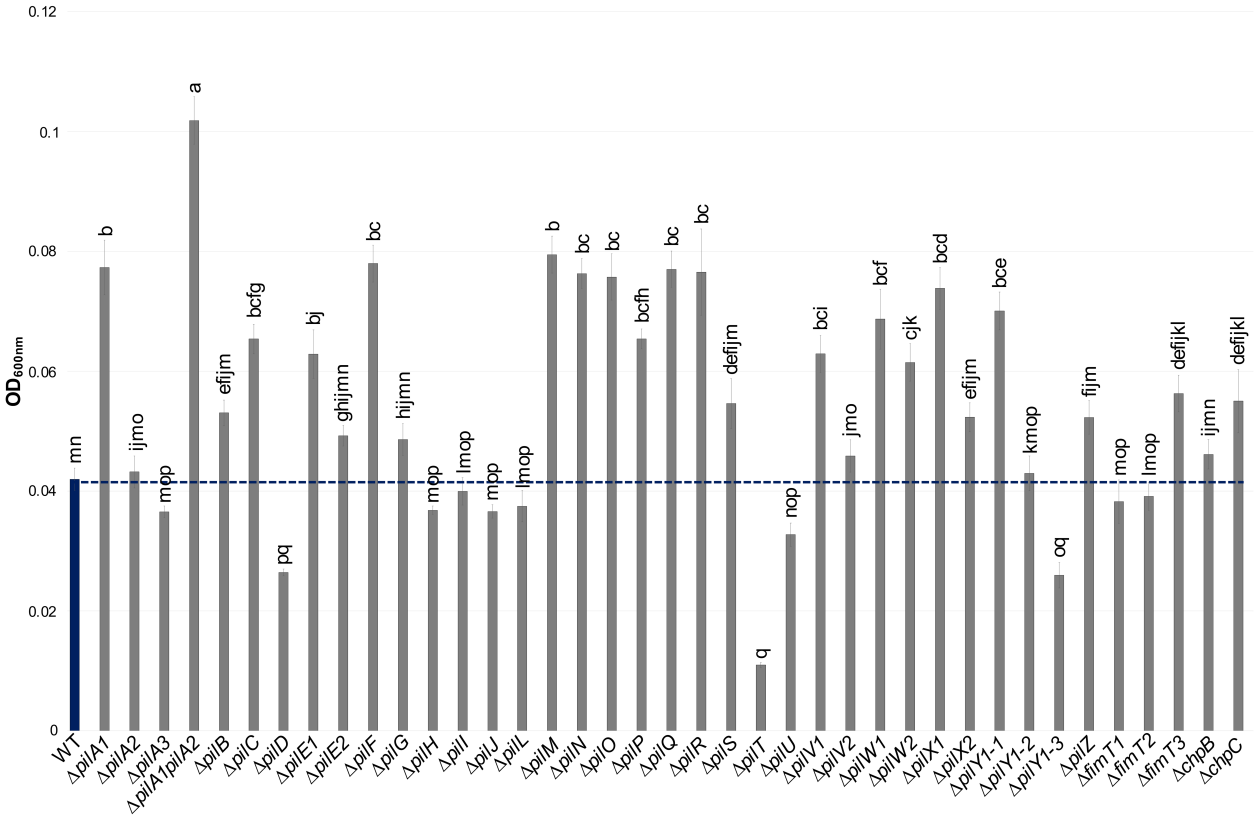

Fig. S5-8. Planktonic growth of *X. fastidiosa* mutant strains used in this study. Planktonic growth was quantified by measuring the optical density at 600 nm (OD_{600nm}) values of the supernatant of each *X. fastidiosa* strain at the end of the growth curve experiment. WT is highlighted in blue, and the dashed blue line indicates the mean value of planktonic growth for the WT. Data represent means and standard errors. Different letters on top of bars indicate significant difference as analyzed by ANOVA followed by Tukey's HSD multiple comparisons of means (P<0.05; n = three to 14 independent replicates with six to eight internal replicates each).

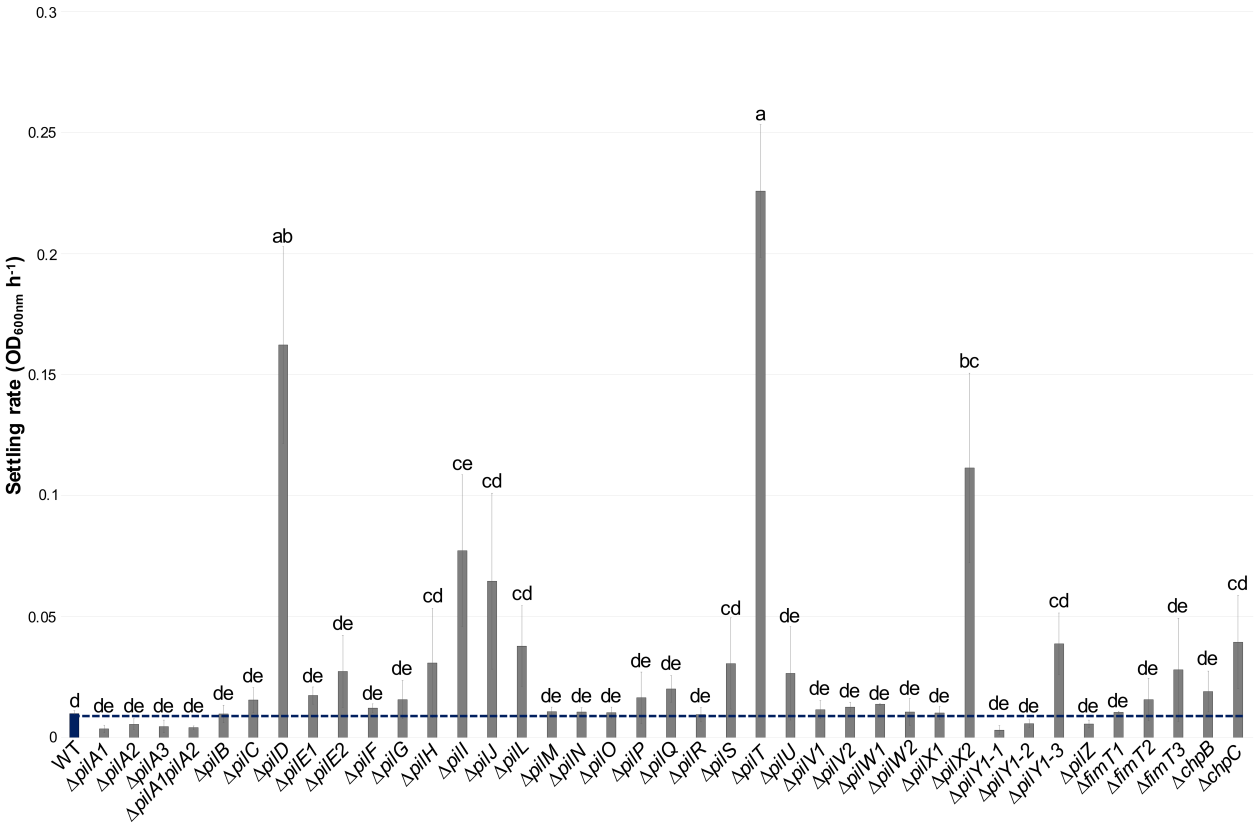

Fig. S5-9. Settling rates of *X. fastidiosa* mutant strains used in this study. Settling rate was measured by suspending (OD_{600nm} = 1.0) the analyzed *X. fastidiosa* strains in a cuvette in 1 ml of PD3 broth and measuring OD_{600nm} values at the initial time point and after 2 hours. WT is highlighted in blue, and the dashed blue line indicates the mean value of settling rate for the WT. Data represent means and standard errors. Different letters on top of bars indicate significant difference as analyzed by ANOVA followed by Tukey's HSD multiple comparisons of means (P<0.05; n = three to 15 independent replicates).

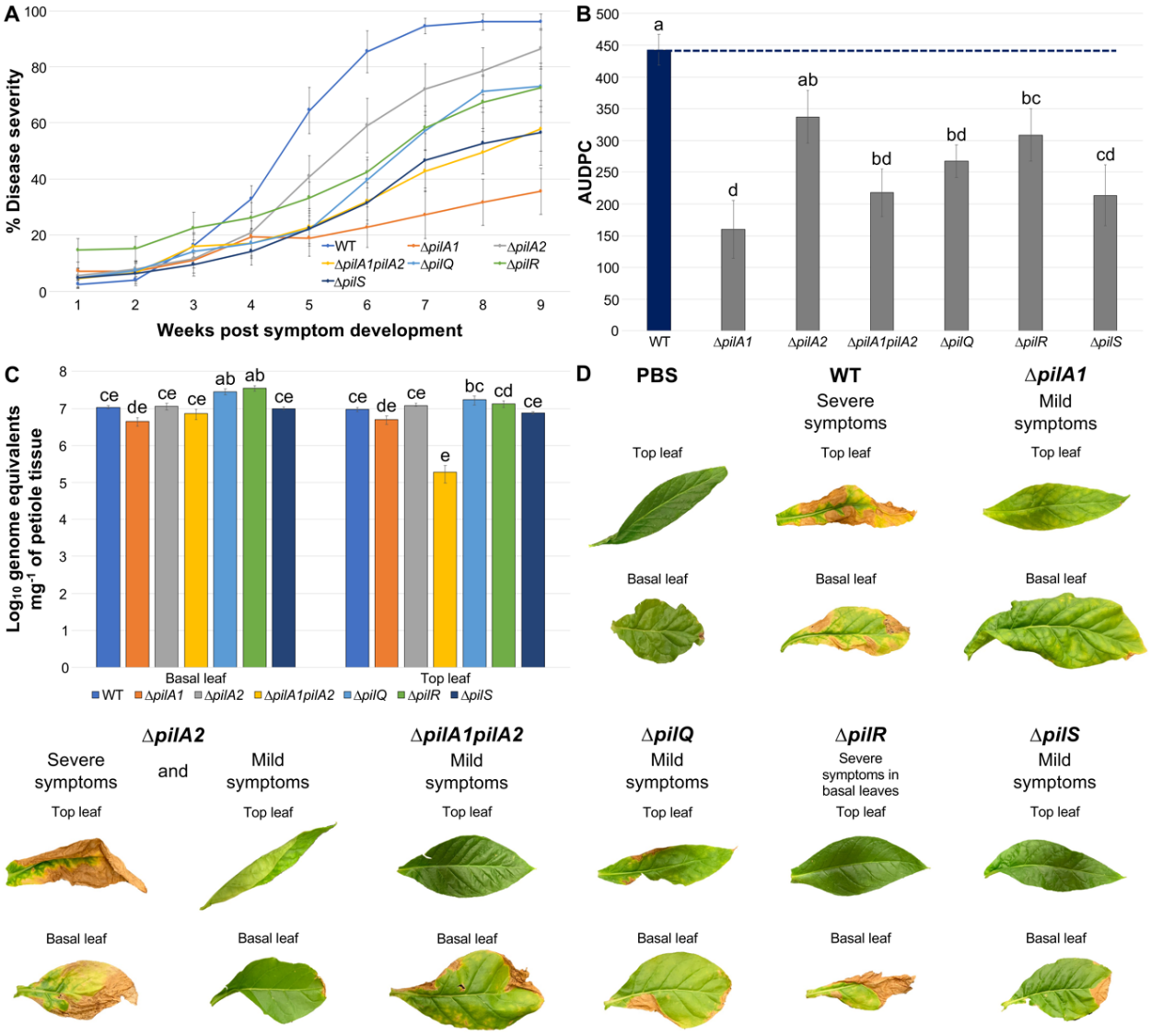

Fig. S5-10. Deletion of *pil* genes negatively affects virulence of *X. fastidiosa*. A. Disease severity progression over time in inoculated tobacco plants. *X. fastidiosa* WT and mutant strains were inoculated into *Nicotiana tabacum* L. cv. Petite Havana SR1 plants (PBS mock inoculation used as control). Mutant strains chosen for inoculation presented different twitching motility phenotypes, including higher twitching motility (Δ*pilA1* and Δ*pilS*), lower twitching motility (Δ*pilA2*) and non-motility (Δ*pilA1pilA2*, Δ*pilQ* and Δ*pilR*). Leaf scorch symptoms were recorded for measurements of disease incidence and severity once a week during nine weeks after appearance of the first disease symptoms. At the final time point of evaluation, disease incidence in all inoculated plants reached 100%, except for plants inoculated with Δ*pilA1*, which reached 88.88% disease incidence (±11.11%, standard error). On the other hand, disease severity reached 96% in the WT, 35% in Δ*pilA1*, 86% in Δ*pilA2*, 57% in Δ*pilA1pilA2*, 73% in Δ*pilQ*, 72% in Δ*pilR* and 56% in Δ*pilS*. Data represent means and standard errors from two independent experiments (n = seven to ten plants in each independent experiment). **B.** Mean AUDPC per treatment group. AUDPC was calculated using data from disease severity over nine weeks after first disease symptom appearance. WT is highlighted in blue, and the dashed blue line indicates the mean value of AUDPC for WT-inoculated plants. AUDPC was significantly lower for plants

inoculated with all mutant strains in comparison to WT-inoculated plants, except for Δ*pilA2*. Data represent means and standard errors. Different letters on top of bars indicate significant difference as analyzed by ANOVA followed by Tukey's HSD multiple comparisons of means (P<0.05; n = two independent experiments with seven to ten plants each). **C.** *X. fastidiosa* in planta population determined by qPCR at the last time point of evaluation. The population of WT and mutant strains throughout inoculated plants was calculated using petioles of basal and top leaves. Δ*pilA1pilA2* cells showed a defect in colonizing the top leaf of plant hosts, while Δ*pilQ* and Δ*pilR* showed a significant higher population in the basal leaf of infected plants. This shows that mutant strains still move inside the xylem of plant hosts, but absence of deleted genes impairs full symptom development. Data represent means and standard errors. Different letters on top of bars indicate significant difference as analyzed by ANOVA followed by Tukey's HSD multiple comparisons of means (P<0.05; n = two independent experiments with three leaf replicates each). **D.** Figure panel with representative pictures of leaf scorch symptoms in WT- and mutant strains-inoculated plants (top and basal leaves), as well as control plants (PBS mock inoculation). Only WT-inoculated plants consistently presented severe leaf scorch symptoms. Similar events were captured in two independent experiments.

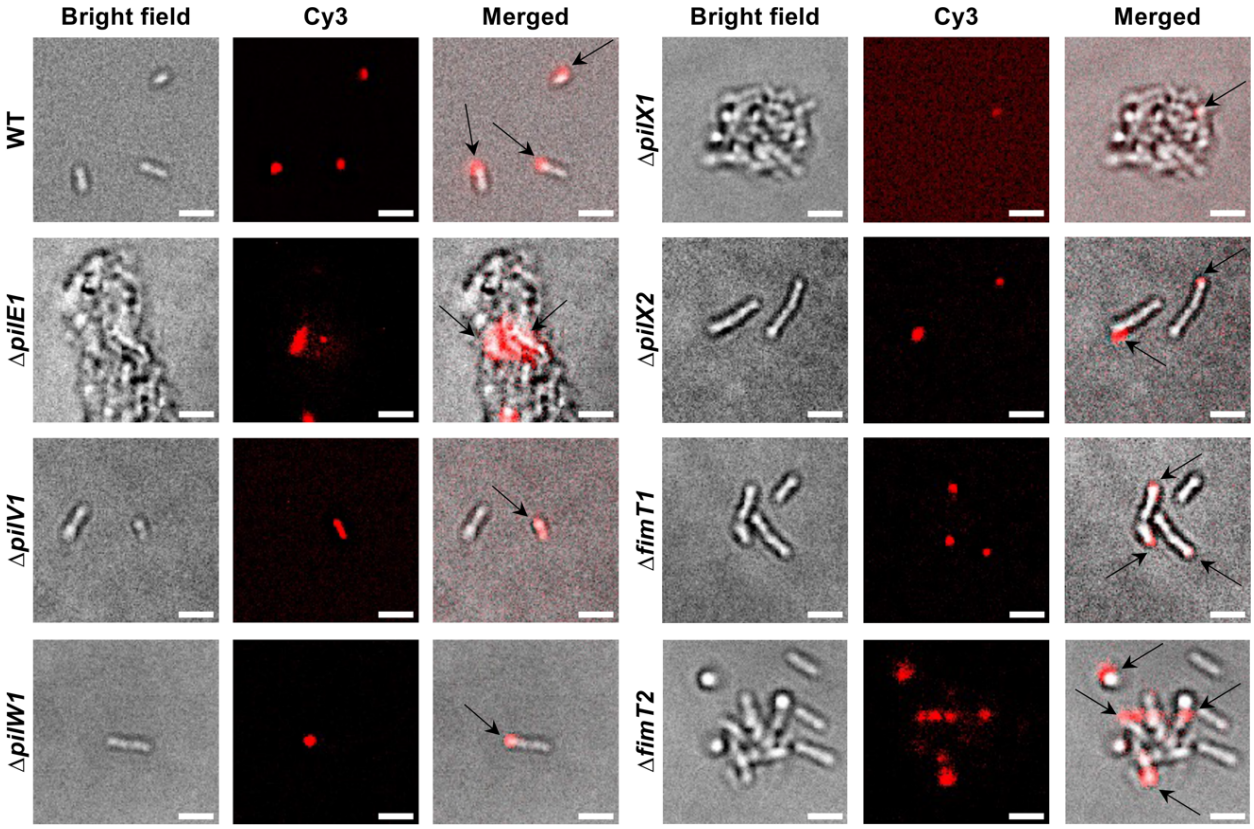

Fig. S5-11. *X. fastidiosa* cells take up Cy-3 labeled DNA into a DNase I resistant state. WT and mutant cells were exposed to Cy-3-labeled pAX1-Cm plasmid (1 µg) for 24 hours, treated with DNase I and DNA foci were observed using a fluorescent microscope. The images shown correspond to the bright field (left), Cy-3 channel (center) and merged fluorescent images (right). In merged fluorescent images, arrows are pointing to fluorescent DNA foci at the poles of cells. Similar events were captured in two to three independent experiments. All evaluated cells presented uptake of Cy-3 labeled DNA. Mutant strains analyzed here correspond to knockout of minor pilins that presented lower recombination through natural competence in comparison to the WT. Δ*fimT1* and Δ*fimT2* were included for comparison with Δ*fimT3*. Images were captured at 100× magnification. Scale bars, 1.5 µm.

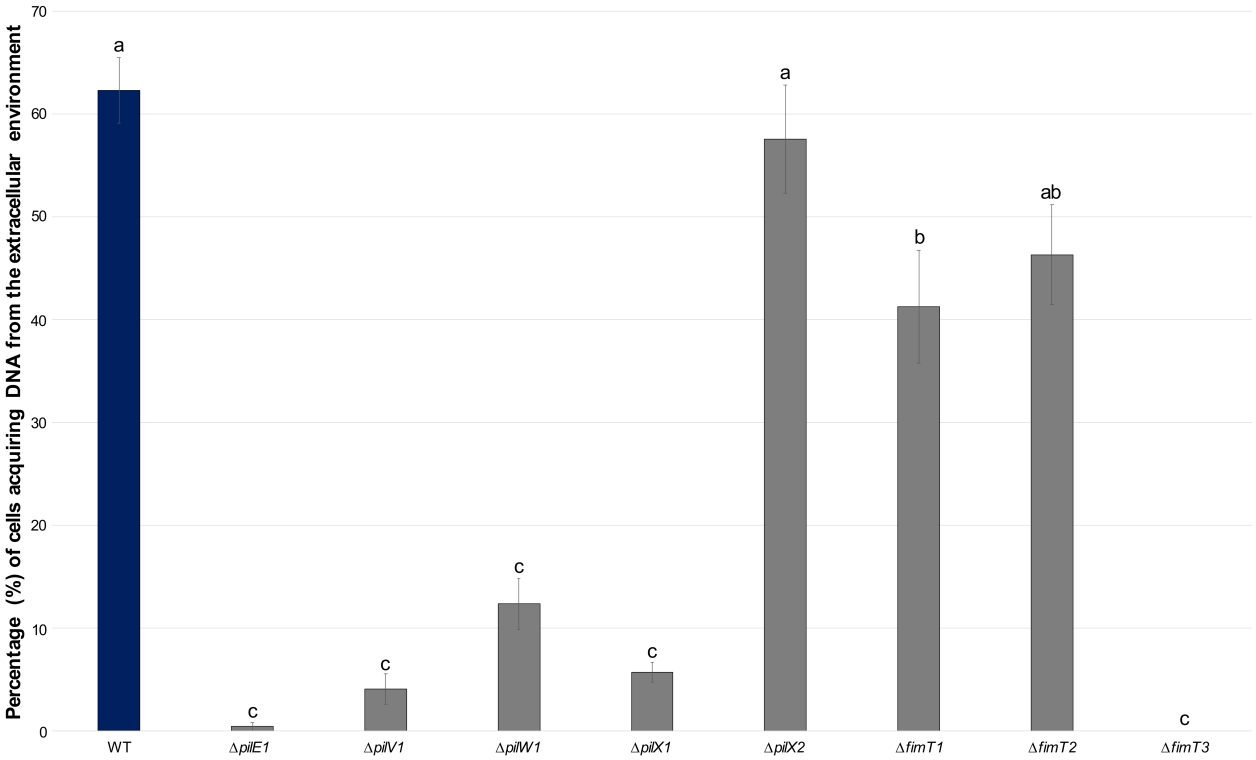

Fig. S5-12. Percentage of *X. fastidiosa* cells that acquired DNA from the extracellular environment during DNA uptake assays in the different analyzed strains. Total cells and cells with DNA foci (Cy-3 labeled pAX1-Cm plasmid) were counted and results are expressed as the percentage of cells with DNA foci. All mutants of minor pilins apart Δ*pilX2* and Δ*fimT2* presented significant lower DNA uptake than WT cells. Data represent means and standard errors. Different letters on top of bars indicate significant difference as analyzed by ANOVA followed by Tukey's HSD multiple comparisons of means (P<0.05; n = two to three independent replicates with three to seven technical replicates each).

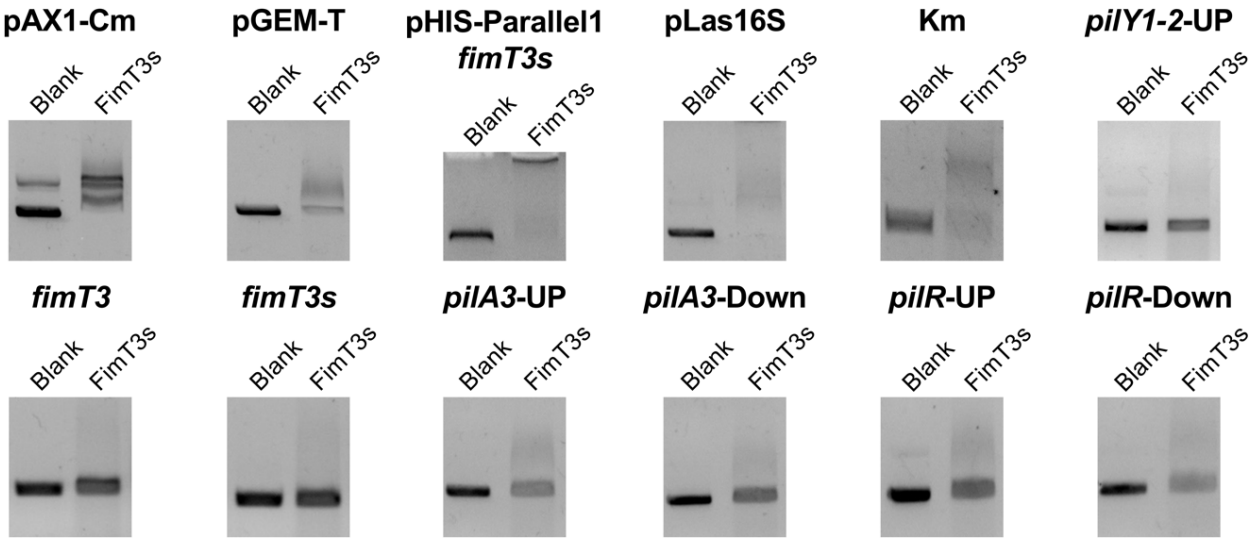

Fig. S5-13. FimT3 DNA binding activity in different DNA sequences. DNA-binding activity of purified FimT3s (5 μM) to different DNA sequences was assessed by agarose EMSA using standard amounts (200 ng) of each DNA sequence. FimT3s was incubated with each DNA sequence for 30 min at 28 ºC and resolved by electrophoresis on a 0.8% agarose gel. Lysis buffer containing 250 μM imidazole, in which proteins were suspended, was included as blank control. DNA binding activity of FimT3s in large sequences (larger than 1,200 bp) is observed as clear shifts in the electrophoretic mobility of bands, while DNA binding activity of FimT3s in small sequences (smaller than 900 bp) is observed as smearing of bands. Amplicon sizes: pAX1-Cm – 4,361 bp; pGEM-T – 3,000 bp; pHIS-Parallel1-*fimT3s* – 5,977 bp; pLas16S – 5,206 bp; Km – 1,202 bp; *pilY1-2*-UP – 988 bp; *fimT3* – 609 bp; *fimT3s* – 519 bp; *pilA3*-UP – 852 bp; *pilA3*-Down – 887 bp; *pilR*-UP – 900 bp; *pilR*-Down – 937 bp. The experiment included DNA sequences with homology to the genome of *X. fastidiosa* TemeculaL (pAX1-Cm, pHIS-Parallel1-*fimT3s*, *pilY1-2*-UP, *fimT3*, *fimT3s*, *pilA3*-UP, *pilA3*-Down, *pilR*-UP and *pilR*-Down), as well as sequences with no apparent homology (pGEM-T, pLas16S and Km resistance cassette). FimT3s did not appear to preferably bind certain DNA sequences, indicating that its DNA-binding ability is non-sequence-specific. *fimT3* – full-length *fimT3* amplified from *X. fastidiosa* TemeculaL; *fimT3s* – soluble portion of *fimT3* amplified from *X. fastidiosa* TemeculaL; sequences labeled with "UP" and "Down" correspond to upstream and downstream sequences, respectively, used to construct the targeting sequences for site-directed mutagenesis of each gene of interest. Similar events were captured in two independent experiments.

Fig. S5-14. Alignment of FimT3 from *X. fastidiosa* to DNA-binding minor pilins from *Neisseria meningitidis* (ComP) and *Vibrio cholerae* (VC0858). The sequence of each protein was obtained from NCBI, aligned through T-Coffee, and visualized using BoxShade. Black shading indicates conserved residues; grey shading indicates conservative mutations; and white color indicates divergence among sequences. **A** and **B** show alignment of FimT3 with ComP and VC0858, respectively. The arginine residue at position 162 (R162) from FimT3 aligned with a lysine of ComP (K108) demonstrated to be essential for the DNA-binding ability of the latter protein. On the other hand, the arginine residue at position 160 (R160) from FimT3 aligned with an arginine of VC0858 (R168) demonstrated to be important for the DNA-binding ability of the *V. cholerae* pilus. Alignment of these specific amino acid residues are highlighted by a yellow box in **A** and **B**.

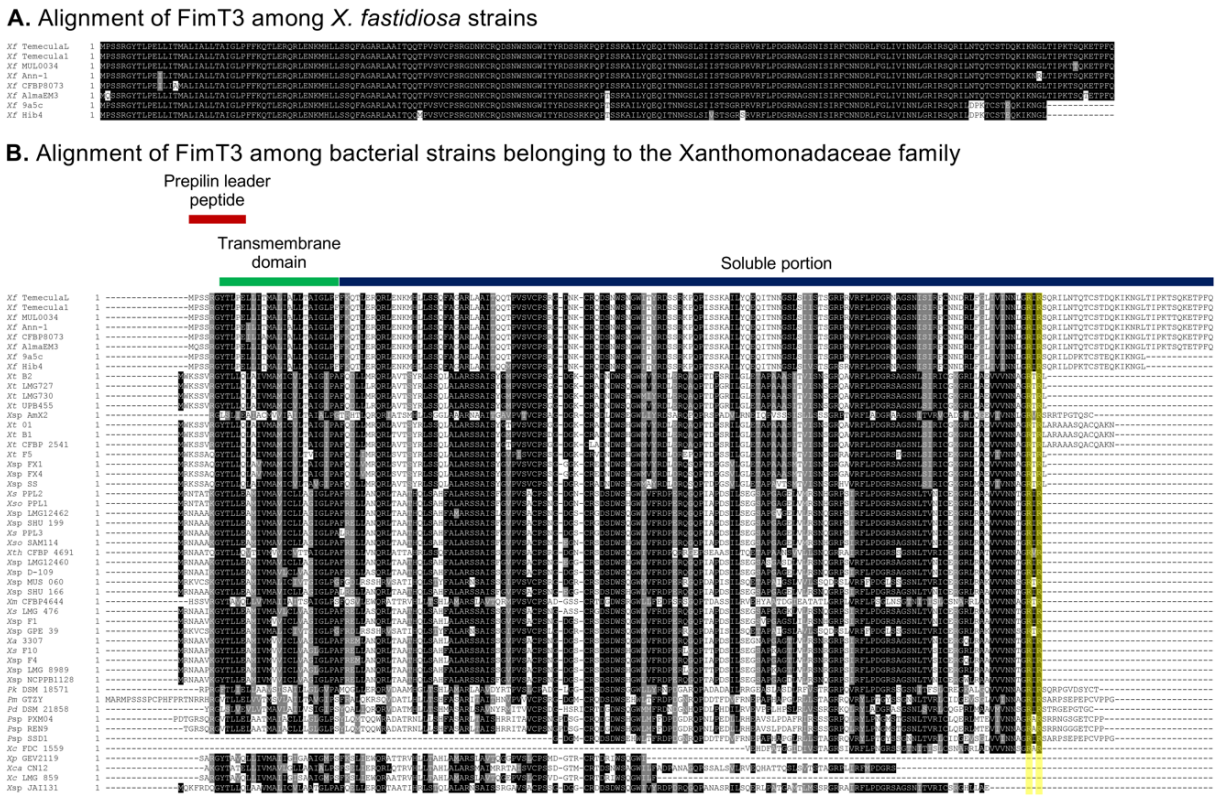

Fig. S5-15. The DNA-binding residues of FimT3 is majorly conserved within bacterial members of the Xanthomonadaceae family encoding this protein. The sequence of each protein was downloaded from NCBI, screened for the presence of FimT3 by tblastn, aligned through MAFFT, and visualized using BoxShade. Black shading indicates conserved residues; grey shading indicates conservative mutations; and white color indicates divergence among sequences. **A.** Alignment of different FimT3 sequences among *X. fastidiosa* strains. FimT3 is nearly identical in all *X. fastidiosa* strains, with strains from subspecies *pauca* (strains 9a5c and Hib4) presenting the highest divergence (97.25% and 95.6% of identical amino acids, respectively, in comparison to FimT3 from strain TemeculaL). **B.** Alignment of FimT3 sequences from all bacterial members of the Xanthomonadaceae family encoding this protein. Although the percentage of identical amino acids ranged from 40.57% to 100%, most sequences aligned with the arginine amino acid residues at positions 160 and 162 of FimT3 from *X. fastidiosa* strain TemeculaL (46 out of 50 different FimT3 sequences; highlighted in yellow in the figure). This indicates that these arginine residues are highly conserved within FimT3 sequences. For conciseness of the figure, only one strain from each group that encodes identical FimT3 sequences is shown in the alignment. Thus, the alignment of only different sequences of FimT3 is shown (except for *X. fastidiosa* strains Temecula1 and TemeculaL). The different portions of FimT3 (prepilin leader peptide, transmembrane domain, and soluble portion) are indicated in the figure. Name coding are as follows: *Xf – Xylella fastidiosa*; *Xt – Xanthomonas translucens*; *Xsp – Xanthomonas* sp.; *Xs – Xanthomonas sacchari*; *Xso – Xanthomonas sontii*; *Xth – Xanthomonas theicola*; *Xm – Xanthomonas melonis*; *Xa – Xanthomonas arboricola*; *Pk – Pseudoxanthomonas kalamensis*; *Pm – Pseudoxanthomonas mexicana*; *Pd – Pseudoxanthomonas dokdonensis*; *Psp – Pseudoxanthomonas* sp.; *Xc – Xanthomonas citri*; *Xp – Xanthomonas perforans*; *Xca – Xanthomonas campestris*.

Table S5-1. Bacterial strains and plasmids used in this study.

Strain name in manuscript or plasmid	Genotype or description	Source
Xylella fastidiosa		
WT	Wild-type *X. fastidiosa* subsp. *fastidiosa* strain TemeculaL	(Potnis et al. 2019)
Δ*pilA1*	*X. fastidiosa* strain TemeculaL with chromosomal *pilA1* (PD1924) deletion, Km^R	(Kandel et al. 2018)
Δ*pilA2*	*X. fastidiosa* strain TemeculaL with chromosomal *pilA2* (PD1926) deletion, Km^R	This study
Δ*pilA3*	*X. fastidiosa* strain TemeculaL with chromosomal *pilA3* (PD1077) deletion, Km^R	This study
Δ*pilA1pilA2*	*X. fastidiosa* strain TemeculaL with chromosomal *pilA1* and *pilA2* (PD1924 and PD1926, respectively) deletion, Km^R, Cm^R	(Kandel et al. 2018)
Δpi*lB*	*X. fastidiosa* strain TemeculaL with chromosomal *pilB* (PD1927) deletion, Km^R	This study
Δ*pilC*	*X. fastidiosa* strain TemeculaL with chromosomal *pilC* (PD1923) deletion, Km^R	This study
Δ*pilD*	*X. fastidiosa* strain TemeculaL with chromosomal *pilD* (PD1922) deletion, Km^R	This study
Δ*pilE1*	*X. fastidiosa* strain TemeculaL with chromosomal *pilE1* (PD0024) deletion, Km^R	This study
Δ*pilE2*	*X. fastidiosa* strain TemeculaL with chromosomal *pilE2* (PD1610) deletion, Km^R	This study
Δ*pilF*	*X. fastidiosa* strain TemeculaL with chromosomal *pilF* (PD1623) deletion, Km^R	This study
Δ*pilG*	*X. fastidiosa* strain TemeculaL with chromosomal *pilG* (PD0845) deletion, Km^R	This study
Δ*pilH*	*X. fastidiosa* strain TemeculaL with chromosomal *pilH* (PD1632) deletion, Km^R	This study
Δ*pilI*	*X. fastidiosa* strain TemeculaL with chromosomal *pilI* (PD0846) deletion, Km^R	This study
Δ*pilJ*	*X. fastidiosa* strain TemeculaL with chromosomal *pilJ* (PD0847) deletion, Km^R	This study
Δ*pilL*	*X. fastidiosa* strain TemeculaL with chromosomal *pilL* (PD0848) deletion, Km^R	This study
Δ*pilM*	*X. fastidiosa* strain TemeculaL with chromosomal *pilM* (PD1695) deletion, Km^R	This study
Δ*pilN*	*X. fastidiosa* strain TemeculaL with chromosomal *pilN* (PD1694) deletion, Km^R	This study
Δ*pilO*	*X. fastidiosa* strain TemeculaL with chromosomal *pilO* (PD1693) deletion, Km^R	This study
Δ*pilP*	*X. fastidiosa* strain TemeculaL with chromosomal *pilP* (PD1694) deletion, Km^R	This study
Δ*pilQ*	*X. fastidiosa* strain TemeculaL with chromosomal *pilQ* (PD1691) deletion, Km^R	This study
Δ*pilR*	*X. fastidiosa* strain TemeculaL with chromosomal *pilR* (PD1928) deletion, Km^R	This study
Δ*pilS*	*X. fastidiosa* strain TemeculaL with chromosomal *pilS* (PD1929) deletion, Km^R	This study
Δ*pilT*	*X. fastidiosa* strain TemeculaL with chromosomal *pilT* (PD1147) deletion, Km^R	This study
Δ*pilU*	*X. fastidiosa* strain TemeculaL with chromosomal *pilU* (PD1148) deletion, Km^R	This study

Δ*pilV1*	*X. fastidiosa* strain TemeculaL with chromosomal *pilV1* (PD0020) deletion, Km^R	This study
Δ*pilV2*	*X. fastidiosa* strain TemeculaL with chromosomal *pilV2* (PD1614) deletion, Km^R	This study
Δ*pilW1*	*X. fastidiosa* strain TemeculaL with chromosomal *pilW1* (PD0021) deletion, Km^R	This study
Δ*pilW2*	*X. fastidiosa* strain TemeculaL with chromosomal *pilW2* (PD1613) deletion, Km^R	This study
Δ*pilX1*	*X. fastidiosa* strain TemeculaL with chromosomal *pilX1* (PD0022) deletion, Km^R	This study
Δ*pilX2*	*X. fastidiosa* strain TemeculaL with chromosomal *pilX2* (PD1612) deletion, Km^R	This study
Δ*pilY1-1*	*X. fastidiosa* strain TemeculaL with chromosomal *pilY1-1* (PD0023) deletion, Km^R	This study
Δ*pilY1-2*	*X. fastidiosa* strain TemeculaL with chromosomal *pilY1-2* (PD1611) deletion, Km^R	This study
Δ*pilY1-3*	*X. fastidiosa* strain TemeculaL with chromosomal *pilY1-3* (PD0502) deletion, Km^R	This study
Δ*pilZ*	*X. fastidiosa* strain TemeculaL with chromosomal *pilZ* (PD1497) deletion, Km^R	This study
Δ*fimT1*	*X. fastidiosa* strain TemeculaL with chromosomal *fimT1* (PD0019) deletion, Km^R	This study
Δ*fimT2*	*X. fastidiosa* strain TemeculaL with chromosomal *fimT2* (PD1615) deletion, Km^R	This study
Δ*fimT3*	*X. fastidiosa* strain TemeculaL with chromosomal *fimT3* (PD1735) deletion, Km^R	This study
Δ*chpB*	*X. fastidiosa* strain TemeculaL with chromosomal *chpB* (PD0849) deletion, Km^R	This study
Δ*chpC*	*X. fastidiosa* strain TemeculaL with chromosomal *chpC* (PD0850) deletion, Km^R	This study
Escherichia coli		
Dh5α	*fhuA2 Δ(argF-lacZ)U169 phoA glnV44 Φ80 Δ(lacZ)M15 gyrA96 recA1 relA1 endA1 thi-1 hsdR17*	New England Biolabs
EAM1	DH5α derivative; Sp^r St^r *attP*$_{HK022}$::($P_{LlacO-1}$-PD1607) Expresses the *X. fastidiosa* subsp. *fastidiosa* strain Temecula1 DNA methylase	(Matsumoto and Igo 2010)
BL21(DE3)	*fhuA2 [lon] ompT gal (λ DE3) [dcm] ΔhsdS λ DE3 = λ sBamHIo ΔEcoRI-B int::(lacI::PlacUV5::T7 gene1) i21 Δnin5*	New England Biolabs
Dh5α-pUC4K	*E. coli* Dh5α bearing the pUC4K plasmid	(Kandel et al. 2018)
EAM1-pAX1-Cm	*E. coli* EAM1 bearing the pAX1-Cm plasmid	(Kandel et al. 2017)
Dh5α-pHIS-Parallel1-*fimT1s*	*E. coli* Dh5α bearing the pHIS-Parallel1-*fimT1s* plasmid	This study
Dh5α-pHIS-Parallel1-*fimT2s*	*E. coli* Dh5α bearing the pHIS-Parallel1-*fimT2s* plasmid	This study
Dh5α-pHIS-Parallel1-*fimT3s*	*E. coli* Dh5α bearing the pHIS-Parallel1-*fimT3s* plasmid	This study
Dh5α-pHIS-Parallel1-*fimT3s*-R160AR162A	*E. coli* Dh5α bearing the pHIS-Parallel1-*fimT3s*-R160AR162A plasmid	This study

BL21(DE3)-pHIS-Parallel1-*fimT1s*	*E. coli* BL21(DE3) bearing the pHIS-Parallel1-*fimT1s* plasmid	This study
BL21(DE3)-pHIS-Parallel1-*fimT2s*	*E. coli* BL21(DE3) bearing the pHIS-Parallel1-*fimT2s* plasmid	This study
BL21(DE3)-pHIS-Parallel1-*fimT3s*	*E. coli* BL21(DE3) bearing the pHIS-Parallel1-*fimT3s* plasmid	This study
BL21(DE3)-pHIS-Parallel1-*fimT3s*-R160AR162A	*E. coli* BL21(DE3) bearing the pHIS-Parallel1-*fimT3s*-R160AR162A plasmid	This study
Dh5α-pLas16S	*E. coli* Dh5α bearing the pLas16S plasmid	(Parker et al. 2014)
Plasmids		
pUC4K	Donor of kanamycin resistance cassette, Km^R Amp^R	(Vieira and Messing 1982)
pAX1-Cm	pGEM-T derivative; contains multiple cloning site Plasmid that recombines into the neutral site 1 (NS1) of *X. fastidiosa* and inserts a chloramphenicol resistance cassette	(Matsumoto et al. 2009)
pHIS-Parallel1	Cloning vector, f1 ori *lacI* T7 promoter (P_{T7}) Amp^R	(Sheffield et al. 1999)
pHIS-Parallel1-*fimT1s*	Amp^R, P_{T7}-*fimT1s*	This study
pHIS-Parallel1-*fimT2s*	Amp^R, P_{T7}-*fimT2s*	This study
pHIS-Parallel1-*fimT3s*	Amp^R, P_{T7}-*fimT3s*	This study
pHIS-Parallel1-*fimT3s*-R160AR162A	Amp^R, P_{T7}-*fimT3s*-R160AR162A	This study
pLas16S[a]	Plasmid standard to quantify the population of '*Candidatus* Liberibacter asiaticus' as genome equivalents through qPCR	(Parker et al. 2014)
pGEM-T	Cloning vector, f1 ori *lacZ* Amp^R	Promega

Km^R – kanamycin-resistant; Cm^R – chloramphenicol-resistant; Amp^R – ampicillin-resistant.
[a]In this study, pLas16S was used for EMSA in agarose gel with FimT3s.

Table S5-2. List of PCR primers and qPCR primers and probe used in this study.

Name	Sequence (5'–3')	Purpose or description	Amplicon size (bp)	Source
Site-directed mutagenesis of genes of interest[a]				
pilA2-Up F	CCTCAGGAATCATCCGTAACC	Amplify the upstream region of *pilA2* (PD1926)	839	This study
pilA2-Up R	**GTCAGCAACACCTTCTTCACGAGGCAGAC**GATGAATCCTTAAATAGCGTTGGTAAG			
pilA2-Down F	**CATCAGAGATTTTGAGACACAACGTGGC**TTAACACCAGCAACAACACGATTC	Amplify the downstream region of *pilA2* (PD1926)	909	This study
pilA2-Down R	GGTGATGCCGACAAGATTGGCTG			
pilA3-Up F	CAGTAGCCCTATCCGTGAATGTGTC	Amplify the upstream region of *pilA3* (PD1077)	823	This study
pilA3-Up R	**GTCAGCAACACCTTCTTCACGAGGCAGAC**AAAAATTCCCCTAATCTTTGAAAGTG			
pilA3-Down F	**CATCAGAGATTTTGAGACACAACGTGGC**CCGAACGAGTAATGAGCGCCGATG	Amplify the downstream region of *pilA3* (PD1077)	859	This study
pilA3-Down R	CCATCACAGACCTATGCGATACTG			
pilB-Up F	GATAACAACGCAGGCCAAGGTG	Amplify the upstream region of *pilB* (PD1927)	973	This study
pilB-Up R	**GTCAGCAACACCTTCTTCACGAGGCAGAC**GAAAAGTTCTCTGGTTACTCTGC			
pilB-Down F	**CATCAGAGATTTTGAGACACAACGTGGC**GCATCAACAACACCTGTTAATGAC	Amplify the downstream region of *pilB* (PD1927)	1,034	This study
pilB-Down R	CCTTGGTGAATCAGGAGTTGG			
pilC-Up F	CAGTGCAGCCGGAAGGTCTCAG	Amplify the upstream region of *pilC* (PD1923)	845	This study
pilC-Up R	**GTCAGCAACACCTTCTTCACGAGGCAGAC**TGCTGTTCTCCCATCCACCGTC			
pilC-Down F	**CATCAGAGATTTTGAGACACAACGTGGC**AACGTTATGGCATTTCTTGATC	Amplify the downstream region of *pilC* (PD1923)	835	This study
pilC-Down R	CCATCCACCAACTGCCAGATAAG			
pilD-Up F	GTATGCGTACGATGGTCAATC	Amplify the upstream region of *pilD* (PD1922)	958	This study
pilD-Up R	**GTCAGCAACACCTTCTTCACGAGGCAGAC**AACGTTTTATCCAACGACAGAAG			

pilD-Down F	**CATCAGAGATTTTGAGACA CAACGTGGC**GTGAGGTTGG AGTTGATGAGTGTC	Amplify the downstream region of *pilD* (PD1922)	851	This study
pilD-Down R	GCAACTCATACATCCATACA C			
pilE1-Up F	CTGTCTGGTGTATTTCCCTGG TC	Amplify the upstream region of *pilE1* (PD0024)	874	This study
pilE1-Up R	**GTCAGCAACACCTTCTTCA CGAGGCAGAC**GGAAGTTAC ATCATTCACGAACATC			
pilE1-Down F	**CATCAGAGATTTTGAGACA CAACGTGGC**GGTGATCTGAT GTTTGGAGTGCTTG	Amplify the downstream region of *pilE1* (PD0024)	952	This study
pilE1-Down R	CAGGAGTCATCCGTCGTCTTT CG			
pilE2-Up F	GCAATCTCTGGAAGTTCAAC CTG	Amplify the upstream region of *pilE2* (PD1610)	912	This study
pilE2-Up R	**GTCAGCAACACCTTCTTCA CGAGGCAGAC**ACGTTCCCAC TTTAGGATCACCATC			
pilE2-Down F	**CATCAGAGATTTTGAGACA CAACGTGGC**CGTGTTCCCGC ATTGCTTTTAGTTG	Amplify the downstream region of *pilE2* (PD1610)	893	This study
pilE2-Down R	CTCATAGACGAACACGAGTA GG			
pilF-Up F	CAAGGTTTTAACCGCAATCT GAC	Amplify the upstream region of *pilF* (PD1623)	855	This study
pilF-Up R	**GTCAGCAACACCTTCTTCA CGAGGCAGAC**GACTAAGCA GCCAGATAAAATC			
pilF-Down F	**CATCAGAGATTTTGAGACA CAACGTGGC**TGTATTGTGAT CAGTGATTTCG	Amplify the downstream region of *pilF* (PD1623)	814	This study
pilF-Down R	GTTCCCAGATTCTTGCACTTC CACC			
pilG-Up F	CAGATAGCGTTGCGCTATTG C	Amplify the upstream region of *pilG* (PD0845)	869	This study
pilG-Up R	**GTCAGCAACACCTTCTTCA CGAGGCAGAC**AGCGCTCTG AATCTAAATACTGTG			
pilG-Down F	**CATCAGAGATTTTGAGACA CAACGTGGC**CCTGACTGTTC ATCTGATGCGTTTCC	Amplify the downstream region of *pilG* (PD0845)	803	This study
pilG-Down R	CAACTGCTGCGACAACACCT G			
pilH-Up F	GAAGTGATAGTTCGCGCGTT ATG	Amplify the upstream region of *pilH* (PD1632)	1,003	This study
pilH-Up R	**GTCAGCAACACCTTCTTCA CGAGGCAGAC**GTCTGCTTCA GCAGTTTAGTGTG			

pilH-Down F	**CATCAGAGATTTTGAGACA CAACGTGGC**GGCACACCAT AACGAGAAACCGGAC	Amplify the downstream region of *pilH* (PD1632)	977	This study
pilH-Down R	GTTATGTTGACTCCCTTCTCT G			
pilI-Up F	CTACCAGGGTGCACATAATG AAG	Amplify the upstream region of *pilI* (PD0846)	845	This study
pilI-Up R	**GTCAGCAACACCTTCTTCA CGAGGCAGAC**CAGATGAAC AGTCAGGTTAAACAG			
pilI-Down F	**CATCAGAGATTTTGAGACA CAACGTGGC**TTGGCGGTCCC GTCTTGCATATTTAG	Amplify the downstream region of *pilI* (PD0846)	977	This study
pilI-Down R	GTTTATCACGTACCGAGCCA ACC			
pilJ-Up F	GGTGTGAGGTGGTTACCGCT ATTG	Amplify the upstream region of *pilJ* (PD0847)	884	This study
pilJ-Up R	**GTCAGCAACACCTTCTTCA CGAGGCAGAC**TCAGGCAGC AGCCTGTCTAAATTCAG			
pilJ-Down F	**CATCAGAGATTTTGAGACA CAACGTGGC**TTGAATGCTTC TCGGCTTGGAAAGG	Amplify the downstream region of *pilJ* (PD0847)	928	This study
pilJ-Down R	GGAAGCATCGACATGGAGCA ATG			
pilL-Up F	CGATAGCCGACGCGATTAAC TGTG	Amplify the upstream region of *pilL* (PD0848)	922	This study
pilL-Up R	**GTCAGCAACACCTTCTTCA CGAGGCAGAC**TCAAGCTGG CAATTTGAAGTTGGCTG			
pilL-Down F	**CATCAGAGATTTTGAGACA CAACGTGGC**TAGCGTCCAAG GTAAGTTGGTTGC	Amplify the downstream region of *pilL* (PD0848)	920	This study
pilL-Down R	GATGCCCAGATTATCCCGAA GCAC			
pilM-Up F	CGTGCATCGGTATTGCTTTTG C	Amplify the upstream region of *pilM* (PD1695)	1,016	This study
pilM-Up R	**GTCAGCAACACCTTCTTCA CGAGGCAGAC**GGGCACTTTT AAGACAGGAACATATC			
pilM-Down F	**CATCAGAGATTTTGAGACA CAACGTGGC**ATGGCCAGAA TTAACTTATTGCCCTG	Amplify the downstream region of *pilM* (PD1695)	987	This study
pilM-Down R	CTTACTAGGCAACTGCCGTA ACATC			
pilN-Up F	GCTTCAAGGTGGAACACTAT GCTG	Amplify the upstream region of *pilN* (PD1694)	994	This study
pilN-Up R	**GTCAGCAACACCTTCTTCA CGAGGCAGAC**TCAGTCAAA ACTCCTCAAAGCCAGAC			

pilN-Down F	**CATCAGAGATTTTGAGACA CAACGTGGC**ATGAGTAAGA ATTCGTTTAAATTGAG	Amplify the downstream region of *pilN* (PD1694)	1,153	This study
pilN-Down R	GTTCGACGCGATCTTCATTCA CC			
pilO-Up F	CTATGCTGGCAGTGAGTACA AC	Amplify the upstream region of *pilO* (PD1693)	920	This study
pilO-Up R	**GTCAGCAACACCTTCTTCA CGAGGCAGAC**TCAATTGTCC TCTGACAGCG			
pilO-Down F	**CATCAGAGATTTTGAGACA CAACGTGGC**ATGAGTACAA AAACCCTCAAAAAAATAG	Amplify the downstream region of *pilO* (PD1693)	912	This study
pilO-Down R	GATCTGGCGTTGCAAGACAG TC			
pilP-Up F	GATAGCAGGGCTCTGCCGTA TG	Amplify the upstream region of *pilP* (PD1692)	853	This study
pilP-Up R	**GTCAGCAACACCTTCTTCA CGAGGCAGAC**TCATGGTCCA TCCTTCTTGC			
pilP-Down F	**CATCAGAGATTTTGAGACA CAACGTGGC**ATGATTGATTT AAGGGATAG	Amplify the downstream region of *pilP* (PD1692)	822	This study
pilP-Down R	CAAATTACTTTCTCATCACGG C			
pilQ-Up F	GAGGTGCTGAAGCAGATGTT AC	Amplify the upstream region of *pilQ* (PD1691)	967	This study
pilQ-Up R	**GTCAGCAACACCTTCTTCA CGAGGCAGAC**TTAATCGTCG AACGAAAGCGC			
pilQ-Down F	**CATCAGAGATTTTGAGACA CAACGTGGC**ATTTCGTCAAT GCACTGCTTTATATCTC	Amplify the downstream region of *pilQ* (PD1691)	897	This study
pilQ-Down R	CAACTCGAAACGCTTGGCAC AAC			
pilR-Up F	CGTTGACTTTGTTGGCGCTTG G	Amplify the upstream region of *pilR* (PD1928)	900	This study
pilR-Up R	**GTCAGCAACACCTTCTTCA CGAGGCAGAC**GAATGCCAA GATAACGCAGCAGAC			
pilR-Down F	**CATCAGAGATTTTGAGACA CAACGTGGC**TGAGAGGAAG CAGGCAACATAGC	Amplify the downstream region of *pilR* (PD1928)	937	This study
pilR-Down R	GGTATCGACAAACTCGGTTA CG			
pilS-Up F	CCATCCAGTGCGTACAAATC C	Amplify the upstream region of *pilS* (PD1929)	924	This study
pilS-Up R	**GTCAGCAACACCTTCTTCA CGAGGCAGAC**GTCACGGTG TCCTAAGGCAGAAGAG			

pilS-Down F	**CATCAGAGATTTTGAGACA CAACGTGGC**GTGCCCCGGTA TTTCATTCACATTC	Amplify the downstream region of *pilS* (PD1929)	881	This study
pilS-Down R	GTATGCGCACCGGTGAAACT C			
pilT-Up F	ACATCATCTGGCACATCAG	Amplify the upstream region of *pilT* (PD1147)	925	This study
pilT-Up R	**GTCAGCAACACCTTCTTCA CGAGGCAGAC**TTGCATAGA CGACGAATGG			
pilT-Down F	**TCAGAGATTTTGAGACACA ACGTGGC**TTACCGCACTATC ACACATAAG	Amplify the downstream region of *pilT* (PD1147)	903	This study
pilT-Down R	GCTTGATTGGCGTTGTTG			
pilU-Up F	GATTCTGGTGACTGGGCCGA CTG	Amplify the upstream region of *pilU* (PD1148)	855	This study
pilU-Up R	**GTCAGCAACACCTTCTTCA CGAGGCAGAC**CGGGTGTTG CTCCTTTGCTGCTATG			
pilU-Down F	**CATCAGAGATTTTGAGACA CAACGTGGC**ATCTATTATGA GGTTATATAATC	Amplify the downstream region of *pilU* (PD1148)	879	This study
pilU-Down R	GTCGATGGTCGCTATGAATT GC			
pilV1-Up F	GGAACGAAGGAGGTCTCAAA GG	Amplify the upstream region of *pilV1* (PD0020)	858	This study
pilV1-Up R	**GTCAGCAACACCTTCTTCA CGAGGCAGAC**AACAGTGTTT TATTCGTCGTTAGG			
pilV1-Down F	**CATCAGAGATTTTGAGACA CAACGTGGC**GTGAACCGTCG GTTTGCCCTGCAAC	Amplify the downstream region of *pilV1* (PD0020)	885	This study
pilV1-Down R	CAAGGCAACTCTAACCGCAA TGAC			
pilV2-Up F	GCTGGCAACGTCAAGGAAGA AG	Amplify the upstream region of *pilV2* (PD1614)	861	This study
pilV2-Up R	**GTCAGCAACACCTTCTTCA CGAGGCAGAC**TCATTGACAC GCGCCCTTCTCCACC			
pilV2-Down F	**CATCAGAGATTTTGAGACA CAACGTGGC**CGATGTATTCC TCACGCTTAGCGCGTC	Amplify the downstream region of *pilV2* (PD1614)	911	This study
pilV2-Down R	CAACGGGCACGATACAGTGA TG			
pilW1-Up F	CAGTGCCAACGAGTTAGTTG CTTC	Amplify the upstream region of *pilW1* (PD0021)	936	This study
pilW1-Up R	**GTCAGCAACACCTTCTTCA CGAGGCAGAC**TCACAGTTTA CTCCTCACTTCAAAAATTTG			

pilW1-Down F	**CATCAGAGATTTTGAGACA CAACGTGGC**ATGAGGATGA CTCACCTCGGGCCGTACAG	Amplify the downstream region of *pilW1* (PD0021)	973	This study
pilW1-Down R	CGTAATTGGCTTGAGGCCTTG GAG			
pilW2-Up F	GCTTATGGTCGTTGTTGCTGT CG	Amplify the upstream region of *pilW2* (PD1613)	988	This study
pilW2-Up R	**GTCAGCAACACCTTCTTCA CGAGGCAGAC**CGTCATAAC ACACTAGTCAGATTG			
pilW2-Down F	**CATCAGAGATTTTGAGACA CAACGTGGC**TGATGAAGTTA CGGGCATTTGTCG	Amplify the downstream region of *pilW2* (PD1613)	1,069	This study
pilW2-Down R	CATACCCGTCATGCGACACA CTAGC			
pilX1-Up F	GAAGTGAGGAGTAAACTGTG AACC	Amplify the upstream region of *pilX1* (PD0022)	997	This study
pilX1-Up R	**GTCAGCAACACCTTCTTCA CGAGGCAGAC**TCATAAATTT CTGTTCCGTAAGCTG			
pilX1-Down F	**CATCAGAGATTTTGAGACA CAACGTGGC**TTGGATTTCTT CAAGATATCGAAATG	Amplify the downstream region of *pilX1* (PD0022)	931	This study
pilX1-Down R	CACCATCAATCAAGTAGCTG TG			
pilX2-Up F	GTAGTGCGTCTGATTGGAAT CC	Amplify the upstream region of *pilX2* (PD1612)	843	This study
pilX2-Up R	**GTCAGCAACACCTTCTTCA CGAGGCAGAC**CATCAGTTCC CGTATAAGCGATTG			
pilX2-Down F	**CATCAGAGATTTTGAGACA CAACGTGGC**GCAATGAAAA AAAACGTTCTGAAGTG	Amplify the downstream region of *pilX2* (PD1612)	849	This study
pilX2-Down R	CGTAACTCATCGGCAACAGA AC			
pilY1-1-Up F	CGATCATCACCGAATTGCGT GCAG	Amplify the upstream region of *pilY1-1* (PD0023)	959	This study
pilY1-1-Up R	**GTCAGCAACACCTTCTTCA CGAGGCAGAC**TTCGATATCT TGAAGAAATCC			
pilY1-1-Down F	**CATCAGAGATTTTGAGACA CAACGTGGC**CGATGTTCGTG AATGATGTAAC	Amplify the downstream region of *pilY1-1* (PD0023)	864	This study
pilY1-1-Down R	CTACGCAAACGTGTTGCCAT ACAG			
pilY1-2-Up F	GGAGTGGAGTCCTTGCAATT TC	Amplify the upstream region of *pilY1-2* (PD1611)	988	This study
pilY1-2-Up R	**GTCAGCAACACCTTCTTCA CGAGGCAGAC**ATTGAGCGG CGGCACCACGTTGCTC			

pilY1-2-Down F	**CATCAGAGATTTTGAGACA CAACGTGGC**TGGTGATCCTA AAGTGGGAACGTG	Amplify the downstream region of *pilY1-2* (PD1611)	1,045	This study
pilY1-2-Down R	CGATTCAATGTCCAGCTGCAT CC			
pilY1-3-Up F	GGTGTATTAGGGATAGTGGA GTTC	Amplify the upstream region of *pilY1-3* (PD0502)	918	This study
pilY1-3-Up R	**GTCAGCAACACCTTCTTCA CGAGGCAGAC**CAAATCTTGT TCCTTCATCCTTGCTC			
pilY1-3-Down F	**CATCAGAGATTTTGAGACA CAACGTGGC**TCCACAAAAA AAGAGATGGATAGAG	Amplify the downstream region of *pilY1-3* (PD0502)	868	This study
pilY1-3-Down R	GCTTCCACACCTCATTATTCT GTC			
pilZ-Up F	GAAGGATTAGGGCAACGTGC GGTTTC	Amplify the upstream region of *pilZ* (PD1497)	883	This study
pilZ-Up R	**GTCAGCAACACCTTCTTCA CGAGGCAGAC**TACTCCTTAC ATTCTGCTCAGCATTC			
pilZ-Down F	**CATCAGAGATTTTGAGACA CAACGTGGC**TTGCTGTTGTG CTTGATGTGTTGCTTG	Amplify the downstream region of *pilZ* (PD1497)	1,028	This study
pilZ-Down R	GAACGAAGATGCTCTAGCAC TGC			
fimT1-Up F	GCTTGGTGCGTATTACTCAGG CCATC	Amplify the upstream region of *fimT1* (PD0019)	909	This study
fimT1-Up R	**GTCAGCAACACCTTCTTCA CGAGGCAGAC**ATTTAGATAC ATATGCCACG			
fimT1-Down F	**CATCAGAGATTTTGAGACA CAACGTGGC**AACACTGTTAT GTCCATCGCAAGC	Amplify the downstream region of *fimT1* (PD0019)	879	This study
fimT1-Down R	CAGAATGCGGATTGCGTCTG TTCC			
fimT2-Up F	CATCGCTGCCGAATCGCCAA ATC	Amplify the upstream region of *fimT2* (PD1615)	880	This study
fimT2-Up R	**GTCAGCAACACCTTCTTCA CGAGGCAGAC**CTAAACGCT CCACAGCGTTAATGTC			
fimT2-Down F	**CATCAGAGATTTTGAGACA CAACGTGGC**GTGTCAATGAA AAAGTGTTCCAATC	Amplify the downstream region of *fimT2* (PD1615)	832	This study
fimT2-Down R	CATCCGCATTGAGAAACAAC GAACG			
fimT3-Up F	GTCTGACCGGTAAGCGGATC GAAC	Amplify the upstream region of *fimT3* (PD1735)	884	This study
fimT3-Up R	**GTCAGCAACACCTTCTTCA CGAGGCAGAC**ACCGATAGT CTCGACAATGTTTAGG			

fimT3-Down F	**CATCAGAGATTTTGAGACA CAACGTGGC**ACACCATCGTA TTCACATGACATTTG	Amplify the downstream region of *fimT3* (PD1735)	900	This study
fimT3-Down R	GCATAAGGATTACGCGCTTT CACC			
chpB-Up F	GTCAGAGCACCTTTGCAGTTC	Amplify the upstream region of *chpB* (PD0849)	845	This study
chpB-Up R	**GTCAGCAACACCTTCTTCA CGAGGCAGAC**CTTACCTTGG ACGCTATCATTCTC			
chpB-Down F	**CATCAGAGATTTTGAGACA CAACGTGGC**TATGTAAGGA AACTACCTTCAATG	Amplify the downstream region of *chpB* (PD0849)	1,042	This study
chpB-Down R	CAACTACGCTCCGATGAGGT AAAGC			
chpC-Up F	CGAATTGATTGCTCGTCGTCA AGG	Amplify the upstream region of *chpC* (PD0850)	984	This study
chpC-Up R	**GTCAGCAACACCTTCTTCA CGAGGCAGAC**TGAAGGTAG TTTCCTTACATATCAATG			
chpC-Down F	**CATCAGAGATTTTGAGACA CAACGTGGC**CATGTGGTGGG ATGAATGTGTTTTG	Amplify the downstream region of *chpC* (PD0850)	857	This study
chpC-Down R	CCAGATTGTCCAGATGGTAA GAG			
Km-F	GTCTGCCTCGTGAAG	Amplify the kanamycin resistance cassette	1,202	(Kandel et al. 2018)
Km-R	AAGCCACGTTGTGT			
Confirmation of site-directed mutagenesis of genes of interest				
pilA2-Fconf	CACTTTGATCGAGCTGATGAT C	Amplify internal sequence of *pilA2* (PD1926)	328	This study
pilA2-Rconf	GTTGTTATCAGCGATGCGGG TCAAG			
pilA2Up-Fconf	CAGGTCACTCCATCTGCCTTA CC	Amplify internal sequence of upstream region of *pilA2* (PD1926) and the kanamycin resistance cassette	972	This study
pilA3-Fconf	CAAGGCTTCACCCTGTTAGA GG	Amplify internal sequence of *pilA3* (PD1077)	410	This study
pilA3-Rconf	CTTGAGCCATGCAAACCTAC ATCG			
pilA3UP-Fconf	CGTCAATAACGCGAACAGCA TC	Amplify internal sequence of upstream region of *pilA3* (PD1077) and the kanamycin resistance cassette	1,119	This study

pilB-Fconf	CTACTGGATGTGTCCGCATTCG	Amplify internal sequence of *pilB* (PD1927)	493	This study
pilB-Rconf	CAGCCTTCAGCAGACCATCAATCC			
pilBUp-Fconf	CCATCCATGCAGCGTTTCCATCTG	Amplify internal sequence of upstream region of *pilB* (PD1927) and the kanamycin resistance cassette	1,130	This study
pilC-Fconf	CATCACGCCTCTTGTGGTTAAG	Amplify internal sequence of *pilC* (PD1923)	649	This study
pilC-Rconf	CAACACCAACCTATCCAACAG			
pilCUp-Fconf	GTTGTACTCTTCCCATCAGCAATC	Amplify internal sequence of upstream region of *pilC* (PD1923) and the kanamycin resistance cassette	1,096	This study
pilD-Fconf	GGAAAACATTCCGGTGCTTAGC	Amplify internal sequence of *pilD* (PD1922)	500	This study
pilD-Rconf	CAAGCCAAACAGAGCCCAATACC			
pilDUp-Fconf	CCAACTTTATGCAGCGGTGGTG	Amplify internal sequence of upstream region of *pilD* (PD1922) and the kanamycin resistance cassette	1,100	This study
pilE1-Fconf	GATGATTGTGGTGGTGATCGTG	Amplify internal sequence of *pilE1* (PD0024)	305	This study
pilE1-Rconf	GTGTGAGCCTGCCACAGTGATC			
pilE1Up-Fconf	CCAGGTACAGATTGTTGATGAGG	Amplify internal sequence of upstream region of *pilE1* (PD0024) and the kanamycin resistance cassette	1,044	This study
pilE2-Fconf	GTTGATGGTTGTGGTCGCTGTC	Amplify internal sequence of *pilE2* (PD1610)	301	This study
pilE2-Rconf	GCACTTGTCGTTTTGCTGAGTGC			
pilE2Up-Fconf	GGTATGTCGATTTGGTGGTACAG	Amplify internal sequence of upstream region of *pilE2* (PD1610) and the kanamycin resistance cassette	1,024	This study
pilF-Fconf	GTTTACAACGTGCGTGATGATG	Amplify internal sequence of *pilF* (PD1623)	388	This study
pilF-Rconf	CACAACCGCCGGAATTGGCTAAAG			

pilFUp-Fconf	CAAACTAATGCGGCAATTTGAC	Amplify internal sequence of upstream region of *pilF* (PD1623) and the kanamycin resistance cassette	878	This study
pilG-Fconf	GTCTTAGGGTGATGGTCATTG	Amplify internal sequence of *pilG* (PD0845)	305	This study
pilG-Rconf	CAGATATTGTTCGGAACCAACCAC			
pilGUp-Fconf	CAGCATTGACTGGAGGATCTTTAC	Amplify internal sequence of upstream region of *pilG* (PD0845) and the kanamycin resistance cassette	1,042	This study
pilH-Fconf	GCATTTTGATCGTCGAGGACTC	Amplify internal sequence of *pilH* (PD1632)	313	This study
pilH-Rconf	GAGAAAGGCTTGGTGATGTAGG			
pilHUp-Fconf	CTGGCTTTGGACATCTTCAGTG	Amplify internal sequence of upstream region of *pilH* (PD1632) and the kanamycin resistance cassette	1,100	This study
pilI-Fconf	GTGTTGGCTATCGTATTGGAAG	Amplify internal sequence of *pilI* (PD0846)	252	This study
pilI-Rconf	CGATAACCAGTGCTGCATTATC			
pilIUp-Fconf	GCGTCTGCTATTGCAGTACACAG	Amplify internal sequence of upstream region of *pilI* (PD0846) and the kanamycin resistance cassette	1,021	This study
pilJ-Fconf	GCTGATCGCTTCGTGAGTAATGTG	Amplify internal sequence of *pilJ* (PD0847)	557	This study
pilJ-Rconf	CCAACAATCGACACTACAGACAGC			
pilJUp-Fconf	CCTGACTGTTCATCTGATGCGTTTC	Amplify internal sequence of upstream region of *pilJ* (PD0847) and the kanamycin resistance cassette	1,072	This study
pilL-Fconf	GCTTGATGAAGAGCAGGGTAATC	Amplify internal sequence of *pilL* (PD0848)	464	This study
pilL-Rconf	GGATTTCACGCAGTACACTGTCC			

pilLUp-Fconf	CGAGATTGCGGCTAGTATCGAAC	Amplify internal sequence of upstream region of *pilL* (PD0848) and the kanamycin resistance cassette	1,236	This study
pilM-Fconf	GCAGGATTTGGAAGCTCAGATAG	Amplify internal sequence of *pilM* (PD1695)	408	This study
pilM-Rconf	CCATAGCGATGCATTACTTCGTC			
pilMUp-Fconf	GTCAATGCCGCTGTGTTCGTAG	Amplify internal sequence of upstream region of *pilM* (PD1695) and the kanamycin resistance cassette	1,049	This study
pilN-Fconf	GGTCAGTGGTCAGAATGATCG	Amplify internal sequence of *pilN* (PD1694)	439	This study
pilN-Rconf	CTTATCTGGCGACTCTGGCTTGG			
pilNUp-Fconf	CAACAACACGGAGATGGTCCAAG	Amplify internal sequence of upstream region of *pilN* (PD1694) and the kanamycin resistance cassette	1,188	This study
pilO-Fconf	GTCATCATGGCTTGGTTCCTC	Amplify internal sequence of *pilO* (PD1693)	377	This study
pilO-Rconf	GGTAAAGAAGCCACACCACTGAC			
pilOUp-Fconf	CACATTGGTGGGTATCCTCGTTTC	Amplify internal sequence of upstream region of *pilO* (PD1693) and the kanamycin resistance cassette	1,105	This study
pilP-Fconf	GTCGGTTTGATTGTTCTCTTGG	Amplify internal sequence of *pilP* (PD1692)	433	This study
pilP-Rconf	GTTCGACGCGATCTTCATTCAC			
pilPUp-Fconf	GCAGCCATTAAAGCAGCAGTTG	Amplify internal sequence of upstream region of *pilP* (PD1692) and the kanamycin resistance cassette	970	This study
pilQ-Fconf	CGTATCGACGCTAAGCCTATGG	Amplify internal sequence of *pilQ* (PD1691)	567	This study
pilQ-Rconf	CATACCTTTGGCTTCTGTCAGTGC			

pilQUp-Fconf	GAGAATCGTACTGCTGATGCTG	Amplify internal sequence of upstream region of *pilQ* (PD1691) and the kanamycin resistance cassette	1,096	This study
pilR-Fconf	CGTATCAGAACGGCAGCTAATCTG	Amplify internal sequence of *pilR* (PD1928)	400	This study
pilR-Rconf	CTTGACTACGCGCCACTTTAGC			
pilRUp-Fconf	CGATGAATACCGCCAGACATTG	Amplify internal sequence of upstream region of *pilR* (PD1928) and the kanamycin resistance cassette	1,137	This study
pilS-Fconf	CTTGTGGAATACATCTGGACTG	Amplify internal sequence of *pilS* (PD1929)	642	This study
pilS-Rconf	CCTTTGATCGCCTTTGTCAAG			
pilSUp-Fconf	CTGTTTCACTTCGTCGGTTGTC	Amplify internal sequence of upstream region of *pilS* (PD1929) and the kanamycin resistance cassette	992	This study
pilT-Fconf	GTGATGACATTGGACGAACTCG	Amplify internal sequence of *pilT* (PD1147)	719	This study
pilT-Rconf	CTTTATCCTTGGCGTATTCACG			
pilTUp-Fconf	CCTTCTTTACTATCTCCTGAGC	Amplify internal sequence of upstream region of *pilT* (PD1147) and the kanamycin resistance cassette	951	This study
pilU-Fconf	CTCAATGGCATCAATGATCAAC	Amplify internal sequence of *pilU* (PD1148)	365	This study
pilU-Rconf	GATTCAGCGACAGATCCATCAG			
pilUUp-Fconf	GATCATCTCGCAAATGTTGTTG	Amplify internal sequence of upstream region of *pilU* (PD1148) and the kanamycin resistance cassette	940	This study
pilV1-Fconf	CGTTAGTTTGATCGAAGTGCTG	Amplify internal sequence of *pilV1* (PD0020)	323	This study
pilV1-Rconf	CATCACAAGAGATCGAACCACAG			

pilV1Up-Fconf	GAACGAAGGAGGTCTCAAAGGAAAGC	Amplify internal sequence of upstream region of *pilV1* (PD0020) and the kanamycin resistance cassette	1,353	This study
pilV2-Fconf	GTGTTCCAATCATCGTTGCCATTG	Amplify internal sequence of *pilV2* (PD1614)	381	This study
pilV2-Rconf	CCATTCGTCGCAAGATTCACC			
pilV2Up-Fconf	CAGACAGTGTTTGCGCTGCACTG	Amplify internal sequence of upstream region of *pilV2* (PD1614) and the kanamycin resistance cassette	1,111	This study
pilW1-Fconf	GAGATTCCGCCACAGAATGGTC	Amplify internal sequence of *pilW1* (PD0021)	405	This study
pilW1-Rconf	CATACCACTGCACTGCACGCAATTC			
pilW1Up-Fconf	CCAACACACGGATGGCTAACAAC	Amplify internal sequence of upstream region of *pilW1* (PD0021) and the kanamycin resistance cassette	1,124	This study
pilW2-Fconf	CGTCATGGACTGCTTACCGTCTTTC	Amplify internal sequence of *pilW2* (PD1613)	408	This study
pilW2-Rconf	GCAGTACCAGAACATCACTTCC			
pilW2Up-Fconf	CAGTTGTTCGTGTCAGTGAAGG	Amplify internal sequence of upstream region of *pilW2* (PD1613) and the kanamycin resistance cassette	1,189	This study
pilX1-Fconf	GCTAACCTCCGTGATCGCAGTTTG	Amplify internal sequence of *pilX1* (PD0022)	409	This study
pilX1-Rconf	CATTGCTAGACGGATCGCTGCTTCG			
pilX1Up-Fconf	CTCAAGGCGTCAGAGGAACAGAC	Amplify internal sequence of upstream region of *pilX1* (PD0022) and the kanamycin resistance cassette	1,148	This study
pilX2-Fconf	GTTGTGCTGGTGGTGTTGGTG	Amplify internal sequence of *pilX2* (PD1612)	350	This study
pilX2-Rconf	CTGAATACAGTGATACGGAAC			

pilX2Up-Fconf	GTTTGAACGAGCGCGGGATTCC	Amplify internal sequence of upstream region of *pilX2* (PD1612) and the kanamycin resistance cassette	940	This study
pilY1-1-Fconf	GCTAATCTGGCCGACACCTACAC	Amplify internal sequence of *pilY1-1* (PD0023)	479	This study
pilY1-1-Rconf	GAATCGTAAGGTTGGCCCTCTGTG			
pilY1-1Up-Fconf	CTGTTCTGCGCACGACGTTACTTC	Amplify internal sequence of upstream region of *pilY1-1* (PD0023) and the kanamycin resistance cassette	1,042	This study
pilY1-2-Fconf	CACATCGCGTATGGATGCTTTGC	Amplify internal sequence of *pilY1-2* (PD1611)	541	This study
pilY1-2-Rconf	CTGGTATGAGCCAGTCAACAGAC			
pilY1-2Up-Fconf	CAAGTTGCAACCATGCAGGAG	Amplify internal sequence of upstream region of *pilY1-2* (PD1611) and the kanamycin resistance cassette	1,044	This study
pilY1-3-Fconf	CAGTGATGGATCGTGCTTATCC	Amplify internal sequence of *pilY1-3* (PD0502)	552	This study
pilY1-3-Rconf	GAGTAGTCGCCTTAGCATCCTCAG			
pilY1-3Up-Fconf	GCATCTCTGGATTGTCAGCATCG	Amplify internal sequence of upstream region of *pilY1-3* (PD0502) and the kanamycin resistance cassette	1,187	This study
pilZ-Fconf	CAGGGTATTCTGTCGCTCACC	Amplify internal sequence of *pilZ* (PD1497)	326	This study
pilZ-Rconf	GTGTGCGTTGGCTTATCTGAG			
pilZUp-Fconf	GCATTGCTGAAGACGCTTGAG	Amplify internal sequence of upstream region of *pilZ* (PD1497) and the kanamycin resistance cassette	1,088	This study
fimT1-Fconf	CAATTCTTGCGGGCCTTGCTTATC	Amplify internal sequence of *fimT1* (PD0019)	396	This study
fimT1-Rconf	GGTTGTTAGCCATCCGTGTGTTGG			

fimT1Up-Fconf	CAAAGGTGTTGATGACCCGATG	Amplify internal sequence of upstream region of *fimT1* (PD0019) and the kanamycin resistance cassette	1,088	This study
fimT2-Fconf	GCTTATGGTCGTTGTTGCTGTCG	Amplify internal sequence of *fimT2* (PD1615)	367	This study
fimT2-Rconf	GTTCGATGCACGCCGTAAGCCATGC			
fimT2Up-Fconf	GTGAAGAACGCAAGGATGCTTATTAC	Amplify internal sequence of upstream region of *fimT2* (PD1615) and the kanamycin resistance cassette	1,014	This study
fimT3-Fconf	CACGATGGCGCTAATCGCATTATTG	Amplify internal sequence of *fimT3* (PD1735)	398	This study
fimT3-Rconf	CATTGTTGCAGAAGCGGATGCTG			
fimT3Up-Fconf	CAACACATCAGAACGTGACAGC	Amplify internal sequence of upstream region of *fimT3* (PD1735) and the kanamycin resistance cassette	1,090	This study
chpB-Fconf	GATTGCTCGTCGTCAAGGTTG	Amplify internal sequence of *chpB* (PD0849)	569	This study
chpB-Rconf	GATCAACTGGCAAAGTGGAGACTC			
chpBUp-Fconf	CACTGGTGATGGTTGTGTGATTG	Amplify internal sequence of upstream region of *chpB* (PD0849) and the kanamycin resistance cassette	1,034	This study
chpC-Fconf	CGAACGAGTGCTATTACCAAATGC	Amplify internal sequence of *chpC* (PD0850)	357	This study
chpC-Rconf	GCTTGAGTTTCACTAAGAAGTACAC			
chpCUp-Fconf	GCATTACCCGCTGGTTTCAAACATC	Amplify internal sequence of upstream region of *chpC* (PD0850) and the kanamycin resistance cassette	1,020	This study

Km-Rconf	GATTCAGTCGTCACTCATGGTG	Pairs with "Up-Fconf" primers to amplify internal sequence of upstream region of the gene of interest and the kanamycin resistance cassette	-	(Gluck-Thaler et al. 2020)
Confirmation of pAX1-Cm recombination into the NS1 region of *X. fastidiosa* TemeculaL				
Cm-F	AATCAGCGACACTGAATACGG	Amplify the chloramphenicol resistance cassette	1,119	(Kandel et al. 2018)
Cm-R	TCACTTATTCAGGCGTAGCAC			
qPCR primers and probe used to quantify the *X. fastidiosa* population				
HL5 Forward	AAGGCAATAAACGCGCACTA	Quantify the *X. fastidiosa* population as genome equivalents	221	(Francis et al. 2006)
HL6 Reverse	GGTTTTGCTGACTGGCAACA			
HLp (probe)	6FAM-TGGCAGGCAGCAACGATACGGCT-QSY			
Cloning into pHIS-Parallel1[b]				
fimT1s-pHIS-F	CATG**CCATGG**ATAATGGTGAGCGCTTG (NcoI)	Amplify *fimT1s* to clone into pHIS-Parallel1	459	This study
fimT1s-pHIS-R	CCG**CTCGAG**TTATTCGTCGTTAGG (XhoI)			
fimT2s-pHIS-F	CATG**CCATGG**ATCGCTCGAATCGAGTG (NcoI)	Amplify *fimT2s* to clone into pHIS-Parallel1	429	This study
fimT2s-pHIS-R	CCG**CTCGAG**TCATTGACACGC (XhoI)			
fimT3s-pHIS-F	CATG**CCATGG**ATAAACAAACTCTGGAAC (NcoI)	Amplify *fimT3s* to clone into pHIS-Parallel1	519	This study
fimT3s-pHIS-R	CCG**CTCGAG**TTATTGGAATGGTGTTTC (XhoI)			
Amino acid exchanges in FimT3s (cloned into pHIS-Parallel1)				
FimT3_R160A R162A-F	GAGTATTAAGTATCCGTTGCGAGGCAATTGCGCCTAAATTGTTGATCACGATGA	Exchange the arginine amino acid residues at positions 160 and 162 of FimT3s cloned into pHIS-Parallel1 by alanine residues	5,859	This study
FimT3_R160A R162A-R	TCATCGTGATCAACAATTTAGGCGCAATTGCCTCGCAACGGATACTTAATACTC			
Sanger sequencing				
T7 promoter - forward	TAATACGACTCACTATAGGG	Amplify the gene cloned downstream of the T7 promoter in pHIS-Parallel1 for Sanger sequencing	variable	Eurofins Genomics LLC

[a]Nucleotides in bold indicate the 5' extended region of each primer that is homologous to the kanamycin resistance cassette sequence to allow fusion of chromosomal sequences to the marker by overlap-extension PCR.
[b]Nucleotides in bold indicate the restriction sites of the endonucleases (specified within parenthesis) used for cloning into pHIS-Parallel1.

Table S5-3. List of *pil* and associated genes deleted in *X. fastidiosa* strain TemeculaL.

Locus ID[a]	Gene	Genome annotation[a]	General description	Reference
Major pilin[b]				
PD1924	*pilA1*	Type IV fimbrial precursor	Major pilin subunit that composes the main structural component of TFP	(Mattick 2002)
PD1926	*pilA2*	Fimbrial protein		
PD1077	*pilA3*	Fimbrillin		
Minor pilin				
PD0024	*pilE1*	Type IV pilin	Minor pilins responsible for priming the assembly of TFP and promoting the display of the PilY1 adhesin at the tip of the pilus	(Nguyen et al. 2015)
PD1610	*pilE2*	Type IV pilin		
PD0020	*pilV1*	Prepilin leader sequence		
PD1614	*pilV2*	Type IV pilus modification protein		
PD0021	*pilW1*	Prepilin type N-terminal cleavage//methylation domain		
PD1613	*pilW2*	Pilus assembly protein		
PD0022	*pilX1*	Type IV fimbrial biogenesis protein		
PD1612	*pilX2*	Type IV fimbrial biogenesis protein		
PD0019	*fimT1*	Prepilin like leader sequence	Minor pilin that interacts directly with PilA and mediates its connection to the other minor pilins subcomplex (PilVWXY1E)	
PD1615	*fimT2*	Prepilin type N-terminal cleavage/methylation domain		
PD1735	*fimT3*	Type IV fimbrial biogenesis protein		
Pilus-associated adhesin				
PD0023	*pilY1-1*	Type IV fimbrial biogenesis protein	TFP tip adhesin	(Alm et al. 1996b)
PD1611	*pilY1-2*	Type IV fimbrial biogenesis protein		
PD0502	*pilY1-3*	Type IV fimbrial biogenesis protein		
Secretin				
PD1691	*pilQ*	Fimbrial assembly protein	Multimeric outer membrane secretin that forms gated pores from which TFP are extruded	(Mattick 2002)
Pilotin				
PD1623	*pilF*	Type IV fimbrial biogenesis protein/stability protein	Pilotin protein required for the outer membrane localization and assembly of the multimeric PilQ secretin	(Koo et al. 2008)
Platform protein				
PD1923	*pilC*	Fimbrial assembly protein	Platform protein that mediates TFP assembly through the polymerization and depolymerization ATPases	(Takhar et al. 2013)

Alignment protein				
PD1695	*pilM*	Fimbrial assembly membrane protein	Alignment subcomplex that is involved in TFP assembly and stabilization by linking the outer membrane secretin pore subcomplex (PilF and PilQ) to the inner membrane motor subcomplex (PilB, PilC, PilD, PilT and PilU)	(Tammam et al. 2013)
PD1694	*pilN*	Fimbrial assembly membrane protein		
PD1693	*pilO*	Fimbrial assembly membrane protein		
PD1692	*pilP*	Fimbrial assembly protein		
Assembly ATPase				
PD1927	*pilB*	Pilus biogenesis protein	TFP polymerization (assembly) ATPase; promotes TFP extension	(Mattick 2002)
Retraction ATPase				
PD1147	*pilT*	Type IV fimbrial biogenesis protein	TFP depolymerization (disassembly) ATPases; promote TFP retraction	(Mattick 2002)
PD1148	*pilU*	Type IV fimbrial biogenesis protein		
Prepilin peptidase				
PD1922	*pilD*	Type IV prepilin leader peptidase	Prepilin peptidase that cleaves the leader peptide of all pilins (major and minor) at the cytoplasmic milieu of the inner membrane and methylates the mature pilin	(Giltner et al. 2010; Strom et al. 1993)
Two-component regulatory system				
PD1928	*pilR*	Two-component system, regulatory protein	Cytoplasmic response regulator that binds to the promoter of *pilA* (together with σ^{54}) to activate transcription of the major pilin	(Ishimoto and Lory 1992; Jin et al. 1994)
PD1929	*pilS*	Two-component system, sensor protein	Sensor kinase that interacts directly with PilA for pilin transcription autoregulation	(Kilmury and Burrows 2016)
Chemotaxis protein				
PD0845	*pilG*	Pilus protein	Chemosensory system composed by a transmembrane chemoreceptor (PilJ), a histidine kinase (PilL), a methylesterase (ChpB), response regulators (PilG and PilH) and coupling proteins (PilI and ChpC), which has been shown to affect twitching motility	(Cursino et al. 2011; Darzins 1994)
PD1632	*pilH*	Regulatory protein		
PD0846	*pilI*	Type IV fimbrial biogenesis protein		
PD0847	*pilJ*	Type IV fimbrial biogenesis protein		
PD0848	*pilL*	Chemotaxis-related protein kinase		
PD0849	*chpB*	Chemotaxis response regulator protein		
PD0850	*chpC*	Chemotaxis protein		

Signal transduction				
PD1497	*pilZ*	Type IV fimbriae assembly protein	Regulatory protein associated with TFP extension in a possible c-di-GMP (3′,5′-cyclic-di-guanylate) - dependent manner	(Alm et al. 1996a; Guzzo et al. 2009)

[a]Locus IDs and genome annotations are from the genome of *X. fastidiosa* subsp. *fastidiosa* reference strain Temecula1, GenBank Accession number AE009442.1. Genome annotation was visualized using Geneious (Biomatters Ltd.).
[b]Genes are organized by functional categories in the table.

Table S5-4. Genomic organization of *pil* and associated genes in *X. fastidiosa* TemeculaL.

Gene(s)[a]	Operon[b]	DNA strand
fimT1 (PD0019), *pilV1* (PD0020), *pilW1* (PD0021), *pilX1* (PD0022), *pilY1-1* (PD0023), *pilE1* (PD0024)	PD0019→PD0020→PD0021→PD0022→PD0023→PD0024	Leading
pilY1-3 (PD0502)	Not in operon	Leading
pilG (PD0845), *pilI* (PD0846), *pilJ* (PD0847), *cheA/pilL* (PD0848), *cheB/chpB* (PD0849), *cheW/chpC* (PD0850)	PD0845→PD0846→PD0847→PD0848→PD0849→PD0850	Leading
pilA3 PD1077	Not in operon	Lagging
pilT (PD1147)	Not in operon	Leading
pilU (PD1148)	Not in operon	Leading
pilZ (PD1497), **PD1498**, **PD1499**	PD1499→PD1498→PD1497	Lagging
pilE2 (PD1610), *pilY1-2* (PD1611)	PD1611→PD1610	Lagging
pilX2 (PD1612), *pilW2* (PD1613), *pilV2* (PD1614), *fimT2* (PD1615)	PD1615→PD1614→PD1613→PD1612	Lagging
pilF PD1623, **PD1622**	PD1623→PD1622	Lagging
pilH (PD1632), **PD1631**	PD1631→PD1632	Leading
pilQ (PD1691), *pilP* (PD1692), *pilO* (PD1693), *pilN* (PD1694), *pilM* (PD1695)	PD1695→PD1694→PD1693→PD1692→ PD1691	Lagging
fimT3 (PD1735)	Not in operon	Leading
PD1921, *pilD* (PD1922), *pilC* (PD1923)	PD1923→PD1922→PD1921	Lagging
pilA1 (PD1924)	Not in operon	Leading
pilA2 (PD1926)	Not in operon	Leading
pilB (PD1927)	Not in operon	Leading
pilR (PD1928)	Not in operon	Lagging
pilS (PD1929)	Not in operon	Lagging

[a]Genes in bold have no apparent effect on type IV pili and/or natural transformation. They are included in the list because they are located within the same operon of *pil* genes.
[b]Operon prediction was retrieved from elsewhere (Parker et al. 2016).

Table S5-5. Pearson's correlation results for the analyzed phenotypic traits of *X. fastidiosa*.

Phenotypic traits[a]	Recombination frequency	Twitching motility	Biofilm formation	Planktonic growth	Growth rate	Settling rate	Total viable CFU/ml[b]
Recombination frequency	-	**R^2 = 0.56 *P*<0.001**	R^2 = -0.23 *P* = 0.15	R^2 = -0.14 *P* = 0.38	R^2 = 0.02 *P* = 0.89	R^2 = -0.11 *P* = 0.47	R^2 = -0.27 *P* = 0.09
Twitching motility	**R^2 = 0.56 *P*<0.001**	-	**R^2 = -0.54 *P*<0.001**	R^2 = -0.14 *P* = 0.38	R^2 = 0.09 *P* = 0.58	R^2 = -0.14 *P* = 0.38	R^2 = -0.10 *P* = 0.51
Biofilm formation	R^2 = -0.23 *P* = 0.15	**R^2 = -0.54 *P*<0.001**	-	R^2 = -0.16 *P* = 0.30	**R^2 = -0.34 *P*<0.05**	**R^2 = 0.59 *P*<0.001**	R^2 = 0.01 *P* = 0.94
Planktonic growth	R^2 = -0.14 *P* = 0.38	R^2 = -0.14 *P* = 0.38	R^2 = -0.16 *P* = 0.30	-	**R^2 = 0.34 *P*<0.05**	**R^2 = -0.55 *P*<0.001**	R^2 = 0 *P* = 1.0
Growth rate	R^2 = 0.02 *P* = 0.89	R^2 = 0.09 *P* = 0.58	**R^2 = -0.34 *P*<0.05**	**R^2 = 0.34 *P*<0.05**	-	**R^2 = -0.51 *P*<0.001**	**R^2 = -0.49 *P*<0.005**
Settling rate	R^2 = -0.11 *P* = 0.47	R^2 = -0.14 *P* = 0.38	**R^2 = 0.59 *P*<0.001**	**R^2 = -0.55 *P*<0.001**	**R^2 = -0.51 *P*<0.001**	-	R^2 = 0.24 *P* = 0.12
Total viable CFU/ml[a]	R^2 = -0.27 *P* = 0.09	R^2 = -0.10 *P* = 0.51	R^2 = 0.01 *P* = 0.94	R^2 = 0 *P* = 1.0	**R^2 = -0.49 *P*<0.005**	R^2 = 0.24 *P* = 0.12	-

[a]Results are shown as correlation coefficients (R^2) and *p*-values (*P*). Results in bold show significant correlations (either positive or negative) among phenotypes.
[b]Total viable CFU/ml obtained in natural competence assays.

Table S5-6. DNA-binding probability of amino acid residues from FimT3.

Amino acid	Position	DNA-binding probability[a]
R (arginine)	160	0.8941
R (arginine)	162	0.8199
W (tryptophan)	81	0.8161
K (lysine)	177	0.784
N (asparagine)	180	0.7829
R (arginine)	93	0.7772
G (glycine)	159	0.7689
K (lysine)	94	0.7577
K (lysine)	179	0.7566
G (glycine)	84	0.7465
R (arginine)	123	0.7433
R (arginine)	54	0.7417
S (serine)	188	0.7412

[a]The DNA-binding probability of each amino acid residue from FimT3 of *X. fastidiosa* strain TemeculaL was calculated using the DRNApred webserver (Yan and Kurgan 2017) and ranges from 0 to 1.0. Only amino acid residues with a DNA-binding probability above 0.74 are shown in the table.

Table S5-7. Homologs of FimT3 are found in many members of the Xanthomonadaceae and few *Pseudomonas* spp.

Bacterial species	Total number of genomes per species[a]	Number of strains encoding FimT3	Identical amino acids (%)[b]
Xylella			
X. fastidiosa	121	121	95.60 – 100
Xanthomonas			
X. translucens	64	53	50.92 – 53.99
X. perforans	149	1	51.19
X. campestris	75	4	50.38
X. citri	193	5	47.37 – 50
X. sontii	3	3	48.77 – 49.38
X. sacchari	7	7	46.91 – 49.38
X. theicola	2	2	48.77
X. melonis	1	1	47.53
X. arboricola	139	1	46.91
X. albilineans	17	17	46.43
X. sp.	52	26	46.91 – 53.57
Pseudoxanthomonas			
P. mexicana	5	5	33.33 – 45.83
P. kalamensis	1	1	46.20
P. wuyuanensis	2	2	42.69 – 45.45
P. gei	1	1	44.31
P. spadix	4	2	41.61 – 43.2
P. dokdonensis	1	1	42.60
P. japonensis	2	2	37.42 – 38.04
P. sp.	43	14	40.57 – 45.24
Stenotrophomonas			
S. acidaminiphila	11	1	34.58
Pseudomonas[c]			
P. boreopolis	1	1	48.50
P. sp. Hp2	1	1	48.50

[a]A total of 2,699 genomes of bacterial species belonging to the Xanthomonadaceae family were downloaded from NCBI on July 3rd, 2021. In the table only the number of genomes from bacterial species that encode homologs of FimT3 are shown.

[b]Sequence alignments to FimT3 of *X. fastidiosa* strain TemeculaL were produced using Clustal Omega (Clustal 12.1). BLASTP searches were also carried out using the FimT3 sequence of *X. fastidiosa* strain TemeculaL.

[c]Only BLASTP searches were performed to identify presence of FimT3 within *Pseudomonas* spp.

Supplementary references

Adams, D. W., Stutzmann, S., Stoudmann, C., and Blokesch, M. 2019a. DNA-uptake pili of *Vibrio cholerae* are required for chitin colonization and capable of kin recognition via sequence-specific self-interaction. Nat Microbiol 4:1545-1557.

Adams, D. W., Pereira, J. M., Stoudmann, C., Stutzmann, S., and Blokesch, M. 2019b. The type IV pilus protein PilU functions as a PilT-dependent retraction ATPase. PLoS Genet 15:e1008393.

Alm, R. A., and Mattick, J. S. 1995. Identification of a gene, *pilV*, required for type 4 fimbrial biogenesis in *Pseudomonas aeruginosa*, whose product possesses a pre-pilin-like leader sequence. Mol Microbiol 16:485-496.

Alm, R. A., and Mattick, J. S. 1996. Identification of two genes with prepilin-like leader sequences involved in type 4 fimbrial biogenesis in *Pseudomonas aeruginosa*. J Bacteriol 178:3809-3817.

Alm, R. A., Bodero, A. J., Free, P. D., and Mattick, J. S. 1996a. Identification of a novel gene, *pilZ*, essential for type 4 fimbrial biogenesis in *Pseudomonas aeruginosa*. J Bacteriol 178:46-53.

Alm, R. A., Hallinan, J. P., Watson, A. A., and Mattick, J. S. 1996b. Fimbrial biogenesis genes of *Pseudomonas aeruginosa*: *pilW* and *pilX* increase the similarity of type 4 fimbriae to the GSP protein-secretion systems and *pilY1* encodes a gonococcal PilC homologuE. Mol Microbiol 22:161-173.

Almeida, R. P. P., Coletta-Filho, H. D., and Lopes, J. R. S. 2014. *Xylella fastidiosa*. Pages 841-850 in: Manual of Security Sensitive Microbes and Toxins. D. Liu, ed. CRC Press, Boca Raton, FL.

Bertrand, J. J., West, J. T., and Engel, J. N. 2010. Genetic analysis of the regulation of type IV pilus function by the Chp chemosensory system of *Pseudomonas aeruginosa*. J Bacteriol 192:994-1010.

Boyd, J. M., and Lory, S. 1996. Dual function of PilS during transcriptional activation of the *Pseudomonas aeruginosa* pilin subunit gene. J Bacteriol 178:831-839.

Boyd, J. M., Koga, T., and Lory, S. 1994. Identification and characterization of PilS, an essential regulator of pilin expression in *Pseudomonas aeruginosa*. Mol Gen Genet 243:565-574.

Burrows, L. L. 2012. *Pseudomonas aeruginosa* twitching motility: type IV pili in action. Annu Rev Microbiol 66:493-520.

Carbonnelle, E., Helaine, S., Nassif, X., and Pelicic, V. 2006. A systematic genetic analysis in *Neisseria meningitidis* defines the Pil proteins required for assembly, functionality, stabilization and export of type IV pili. Mol Microbiol 61:1510-1522.

Chatterjee, S., Newman, K. L., and Lindow, S. E. 2008a. Cell-to-Cell signaling in *Xylella fastidiosa* suppresses movement and xylem vessel colonization in grape. Mol Plant Microbe Interact 21:1309-1315.

Chatterjee, S., Almeida, R. P. P., and Lindow, S. 2008b. Living in two worlds: the plant and insect lifestyles of *Xylella fastidiosa*. Annu Rev Phytopathol 46:243-271.

Chiang, P., Sampaleanu, L. M., Ayers, M., Pahuta, M., Howell, P. L., and Burrows, L. L. 2008. Functional role of conserved residues in the characteristic secretion NTPase motifs of the *Pseudomonas aeruginosa* type IV pilus motor proteins PilB, PilT and PilU. Microbiology 154:114-126.

Chlebek, J. L., Hughes, H. Q., Ratkiewicz, A. S., Rayyan, R., Wang, J. C., Herrin, B. E., Dalia, T. N., Biais, N., and Dalia, A. B. 2019. PilT and PilU are homohexameric ATPases that coordinate to retract type IVa pili. PLoS Genet 15:e1008448.

Craig, L., Pique, M. E., and Tainer, J. A. 2004. Type IV pilus structure and bacterial pathogenicity. Nat Rev Microbiol 2:363-378.

Cruz, L. F., Cobine, P. A., and De La Fuente, L. 2012. Calcium increases *Xylella fastidiosa* surface attachment, biofilm formation, and twitching motility. Appl Environ Microbiol 78:1321-1331.

Cruz, L. F., Parker, J. K., Cobine, P. A., and De La Fuente, L. 2014. Calcium-enhanced twitching motility in *Xylella fastidiosa* is linked to a single PilY1 homolog. Appl Environ Microbiol 80:7176-7185.

Cursino, L., Galvani, C. D., Athinuwat, D., Zaini, P. A., Li, Y., De La Fuente, L., Hoch, H. C., Burr, T. J., and Mowery, P. 2011. Identification of an operon, Pil-Chp, that controls twitching motility and virulence in *Xylella fastidiosa*. Mol Plant Microbe Interact 24:1198-1206.

Cursino, L., Athinuwat, D., Patel, K. R., Galvani, C. D., Zaini, P. A., Li, Y., De La Fuente, L., Hoch, H. C., Burr, T. J., and Mowery, P. 2015. Characterization of the *Xylella fastidiosa* PD1671 gene encoding degenerate c-di-GMP GGDEF/EAL domains, and its role in the development of Pierce's disease. PLoS One 10:e0121851.

da Silva Neto, J. F., Koide, T., Abe, C. M., Gomes, S. L., and Marques, M. V. 2008. Role of σ54 in the regulation of genes involved in type I and type IV pili biogenesis in *Xylella fastidiosa*. Arch Microbiol 189:249-261.

Darzins, A. 1993. The *pilG* gene product, required for *Pseudomonas aeruginosa* pilus production and twitching motility, is homologous to the enteric, single-domain response regulator CheY. J Bacteriol 175:5934-5944.

Darzins, A. 1994. Characterization of a *Pseudomonas aeruginosa* gene cluster involved in pilus biosynthesis and twitching motility: sequence similarity to the chemotaxis proteins of enterics and the gliding bacterium *Myxococcus xanthus*. Mol Microbiol 11:137-153.

Darzins, A. 1995. The *Pseudomonas aeruginosa pilK* gene encodes a chemotactic methyltransferase (CheR) homologue that is translationally regulated. Mol Microbiol 15:703-717.

De La Fuente, L., Burr, T. J., and Hoch, H. C. 2007. Mutations in type I and type IV pilus biosynthetic genes affect twitching motility rates in Xylella fastidiosa. J Bacteriol 189:7507-7510.

de Souza, A. A., Ionescu, M., Baccari, C., da Silva, A. M., and Lindow, S. E. 2013. Phenotype overlap in *Xylella fastidiosa* is controlled by the cyclic di-GMP phosphodiesterase Eal in response to antibiotic exposure and diffusible signal factor-mediated cell-cell signaling. Appl Environ Microbiol 79:3444-3454.

Doyle, J., and Doyle, J. L. 1987. Genomic plant DNA preparation from fresh tissue—CTAB method. Phytochem. Bull. 19:11-15.

Francis, M., Civerolo, E. L., and Bruening, G. 2008. Improved bioassay of *Xylella fastidiosa* using *Nicotiana tabacum* cultivar SR1. Plant Dis 92:14-20.

Francis, M., Lin, H., Rosa, J. C.-L., Doddapaneni, H., and Civerolo, E. L. 2006. Genome-based PCR primers for specific and sensitive detection and quantification of *Xylella fastidiosa*. European Journal of Plant Pathology 115:203-213.

Fulcher, N. B., Holliday, P. M., Klem, E., Cann, M. J., and Wolfgang, M. C. 2010. The *Pseudomonas aeruginosa* Chp chemosensory system regulates intracellular cAMP levels by modulating adenylate cyclase activity. Mol Microbiol 76:889-904.

Giltner, C. L., Habash, M., and Burrows, L. L. 2010. *Pseudomonas aeruginosa* minor pilins are incorporated into type IV pili. J Mol Biol 398:444-461.

Giltner, C. L., Nguyen, Y., and Burrows, L. L. 2012. Type IV pilin proteins: versatile molecular modules. Microbiol Mol Biol Rev 76:740-772.

Giltner, C. L., Rana, N., Lunardo, M. N., Hussain, A. Q., and Burrows, L. L. 2011. Evolutionary and functional diversity of the *Pseudomonas* type IVa pilin island. Environ Microbiol 13:250-264.

Gluck-Thaler, E., Cerutti, A., Perez-Quintero, A. L., Butchacas, J., Roman-Reyna, V., Madhavan, V. N., Shantharaj, D., Merfa, M. V., Pesce, C., Jauneau, A., Vancheva, T., Lang, J. M., Allen, C., Verdier, V., Gagnevin, L., Szurek, B., Beckham, G. T., De La Fuente, L., Patel, H. K., Sonti, R. V., Bragard, C., Leach, J. E., Noël, L. D., Slot, J. C., Koebnik, R., and Jacobs, J. M. 2020. Repeated gain and loss of a single gene modulates the evolution of vascular plant pathogen lifestyles. Sci Adv 6:eabc4516.

Goosens, V. J., Busch, A., Georgiadou, M., Castagnini, M., Forest, K. T., Waksman, G., and Pelicic, V. 2017. Reconstitution of a minimal machinery capable of assembling periplasmic type IV pili. Proc Natl Acad Sci U S A 114:E4978-E4986.

Guzzo, C. R., Salinas, R. K., Andrade, M. O., and Farah, C. S. 2009. PILZ protein structure and interactions with PILB and the FIMX EAL domain: implications for control of type IV pilus biogenesis. J Mol Biol 393:848-866.

Harvey, H., Habash, M., Aidoo, F., and Burrows, L. L. 2009. Single-residue changes in the C-terminal disulfide-bonded loop of the *Pseudomonas aeruginosa* type IV pilin influence pilus assembly and twitching motility. J Bacteriol 191:6513-6524.

Hazelbauer, G. L., Falke, J. J., and Parkinson, J. S. 2008. Bacterial chemoreceptors: high-performance signaling in networked arrays. Trends Biochem Sci 33:9-19.

Ionescu, M., Baccari, C., Da Silva, A. M., Garcia, A., Yokota, K., and Lindow, S. E. 2013. Diffusible signal factor (DSF) synthase RpfF of *Xylella fastidiosa* is a multifunction protein also required for response to DSF. J Bacteriol 195:5273-5284.

Ishimoto, K. Y., and Lory, S. 1992. Identification of pilR, which encodes a transcriptional activator of the *Pseudomonas aeruginosa* pilin gene. J Bacteriol 174:3514-3521.

Jha, G., Rajeshwari, R., and Sonti, R. V. 2005. Bacterial type two secretion system secreted proteins: double-edged swords for plant pathogens. Mol Plant Microbe Interact 18:891-898.

Jin, S., Ishimoto, K. Y., and Lory, S. 1994. PilR, a transcriptional regulator of piliation in *Pseudomonas aeruginosa*, binds to a *cis*-acting sequence upstream of the pilin gene promoter. Mol Microbiol 14:1049-1057.

Jouravleva, E. A., McDonald, G. A., Marsh, J. W., Taylor, R. K., Boesman-Finkelstein, M., and Finkelstein, R. A. 1998. The *Vibrio cholerae* mannose-sensitive hemagglutinin is the receptor for a filamentous bacteriophage from *V. cholerae* O139. Infect Immun 66:2535-2539.

Kandel, P. P., Chen, H., and De La Fuente, L. 2018. A short protocol for gene knockout and complementation in *Xylella fastidiosa* shows that one of the type IV pilin paralogs (PD1926) is needed for twitching while another (PD1924) affects pilus number and location. Appl Environ Microbiol 84:e01167-01118.

Kandel, P. P., Lopez, S. M., Almeida, R. P. P., and De La Fuente, L. 2016. Natural competence of *Xylella fastidiosa* occurs at a high frequency inside microfluidic chambers mimicking the bacterium's natural habitats. Appl Environ Microbiol 82:5269-5277.

Kandel, P. P., Almeida, R. P. P., Cobine, P. A., and De La Fuente, L. 2017. Natural competence rates are variable among *Xylella fastidiosa* strains and homologous recombination occurs in vitro between subspecies *fastidiosa* and *multiplex*. Mol Plant Microbe Interact 30:589-600.

Kang, Y., Liu, H., Genin, S., Schell, M. A., and Denny, T. P. 2002. *Ralstonia solanacearum* requires type 4 pili to adhere to multiple surfaces and for natural transformation and virulence. Mol Microbiol 2:427-437.

Kilmury, S. L., and Burrows, L. L. 2016. Type IV pilins regulate their own expression via direct intramembrane interactions with the sensor kinase PilS. Proc Natl Acad Sci U S A 113:6017-6022.

Kilmury, S. L. N., and Burrows, L. L. 2018. The *Pseudomonas aeruginosa* PilSR two-component system regulates both twitching and swimming motilities. mBio 9:e01310-01318.

Kim, E. S., Bae, H. W., and Cho, Y. H. 2018. A pilin region affecting host range of the *Pseudomonas aeruginosa* RNA phage, PP7. Front Microbiol 9:247.

Koo, J., Tammam, S., Ku, S. Y., Sampaleanu, L. M., Burrows, L. L., and Howell, P. L. 2008. PilF is an outer membrane lipoprotein required for multimerization and localization of the *Pseudomonas aeruginosa* Type IV pilus secretin. J Bacteriol 190:6961-6969.

Krogh, A., Larsson, B., von Heijne, G., and Sonnhammer, E. L. 2001. Predicting transmembrane protein topology with a hidden Markov model: application to complete genomes. J Mol Biol 305:567-580.

Kung, S. H., and Almeida, R. P. P. 2014. Biological and genetic factors regulating natural competence in a bacterial plant pathogen. Microbiology 160:37-46.

Leong, C. G., Bloomfield, R. A., Boyd, C. A., Dornbusch, A. J., Lieber, L., Liu, F., Owen, A., Slay, E., Lang, K. M., and Lostroh, C. P. 2017. The role of core and accessory type IV pilus genes in natural transformation and twitching motility in the bacterium *Acinetobacter baylyi*. PLoS One 12:e0182139.

Li, Y., Hao, G., Galvani, C. D., Meng, Y., De La Fuente, L., Hoch, H. C., and Burr, T. J. 2007. Type I and type IV pili of *Xylella fastidiosa* affect twitching motility, biofilm formation and cell-cell aggregation. Microbiology 153:719-726.

Liu, H., Kang, Y., Genin, S., Schell, M. A., and Denny, T. P. 2001. Twitching motility of *Ralstonia solanacearum* requires a type IV pilus system. Microbiology 147:3215-3229.

Matsumoto, A., and Igo, M. M. 2010. Species-specific type II restriction-modification system of *Xylella fastidiosa* Temecula1. Appl Environ Microbiol 76:4092-4095.

Matsumoto, A., Young, G. M., and Igo, M. M. 2009. Chromosome-based genetic complementation system for *Xylella fastidiosa*. Appl Environ Microbiol 75:1679-1687.

Mattick, J. S. 2002. Type IV pili and twitching motility. Annu Rev Microbiol 56:289-314.

Meng, Y., Li, Y., Galvani, C. D., Hao, G., Turner, J. N., Burr, T. J., and Hoch, H. C. 2005. Upstream migration of *Xylella fastidiosa* via pilus-driven twitching motility. J Bacteriol 187:5560-5567.

Newman, K. L., Almeida, R. P. P., Purcell, A. H., and Lindow, S. E. 2004. Cell-cell signaling controls *Xylella fastidiosa* interactions with both insects and plants. Proc Natl Acad Sci U S A 101:1737-1742.

Nguyen, Y., Sugiman-Marangos, S., Harvey, H., Bell, S. D., Charlton, C. L., Junop, M. S., and Burrows, L. L. 2015. *Pseudomonas aeruginosa* minor pilins prime type IVa pilus assembly and promote surface display of the PilY1 adhesin. J Biol Chem 290:601-611.

Nolan, L. M., Turnbull, L., Katrib, M., Osvath, S. R., Losa, D., Lazenby, J. J., and Whitchurch, C. B. 2020. *Pseudomonas aeruginosa* is capable of natural transformation in biofilms. Microbiology 166:995-1003.

Nunn, D. 1999. Bacterial Type II protein export and pilus biogenesis: more than just homologies? Trends Cell Biol 9:402-408.

Orans, J., Johnson, M. D., Coggan, K. A., Sperlazza, J. R., Heiniger, R. W., Wolfgang, M. C., and Redinbo, M. R. 2010. Crystal structure analysis reveals *Pseudomonas* PilY1 as an essential calcium-dependent regulator of bacterial surface motility. Proc Natl Acad Sci U S A 107:1065-1070.

Parker, D., Kennan, R. M., Myers, G. S., Paulsen, I. T., Songer, J. G., and Rood, J. I. 2006. Regulation of type IV fimbrial biogenesis in *Dichelobacter nodosus*. J Bacteriol 188:4801-4811.

Parker, J. K., Chen, H., McCarty, S. E., Liu, L. Y., and De La Fuente, L. 2016. Calcium transcriptionally regulates the biofilm machinery of *Xylella fastidiosa* to promote continued biofilm development in batch cultures. Environ Microbiol 18:1620-1634.

Parker, J. K., Wisotsky, S. R., Johnson, E. G., Hijaz, F. M., Killiny, N., Hilf, M. E., and De La Fuente, L. 2014. Viability of '*Candidatus* Liberibacter asiaticus' prolonged by addition of citrus juice to culture medium. Phytopathology 104:15-26.

Potnis, N., Kandel, P. P., Merfa, M. V., Retchless, A. C., Parker, J. K., Stenger, D. C., Almeida, R. P. P., Bergsma-Vlami, M., Westenberg, M., Cobine, P. A., and De La Fuente, L. 2019. Patterns of inter- and intrasubspecific homologous recombination inform eco-evolutionary dynamics of *Xylella fastidiosa*. ISME J 13:2319-2333.

Pratt, J. T., Tamayo, R., Tischler, A. D., and Camilli, A. 2007. PilZ domain proteins bind cyclic diguanylate and regulate diverse processes in *Vibrio cholerae*. J Biol Chem 282:12860-12870.

Rudel, T., Facius, D., Barten, R., Scheuerpflug, I., Nonnenmacher, E., and Meyer, T. F. 1995. Role of pili and the phase-variable PilC protein in natural competence for transformation of *Neisseria gonorrhoeae*. Proc Natl Acad Sci U S A 92:7986-7990.

Russell, M. A., and Darzins, A. 1994. The *pilE* gene product of *Pseudomonas aeruginosa*, required for pilus biogenesis, shares amino acid sequence identity with the *N*-termini of type 4 prepilin proteins. Mol Microbiol 13:973-985.

Ryjenkov, D. A., Simm, R., Römling, U., and Gomelsky, M. 2006. The PilZ domain is a receptor for the second messenger c-di-GMP: the PilZ domain protein YcgR controls motility in enterobacteria. J Biol Chem 281:30310-30314.

Schneider, C. A., Rasband, W. S., and Eliceiri, K. W. 2012. NIH Image to ImageJ: 25 years of image analysis. Nat Methods 9:671-675.

Seitz, P., and Blokesch, M. 2013. DNA-uptake machinery of naturally competent *Vibrio cholerae*. Proc Natl Acad Sci U S A 110:17987-17992.

Sheffield, P., Garrard, S., and Derewenda, Z. 1999. Overcoming expression and purification problems of RhoGDI using a family of "Parallel" expression vectors. Protein Expr. Purif. 15:34-39.

Shi, X., and Lin, H. 2016. Visualization of twitching motility and characterization of the role of the *PilG* in *Xylella fastidiosa*. J Vis Exp:e53816.

Shi, X., and Lin, H. 2018. The chemotaxis regulator *pilG* of *Xylella fastidiosa* is required for virulence in *Vitis vinifera* grapevines. Eur J Plant Pathol 150:351-362.
Simko, I., and Piepho, H.-P. 2012. The area under the disease progress stairs: Calculation, advantage, and application. Phytopathology 102:381-389.
Strom, M. S., Nunn, D. N., and Lory, S. 1993. A single bifunctional enzyme, PilD, catalyzes cleavage and N-methylation of proteins belonging to the type IV pilin family. Proc Natl Acad Sci U S A 90:2404-2408.
Takhar, H. K., Kemp, K., Kim, M., Howell, P. L., and Burrows, L. L. 2013. The platform protein is essential for type IV pilus biogenesis. J Biol Chem 288:9721-9728.
Talà, L., Fineberg, A., Kukura, P., and Persat, A. 2019. *Pseudomonas aeruginosa* orchestrates twitching motility by sequential control of type IV pili movements. Nat Microbiol 4:774-780.
Tammam, S., Sampaleanu, L. M., Koo, J., Manoharan, K., Daubaras, M., Burrows, L. L., and Howell, P. L. 2013. PilMNOPQ from the *Pseudomonas aeruginosa* type IV pilus system form a transenvelope protein interaction network that interacts with PilA. J Bacteriol 195:2126-2135.
Taylor, R. K., Miller, V. L., Furlong, D. B., and Mekalanos, J. J. 1987. Use of *phoA* gene fusions to identify a pilus colonization factor coordinately regulated with cholera toxin. Proc Natl Acad Sci U S A 84:2833-2837.
Vesel, N., and Blokesch, M. 2021. Pilus production in *Acinetobacter baumannii* is growth phase dependent and essential for natural transformation. J Bacteriol 203:e00034- 00021.
Vieira, J., and Messing, J. 1982. The pUC plasmids, an M13mp7-derived system for insertion mutagenesis and sequencing with synthetic universal primers. Gene 19:259-268.
Watson, A. A., Alm, R. A., and Mattick, J. S. 1996. Identification of a gene, *pilF*, required for type 4 fimbrial biogenesis and twitching motility in *Pseudomonas aeruginosa*. Gene 180:49-56.
West, A. H., and Stock, A. M. 2001. Histidine kinases and response regulator proteins in two-component signaling systems. Trends Biochem Sci 26:369-376.
Whitchurch, C. B., Leech, A. J., Young, M. D., Kennedy, D., Sargent, J. L., Bertrand, J. J., Semmler, A. B., Mellick, A. S., Martin, P. R., Alm, R. A., Hobbs, M., Beatson, S. A., Huang, B., Nguyen, L., Commolli, J. C., Engel, J. N., Darzins, A., and Mattick, J. S. 2004. Characterization of a complex chemosensory signal transduction system which controls twitching motility in *Pseudomonas aeruginosa*. Mol Microbiol 52:873-893.
Yan, J., and Kurgan, L. 2017. DRNApred, fast sequence-based method that accurately predicts and discriminates DNA- and RNA-binding residues. Nucleic Acids Res 45:e84.
Yang, F., Tian, F., Li, X., Fan, S., Chen, H., Wu, M., Yang, C. H., and He, C. 2014. The degenerate EAL-GGDEF domain protein Filp functions as a cyclic di-GMP receptor and specifically interacts with the PilZ-domain protein PXO_02715 to regulate virulence in *Xanthomonas oryzae* pv. *oryzae*. Mol Plant Microbe Interact 27:578-589.
Yu, C., Nguyen, D. P., Ren, Z., Liu, J., Yang, F., Tian, F., Fan, S., and Chen, H. 2020. The RpoN2-PilRX regulatory system governs type IV pilus gene transcription and is required for bacterial motility and virulence in *Xanthomonas oryzae* pv. *oryzae*. Mol Plant Pathol 21:652-666.

Chapter 6

Patterns of inter- and intra-subspecific homologous recombination inform eco-evolutionary dynamics of *Xylella fastidiosa*

Note – This study was previously published with the following citation:

Potnis, N.*, Kandel, P. P.*, **MERFA, M. V.***, Retchless, A. C., Parker, J. K., Stenger, D. C., Almeida, R. P. P., Bergsma-Vlami, M., Westenberg, M., Cobine, P. A., and De La Fuente, L. 2019. Patterns of inter- and intrasubspecific homologous recombination inform eco-evolutionary dynamics of *Xylella fastidiosa*. ISME J 13:2319-2333. ***Co-first authorship.**

This work performed as a three-way collaboration. My part of the collaboration was to identify and count the recent recombined genes in *X. fastidiosa* strains belonging to different subspecies. These results are shown in **Table 6-1**, **S6-6** and **S6-7**, as well as in **Fig. 6-7**, and are mainly described in subsection 'Recombinant regions shared among subspecies inform eco-evolutionary dynamics of *X. fastidiosa*-host interactions' of the 'Results' section. The entire study is included in this chapter to maintain its cohesion and understanding.

Abstract

High rates of homologous recombination (HR) in the bacterial plant pathogen *Xylella fastidiosa* have been previously detected. This study aimed to determine the extent and explore the ecological significance of HR in the genomes of recombinants experimentally-generated by natural transformation and wild-type isolates. Both set of strains displayed widespread HR and similar average size of recombined fragments consisting of random events (2-10kb) of inter- and intra-subspecific recombination. Significantly higher proportion and greater lengths (>10 kb,

maximum 31.5 kb) of recombined fragments were observed in subsp. *morus* and in strains isolated in Europe from intercepted coffee plants shipped from the Americas. Such highly recombinant strains pose a serious risk of emergence of novel variants as genetically-distinct and formerly geographically-isolated genotypes are brought in close proximity by global trade. Recently-recombined regions in wild-type strains included genes involved in regulation and signaling, host colonization, nutrient acquisition and host evasion, all fundamental traits for *X. fastidiosa* ecology. Identification of four recombinant loci shared between wild-type and experimentally-generated recombinants suggest potential hotspots of recombination in this naturally-competent pathogen. These findings provide insights into evolutionary forces possibly affecting the adaptive potential to colonize the host environments of *X. fastidiosa*.

Introduction

Horizontal gene transfer, a fundamental mechanism of evolution in bacteria, occurs by conjugation, transduction, and transformation (Thomas and Nielsen 2005). These processes lead to homologous recombination (HR) that mediates exchange of genetic material among related taxa, including acquisition of novel genetic elements such as antibiotic resistance and virulence factors that can result in emergence of new pathotypes (Hacker and Carniel 2001). In bacteria, HR is proposed to play a key role in repairing damaged DNA (Michod et al. 2008) to promote survival under stressful conditions. But HR may also give rise to new variants if the homologous DNA originates from a closely related but genetically-distinct donor (Guttman 1997). New genetic variants can result in profound phenotypic changes; such as evasion of host defenses by creating variation in surface structures (Feil and Spratt 2001; Nelson and Selander 1994), facilitate disease emergence (Yan et al. 2008), or enhance adaptation to new environments

(Baltrus et al. 2008). The relative role of HR and point mutations in generating genetic variation differs among bacterial species (Feil et al. 2001), with HR expected to play a major role in naturally-transformable bacteria.

The first observation of HR was achieved by detection of mosaic genes that contained fragments originating from different taxa of the same genus (Spratt et al. 1992). Use of multilocus sequence typing/analysis (MLST/MLSA), a technique to assess genetic diversity within a species by sequence analysis of 5-11 housekeeping genes scattered across the genome (Maiden 2006), has revealed HR in bacterial genomes. Until recently, MLST was a signature tool for bacterial phylogenetic studies and detection of HR (Freel et al. 2013; Kong et al. 2013; Nunney et al. 2014a; Timilsina et al. 2015). However, examination of only few genes with presumed neutral variation will overlook HR present in other genomic regions, including genes involved in host adaptation and/or virulence (Parker et al. 2012). Whole genome sequence (WGS) comparisons provide a superior approach for detecting HR in bacterial genomes (Croucher et al. 2015; Marttinen et al. 2012; Yahara et al. 2014).

Xylella fastidiosa is a plant pathogenic bacterium that causes massive economic losses and was believed to be limited to the Americas, but recently has emerged as an important pathogen in other regions of the world (Almeida and Nunney 2015), including Europe (Saponari et al. 2013; Strona et al. 2017) and Asia (Su et al. 2016). *X. fastidiosa* exclusively colonizes two habitats: the plant xylem vessels and foregut of insect vectors (sharpshooter leafhoppers and spittlebugs) (Hopkins and Purcell 2002). Taxonomically, strains within *X. fastidiosa* are generally categorized into three subspecies (i.e., *fastidiosa, multiplex,* and *pauca*) (Marcelletti

and Scortichini 2016; Schaad et al. 2004b; Schaad et al. 2004a), although additional subspecies have been suggested (i.e., *morus, sandyi*) (Nunney et al. 2014c; Scally et al. 2005). While the species has a very broad plant host range (EFSA 2018), this differs amongst subspecies. However, mechanisms of host specificity are still unknown (Nunney et al. 2012).

Extensive HR has been identified in *X. fastidiosa* based on genetic diversity and phylogenetic patterns revealed by MLST (Almeida et al. 2008; Coletta-Filho et al. 2017; Nunney et al. 2010; Nunney et al. 2012; Scally et al. 2005). These studies made notable speculations on the impacts of HR on host range expansion in *X. fastidiosa* strains, including those strains that infect citrus, mulberry, and blueberry (Nunney et al. 2014a; Nunney et al. 2014c; Nunney et al. 2010). However, these inferences were made based on the evidence of HR in housekeeping genes, rather than taking advantage of whole genomes.

Experimental studies have demonstrated natural competence and HR in *X. fastidiosa* both in vitro (Kung and Almeida 2011) and in artificial habitats mimicking the natural growth environment of the bacterium (Kandel et al. 2016). Moreover, intersubspecific HR (IHR) between *X. fastidiosa* subsp. *fastidiosa* and *multiplex* was recently demonstrated experimentally (Kandel et al. 2017). The objective of this study was to use WGS analysis to identify the extent of intra- and intersubspecific HR in *X. fastidiosa*. We did this by first focusing on *X. fastidiosa* recombinant strains experimentally generated in vitro (Kandel et al. 2017), and later by studying multiple strains isolated from field infections around the world. Extensive inter- and intrasubspecific recombination of both ancient and recent origins was detected in the genomes of *X. fastidiosa*, indicating patterns of gene flow and associated phenotypes among different

subspecies. The increased global movement of strains through trade of plant materials can lead to introduction of novel genotypes into endemic pathogen population. HR can play a significant role in such cases, where novel genotypes might exchange adaptive alleles with existing population, resulting in niche-adapted recombinant strains with greater fitness than existing population.

Materials and methods

Bacterial strains, media, and culture conditions

Strains and mutants used in this study are listed in **Table S6-1**. For explanation on recombinant mutants generated in vitro see Supplementary Methods and **Fig. 6-1**. A Temecula1 variant strain, that differed based on whole genome sequence analysis in this study, was named here as TemeculaL (Kandel et al. 2018). Temecula1* was also a variant of the Temecula1 strain that showed reduced virulence in our previous study (Oliver et al. 2014). Strains PD7202 and PD7211 were isolated from coffee plants shipped from Costa Rica and intercepted in the Netherlands (Bergsma-Vlami et al. 2017). Strains were cultured in PW (Davis et al. 1981) modified agar without phenol red and with 1.8 g litre^{-1} Bovine Serum Albumin (BSA) (Gibco Life Sciences Technology) for a week at 28°C from -80°C stock, re-streaked, and cultured for another week before use. Kanamycin (Km) and Chloramphenicol (Cm) were used at 30 and 10 μg ml^{-1}, respectively.

DNA extraction, library preparation, sequencing and assembly

In this study 17 novel *X. fastidiosa* genome sequences (including 9 WT, five in vitro recombinant strains, and three parental strains) were generated (**Table S6-1**). Genomic DNA

extraction, library preparation and MiSeq/Pacific Biosciences (PacBio) sequencing protocol, quality filtering, trimming, assembly and annotation details are presented in Supplementary Methods. Briefly, paired-end MiSeq FASTQ files were quality assessed with FastQC (Babraham Bioinformatics) and trimmed with Trimmomatic-0.35 (Bolger et al. 2014). Trimmed reads (>36 bp) were *de novo* assembled using SPAdes 3.9.0 (Bankevich et al. 2012). For WM1-1 and AlmaEM3, sequenced by both MiSeq and PacBio, a hybrid assembly of SPAdes 3.9.0 was used. Information for read and assembly statistics, breadth and depth of coverage, and annotation results are summarized in **Tables S6-2** and **S6-3**.

Core genome prediction

Complete or draft genomes of 55 strains of *X. fastidiosa* sequenced here or obtained from NCBI (**Table S6-1**) were aligned using progressiveMauve (Darling et al. 2010) using default settings. Core genome alignment was obtained by removing the accessory regions from the alignment using stripSubsetLCBs script on the aligned Locally Collinear Blocks (LCBs) (Darling et al. 2010), https://github.com/xavierdidelot/ClonalOrigin/wiki/Usage, after discarding core LCBs shorter than 500 nt. Same steps were followed to obtain the core genome of 57 *X. fastidiosa* strains when two additional intercepted strains PD7202 and PD7211 (Bergsma-Vlami et al. 2017) were added to our database. Implementing the Mauve approach instead of using alignment of concatenated core genes allowed us to include intergenic regions and contiguous order in recombination analysis. For the model implemented in BratNextGen, contiguously ordered core genome alignment is preferred, which was obtained by concatenation of core LCBs.

Population structure and inference of recombination

Population structure was defined with BAPS 6.0 (hierBAPS module for hierarchical BAPS) using the default settings (Cheng et al. 2013). The core genome (i.e. LCBs) obtained from Mauve alignment of 55 *X. fastidiosa* genomes was used as input in BAPS 6.0 to obtain the population structure. A total of 33824 backbone entries were concatenated to obtain core genome alignment of the 55 genomes. In addition, the core genome from Mauve alignment of 13 genomes of in vitro recombinants and their parents was used as input for analyzing population structure for in vitro recombinants. These core genome alignments were used to infer maximum likelihood (ML) phylogeny estimated with RAxML v 8.2.11 under the generalized time-reversible model (GTRGAMMA) with 1000 bootstrap replicates (Stamatakis 2014). Mid-point rooted ML trees were visualized and annotated using FigTree (v.1.4.2, http://tree.bio.ed.ac.uk/software/figtree/).

For genealogy reconstruction, recombination was identified from the core genome alignments using BratNextGen algorithm. The cut-off level for obtaining clusters from the proportion of shared ancestry tree (PSA tree) was guided by the number of clusters determined by hierBAPS. Recombination was estimated with 20 iterations of the HMM estimation algorithm and 100 permutations with a 5% significance threshold (Marttinen et al. 2012). To analyze the origin of recombination, we used the fastGEAR algorithm, which employs hierBAPS to identify lineages as clusters of genomes that share a monophyletic signal in at least 50% of the sites. Recombination events between *X. fastidiosa* lineages that affected a subset of recipient lineages are considered “recent” with the origin of the recombinant sequence assigned to the lineage with the highest probability at that position. Regions affected by recent recombination were removed

prior to detection of "ancestral" recombination events that are shared by all strains which comprise a lineage. The origin of these ancestral recombination events cannot be inferred due to their conserved nature (Mostowy et al. 2017). In identifying both recent and ancestral recombination events, Bayes factor >1 or >10, respectively, was used for testing the statistical significance. We conducted this fastGEAR analysis on the core genome alignments for both sets of 55 and 57 *X. fastidiosa* strains (including newly intercepted strains PD7202 and PD7211). Next, to obtain recombination-filtered core-genome alignment, positions in the core genome alignment that corresponded to the predicted recent recombination events by fastGEAR were masked using the Perl script, bng-mask_recombination.pl (https://github.com/tseemann/bng-tools/blob/master/bng-mask_recombination.pl). Gaps were then removed from the alignment using trimal (v1.2) with the '-nogaps' option (Capella-Gutierrez et al. 2009). This recombination-filtered core genome alignment was then used to construct a ML phylogeny as described above. Further analysis of recently-recombined regions was carried out to understand ecological significance of intersubspecies recombination. Detailed methodology of extracting co-ordinates for recently recombined genes as well as annotations is described in **Fig. S6-1**.

Accession numbers

The genomes and the raw reads generated in this study have been deposited in NCBI GenBank under BioProject PRJNA433735 with BioSample numbers SAMN08537137-SAMN08537151, SAMN10499944, and SAMN10499946. GenBank accession numbers are included in **Table S6-1**.

Results and discussion

Recombination by natural competence in vitro leads to multiple events of DNA exchange across the genome

Previously, we performed in vitro natural transformation experiments of *X. fastidiosa* by co-culturing combinations of either live or heat-killed donor and live recipient strains, generating recombinant strains that were selected based solely on the acquisition of antibiotic-resistance markers (Kandel et al. 2017; Kandel et al. 2016) (**Fig. 6-1**). Complete genomes were analyzed to determine the overall distribution of recombination events that occurred, including the length of DNA flanking the selection marker. Initially, the presence of recombinogenic regions were identified by reference mapping of the reads and alignment of contigs to the parental strain genome (**Fig. S6-2**).

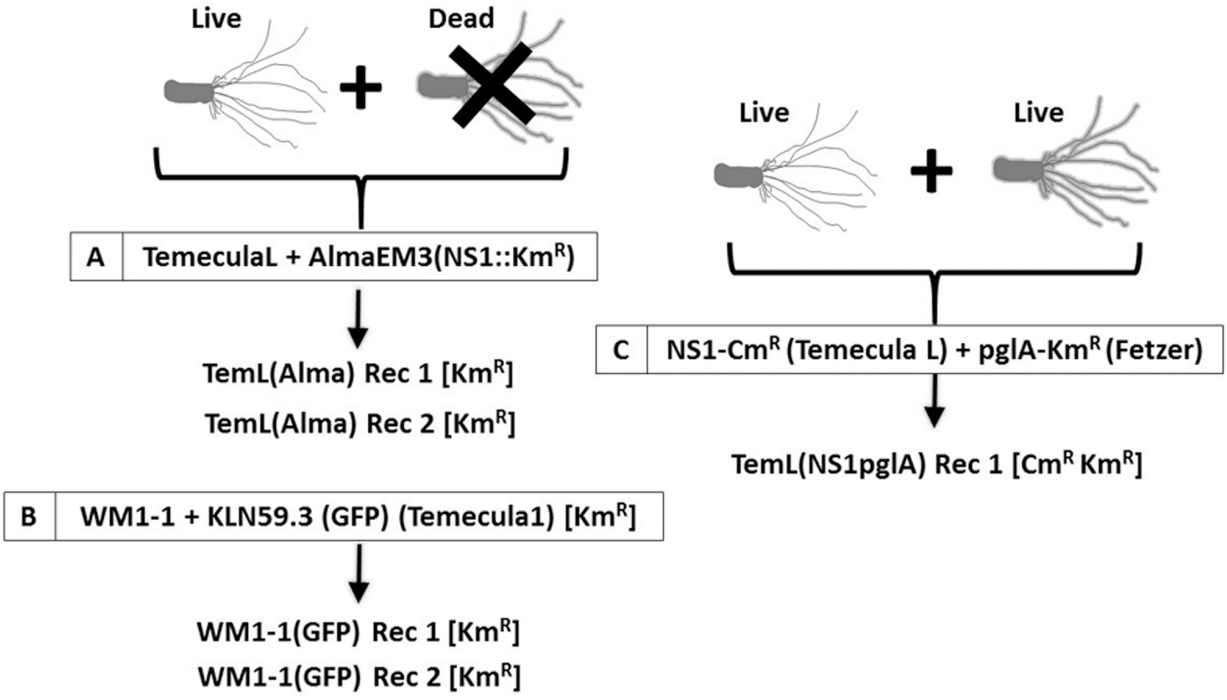

Fig. 6-1. **Diagram summarizing the lineage of the recombinant strains used in this study.** Parental strains are highlighted in boxes. Recombinant strains were obtained by mixing either one live strain with DNA from another dead strain (**A**, **B**), or by co-culturing two live strains (**C**).

Denomination between parenthesis after the strain names correspond to antibiotic-resistance markers used for selection: Km, kanamycin; Cm, chloramphenicol. Whenever available, selection was also done by GFP production in addition to antibiotic resistance. Parental strains include *Xylella fastidiosa* subsp. *fastidiosa* wild-type TemeculaL, WM1-1, and mutants KLN59.3 (GFP) [a Km^R and GFP-marked mutant of Temecula1, (Newman et al. 2003)], NS1-Cm^R [a Cm^R cassette inserted in the non-coding region NS1 of TemeculaL (Matsumoto et al. 2009)], and pglA-Km^R [a Cm^R *pglA* mutant of strain Fetzer, (Roper et al. 2007)]. *X. fastidiosa* subsp. *multiplex* AlmaEm3 (marked with a Km^R cassette in the NS1 site) was the only strain classified in a different subspecies. The genome of all parental and recombinant strains shown here were sequenced for this study. For more details see Supplementary methods.

To further analyze recombinant regions beyond those flanking selection markers, we classified strains used in vitro by hierBAPS that identified five clusters among parental and recombinant strains (**Fig. 6-2A**). One interesting observation of this analysis was that strains referred to as "Temecula1" in previous reports are actually different strains that were classified in two different clusters: cluster 5 [TemeculaL, NS1-Cm^R(TemeculaL)]; and cluster 4 [Temecula1, Temecula1*, KLN59.3(GFP)(Temecula1)]. The NCBI-deposited Temecula1 genome (**Table S6-1**) differs from the genome of other strains that have been referred to in the literature by the same name. For instance, clustering showed that NS1-Cm^R (TemeculaL) has TemeculaL as background and not Temecula1 as previously thought (Kung and Almeida 2011). Recombinant regions shared among Temecula1 and Temecula1* represented different alleles compared to TemeculaL, further highlighting the differences among strains referred to with the same name.

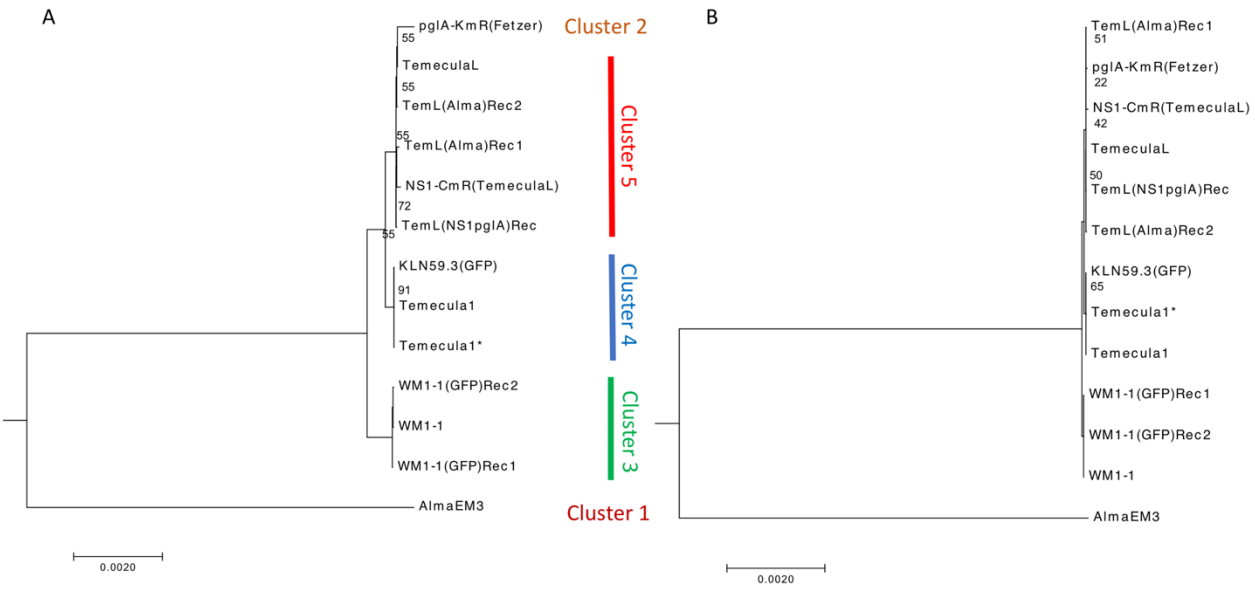

Fig. 6-2. **Maximum likelihood phylogeny of the core genome alignment of 13 strains of *X. fastidiosa* in vitro recombinants and their donor and recipient parental strains before (A) and after (B) recombination filtering.** Population structure was inferred using nested clustering implemented in hierBAPS. For **B**, recombinant regions detected by BratNextGen in the genomes were excluded to build a recombination-free phylogenetic tree. Overall topology remained similar but the phylogenetic distance decreased among the genomes after recombination filtering. The phylogenetic tree was mid-point rooted, representing increasing order of nodes. Bootstrap support was >98% for all nodes except where otherwise indicated.

To further investigate variable regions, we used more robust detection tools that detect recombination events at the intrasubspecific level (within subspecies *fastidiosa*; BratNextGen) and at the intersubspecific level (between subspecies *fastidiosa* and *multiplex*; fastGEAR). BratNextGen and fastGEAR identified recombination events in the core genome of *X. fastidiosa* subsp. *fastidiosa* WT and in vitro recombinant strains, with prediction of 72 recombination events (**Fig. 6-3**). Influence of recombination on phylogenetic relationships among in vitro recombinants and their parents was evident based on recombination-free tree topology that showed increased cohesiveness among clusters within *X. fastidiosa* subsp. *fastidiosa* and reduced branch length among subspecies *fastidiosa* and *multiplex* strains (**Fig. 6-2B**).

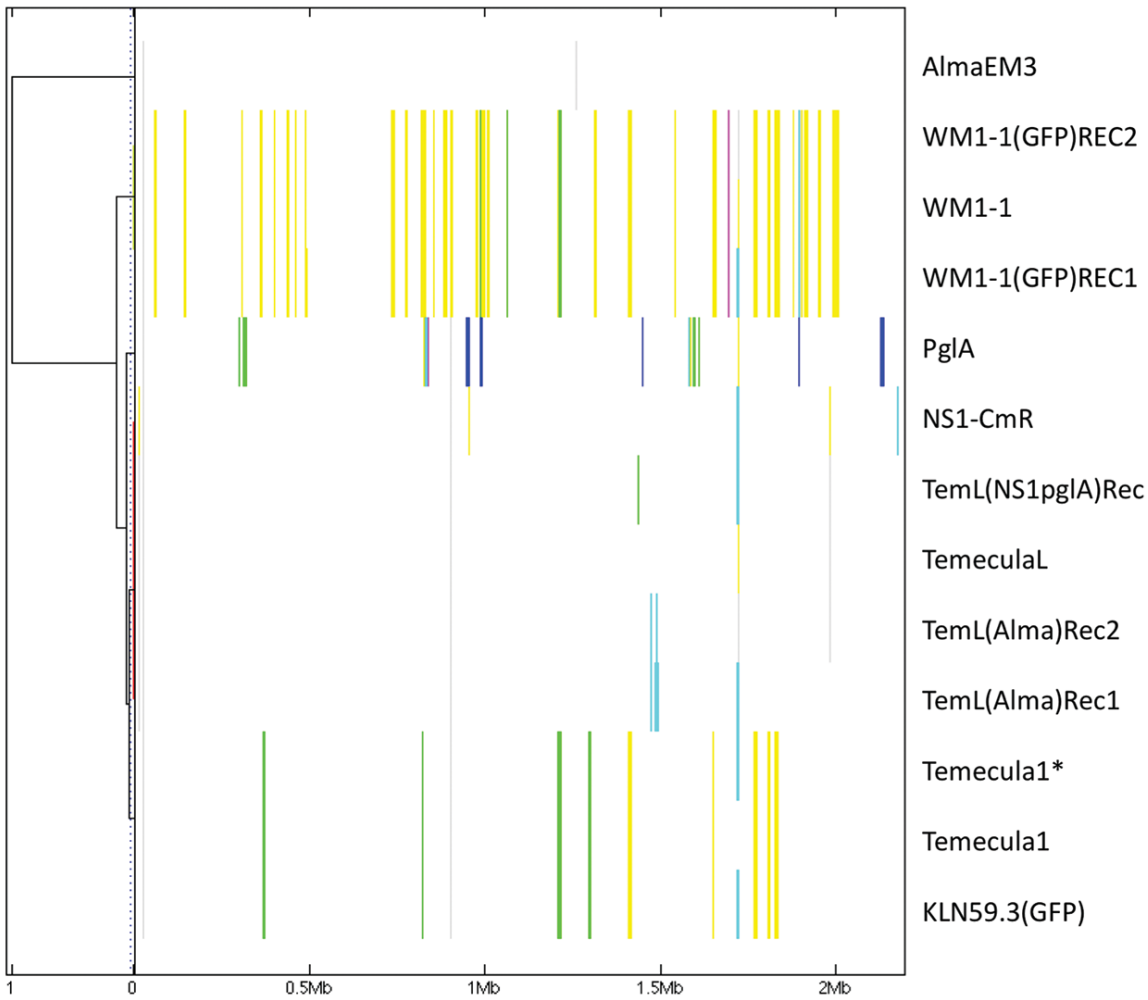

Fig. 6-3. **Detection of recombinogenic regions in the core genomes of *X. fastidiosa* in vitro recombinants and their parental strains using BratNextGen.** Core genome alignment obtained with progressiveMauve was used for genealogy reconstruction, and recombination was identified using BratNextGen algorithm. The estimation of recombination was performed with 20 iterations of the HMM estimation algorithm and 100 permutations with 5% significance threshold. The left panel corresponds to the Proportion of Shared Ancestry (PSA) tree computed by BratNextGen. In PSA tree, strains are clustered according to the proportion of sequence shared including recombinant regions. In the right panel, recombinant segments identified by BratNextGen for each strain are shown. The colors are arbitrarily assigned. The fragments of the same color present in the same column share the same origin. BratNextGen identified intrasubspecies recombination events (within *fastidiosa* subspecies), also indicating differences among different "Temecula" strains (see text for more details).

Recombinants representing an intersubspecific strain combination, i.e. heat-killed *X. fastidiosa* subsp. *multiplex* strain AlmaEM3 as a donor and *X. fastidiosa* subsp. *fastidiosa* strain TemeculaL as recipient (**Fig. 6-1A**), showed recombination only around the Km marker cassette,

as identified by both fastGEAR and the stringent method BratNextGen (data not shown). The lengths of recombining regions varied in the case of the two recombinants, with TemL(Alma) Rec1 showing a total of 10 kb region (spanning five recombination events surrounding the Km marker gene) and TemL(Alma) Rec2 showing a 3.5 kb region (spanning one recombination event) flanking the Km marker cassette as was observed in reference mapping and alignment (**Fig. S6-2**). No additional recombinant regions were identified, indicating that recombination in this case was confined to the flanking regions of the Km selection marker insertion site.

On the other hand, in the case of in vitro intrasubspecific recombinants generated by mixing live cells of *X. fastidiosa* subsp. *fastidiosa* WM1-1 (hierBAPS cluster 3, **Fig. 6-2A**) with heat-killed cells of *X. fastidiosa* subsp. *fastidiosa* KLN59.3(GFP) (hierBAPS cluster 4) (**Fig. 6-1B**), recombination events were detected away from the GFP marker using BratNextGen and fastGEAR analysis in WM1-1(GFP) Rec1 and WM1-1(GFP) Rec2 (10.5kb region identified in both recombinants and an additional 6.1kb in WM1-1(GFP) Rec1). Such random recombination events away from the selection marker were also observed in in vitro recombinants of *Helicobacter pylori* (Bubendorfer et al. 2016). We scanned these recombinant regions for polymorphisms in amino acid sequences, and identified polymorphisms in genes encoding lipase/alpha-beta hydrolase and putative Ctpa-like serine protease/peptidase S41 (**Table 6-1**). Previously, homologous serine proteases have been linked to virulence of *X. fastidiosa* (Gouran et al. 2016; Zhang et al. 2015).

Finally, we assessed the extent of recombination in another intrasubspecific in vitro recombinant. TemL(NS1pglA) Rec1 was obtained by co-culturing live donor and recipient

parents NS1-Cm^R (TemeculaL) and pglA-Km^R, belonging to clusters 5 and 2, respectively (**Fig. 6-1C** and **6-2A**). Upon analyzing the flanking region of the Km marker cassette in the recombinant genome, a 6 kb region upstream of the cassette was identical to the region from pglA-Km^R, indicating recombination at this region. A 5 kb region downstream of the Km cassette was identical in both pglA-Km^R as well as NS1-Cm^R. In addition to recombination near the Km cassette, we identified three recombination events (320 bp, 1.5 kb, and 3 kb) away from the Km cassette, similar to what was described above. Scanning these regions for changes in amino acid polymorphisms in protein-coding genes indicated recombinant genes encoding extracellular serine protease, Ctpa-like serine protease, hypothetical proteins and translocation and assembly module TamA/surface antigen/autotransporter domain (**Table 6-1**). Except for the last two, all the other proteins were identified also as recombinants in WT strains (**Table 6-1**).

Interestingly, recombinant gene encoding Ctpa-like serine protease, identified in this in vitro recombinant, is present upstream of the recombinant gene (also encoding Ctpa-like serine protease) (Carroll et al. 2014) in WM1-1(GFP) Rec1 (see above). Presence of recombination in similar regions of the genome in two independent recombinants arising from different parents is surprising. Ctpa-like serine protease was also identified to be a recombinant locus in *morus/sandyi, multiplex* and *fastidiosa* subspecies in WT strains (**Table 6-1**), suggesting this region as a possible recombination hotspot. Potential role of these genes in the interaction of *X. fastidiosa* with its host plants is described in **Table 6-1**.

Table 6-1. List of recent recombination events in genes/categories identified in WT strains and their possible ecological role in host adaptation.

Recent recombined genes[a]		Recombined subspecies (number of recombination events)				Recombination origin					Ecological role	References
		morus/ sandyi (4)[b]	*multiplex* (12)	*fastidiosa* (20)	*pauca* (19)	*morus/ sandyi*	*multiplex*	*fastidiosa*	*pauca*	Outside		
1. Movement	Type IV pili genes	**S** (31)[c]	**M** (52)	**F** (3)	**P** (22)	**M F P**[d]	**S P**	**S M P**	**S**	**P**	Xf[e]: Plant colonization via twitching motility; virulence determinant.	(Meng et al. 2005)
2. Attachment	Type I pili	-	**M** (14)	**F** (3)	**P** (55)	**M F P**		**P**	**F**	**P**	Xf: Cell-cell aggregation, attachment to surfaces and biofilm formation; important for colonization of plant and insect hosts and virulence determinant.	(De La Fuente et al. 2007; Feil et al. 2007; Killiny and Almeida 2014)
	Afimbrial adhesin genes	**S** (14)	**M** (1)	**F** (5)	**P** (18)	**F P**	**S F P**	**S**		**M P**		
3. Exoenzymes	TIISS genes	**S** (18)	**M** (29)	**F** (4)	**P** (18)	**M F P**	**S P**	**S M P**	**S**	**P**	Xf: Hydrolytic enzymes are important for degrading plant structural components and therefore colonization.	(Gouran et al. 2016; Roper et al. 2007)
	Xylan 1,4-xylosidase	**S** (9)	-	**F** (7)	-	**F**	**S F**	**S**		**S**		
4. Regulation and signaling	DSF (*rpfF*/*rpfC*/*rpfG*)	**S** (14)	**M** (54)	**F** (2)	**P** (34)	**M F P**	**S**	**S M P**		**P**	Xf: Diffusible Signaling Factor (DSF) is a quorum sensing molecule important for plant host specificity and switching between plant and insect environments.	(Chatterjee et al. 2008; Killiny and Almeida 2011)
	Sensor kinases	**S** (53)	**M** (29)	**F** (6)	**P** (15)	**M F P**	**S**	**S M P**		**P**	Part of two-component signal transduction pathways responding to external stimuli for adaptation to different environments.	(Capra and Laub 2012)

	phoP/phoQ	**S** (14)	**M** (29)	**F** (4)	**P** (5)	**M F P**	**S**	**S M**		**S**	Xf: Essential for survival in plant host.	(Pierce and Kirkpatrick 2015)
	Vitamin B12 transporter BtuB	**S** (33)	**M** (39)	**F** (30)	**P** (59)	**M F P**	**S F P**	**S M P**	**S**	**S F P**	Regulatory system affecting gene expression, enzyme activity, organism abundance; affects virulence and biofilm formation.	(Cordonnier et al. 2016; Lee et al. 2012; Rosnow et al. 2018)
	RNA binding Hfq	**S** (2)	**M** (6)	-	-	**M**	**S**				Small RNAs chaperone, regulates virulence and stress adaptation.	(Kavita et al. 2018)
5. Nutrient acquisition	Tryptophan metabolism	**S** (10)	**M** (5)	**F** (1)	**P** (9)	**M F P**	**S P**	**S**			Important for interaction host-microflora in humans.	(O'Mahony et al. 2015)
	Phosphate assimilation	**S** (39)	**M** (53)	**F** (20)	**P** (22)	**M F P**	**S F**	**S M**		**S P**	Xf: Indirect evidence suggests phosphorus metabolism important for plant colonization.	(De La Fuente et al. 2013; Rock 2013)
6. Adaptation to new conditions	Recombination genes	**S** (26)	**M** (11)	**F** (19)	**P** (7)	**M F P**	**S F P**	**S M P**	**S**	**P**	Xf: Acquisition of new genomic information, evolution.	(Kung and Almeida 2011)
	tRNA biosynthesis / modification genes	**S** (17)	**M** (37)	**F** (8)	**P** (17)	**M F P**	**S F**	**S M P**		**P**	Optimization of translation, adaptation to changes.	(Bjork et al. 1987)
7. Cell envelope structure	Peptidoglycan biosynthesis genes	**S** (42)	**M** (71)	**F** (12)	**P** (38)	**M F P**	**S P**	**S M P**	**S**	**S P**	Plant host recognition, bacterial growth.	(Antolin-Llovera et al. 2012; Typas et al. 2012)
	Lipopolysaccharide genes	**S** (24)	**M** (24)	**F** (9)	**P** (12)	**M F P**	**S F**	**S M P**		**S P**	Xf: Lipopolysaccharide O-antigen allows to delay initial recognition by plant innate immune system.	(Rapicavoli et al. 2018)
	3-Oxoacyl [acyl-carrier-proteins]	**S** (34)	**M** (48)	**F** (14)	**P** (6)	**M F**	**S F**	**S M P**	**F**		Involved in fatty acid metabolism, influence membrane structure and quorum sensing signaling.	(Filip'echeva et al. 2018; Hu et al. 2018; Mao et al. 2016)

Recently recombined genes in experimentally-generated recombinants[f]												
WM1-1 (GFP) Rec1[f]	Lipase/alpha-beta hydrolase (PD1702)[g]	**S** (2)	-	-	**P** (11)	**P**	**P**	**S P**		**P**	Xf: Homolog (PD1703) identified as pathogenicity effector.	(Zhang et al. 2015)
	Putative Ctpa-like serine protease /peptidase S41 (PD0948) [g]	**S** (1)	**M** (15)	**F** (1)	-	**M F**		**S M**			Associated with virulence of other bacterial species.	(Carroll et al. 2014)
TemL(NS1-pgla)Rec 1[f]	Hypothetical proteins (PD1421, PD1422, PD1423)[g]	-	-	-	-						Unknown.	
	Extracellular serine protease (PD0950)[g]	-	**M** (14)	**F** (2)	**P** (1)	**M F P**					Xf: Serine protease PD0956 identified as pathogenicity effector.	(Zhang et al. 2015)
	Putative Ctpa-like serine protease/ C-terminal processing protease CtpA/Prc, contains a PDZ domain (PD0949)[g]	-	**M** (8)	-	-	**M**		**M**			Associated with virulence of other bacterial species.	(Carroll et al. 2014)
	Translocation and assembly module TamA/ outer membrane protein assembly factor (PD0507)[g]	-	-	-	-						Secretion of adhesion protein.	(Selkrig et al. 2015)

[a]For a complete list of genes considered for each category see **Table S6-6**.

[b]Number in parenthesis indicates the total number of strains considered for each subspecies, see **Table S6-1** for details.

[c]The number of recent recombination events in parenthesis is categorized by *X. fastidiosa* subspecies for each gene/category shown in the table. Different letters indicate presence of recombination in each subspecies for each analyzed gene/category. Letters represent each subspecies, i.e., S: subsp. *morus/sandyi*; M: subsp. *multiplex;* F: subsp. *fastidiosa;* P: subsp. *pauca*.

[d]Presence of letters in the columns under "Recombination origin" shows which subspecies acted as donor for the recombination event, according to the letter coding of each subspecies used in "Recombined subspecies" column. For instance, if a "M" (subspecies *multiplex*) is in the "Recombination origin" column of subspecies "*fastidiosa*", it means that the latter was the donor for that recombination event(s) in subspecies *multiplex*.

[e]Presence of "Xf" means that the ecological role of genes belonging to these categories was functionally studied in *X. fastidiosa* and references appear in the following column. In the absence of "Xf" the description and corresponding references represent knowledge gained in other bacteria.

[f]Experimentally-generated recombinants strains where recombined regions were found, and were searched in WT strains.

[g]Corresponding locus tag from *X. fastidiosa* Temecula1 for each gene is included in parenthesis.

Our results indicate that in vitro recombination by natural competence is not limited to a small fraction of the genome, and it is variable, even when considering the same pair of strains under controlled conditions in the same experiment (Kandel et al. 2017), as seen in case of two TemL(Alma) recombinants that vary in the extent of integration of transformed DNA. While this study analyzed recombinants obtained after a single cycle of transformation, frequency of recombination upon natural competence is expected to increase dramatically after several cycles (Bubendorfer et al. 2016). Thus, co-infection of plants (Denancé et al. 2017) or insects with different strains of a single or multiple subspecies is expected to result in unpredictable widespread exchanges of genetic material.

Interestingly, we found that in the case of intersubspecific recombination (**Fig. 6-1A**) only the region of the selection marker was exchanged, while in intrasubspecific recombination (**Fig. 6-1B** and **C**) additional regions away from the selection marker were also exchanged. This may indicate that in nature, intra-subspecific HR may be more widespread in the genome than inter-subspecific recombination, where it could be inhibited by sequence divergence (Fraser et al. 2007), or possibly by different restriction-modification systems (Bubendorfer et al. 2016). Testing this hypothesis would require extensive sampling and genome analysis of strains belonging to each subspecies from wild populations followed by genome sequencing.

Ancient and recent recombinogenic regions are common among *X. fastidiosa* strains

Analysis of in vitro transformation detected multiple recombination events within and between subspecies *multiplex* and *fastidiosa*. To estimate the influence of recombination on the evolution of *X. fastidiosa* at the intersubspecific level, we analyzed 55 genomes belonging to all

X. fastidiosa subspecies described/available to date [i.e. subsp. *fastidiosa, multiplex, pauca, morus*, and *sandyi* (15 sequenced in this study and 40 obtained from NCBI GenBank)] (**Table S6-1**). Population structure of all the genomes inferred using nested clustering implemented in hierBAPS identified five clusters: one cluster each representing subsp. *fastidiosa* and *multiplex*, two clusters within subsp. *pauca*, and a single cluster representing subsp. *morus* and *sandyi* (**Fig. 6-4A**).

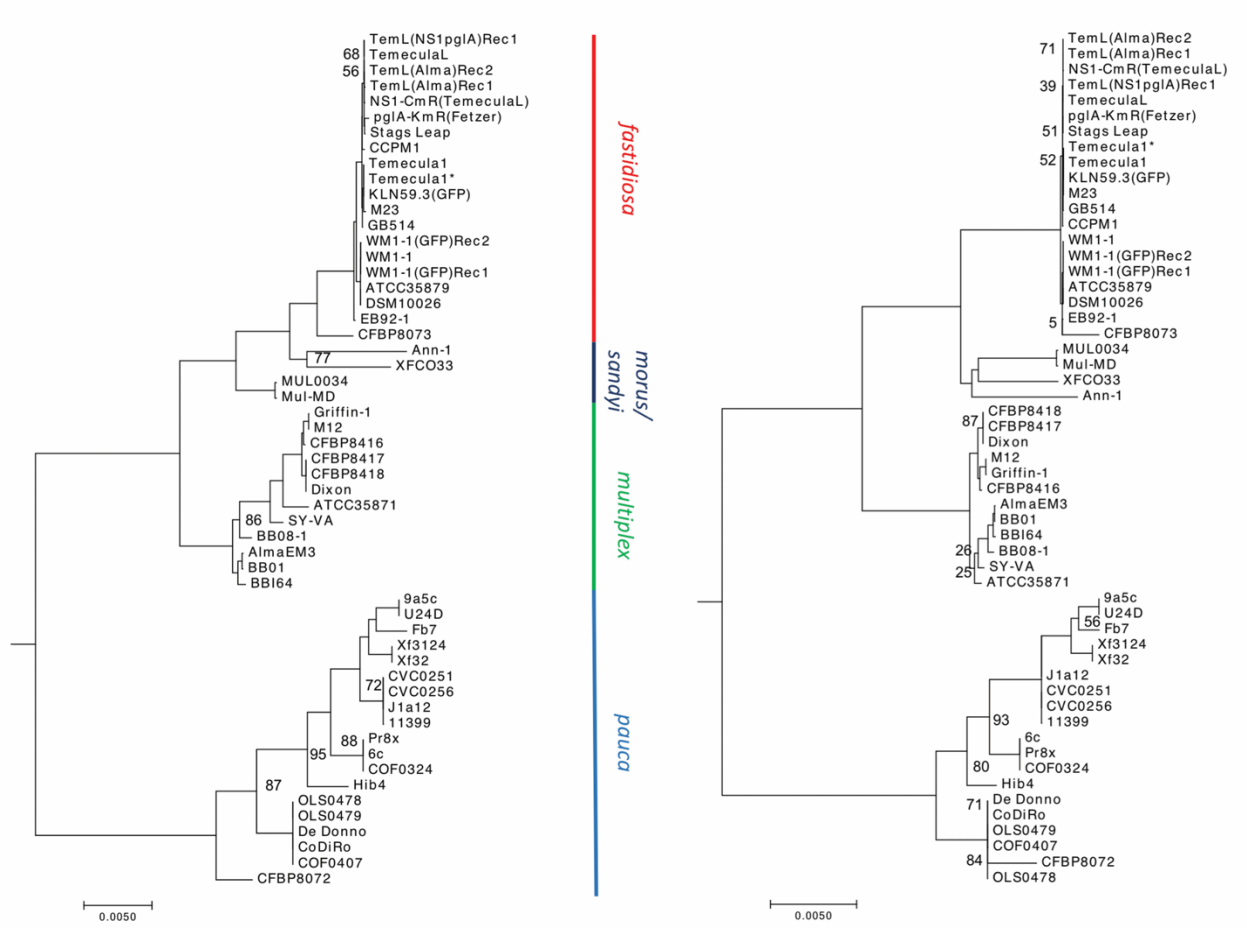

Fig. 6-4. **Population structure of *X. fastidiosa*.** Maximum likelihood phylogeny of core genome alignment of 1.79 Mb of 55 *X. fastidiosa* strains analyzed in this study, before (**A**) and after (**B**) filtering for the recombinant regions. The phylogenetic tree was mid-point rooted, representing increasing order of nodes. For **A**, a total of 33,824 backbone entries were concatenated to obtain core genome alignments of 1.79 MB. Population structure was inferred using nested clustering implemented in hierBAPS. For **B**, recombinant regions detected by fastGEAR in all subspecies

of *X. fastidiosa* were excluded to build a recombination-free phylogenetic tree. Bootstrap support was > 98% for all nodes except where otherwise indicated.

The secondary level clustering further divided the cluster containing subspecies *morus* and *sandyi* into individual subspecies clusters, and a cluster containing *multiplex* into two clusters (as seen by two subclades within subspecies *multiplex*). The core genome alignment of 1.79 MB was used for the construction of a phylogenetic tree (**Fig. 6-4A**). Subspecies *morus* and *sandyi* were positioned in a "hybrid" subclade between *fastidiosa* and *multiplex*; this is in agreement with the phylogeny based on MLST (Almeida and Nunney 2015). While BratNextGen allowed us to detect recombination within a single lineage (subsp. *fastidiosa*), it did not provide enough resolution when diverse lineages belonging to subspecies were included, with no recombination identified in subsp. *multiplex* or *pauca* (**Fig. S6-3**).

To address this limitation, we used fastGEAR software that inferred recombination between lineages as well as from external origins (Mostowy et al. 2017). As evident from **Fig. 6-5**, subsp. *morus* and *sandyi* showed mosaic/chimeric genomes due to relatively high degree of recent (**Table S6-4**) as well as ancient (**Table S6-5**) recombination events, thus, confirming previous observations (Nunney et al. 2014c).

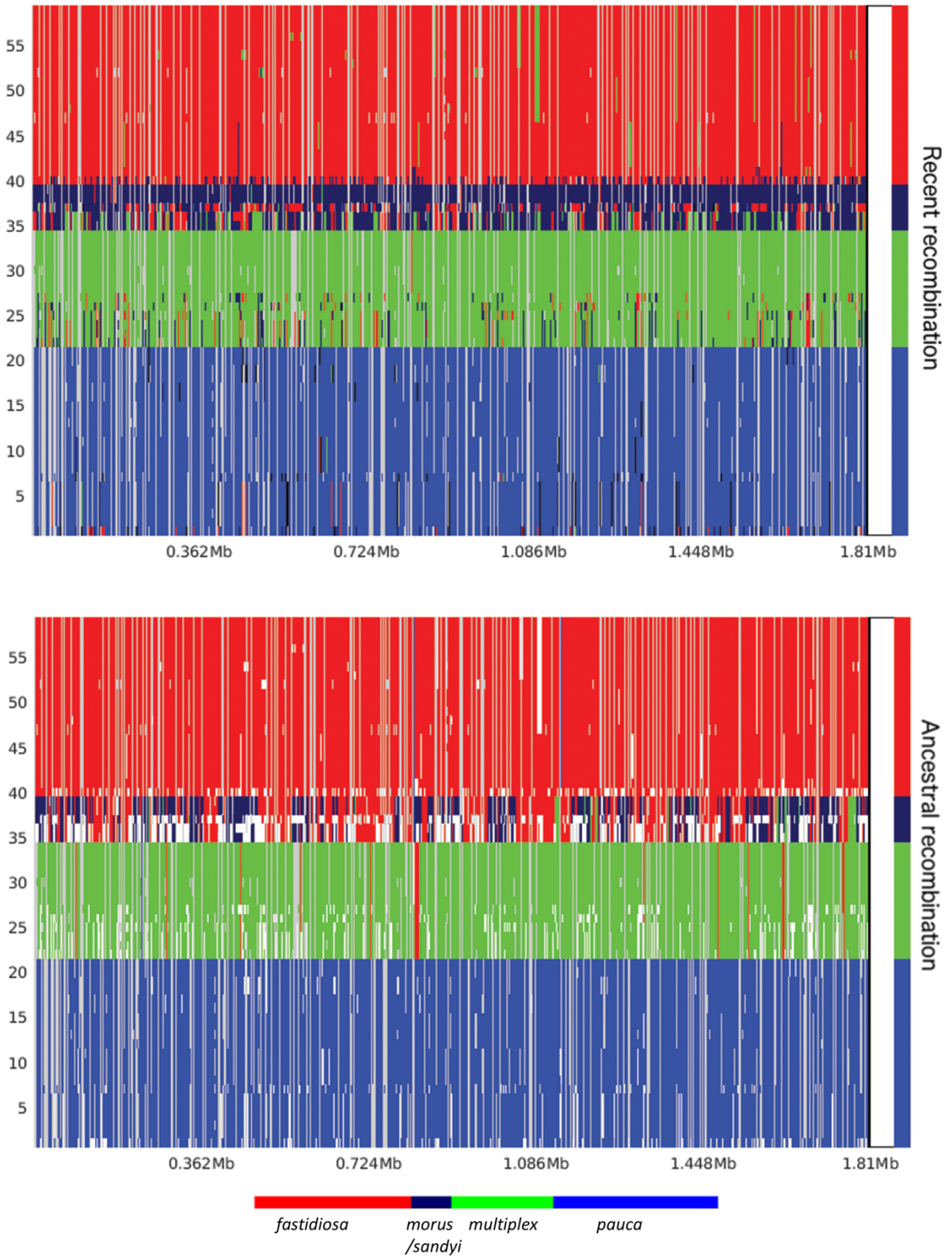

Fig. 6-5. **Interlineage recombination.** Distribution, origin and proportion of recent (**A**) and ancestral (**B**) recombination events across the *X. fastidiosa* core genome as predicted by

fastGEAR. The lineage predictions are based on hierBAPS analysis and are color-coded and clade designations are labeled accordingly. Presence of a differently colored markings within a given lineage indicates recombination event relative to the genomic position shown in the X-axis. Predicted recent recombination events were removed prior to the analysis of ancestral recombination, which are represented by white gaps in **B**. Subspecies *morus* and *sandyi* showed high degree of both ancestral and recent recombination indicating mosaicism in these two subspecies.

Next, we assessed the influence of recent recombination events on different subspecies. Subspecies *pauca* has experienced recent recombination events originating from all three lineages, *morus/sandyi* (27% of the events), *multiplex* (16% events), and *fastidiosa* (16% of the events) subspecies, as well as from possibly other bacteria (40% of the total recombination events) (**Table S6-4**). There are multiple reports of co-existence in the same geographic areas of subsp. *pauca* and other subspecies, that can explain the exchange of DNA leading to recombination (Coletta-Filho et al. 2017; Nunney et al. 2014b). The total size of recombination events varied from 530 bp to ~250 kb, representing ~ 0.02-10% of the genome (**Table S6-4**). We identified CFBP8072 as highly recombinant among *pauca* strains, showing a total of 376 recombination events, with origins in all other subspecies of *X. fastidiosa* and possible outside sources. This strain, isolated in France from intercepted coffee plants imported from Ecuador, was previously identified as a recombinant strain based on MLSA (Jacques et al. 2016). Analysis of length distribution of recombination events across genomes of subsp. *pauca* indicated average size of 1 kb, ranging from 25 bp to 3,791 bp, with the exception of 4,423 bp for CFBP8072 (**Fig. 6-6**). Plot of frequency of specific lengths of recombinant segments showed a normal distribution, and a small peak at 25 bp followed by a large peak at 300 bp (without outlier CFBP8072), indicating two frequently recombined lengths across *pauca* subspecies. This bimodal distribution model is similar to what has been observed in other bacteria (Bubendorfer et al. 2016; Mostowy et al. 2014), but the mechanism(s) behind it is still unclear.

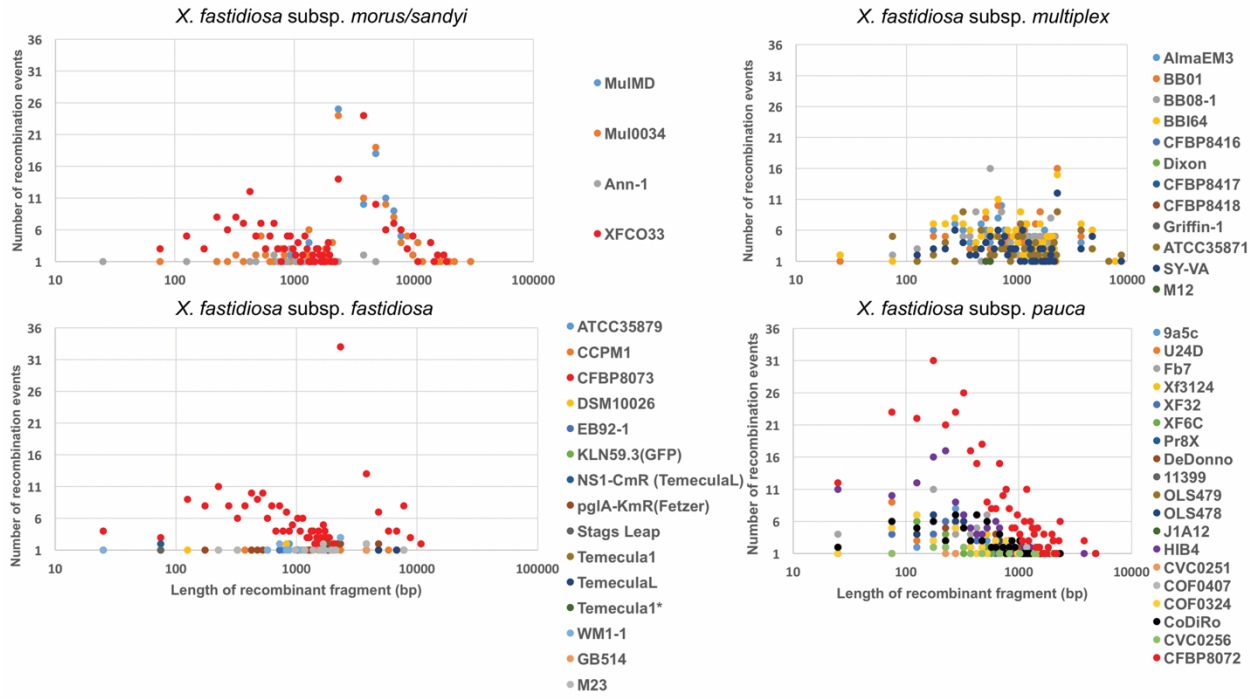

Fig. 6-6. Distribution of length of recombinant fragments and the number of recombination events for each subspecies of *X. fastidiosa*. The number of recent recombination events identified by fastGEAR were plotted on Y-axis, with the lengths of recombination events plotted on X-axis using a logarithmic scale. Average length of recombined fragment was around 1,000 bp for all subspecies, with 10,000 bp being a higher limit for the recombined fragment length (subsp. *morus* as an exception). Higher incidence of recombination as well as the greater lengths of recombinant fragments were observed in subsp. *morus* (31,554 bp as the longest recombinant fragment) as well as in strains isolated from intercepted coffee plants (XFCO33, CFBP8072, and CFBP8073, marked in red, 19,280 bp as the longest recombinant fragment).

Subspecies *fastidiosa* has experienced relatively low levels of recombination events compared to other subspecies, except for an outlier strain, CFBP8073, which is highly recombinant (**Fig. 6-6**). Overall number of recombination events experienced by subsp. *fastidiosa* strains, except CFBP8073, were 235 in total, of which 87% of the events originated in subsp. *multiplex*, 11% originated in subsp. *morus/sandyi*, 2% originated from outside species, with none from subsp. *pauca*. Highly recombinant strain CFBP8073 contains recombinant regions with 83% of the events originating in *morus/sandyi* subspecies. This is in contrast with other subsp. *fastidiosa* strains that contained recombination origins in subsp. *multiplex*.

Interestingly strain CFBP8073 was also intercepted in Europe in coffee plants shipped from Mexico (Jacques et al. 2016). Despite a comparatively low rate of recombination in subsp. *fastidiosa*, two frequently recombined segments included 75 bp and 2,325 bp, indicating a similar pattern as observed above, including a normal distribution. The maximum length of a recombinant segment was 10,909 bp (**Fig. 6-6**). These lengths are comparable to the recombinant segment lengths observed in experimentally-generated recombinants.

Population structure using hierBAPS indicated that subspecies *multiplex* is diverse (**Fig. 6-4A**), with at least 5 subclades. Sublineage within *multiplex* consisting of Dixon and Griffin-1 strains was minimally affected by recombination (**Fig. 6-5**, **Table S6-4**). However, sublineages containing susbp. *multiplex* ATCC35871, SY-VA, and BB08-1-containing subclades were significantly affected by recombination, with donor lineages being *morus/sandyi* (51% of recombination events) and *fastidiosa* (48% of recombination events) (**Fig. 6-5**, **Table S6-4**). The length distribution of recombinant events also followed a normal curve for subsp. *multiplex,* with the two most frequently recombined fragments of 649 bp and 2,318 bp.

In addition to ancient recombination, subsp. *morus* and *sandyi* have also undergone recent recombination. It is interesting to note that these two subspecies have different origins of recombination, with *morus* showing higher proportion of recombination originating in *multiplex* (56% in *multiplex* compared to 41% recombination originating in *fastidiosa*), and with *sandyi* showing higher proportion of recombination originating in *fastidiosa* (64% of the events originating in *fastidiosa* and 20% originating in *multiplex*). Strain XFC033 belonging to subspecies *sandyi* can be referred to as a hybrid strain, with origins in *pauca, fastidiosa* and

multiplex. Interestingly, this strain was identified from symptomatic coffee leaves originating in Costa Rica and intercepted in northern Italy (Giampetruzzi et al. 2015). Although similar to other subspecies, fragments of ~1 kb were frequently recombined in *morus/sandyi* strains; subsp. *morus* contains the largest recombined fragment of 31.5 kb. The two subsp. also contained at least 9 fragment sizes >10 kb, reiterating the highly recombinant nature of these subspecies. The widespread recombination found here is in concordance with *X. fastidiosa* being an γ proteobacteria, since this group is considered to have the 'most chameleonic-like evolutionary history' (Kloesges et al. 2011).

Phylogenetic relationships are influenced by recombination events between *X. fastidiosa* subspecies

To understand the influence of recombination on the overall topology of the *X. fastidiosa* phylogeny, we filtered core genome alignments to exclude the regions identified as recent recombinant events predicted by fastGEAR. The remaining non-recombinant regions were then used to build a recombination-free phylogenetic tree. As shown in **Fig. 6-4B**, the overall topology of the tree appeared similar to that of the unfiltered tree, showing similar major clades and subclades. Recombinant-filtering resulted in a strongly increased cohesiveness within subsp. *fastidiosa*, *multiplex,* and *pauca*. The most notable observation after recombinant-filtering was the shift of subclades *morus* and *sandyi* with respect to their relatedness to *fastidiosa* and *multiplex* (**Fig. 6-4B**). When we compared branch-length distances from both trees, average distance between *morus* and *sandyi* decreased (from 0.015 to 0.010), whereas that between *morus* and *multiplex* significantly increased (from 0.014 to 0.019) upon recombinant filtering. This led to a shift in the position of subsp. *morus* closer to *sandyi* in the recombinant-filtered

phylogeny. These observations indicate that recombination plays an important role in *X. fastidiosa* evolution.

Majority of strains from intercepted plants are highly recombinant

The findings that: i) different degrees of ancestral and recent recombination have shaped the population structure of *X. fastidiosa*; and ii) each lineage contains different degrees of recombination with origins in other subspecies; show that a shared ecological niche (Coletta-Filho et al. 2017; Nunney et al. 2014b) of these diverse lineages could have contributed to the emergence of the recombinant strains. Interestingly, the highly recombinant strains CFBP8072, CFBP8073, and XFC033, were strains isolated from intercepted infected coffee plants, with origin in American countries. We further included two additional strains belonging to subspecies *pauca*, PD7202 (CFBP8495, belonging to Sequence Type 53, ST53) and PD7211 (CFBP8498, belonging to ST73) (**Table S6-1**), that were isolated from asymptomatic coffee plants intercepted in the Netherlands with origin in Central America. Based on our findings, we hypothesized that these two strains are highly recombinant. Upon analyzing recombination using fastGEAR, we found PD7211 to contain in total 99 recent recombination events, with recombination regions shared with CFBP8072. On the contrary, strain PD7202 contained 49 recent recombination events, similar to other *pauca* strains, indicating that not all intercepted strains were highly recombinant (**Fig. S6-4**). Maximum likelihood phylogeny of core genome indicated that PD7202 belongs to the same clade as subsp. *pauca* strains, containing CoDiRo and DeDonno, while PD7211 with higher degree of recombination formed a distinct clade (**Fig. S6-5**). Presence of all subspecies has been identified in countries of the American continents in different hosts (Coletta-Filho et al. 2017; Nunney et al. 2014b). It is likely that recombination events are rampant in the

case of plants co-infected by multiple strains (Denancé et al. 2017). Presence of multiple subspecies in certain hosts or vectored by insects can foster recombination among these subspecies, resulting in emergence of recombinant strains. The importance of these recombinant regions in the epistatic contribution of each strain background (Arnold et al. 2018) in terms of host range expansion, or aggressiveness of strains, remains to be investigated. Movement of these highly recombinant strains, that have acquired genomic regions from diverse subspecies, across the globe via shipment of asymptomatic plant material, is a major concern. Such introduction of novel variants to a new geographic area could further foster generation of new recombinants. Acquisition of novel traits by endemic pathogenic species could lead to increasing losses due to changes in host adaptation.

Recombinant regions shared among subspecies inform eco-evolutionary dynamics of *X. fastidiosa*-host interactions

Functional significance of 1,026 genes (~40% of the *X. fastidiosa* genome), that were identified in recombinant regions, was analyzed. We focused on recently-recombined annotated loci that were included among the top 10% in terms of frequency of recombination events (105 genes with 19 recombination events or higher, see **Table S6-7** genes highlighted in yellow). The predicted functions of genes encoded in these loci can be considered to play roles in adjustment to and/or transition between the two ecological niches experienced by the pathogen during its life cycle, i.e., plant xylem and insect foregut (Chatterjee et al. 2008) (**Tables 6-1**, **S6-6**, **S6-7** and **Fig. 6-7**). Thus, they have a major impact on the ecology of *X. fastidiosa*. Cell attachment (De La Fuente et al. 2007) is a fundamental feature needed to live in physically-restricted environments with strong liquid flow, including xylem and insect foregut (Feil et al. 2007; Killiny and Almeida

2014), while movement against flow (twitching motility) (Meng et al. 2005) and secretion of degrading enzymes (Roper et al. 2007) are crucial for colonization of xylem vessels.

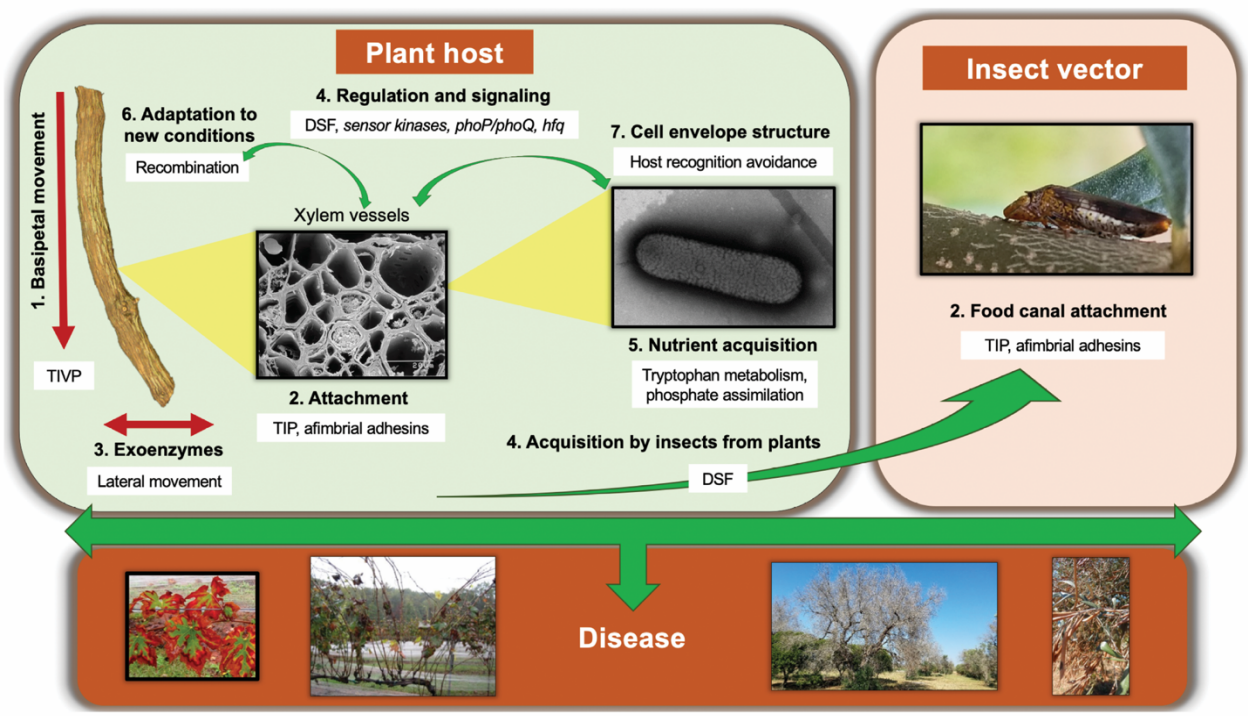

Fig. 6-7. Diagram illustrating the ecological role of genes found to be under recent recombination in *Xylella fastidiosa*. *X. fastidiosa* is only found in two very specific ecological niches: xylem vessels of host plants and food canal of xylem-feeding insects. Genes that were identified through our analysis as having the highest rate of recent intersubspecific recombination are listed in **Tables 6-1**, **S6-6** and **S6-7**. Based on the functional classification of these genes (**Table 6-1**), we placed these functions in the context of the ecology of *X. fastidiosa* during its life cycle. Briefly, in plant hosts (left panel), *X. fastidiosa* needs twitching motility (1) and exoenzymes (3) to colonize the xylem system inside plants, where nutrients are very limited (5). While colonizing xylem vessels they need attachment (2) to withstand constant liquid flow in the vascular system and to form biofilms. Proteins in the cell envelope are fundamental for recognition by the plant (7). When colonizing a new host, *X. fastidiosa* most likely needs to acquire new genetic information for adaptation to new conditions (6). Several regulatory cascades detected to be under recombination, have been implicated in regulating bacterial colonization and virulence (4). DSF quorum sensing molecule has a role in causing an increase in *X. fastidiosa* attachment and biofilm formation that is important to increase cell stickiness and therefore insect acquisition (4). In the food canal of xylem-feeding insect (right panel) attachment by TIP and afimbrial adhesins (2) is important to sustain population under high liquid flow. TIVP: type IV pili; TIP: type I pili; T2SS: type two secretion system; DSF: diffusible signal factor. Numbers of the highlighted *X. fastidiosa* traits from 1 to 7 correlate to the categories described in **Table 6-1**. For more information refer to the text and **Table 6-1**. Photo

credits: plant host 1, 2: Harvey Hoch (Cornell University); insect vector 2: Phil Brannen (University of Georgia). All other pictures are credited to the authors.

Although it is not completely understood how the plant host recognizes *X. fastidiosa*, lipopolysaccharide (LPS) (Rapicavoli et al. 2018) has been suggested as a key target, and other cell envelope structures could be involved in evading recognition by the host innate immune system (Rapicavoli et al. 2018). Recombinant alleles for genes encoding utilization of specific nutrients such as mineral elements (Oliver et al. 2014) or amino acids indicate adaptation of pathogen to the nutritionally-constrained environment. A great number of genes involved in regulatory and signaling cascades were detected as recombinants. Interestingly, genes involved in production (*rpfF*) and sensing (*rpfC* and *rpfG*) of the quorum sensing molecule diffusible signal factor (DSF), which is critical for acquisition of *X. fastidiosa* by insects from plants (Chatterjee et al. 2008), and regulates plant host specificity (Killiny and Almeida 2011), were detected in high frequencies. Other regulatory genes detected here, have been shown to be important for virulence of *X. fastidiosa*, interestingly *phoP/phoQ* (Pierce and Kirkpatrick 2015) that were shown to be needed for survival in plants.

Notably, the vitamin B_{12} transporter BtuB was the single gene with the highest recombination events (165) across subspecies, and was among the most frequently recombined genes for each subspecies (**Table S6-7**). Interestingly, vitamin B_{12} regulates gene expression, enzyme activity and abundance of microorganisms (Rosnow et al. 2018), and has been related to virulence (Cordonnier et al. 2016) and biofilm formation (Lee et al. 2012) in bacterial human pathogens, but has not been studied in *X. fastidiosa*. Presence of greater number of recombination events (collectively 2,631 events) in genes encoding “hypothetical proteins”,

brings attention to functionally uncharacterized proteins. Four genes, encoding lipase, Ctpa-like serine proteases, and extracellular serine protease, were common recombinant loci in intrasubspecific recombination (in vitro recombinants), as well as in intersubspecific recombination in WT strains (**Table 6-1**). Genes identified to be highly recombinant across different subspecies and encoding functions not previously shown to be important in *X. fastidiosa*, are of great interest to further understand the ecological adaptation of *X. fastidiosa* to specific environmental niches. Recombination in tRNA modification genes and recombination machinery indicates adaptability to receive and successfully integrate foreign DNA (from different subspecies) in order to obtain adaptive alleles that provide overall fitness to this naturally competent pathogen (Bjork et al. 1987; Kung and Almeida 2011).

Conclusions

In this study we assessed the effect of HR on the diversity of the bacterial plant pathogen *X. fastidiosa*. Through our comparison of both experimentally-generated recombinants and WT strains, we conclude that recombination occurs randomly and with varying lengths of DNA recombination across the genome. While extent of recombination in different subspecies varies among WT strains, all subspecies were affected by recent intersubspecific recombination at common loci, encoding important functions such as host colonization, nutrient acquisition, gene regulation/signaling. Four of such recombinant loci were also identified under intrasubspecific recombination in experimentally-generated recombinants, further supporting importance of in vitro studies to understand recombination potential of these naturally competent strains. These findings underline the prominent ability of this pathogen to evolve and adapt to new conditions by acquiring new DNA, which is facilitated by the lifestyle of this bacterium that is restricted to

xylem vessels of plants or mouthparts of insect vectors (Chatterjee et al. 2008), where it can easily encounter other bacteria in very confined spaces.

Acknowledgements

This project was funded by Agriculture and Food Research Initiative competitive grant no. 2015-67014-23085 from the USDA National Institute of Food and Agriculture, and HATCH AAES (Alabama Agricultural Experiment Station) program provided to N.P and L.D, and partly supported by research grant OS 2015330 of the Ministry of Economic Affairs in the Netherlands. We thank the Alabama Supercomputing Authority for granting access to their high-performance computing platform.

References

Almeida, R. P. P., and Nunney, L. 2015. How do plant diseases caused by *Xylella fastidiosa* emerge? Plant Dis 99:1457-1467.

Almeida, R. P. P., Nascimento, F. E., Chau, J., Prado, S. S., Tsai, C. W., Lopes, S. A., and Lopes, J. R. S. 2008. Genetic structure and biology of *Xylella fastidiosa* strains causing disease in citrus and coffee in Brazil. Appl Environ Microbiol 74:3690-3701.

Antolin-Llovera, M., Ried, M. K., Binder, A., and Parniske, M. 2012. Receptor kinase signaling pathways in plant-microbe interactions. Annu Rev Phytopathol 50:451-473.

Arnold, B. J., Gutmann, M. U., Grad, Y. H., Sheppard, S. K., Corander, J., Lipsitch, M., and Hanage, W. P. 2018. Weak epistasis may drive adaptation in recombining bacteria. Genetics 208:1247-1260.

Baltrus, D. A., Guillemin, K., and Phillips, P. C. 2008. Natural transformation increases the rate of adaptation in the human pathogen *Helicobacter pylori*. Evolution 62:39-49.

Bankevich, A., Nurk, S., Antipov, D., Gurevich, A. A., Dvorkin, M., Kulikov, A. S., Lesin, V. M., Nikolenko, S. I., Pham, S., Prjibelski, A. D., Pyshkin, A. V., Sirotkin, A. V., Vyahhi, N., Tesler, G., Alekseyev, M. A., and Pevzner, P. A. 2012. SPAdes: a new genome assembly algorithm and its applications to single-cell sequencing. Journal of computational biology : a journal of computational molecular cell biology 19:455-477.

Bergsma-Vlami, M., van de Bilt, J. L. J., Tjou-Tam-Sin, N. N. A., Helderman, C. M., Gorkink-Smits, P., Landman, N. M., van Nieuwburg, J. G. W., van Veen, E. J., and Westenberg, M. 2017. Assessment of the genetic diversity of *Xylella fastidiosa* in imported ornamental *Coffea arabica* plants. Plant Pathology 66:1065-1074.

Bjork, G. R., Ericson, J. U., Gustafsson, C. E. D., Hagervall, T. G., Jonsson, Y. H., and Wikstrom, P. M. 1987. Transfer RNA modification. Annu Rev Biochem 56:263-287.

Bolger, A. M., Lohse, M., and Usadel, B. 2014. Trimmomatic: a flexible trimmer for Illumina sequence data. Bioinformatics 30:2114-2120.

Bubendorfer, S., Krebes, J., Yang, I., Hage, E., Schulz, T. F., Bahlawane, C., Didelot, X., and Suerbaum, S. 2016. Genome-wide analysis of chromosomal import patterns after natural transformation of *Helicobacter pylori*. Nat Commun 7:11995-11995.

Capella-Gutierrez, S., Silla-Martinez, J. M., and Gabaldon, T. 2009. trimAl: a tool for automated alignment trimming in large-scale phylogenetic analyses. Bioinformatics 25:1972-1973.

Capra, E. J., and Laub, M. T. 2012. Evolution of two-component signal transduction systems. Annu Rev Microbiol 66:325-347.

Carroll, R. K., Rivera, F. E., Cavaco, C. K., Johnson, G. M., Martin, D., and Shaw, L. N. 2014. The lone S41 family C-terminal processing protease in *Staphylococcus aureus* is localized to the cell wall and contributes to virulence. Microbiology 160:1737-1748.

Chatterjee, S., Almeida, R. P. P., and Lindow, S. 2008. Living in two worlds: the plant and insect lifestyles of *Xylella fastidiosa*. Annu Rev Phytopathol 46:243-271.

Cheng, L., Connor, T. R., Siren, J., Aanensen, D. M., and Corander, J. 2013. Hierarchical and spatially explicit clustering of DNA sequences with BAPS software. Mol Biol and Evol 30:1224-1228.

Coletta-Filho, H. D., Francisco, C. S., Lopes, J. R. S., Muller, C., and Almeida, R. P. P. 2017. Homologous recombination and *Xylella fastidiosa* host-pathogen associations in South America. Phytopathology 107:305-312.

Cordonnier, C., Le Bihan, G., Emond-Rheault, J. G., Garrivier, A., Harel, J., and Jubelin, G. 2016. Vitamin B12 uptake by the gut commensal bacteria *Bacteroides thetaiotaomicron* limits the production of Shiga toxin by enterohemorrhagic *Escherichia coli*. Toxins 8:14.

Croucher, N. J., Page, A. J., Connor, T. R., Delaney, A. J., Keane, J. A., Bentley, S. D., Parkhill, J., and Harris, S. R. 2015. Rapid phylogenetic analysis of large samples of recombinant bacterial whole genome sequences using Gubbins. Nucleic Acids Res 43:e15.

Darling, A. E., Mau, B., and Perna, N. T. 2010. progressiveMauve: multiple genome alignment with gene gain, loss and rearrangement. PLoS One 5:e11147.

Davis, M. J., French, W. J., and Schaad, N. W. 1981. Axenic culture of the bacteria associated with phony disease of peach and plum leaf scald. Curr Microbiol 6:309-314.

De La Fuente, L., Montanes, E., Meng, Y., Li, Y., Burr, T. J., Hoch, H. C., and Wu, M. 2007. Assessing adhesion forces of type I and type IV pili of *Xylella fastidiosa* bacteria by use of a microfluidic flow chamber. Appl Environ Microbiol 73:2690-2696.

De La Fuente, L., Parker, J. K., van Santen, E., Oliver, J. E., Brannen, P., Granger, S., and Cobine, P. A. 2013. The bacterial pathogen *Xylella fastidiosa* affects the leaf ionome of plant hosts during infection. PLoS ONE 8:e62945.

Denancé, N., Legendre, B., Briand, M., Olivier, V., de Boisseson, C., Poliakoff, F., and Jacques, M. A. 2017. Several subspecies and sequence types are associated with the emergence of *Xylella fastidiosa* in natural settings in France. Plant Pathology 66:1054-1064.

EFSA. 2018. Update of the *Xylella* spp. host plant database. EFSA Journal 16:5408.

Feil, E. J., and Spratt, B. G. 2001. Recombination and the population structures of bacterial pathogens. Annu Rev Microbiol 55:561-590.

Feil, E. J., Holmes, E. C., Bessen, D. E., Chan, M. S., Day, N. P., Enright, M. C., Goldstein, R., Hood, D. W., Kalia, A., Moore, C. E., Zhou, J., and Spratt, B. G. 2001. Recombination within natural populations of pathogenic bacteria: short-term empirical estimates and long-term phylogenetic consequences. Proc Natl Acad Sci U S A 98:182-187.

Feil, H., Feil, W. S., and Lindow, S. E. 2007. Contribution of fimbrial and afimbrial adhesins of *Xylella fastidiosa* to attachment to surfaces and virulence to grape. Phytopathology 97:318-324.

Filip'echeva, Y. A., Shelud'ko, A. V., Prilipov, A. G., Burygin, G. L., Telesheva, E. M., Yevstigneyeva, S. S., Chernyshova, M. P., Petrova, L. P., and Katsy, E. I. 2018. Plasmid AZOBR_p1-borne *fabG* gene for putative 3-oxoacyl- acyl-carrier protein reductase is essential for proper assembly and work of the dual flagellar system in the alphaproteobacterium *Azospirillum brasilense* Sp245. Can J Microbiol 64:107-118.

Fraser, C., Hanage, W. P., and Spratt, B. G. 2007. Recombination and the nature of bacterial speciation. Science 315:476-480.

Freel, K. C., Millán-Aguiñaga, N., and Jensen, P. R. 2013. Multilocus sequence typing reveals evidence of homologous recombination linked to antibiotic resistance in the genus *Salinispora*. Appl Environ Microbiol 79:5997-6005.

Giampetruzzi, A., Loconsole, G., Boscia, D., Calzolari, A., Chiumenti, M., Martelli, G. P., Saldarelli, P., Almeida, R. P., and Saponari, M. 2015. Draft Genome Sequence of CO33, a Coffee-Infecting Isolate of *Xylella fastidiosa*. Genome Announc 3:e01472-01415.

Gouran, H., Gillespie, H., Nascimento, R., Chakraborty, S., Zaini, P. A., Jacobson, A., Phinney, B. S., Dolan, D., Durbin-Johnson, B. P., Antonova, E. S., Lindow, S. E., Mellema, M. S., Goulart, L. R., and Dandekar, A. M. 2016. The secreted protease PrtA controls cell growth, biofilm formation and pathogenicity in *Xylella fastidiosa*. Sci Rep 6:31098.

Guttman, D. S. 1997. Recombination and clonality in natural populations of *Escherichia coli*. Trends in Ecology & Evolution 12:16-22.
Hacker, J., and Carniel, E. 2001. Ecological fitness, genomic islands and bacterial pathogenicity. A Darwinian view of the evolution of microbes. EMBO Reports 2:376-381.
Hopkins, D. L., and Purcell, A. H. 2002. *Xylella fastidiosa*: Cause of Pierce's Disease of grapevine and other emergent diseases. Plant Dis 86:1056-1066.
Hu, Z., Dong, H. J., Ma, J. C., Yu, Y. H., Li, K. H., Guo, Q. Q., Zhang, C., Zhang, W. B., Cao, X. Y., Cronan, J. E., and Wang, H. H. 2018. Novel *Xanthomonas campestris* long-chain-specific 3-oxoacyl-acyl carrier protein reductase involved in diffusible signal factor synthesis. Mbio 9.
Jacques, M. A., Denancé, N., Legendre, B., Morel, E., Briand, M., Mississipi, S., Durand, K., Olivier, V., Portier, P., Poliakoff, F., and Crouzillat, D. 2016. New coffee plant-infecting *Xylella fastidiosa* variants derived via homologous recombination. Appl Environ Microbiol 82:1556-1568.
Kandel, P. P., Chen, H., and De La Fuente, L. 2018. A short protocol for gene knockout and complementation in *Xylella fastidiosa* shows that one of the type IV pilin paralogs (PD1926) is needed for twitching while another (PD1924) affects pilus number and location. Appl Environ Microbiol 84:e01167-01118.
Kandel, P. P., Lopez, S. M., Almeida, R. P. P., and De La Fuente, L. 2016. Natural competence of *Xylella fastidiosa* occurs at a high frequency inside microfluidic chambers mimicking the bacterium's natural habitats. Appl Environ Microbiol 82:5269-5277.
Kandel, P. P., Almeida, R. P. P., Cobine, P. A., and De La Fuente, L. 2017. Natural competence rates are variable among *Xylella fastidiosa* strains and homologous recombination occurs in vitro between subspecies *fastidiosa* and *multiplex*. Mol Plant Microbe Interact 30:589-600.
Kavita, K., de Mets, F., and Gottesman, S. 2018. New aspects of RNA-based regulation by Hfq and its partner sRNAs. Curr Opin Microbiol 42:53-61.
Killiny, N., and Almeida, R. P. P. 2011. Gene regulation mediates host specificity of a bacterial pathogen. Environ Microbiol Rep 3:791-797.
Killiny, N., and Almeida, R. P. P. 2014. Factors affecting the initial adhesion and retention of the plant pathogen *Xylella fastidiosa* in the foregut of an insect vector. Appl Environ Microbiol 80:420-426.
Kloesges, T., Popa, O., Martin, W., and Dagan, T. 2011. Networks of gene sharing among 329 proteobacterial genomes reveal differences in lateral gene transfer frequency at different phylogenetic depths. Mol Biol Evol 28:1057-1074.
Kong, Y., Ma, J. H., Warren, K., Tsang, R. S. W., Low, D. E., Jamieson, F. B., Alexander, D. C., and Hao, W. 2013. Homologous recombination drives both sequence diversity and gene content variation in *Neisseria meningitidis*. Genome Biol Evol 5:1611-1627.
Kung, S. H., and Almeida, R. P. P. 2011. Natural competence and recombination in the plant pathogen *Xylella fastidiosa*. Appl Environ Microbiol 77:5278-5284.
Lee, K. M., Go, J., Yoon, M. Y., Park, Y., Kim, S. C., Yong, D. E., and Yoon, S. S. 2012. Vitamin B_{12}-mediated restoration of defective anaerobic growth leads to reduced biofilm formation in *Pseudomonas aeruginosa*. Infect Immun 80:1639-1649.
Maiden, M. C. 2006. Multilocus sequence typing of bacteria. Annu Rev Microbiol 60:561-588.

Mao, Y. H., Li, F., Ma, J. C., Hu, Z., and Wang, H. H. 2016. *Sinorhizobium meliloti* functionally replaces 3-oxoacyl-acyl carrier protein reductase (FabG) by overexpressing NodG during fatty acid synthesis. Mol Plant Microbe Interact 29:458-467.

Marcelletti, S., and Scortichini, M. 2016. Genome-wide comparison and taxonomic relatedness of multiple *Xylella fastidiosa* strains reveal the occurrence of three subspecies and a new *Xylella species*. Arch Microbiol 198:803-812.

Marttinen, P., Hanage, W. P., Croucher, N. J., Connor, T. R., Harris, S. R., Bentley, S. D., and Corander, J. 2012. Detection of recombination events in bacterial genomes from large population samples. Nucleic Acids Res 40:e6.

Matsumoto, A., Young, G. M., and Igo, M. M. 2009. Chromosome-based genetic complementation system for *Xylella fastidiosa*. Appl Environ Microbiol 75:1679-1687.

Meng, Y., Li, Y., Galvani, C. D., Hao, G., Turner, J. N., Burr, T. J., and Hoch, H. C. 2005. Upstream migration of *Xylella fastidiosa* via pilus-driven twitching motility. J Bacteriol 187:5560-5567.

Michod, R. E., Bernstein, H., and Nedelcu, A. M. 2008. Adaptive value of sex in microbial pathogens. Infect Genet Evol 8:267-285.

Mostowy, R., Croucher, N. J., Hanage, W. P., Harris, S. R., Bentley, S., and Fraser, C. 2014. Heterogeneity in the frequency and characteristics of homologous recombination in pneumococcal evolution. Plos Genet 10:e1004300.

Mostowy, R., Croucher, N. J., Andam, C. P., Corander, J., Hanage, W. P., and Marttinen, P. 2017. Efficient inference of recent and ancestral recombination within bacterial populations. Mol Biol Evol 34:1167-1182.

Nelson, K., and Selander, R. K. 1994. Intergeneric transfer and recombination of the 6-phosphogluconate dehydrogenase gene (*gnd*) in enteric bacteria. Proc Natl Acad Sci U S A 91:10227-10231.

Newman, K. L., Almeida, R. P., Purcell, A. H., and Lindow, S. E. 2003. Use of a green fluorescent strain for analysis of *Xylella fastidiosa* colonization of *Vitis vinifera*. Applied and environmental microbiology 69:7319-7327.

Nunney, L., Yuan, X., Bromley, R. E., and Stouthamer, R. 2012. Detecting genetic introgression: high levels of intersubspecific recombination found in *Xylella fastidiosa* in Brazil. Appl Environ Microbiol 78:4702-4714.

Nunney, L., Hopkins, D. L., Morano, L. D., Russell, S. E., and Stouthamer, R. 2014a. Intersubspecific recombination in *Xylella fastidiosa* strains native to the United States: infection of novel hosts associated with an unsuccessful invasion. Appl Environ Microbiol 80:1159-1169.

Nunney, L., Ortiz, B., Russell, S. A., Sanchez, R. R., and Stouthamer, R. 2014b. The complex biogeography of the plant pathogen *Xylella fastidiosa*: genetic evidence of introductions and subspecific introgression in Central America. PLoS One 9:e112463.

Nunney, L., Schuenzel, E. L., Scally, M., Bromley, R. E., and Stouthamer, R. 2014c. Large-scale intersubspecific recombination in the plant-pathogenic bacterium *Xylella fastidiosa* is associated with the host shift to mulberry. Appl Environ Microbiol 80:3025-3033.

Nunney, L., Yuan, X., Bromley, R., Hartung, J., Montero-Astúa, M., Moreira, L., Ortiz, B., and Stouthamer, R. 2010. Population genomic analysis of a bacterial plant pathogen: novel insight into the origin of Pierce's disease of grapevine in the U.S. PLoS One 5:e15488.

O'Mahony, S. M., Clarke, G., Borre, Y. E., Dinan, T. G., and Cryan, J. F. 2015. Serotonin, tryptophan metabolism and the brain-gut-microbiome axis. Behav Brain Res 277:32-48.

Oliver, J. E., Sefick, S. A., Parker, J. K., Arnold, T., Cobine, P. A., and De La Fuente, L. 2014. Ionome changes in *Xylella fastidiosa*-infected *Nicotiana tabacum* correlate with virulence and discriminate between subspecies of bacterial isolates. Mol Plant Microbe Interact 27:1048-1058.

Parker, J. K., Havird, J. C., and De La Fuente, L. 2012. Differentiation of *Xylella fastidiosa* strains via multilocus sequence analysis of environmentally mediated genes (MLSA-E). Appl Environ Microbiol 78:1385-1396.

Pierce, B. K., and Kirkpatrick, B. C. 2015. The PhoP/Q two-component regulatory system is essential for *Xylella fastidiosa* survival in *Vitis vinifera* grapevines. Physiol Mol Plant Path 89:55-61.

Rapicavoli, J. N., Blanco-Ulate, B., Muszyński, A., Figueroa-Balderas, R., Morales-Cruz, A., Azadi, P., Dobruchowska, J. M., Castro, C., Cantu, D., and Roper, M. C. 2018. Lipopolysaccharide O-antigen delays plant innate immune recognition of *Xylella fastidiosa*. Nat Commun 9:390.

Rock, C. D. 2013. Trans-acting small interfering RNA4: key to nutraceutical synthesis in grape development? Trends Plant Sci 18:601-610.

Roper, M. C., Greve, L. C., Warren, J. G., Labavitch, J. M., and Kirkpatrick, B. C. 2007. *Xylella fastidiosa* requires polygalacturonase for colonization and pathogenicity in *Vitis vinifera* grapevines. Mol Plant Microbe Interact 20:411-419.

Rosnow, J. J., Hwang, S., Killinger, B. J., Kim, Y. M., Moore, R. J., Lindemann, S. R., Maupin-Furlow, J. A., and Wright, A. T. 2018. A cobalamin activity-Based probe enables microbial cell growth and finds new cobalamin-protein interactions across domains. Appl Environ Microbiol 84:e00955-00918.

Saponari, M., Boscia, D., Nigro, F., and Martelli, G. P. 2013. Identification of DNA sequences related to *Xylella fastidiosa* in oleander, almond and olive trees exhibiting leaf scorch symptoms in Apulia (Southern Italy). J. Plant Pathol. 95:668.

Scally, M., Schuenzel, E. L., Stouthamer, R., and Nunney, L. 2005. Multilocus sequence type system for the plant pathogen *Xylella fastidiosa* and relative contributions of recombination and point mutation to clonal diversity. Appl Environ Microbiol 71:8491-8499.

Schaad, N. W., Postnikova, E., Lacy, G., Fatmi, M. B., and Chang, C. J. 2004a. *Xylella fastidiosa* subspecies: *X-fastidiosa* subsp *piercei*, subsp nov., *X-fastidiosa* subsp *multiplex* subsp. nov., and *X-fastidiosa* subsp *pauca* subsp nov. Syst Appl Microbiol 27:290-300.

Schaad, N. W., Postnikova, E., Lacy, G., Fatmi, M., and Chang, C. J. 2004b. *Xylella fastidiosa* subspecies: *X. fastidiosa* subsp *piercei*, subsp. nov., *X. fastidiosa* subsp. *multiplex* subsp. nov., and *X. fastidiosa* subsp. *pauca* subsp. nov. Syst Appl Microbiol 27:763.

Selkrig, J., Belousoff, M. J., Headey, S. J., Heinz, E., Shiota, T., Shen, H. H., Beckham, S. A., Bamert, R. S., Phan, M. D., Schembri, M. A., Wilce, M. C. J., Scanlon, M. J., Strugnell, R. A., and Lithgow, T. 2015. Conserved features in TamA enable interaction with TamB to drive the activity of the translocation and assembly module. Sci Rep 5:12905.

Spratt, B. G., Bowler, L. D., Zhang, Q. Y., Zhou, J., and Smith, J. M. 1992. Role of interspecies transfer of chromosomal genes in the evolution of penicillin resistance in pathogenic and commensal *Neisseria species*. J Mol Evol 34:115-125.

Stamatakis, A. 2014. RAxML version 8: a tool for phylogenetic analysis and post-analysis of large phylogenies. Bioinformatics 30:1312-1313.

Strona, G., Carstens, C. J., and Beck, P. S. 2017. Network analysis reveals why *Xylella fastidiosa* will persist in Europe. Sci Rep 7:71.

Su, C. C., Deng, W. L., Jan, F. J., Chang, C. J., Huang, H., Shih, H. T., and Chen, J. 2016. *Xylella taiwanensis* sp. nov., causing pear leaf scorch disease. Int J Syst Evol Microbiol 66:4766-4771.

Thomas, C. M., and Nielsen, K. M. 2005. Mechanisms of, and barriers to, horizontal gene transfer between bacteria. Nat Rev Microbiol 3:711-721.

Timilsina, S., Jibrin, M. O., Potnis, N., Minsavage, G. V., Kebede, M., Schwartz, A., Bart, R., Staskawicz, B., Boyer, C., and Vallad, G. E. 2015. Multilocus sequence analysis of xanthomonads causing bacterial spot of tomato and pepper plants reveals strains generated by recombination among species and recent global spread of *Xanthomonas gardneri*. Appl Environ Microbiol 81:1520-1529.

Typas, A., Banzhaf, M., Gross, C. A., and Vollmer, W. 2012. From the regulation of peptidoglycan synthesis to bacterial growth and morphology. Nat Rev Microbiol 10:123-136.

Yahara, K., Didelot, X., Ansari, M. A., Sheppard, S. K., and Falush, D. 2014. Efficient inference of recombination hot regions in bacterial genomes. Mol Biol Evol 31:1593-1605.

Yan, S., Liu, H., Mohr, T. J., Jenrette, J., Chiodini, R., Zaccardelli, M., Setubal, J. C., and Vinatzer, B. A. 2008. Role of recombination in the evolution of the model plant pathogen *Pseudomonas syringae* pv. tomato DC3000, a very atypical tomato strain. Appl Environ Microbiol 74:3171-3181.

Zhang, S., Chakrabarty, P. K., Fleites, L. A., Rayside, P. A., Hopkins, D. L., and Gabriel, D. W. 2015. Three new Pierce's disease pathogenicity effectors identified using *Xylella fastidiosa* biocontrol strain EB92-1. PLoS One 10:e0133796.

Supplementary material for chapter 6

Supplementary Methods

Strains used for the generation of recombinants in vitro

Strains and mutants used in this study are listed in **Table S6-1**. Briefly, *X. fastidiosa* subsp. *fastidiosa* WT strains WM1-1, CCPM1, and Temecula1*; and *X. f.* subsp. *multiplex* strain AlmaEM3, BBI64, and BB08-1 were used. 'Temecula1' corresponds to the genome deposited in NCBI under this strain name. A variant strain that was isolated from infected grapevines in California and was initially presumed to be Temecula1, but differed based on whole genome sequence analysis in this study, was named here as 'TemeculaL'. Temecula1* was also a variant of the Temecula1 strain that showed reduced virulence in our previous studies (Oliver et al. 2014). Mutant strain NS1-Cm^R has a chloramphenicol (Cm) resistant gene inserted in the neutral site 1 (NS1) of TemeculaL (previously identified as Temecula1) chromosome (Matsumoto et al. 2009).

A diagram explaining the generation of the recombinants is presented in **Fig. 6-1**. Parental mutant strain NS1-Cm^R was described above. Parental mutant pglA-Km^R has a kanamycin (Km) resistant gene inserted to disrupt the polygalacturonase (*pglA*) gene in strain Fetzer (Roper et al. 2007). Parental mutant KLN59.3 has green fluorescent protein (GFP) and Km genes inserted in strain Temecula1 (Newman et al. 2003). Parental mutant strain AlmaEM3 (NS1::Km^R) was generated by transforming WT AlmaEM3 with pAX1.Km plasmid (Matsumoto et al. 2009). These antibiotic resistant and GFP-tagged mutants and wild-type (WT) strains were used as donor or recipient (Kandel et al. 2017; Kandel et al. 2016) to generate in vitro recombinant mutants (**Fig. 6-1**) that are explained as follows. TemL(Alma) Rec 1 and 2 were

generated by mixing heat-killed AlmaEM3(NS1::Km^R) with WT TemeculaL as previously described (Kandel et al. 2017). TemL (NS1-pglA) Rec 1 was generated by co-culturing strains NS1-Cm^R (strain TemeculaL background) and pglA-Km^R (strain Fetzer background) in PD3 agar (Kandel et al. 2016). WM1-1(GFP) Rec 1 and 2 were generated by mixing heat-killed KLN59.3 (GFP-marked Temecula1) with WM1-1 cells on PD3 agar medium as previously described (Kandel et al. 2017).

DNA extraction, library preparation, and sequencing

Genomic DNA was extracted from *X. fastidiosa* cultured on PW agar plates using a modified CTAB protocol (Doyle and Dickson 1987) followed by treatment with RNaseA (ThermoFisher Scientific). Strains WM1-1, TemeculaL, Temecula1*, AlmaEM3; mutants NS1-Cm^R, pglA-Km^R, KLN59.3 and in vitro recombinant strains TemL(Alma) Rec 1 and 2, TemL(NS1pglA) Rec 1, and WM1-1(GFP) Rec 1 and 2 were sequenced. DNA libraries were prepared using the Nextera® DNA Library Preparation Kit (Illumina) using the manufacturer's protocol. Twelve separate genomic libraries were multiplexed. Sequencing was performed on a MiSeq System (Illumina) using MiSeq reagent kit V2. Paired-end sequencing was performed with 250 cycles.

The strains WM1-1, CCPM1, AlmaEM3, BBI64, and BB08-1 were also sequenced using the Pacific Biosciences (PacBio) RS instrument at the Allegheny-Singer Research Institute's Center for Genomic Sciences using the manufacturer's protocol. PD7202 and PD7211 DNA was isolated from PW broth cultures using the Blood & Cell Culture DNA Midi Kit (Qiagen). Sequencing was performed at Baseclear BV (Leiden, The Netherlands). Libraries were made

with the Nextera XT DNA Library Prep Kit (Illumina) and sequenced (PE-125) on an Illumina 2500 with 500 Mb output; and with PacBio RS II following manufacturer's protocol. Genome sequences of other *X. fastidiosa* strains were retrieved from NCBI gene bank database (https://www.ncbi.nlm.nih.gov/genome/173) (**Table S6-1**).

Quality filtering, trimming, assembly, and annotation

Paired-end MiSeq FASTQ files were quality assessed with FastQC (Babraham Bioinformatics) and trimmed with Trimmomatic-0.35 (Bolger et al. 2014). Trimming removed adapter sequences, bases with Phred quality scores < 20 (1% error probability) from the beginning and end of the reads, and reads that contained <20 phred score for an average of four contiguous bases (sliding window trimming of 4:20). Trimmed reads (>36 bp) were *de novo* assembled using SPAdes 3.9.0 (Bankevich et al. 2012) with careful mode and k-mer sizes of 21, 33, 55, 77, 99, and 127. For WM1-1 and AlmaEM3, sequenced by both MiSeq and PacBio, a hybrid assembly of SPAdes 3.9.0 was used. Resulting draft assemblies (contigs shorter than 200bp were discarded) were quality assessed with QUAST (Gurevich et al. 2013) using the Temecula1 genome as reference (Van Sluys et al. 2003). For reference alignment, forward and reverse reads were paired and mapped to the Temecula1 reference using Geneious map to reference algorithm using default settings for medium sensitivity. For PD7202 and PD7211, which were also sequenced by both Illumina and PacBio platforms, quality filtering was performed as per the instrument guidelines and also by FastQC. *De novo* assembly for sample PD7202 was performed using the long read assembler HINGE (Kamath et al. 2017). The assembly of sample PD7211 was performed using the HGAP and Quiver assembly protocol through the Pacific Biosciences SMRT Portal version 2.3.0, followed by manual scaffolding

guided by alignment of the assembled contigs against themselves and the PacBio reads. Misassemblies and nucleotide disagreement between the Illumina data and the assembled sequences were corrected with Pilon (Walker et al. 2014) version 1.21 for both samples.

Long PacBio sequence reads from a 10kb library were error-corrected with the PacBio SMRT-Portal software for the RS instrument using circular consensus PacBio sequence reads from a 2kb library. Reads longer than 100 bp and greater than 75% estimated accuracy were included in the final assembly, resulting in at least 24X depth of coverage.

Annotation of draft assemblies was performed by Prokaryotic Genome Annotation Pipeline and web-based RAST server (Aziz et al. 2008). Information for read and assembly statistics, breadth and depth of coverage, and annotation results are summarized in **Tables S6-2** and **S6-3**. The hybrid assembly using reads from MiSeq and PacBio greatly improved the assembly as indicated by reduction in the number of contigs and an increase in N50 values (**Table S6-2**). However, even with the hybrid approach, most assemblies were still fragmented possibly due to the presence of repeat regions >7kb, as analyzed by repeat finder algorithm in Geneious for Temecula1. Previous draft genome assemblies of *X. fastidiosa* have also reported similar genome fragmentation (Chen et al. 2016; Zhang et al. 2011).

References

Aziz, R. K., Bartels, D., Best, A. A., DeJongh, M., Disz, T., Edwards, R. A., Formsma, K., Gerdes, S., Glass, E. M., and Kubal, M. 2008. The RAST Server: rapid annotations using subsystems technology. BMC Genomics 9:75.

Bankevich, A., Nurk, S., Antipov, D., Gurevich, A. A., Dvorkin, M., Kulikov, A. S., Lesin, V. M., Nikolenko, S. I., Pham, S., Prjibelski, A. D., Pyshkin, A. V., Sirotkin, A. V., Vyahhi, N., Tesler, G., Alekseyev, M. A., and Pevzner, P. A. 2012. SPAdes: a new genome assembly algorithm and its applications to single-cell sequencing. Journal of computational biology: a journal of computational molecular cell biology 19:455-477.

Bolger, A. M., Lohse, M., and Usadel, B. 2014. Trimmomatic: a flexible trimmer for Illumina sequence data. Bioinformatics 30:2114-2120.

Chen, J., Wu, F., Zheng, Z., Deng, X., Burbank, L. P., and Stenger, D. C. 2016. Draft Genome Sequence of *Xylella fastidiosa* subsp. *fastidiosa* Strain Stag's Leap. Genome Announc 4:e00240-00216.

Doyle, J. J., and Dickson, E. E. 1987. Preservation of plant samples for DNA restriction endonuclease analysis. Taxon 36:715-722.

Gurevich, A., Saveliev, V., Vyahhi, N., and Tesler, G. 2013. QUAST: quality assessment tool for genome assemblies. Bioinformatics 29:1072-1075.

Kamath, G. M., Shomorony, I., Xia, F., Courtade, T. A., and Tse, D. N. 2017. HINGE: long-read assembly achieves optimal repeat resolution. Genome Res 27:747-756.

Kandel, P. P., Lopez, S. M., Almeida, R. P., and De La Fuente, L. 2016. Natural Competence of *Xylella fastidiosa* Occurs at a High Frequency Inside Microfluidic Chambers Mimicking the Bacterium's Natural Habitats. Appl Environ Microbiol 82:5269-5277.

Kandel, P. P., Almeida, R. P. P., Cobine, P. A., and De La Fuente, L. 2017. Natural competence rates are variable among *Xylella fastidiosa* strains and homologous recombination occurs in vitro between subspecies *fastidiosa* and *multiplex*. Mol Plant Microbe Interact 30:589-600.

Matsumoto, A., Young, G. M., and Igo, M. M. 2009. Chromosome-based genetic complementation system for *Xylella fastidiosa*. Appl Environ Microbiol 75:1679-1687.

Newman, K. L., Almeida, R. P., Purcell, A. H., and Lindow, S. E. 2003. Use of a green fluorescent strain for analysis of *Xylella fastidiosa* colonization of *Vitis vinifera*. Appl Environ Microbiol 69:7319-7327.

Oliver, J. E., Sefick, S. A., Parker, J. K., Arnold, T., Cobine, P. A., and De La Fuente, L. 2014. Ionome changes in *Xylella fastidiosa*-infected *Nicotiana tabacum* correlate with virulence and discriminate between subspecies of bacterial isolates. Mol Plant Microbe Interact 27:1048-1058.

Roper, M. C., Greve, L. C., Warren, J. G., Labavitch, J. M., and Kirkpatrick, B. C. 2007. *Xylella fastidiosa* requires polygalacturonase for colonization and pathogenicity in *Vitis vinifera* grapevines. Mol Plant Microbe Interact 20:411-419.

Van Sluys, M. A., de Oliveira, M. C., Monteiro-Vitorello, C. B., Miyaki, C. Y., Furlan, L. R., Camargo, L. E., da Silva, A. C., Moon, D. H., Takita, M. A., Lemos, E. G., Machado, M. A., Ferro, M. I., da Silva, F. R., Goldman, M. H., Goldman, G. H., Lemos, M. V., El-Dorry, H., Tsai, S. M., Carrer, H., Carraro, D. M., de Oliveira, R. C., Nunes, L. R., Siqueira, W. J., Coutinho, L. L., Kimura, E. T., Ferro, E. S., Harakava, R., Kuramae, E. E., Marino, C. L., Giglioti, E., Abreu, I. L., Alves, L. M., do Amaral, A. M., Baia, G. S., Blanco, S. R., Brito, M. S., Cannavan, F. S., Celestino, A. V., da Cunha, A. F., Fenille, R. C., Ferro, J. A., Formighieri, E. F., Kishi, L. T., Leoni, S. G., Oliveira, A. R., Rosa, V. E., Jr., Sassaki, F. T., Sena, J. A., de Souza, A. A., Truffi, D., Tsukumo, F., Yanai, G. M., Zaros, L. G., Civerolo, E. L., Simpson, A. J., Almeida, N. F., Jr., Setubal, J. C., and Kitajima, J. P. 2003. Comparative analyses of the complete genome sequences of Pierce's disease and citrus variegated chlorosis strains of *Xylella fastidiosa*. J Bacteriol 185:1018-1026.

Walker, B. J., Abeel, T., Shea, T., Priest, M., Abouelliel, A., Sakthikumar, S., Cuomo, C. A., Zeng, Q. D., Wortman, J., Young, S. K., and Earl, A. M. 2014. Pilon: An Integrated Tool

for Comprehensive Microbial Variant Detection and Genome Assembly Improvement. PLoS One 9:e112963.
Zhang, S., Flores-Cruz, Z., Kumar, D., Chakrabarty, P., Hopkins, D. L., and Gabriel, D. W. 2011. The *Xylella fastidiosa* biocontrol strain EB92-1 genome is very similar and syntenic to Pierce's disease strains. J Bacteriol 193:5576-5577.

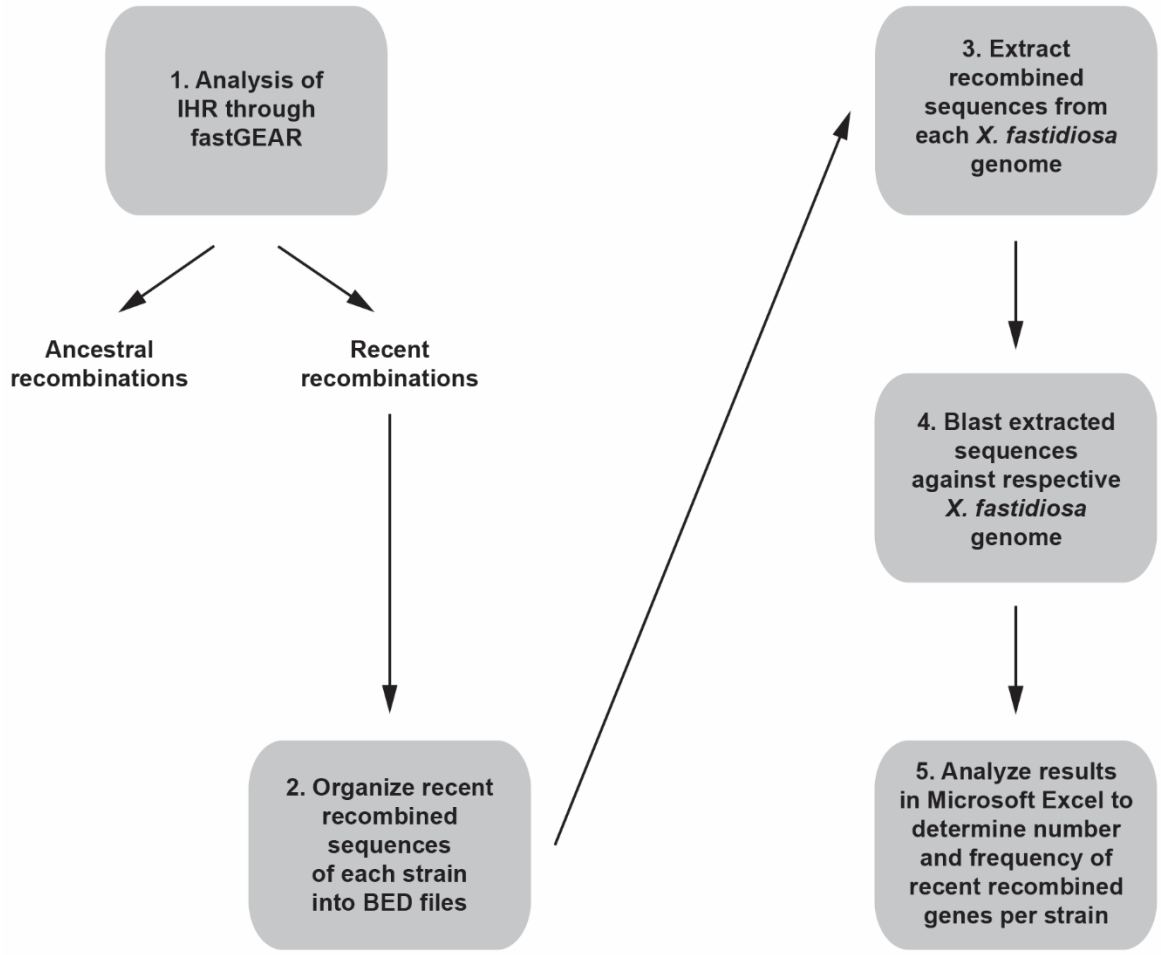

Fig. S6-1. Pipeline to determine the number and frequency of recent recombination events of each gene per *X. fastidiosa* strain. The recent recombination events output from fastGEAR were organized into separate BED files for each *X. fastidiosa* strain. Then, the recombined sequences were extracted from their respective genome using the GetFastaBed tool. Extracted sequences were submitted to blastx using as database the annotated genome of its respective *X. fastidiosa* genome. At last, the obtained hits were analyzed using Microsoft Excel to determine the number and frequency of recent recombined genes per strain.

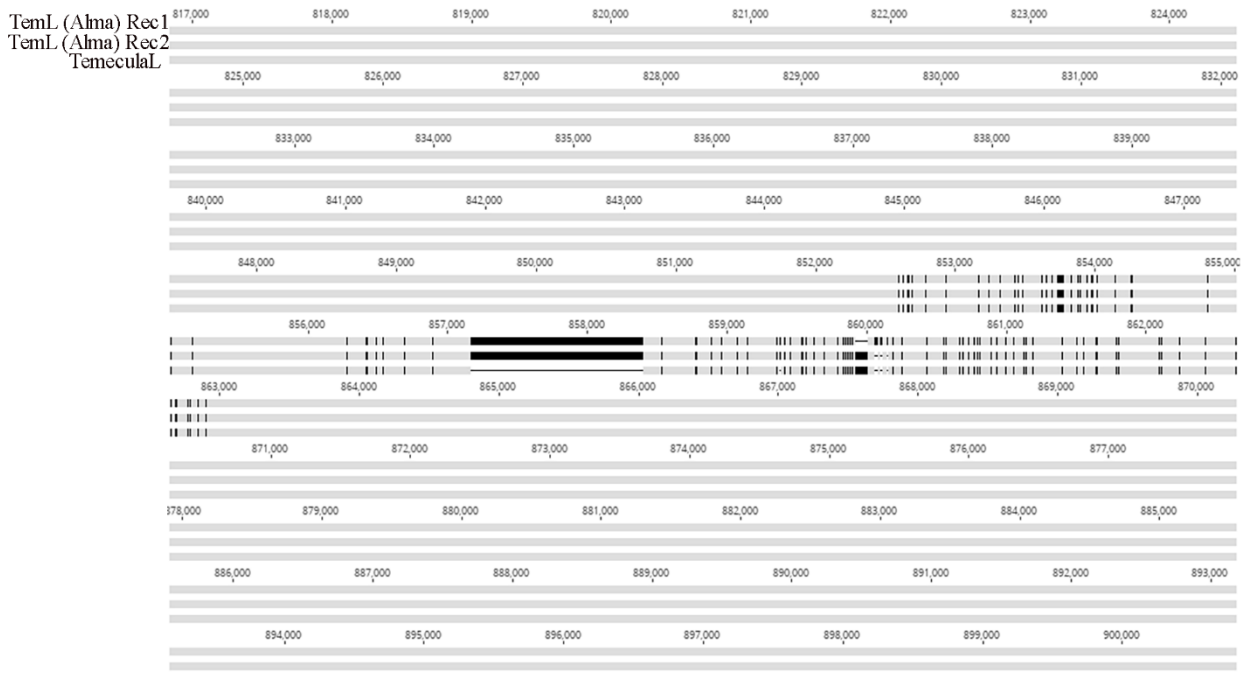

Fig. S6-2. Detection of intersubspecific recombination in the flanking region of the Kanamycin (Km)-resistance insertion site in the in vitro recombinants produced by mixing live cells of TemeculaL with heat-killed cells of AlmaEM3(NS1::Km^{R}). Genomic sequences of the two recombinants [TemL(Alma) Rec1 and Rec2] were aligned with the TemeculaL recipient sequence (alignment was wrapped to show bigger region). A 10kb region indicated by dark vertical strips in the alignment is the recombined region in TemL (Alma) Rec1. The kanamycin region is indicated by continuous horizontal strip that is only present in the recombinants and not in the recipient TemeculaL (indicated by narrow line below the continuous black strip). TemL (Alma) Rec 2 showed only a 3.5 kb region that was recombined from the donor. Except at the flanking region of Km insertion, other regions were identical in the three sequences as indicated by lack of polymorphisms (no black strips) according to this analysis.

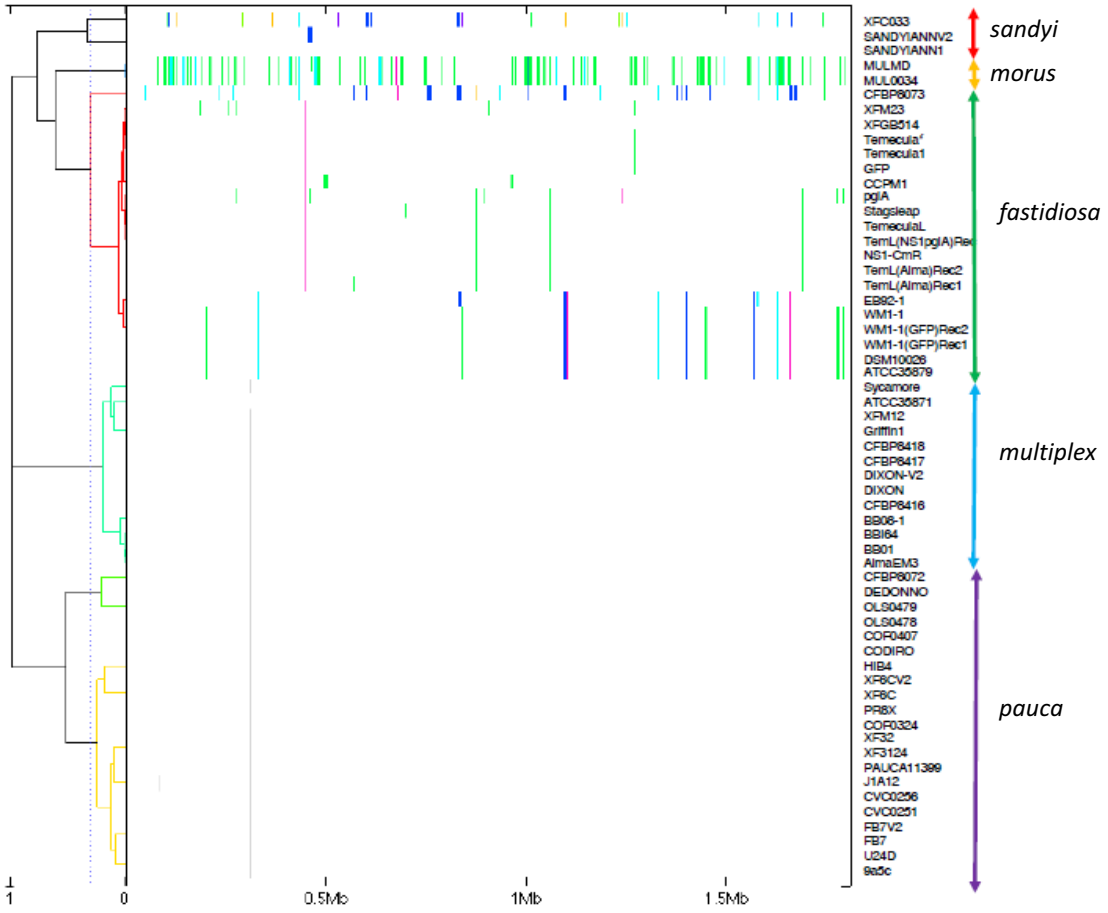

Fig. S6-3. Recombination analysis performed using BratNextGen on the core genome alignment of 55 *X. fastidiosa* strains analyzed in this study. The left panel corresponds to the Proportion of Shared Ancestry (PSA) tree computed by BratNextGen. In the PSA tree, strains are clustered together according to the proportion of sequence they share, including recombinant regions. The right panel shows a horizontal representation of the recombinant segments predicted for each strain. Colors were arbitrarily assigned, fragments of the same color and in the same column are from the same origin across different strains. Recombinant regions were detected in the genomes of subsp. *fastidiosa*, *morus*, and *sandyi*, but not in subsp. *multiplex* and *pauca*.

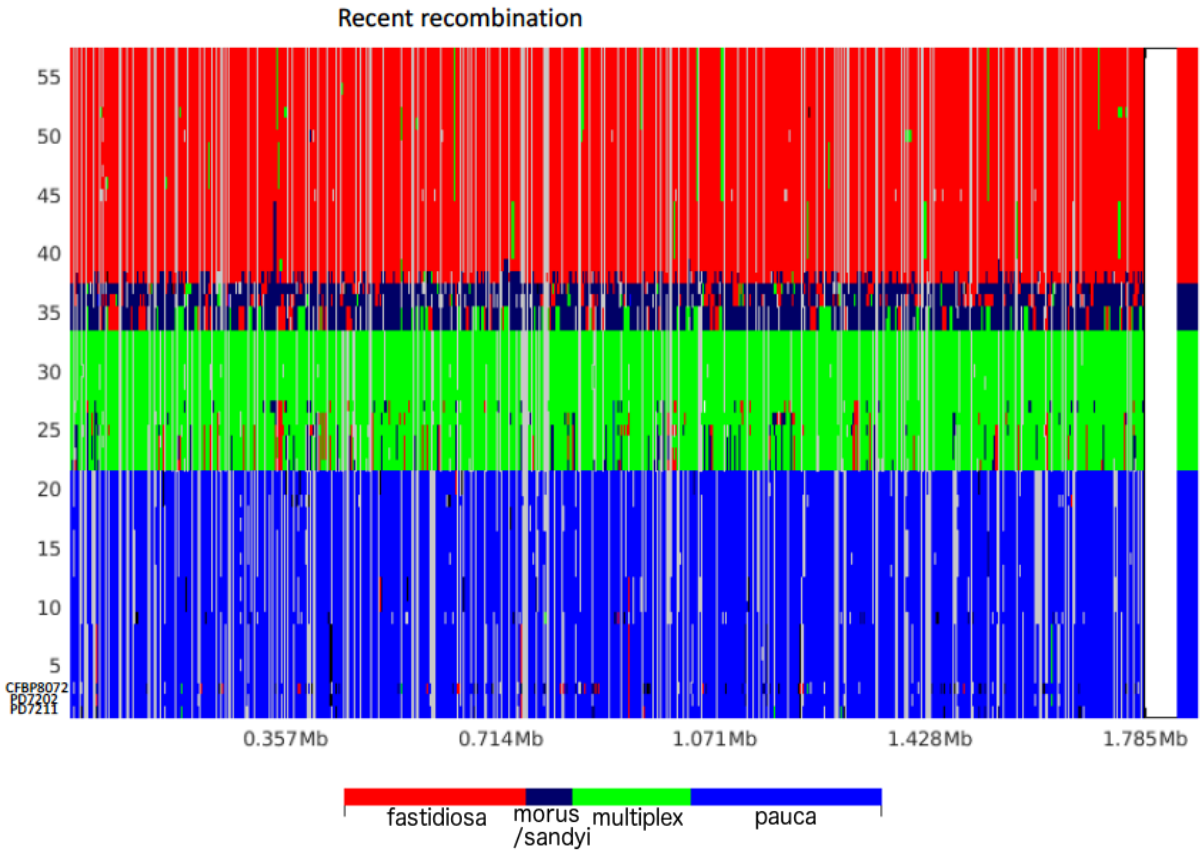

Fig. S6-4. Distribution, origin and proportion of recent recombination events across the *X. fastidiosa* core genome of 57 strains as predicted by fastGEAR as described in materials and methods and Fig. 6-5. This core genome included two strains isolated in the Netherlands from intercepted coffee plants shipped from Costa Rica, PD7202 and PD7211. The recent recombination events were detected in PD7211 and CFBP8072 to a greater extent as compared to PD7202.

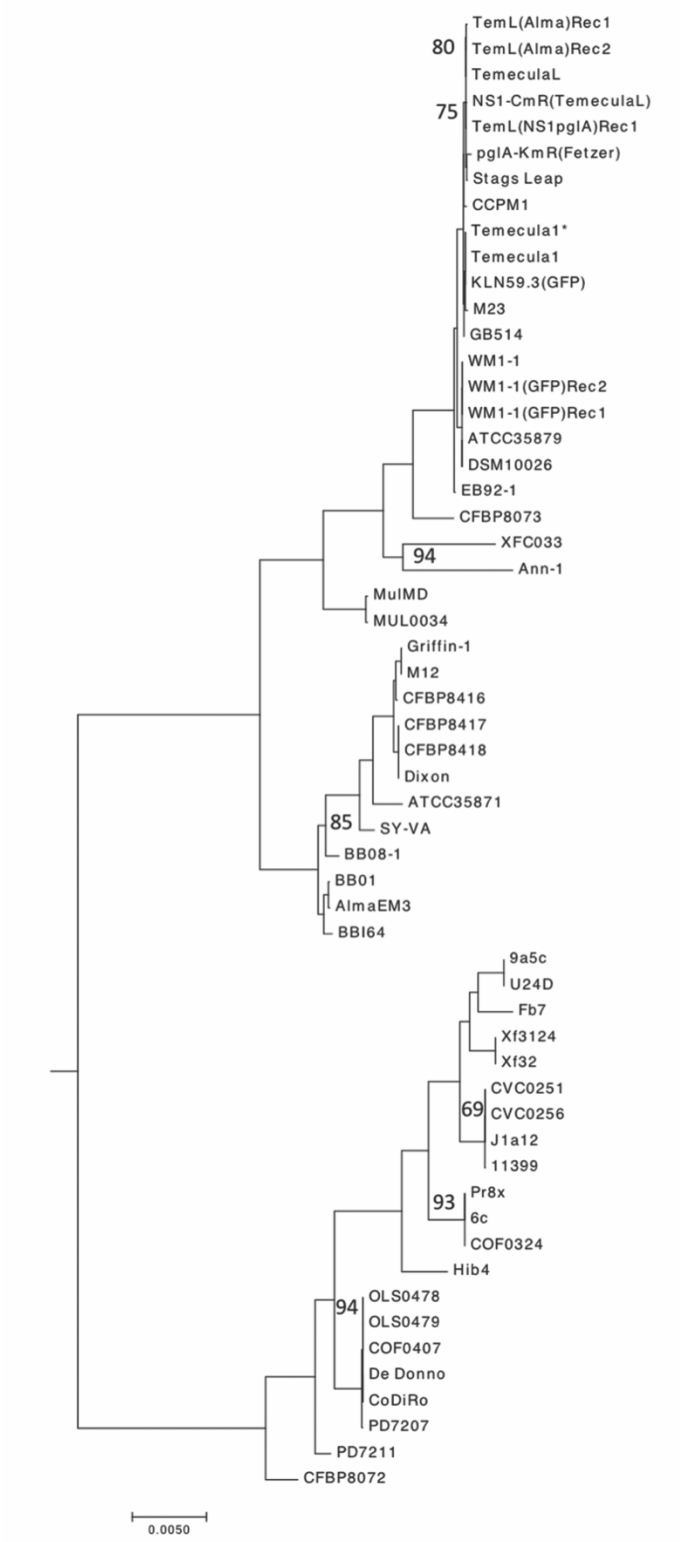

Fig. S6-5. Maximum likelihood phylogeny of core genome alignment of *X. fastidiosa* strains including intercepted strains PD7202 and PD7211. The phylogenetic tree was mid-point rooted, representing increasing order of nodes. Bootstrap support was > 98% for all nodes except where otherwise indicated.

Table S6-1. Strains, mutants, and recombinants used in this study.

Strain	Host plant	Sequence type[g]	Place of isolation	Reference	GenBank Accession
X.f.* subsp. *fastidiosa					
WM1-1	Grape	ST 2	USA (GA)	(Parker et al. 2012)	PUJK00000000
CCPM1	Grape	ST 1	USA (GA)	(Parker et al. 2012)	PUJB00000000
Temecula1[a]	Grape	ST 1	USA (CA)	(Van Sluys et al. 2003)	AE009442.1
Temecula1*	Grape	ST 1	USA (CA)	(Oliver et al. 2014)	PUJI00000000
TemeculaL[b]	Grape	ST 1	USA (CA)	This study	PUJJ00000000
pglA-Km^R (Fetzer)[c]	Grape	ST 4	USA (CA)	(Roper et al. 2007)	PUJH00000000
M23[a]	Almond	ST 1	USA (CA)	(Chen et al. 2010)	CP001011.1
Stags Leap[a]	Grape	ST 1	USA (CA)	(Chen et al. 2016)	LSMJ00000000.1
GB154[a]	Grape	ST 1	USA (TX)	(Schreiber et al. 2010)	CP002165.1
ATCC35879[a]	Grape	ST 2	USA (FL)	(Chen J, unpublished)	JQAP00000000.1
DSM10026[a]	Grape	ST 2	USA (FL)	(Varghese JN, unpublished)	FQWN00000000.1
EB92-1[a]	Elderberry	ST 1	USA (FL)	(Zhang et al. 2011)	AFDJ00000000.1
NS1-Cm^R (TemeculaL)[c]	Mutant of TemeculaL[f]	ST 1	In vitro	(Matsumoto et al. 2009)	PUJF00000000
KLN59.3 (GFP) (Temecula1)[c]	Mutant of Temecula1	ST 1	In vitro	(Newman et al. 2003)	PUJC00000000
TemL(NS1pglA) Rec 1[d]	Recombinant of NS1-CmR and pglA-KmR	ST 1	In vitro	(Kandel et al. 2016)	PUJG00000000
TemL(Alma) Rec 1[e]	Recombinant of TemeculaL with AlmaEM3 donor	ST 1	In vitro	This study	PUIW00000000
TemL(Alma) Rec 2[e]	Recombinant of TemeculaL with AlmaEM3 donor	ST 1	In vitro	This study	PUIX00000000
WM1-1(GFP) Rec 1[e]	Recombinants of WM1-1 with	ST 2	In vitro	(Kandel et al. 2017)	PUJD00000000

	KLN59.3 donor				
WM1-1 (GFP) Rec 2[e]	Recombinants of WM1-1 with KLN59.3 donor	ST 2	In vitro	(Kandel et al. 2017)	PUJE00000000
CFBP8073[a]	Coffee	ST 75	France (imported from Mexico)	(Jacques et al. 2016)	LKES00000000.1
X.f.* subsp. *sandyi					
Ann-1[a]	Oleander	ST 5	USA (CA)	(Schuenzel et al. 2005)	AAAM00000000.4
XFCO33[a]	Coffee	ST 72	Italy (imported from Costa Rica)	(Giampetruzzi et al. 2015a)	LJZW00000000.1
X.f.* subsp. *morus					
MUL0034[a]	Mulberry	ST 30	USA (CA)	(Schuenzel et al. 2005)	CP006740.1
Mul-MD[a]	Mulberry	ST 29	USA(MD)	(Guan et al. 2014)	AXDP00000000.1
X.f.* subsp. *multiplex					
AlmaEM3	Blueberry (Emerald)	ST 42	USA(GA)	(Oliver et al. 2014)	PUIY00000000
AlmaEM3(NS1::Km)	Recombinant of AlmaEM3 and plasmid containing KmR targeted to NS1 site	ST 42	In vitro	This study	
BBI64	Blueberry	ST 42	USA(GA)	(Oliver et al. 2014)	PUJA00000000
BB08-1	Blueberry	ST 43	USA(FL)	(Oliver et al. 2014)	PUIZ00000000
BB01[a]	Blueberry	ST 42	USA (GA)	(Van Horn et al. 2017)	MPAZ00000000.1
ATCC35871[a]	Hybrid Plum	ST 41	USA (GA)	(Kyrpides et al, unpublished)	AUAJ00000000.1
Griffin-1[a]	Oak	ST 7	USA (GA)	(Chen et al. 2013)	AVGA00000000.1
Dixon[a]	Almond	ST 6	USA (CA)	(Copeland et al, unpublished)	AAAL00000000.2
SY-VA[a]	Sycamore	ST 8	USA (VA)	(Guan et al. 2014)	JMHP00000000.1

CFBP8416[a]	Myrtle-leaf milkwort	ST 7	France	(Denance et al. 2017)	GCA_001971475.1
CFBP8417[a]	Spanish Broom	ST 6	France	(Denance et al. 2017)	LUYB00000000.1
CFBP8418[a]	Spanish Broom	ST 6	France	(Denance et al. 2017)	LUYA00000000.1
M12[a]	Almond	ST 7	USA (CA)	(Chen et al. 2010)	CP000941.1
X.f.* subsp. *pauca					
9a5c[a]	Sweet orange	ST 13	Brazil (São Paulo)	(Simpson et al. 2000)	AE003849.1
U24D[a]	Sweet orange	ST 13	Brazil (São Paulo)	(Da Silva, 2017 unpublished)	CP009790.1
J1a12[a]	Sweet orange	ST 11	Brazil (São Paulo)	(Pierry and da Silva, 2017, unpublished)	CP009823.1
CVC0256[a]	Sweet orange	ST 11	Brazil	(Knight et al, 2017, unpublished)	LRVF00000000.1
CVC0251[a]	Sweet orange	ST 11	Brazil	(Knight et al, 2017, unpublished)	LRVE00000000.1
11399[a]	Orange	ST 11	Brazil	(Niza et al. 2016)	JNBT00000000.1
Hib4[a]	Hibiscus	ST 70	Brazil (São Paulo)	(Pierry and da Silva, 2017, unpublished)	CP009885.1
COF0324[a]	Coffee	ST 14	Brazil	(Knight et al, 2017, unpublished)	LRVG00000000.1
Xf32[a]	Coffee	ST 16	Brazil (São Paulo)	(Alencar et al. 2014)	AWYH00000000.1
6c[a]	Coffee	ST 14	Brazil (São Paulo)	(Alencar et al. 2014)	AXBS00000000.2
Fb7[a]	Sweet orange	ST 69	Argentina (Corrientes)	(da Silva et al. 2007)	CP010051.2
Xf3124[a]	Coffee	ST 16	Brazil (São Paulo)	(Li et al. 2001)	CP009829.1
Pr8x[a]	Plum	ST 14	Brazil (São Paulo)	(Pierry and da Silva 2015, unpublished)	CP009826.1
CFBP8072[a]	Coffee	ST 74	France (imported	(Jacques et al. 2016)	LKDK00000000.1

			from Ecuador)		
CoDiRo[a]	Olive	ST 53	Italy (Apulia)	(Giampetruzzi et al. 2015b)	JUJW00000000.1
De Donno[a]	Olive	ST 53	Italy (Apulia)	(Giampetruzzi et al. 2017)	CP020870.1
COF0407[a]	Coffee	ST 53	Costa Rica	(Knight et al, 2017, unpublished)	LRVJ00000000.1
OLS0478[a]	Oleander	ST 53	Costa Rica	(Knight et al, 2017, unpublished)	LRVI00000000.1
OLS0479[a]	Oleander	ST 53	Costa Rica	(Knight et al, 2017, unpublished)	LRVH00000000.1
PD7202	Coffee	ST 53[h]	Netherlands (imported from Costa Rica)	(Bergsma-Vlami et al. 2017)	RRUA00000000
PD7211	Coffee	ST 73[h]	Netherlands (imported from Costa Rica)	(Bergsma-Vlami et al. 2017)	RRTZ00000000

[a]Genomes were obtained from NCBI. All other genomes were sequenced in this study.
[b]Variant of Temecula1 confirmed by whole genome sequencing in this study.
[c]Name in parenthesis indicate wild type background used for mutation.
[d]Recombinant produced by co-culturing live donor and recipient cells (Kandel et al., 2016). Name between parentheses indicate source of donor DNA.
[e]Recombinant produced by co-culturing heat-killed donor and live recipient cells (Kandel et al., 2017). Name between parentheses indicate source of donor DNA.
[f]This study determined the background strain of this mutant to be TemeculaL.
[g]Sequence type information obtained from the *Xylella fastidiosa* MLST databases (<https://pubmlst.org/xfastidiosa/>).
[h]Sequence type information taken from Bergsma-Vlami et al., 2017.

References

Alencar, V. C., Barbosa, D., Santos, D. S., Oliveira, A. C., de Oliveira, R. C., and Nunes, L. R. 2014. Genomic Sequencing of Two Coffee-Infecting Strains of *Xylella fastidiosa* Isolated from Brazil. Genome Announc 2:e01190-13.

Bergsma-Vlami, M., van de Bilt, J. L. J., Tjou-Tam-Sin, N. N. A., Helderman, C. M., Gorkink-Smits, P., Landman, N. M., van Nieuwburg, J. G. W., van Veen, E. J., and Westenberg, M. 2017. Assessment of the genetic diversity of *Xylella fastidiosa* in imported ornamental *Coffea arabica* plants. Plant Pathology 66:1065-1074.

Chen, J., Huang, H., Chang, C. J., and Stenger, D. C. 2013. Draft Genome Sequence of *Xylella fastidiosa* subsp. *multiplex* Strain Griffin-1 from *Quercus rubra* in Georgia. Genome Announc 1:e00756-13.

Chen, J., Xie, G., Han, S., Chertkov, O., Sims, D., and Civerolo, E. L. 2010. Whole genome sequences of two *Xylella fastidiosa* strains (M12 and M23) causing almond leaf scorch disease in California. J Bacteriol 192:4534.

Chen, J., Wu, F., Zheng, Z., Deng, X., Burbank, L. P., and Stenger, D. C. 2016. Draft Genome Sequence of *Xylella fastidiosa* subsp. *fastidiosa* Strain Stag's Leap. Genome Announc 4:e00240-00216.

da Silva, V. S., Shida, C. S., Rodrigues, F. B., Ribeiro, D. C. D., de Souza, A. A., Coletta-Filho, H. D., Machado, M. A., Nunes, L. R., and de Oliveira, R. C. 2007. Comparative genomic characterization of citrus-associated *Xylella fastidiosa* strains. BMC Genomics 8:474-474.

Denance, N., Legendre, B., Briand, M., Olivier, V., de Boisseson, C., Poliakoff, F., and Jacques, M. A. 2017. Several subspecies and sequence types are associated with the emergence of *Xylella fastidiosa* in natural settings in France. Plant Pathology 66:1054-1064.

Giampetruzzi, A., Saponari, M., Almeida, R. P. P., Essakhi, S., Boscia, D., Loconsole, G., and Saldarelli, P. 2017. Complete Genome Sequence of the Olive-Infecting Strain *Xylella fastidiosa* subsp. *pauca* De Donno. Genome announcements 5:e00569-00517.

Giampetruzzi, A., Loconsole, G., Boscia, D., Calzolari, A., Chiumenti, M., Martelli, G. P., Saldarelli, P., Almeida, R. P., and Saponari, M. 2015a. Draft Genome Sequence of CO33, a Coffee-Infecting Isolate of *Xylella fastidiosa*. Genome Announc 3:e01472-15.

Giampetruzzi, A., Chiumenti, M., Saponari, M., Donvito, G., Italiano, A., Loconsole, G., Boscia, D., Cariddi, C., Martelli, G. P., and Saldarelli, P. 2015b. Draft Genome Sequence of the *Xylella fastidiosa* CoDiRO Strain. Genome Announc 3:e01538-14.

Guan, W., Shao, J., Davis, R. E., Zhao, T., and Huang, Q. 2014. Genome Sequence of a *Xylella fastidiosa* Strain Causing Sycamore Leaf Scorch Disease in Virginia. Genome Announc 2:e00773-14.

Jacques, M. A., Denance, N., Legendre, B., Morel, E., Briand, M., Mississipi, S., Durand, K., Olivier, V., Portier, P., Poliakoff, F., and Crouzillat, D. 2016. New Coffee Plant-Infecting *Xylella fastidiosa* Variants Derived via Homologous Recombination. Appl Environ Microbiol 82:1556-1568.

Kandel, P. P., Lopez, S. M., Almeida, R. P., and De La Fuente, L. 2016. Natural Competence of *Xylella fastidiosa* Occurs at a High Frequency Inside Microfluidic Chambers Mimicking the Bacterium's Natural Habitats. Appl Environ Microbiol 82:5269-5277.

Kandel, P. P., Almeida, R. P. P., Cobine, P. A., and De La Fuente, L. 2017. Natural competence rates are variable among *Xylella fastidiosa* strains and homologous recombination occurs in vitro between subspecies *fastidiosa* and *multiplex*. Mol Plant Microbe Interact 30:589-600.

Li, W. B., D. Pria, W., Teixeira, D., Miranda, V., Ayres, A. J., F. Franco, C., Costa, M., He, C. X., Costa, P., and Hartung, J. 2001. Coffee Leaf Scorch Caused by a Strain of *Xylella fastidiosa* from Citrus. Plant Dis 85:501-505.

Matsumoto, A., Young, G. M., and Igo, M. M. 2009. Chromosome-based genetic complementation system for *Xylella fastidiosa*. Appl Environ Microbiol 75:1679-1687.

Newman, K. L., Almeida, R. P., Purcell, A. H., and Lindow, S. E. 2003. Use of a green fluorescent strain for analysis of *Xylella fastidiosa* colonization of *Vitis vinifera*. Appl Environ Microbiol 69:7319-7327.

Niza, B., Merfa, M. V., Alencar, V. C., Menegidio, F. B., Nunes, L. R., Machado, M. A., Takita, M. A., and de Souza, A. A. 2016. Draft Genome Sequence of 11399, a Transformable Citrus-Pathogenic Strain of *Xylella fastidiosa.* Genome Announc 4:e01124-01116.

Oliver, J. E., Sefick, S. A., Parker, J. K., Arnold, T., Cobine, P. A., and De La Fuente, L. 2014. Ionome changes in *Xylella fastidiosa*-infected *Nicotiana tabacum* correlate with virulence and discriminate between subspecies of bacterial isolates. Mol Plant Microbe Interact 27:1048-1058.

Parker, J. K., Havird, J. C., and De La Fuente, L. 2012. Differentiation of *Xylella fastidiosa* strains via multilocus sequence analysis of environmentally mediated genes (MLSA-E). Appl Environ Microbiol 78:1385-1396.

Roper, M. C., Greve, L. C., Warren, J. G., Labavitch, J. M., and Kirkpatrick, B. C. 2007. *Xylella fastidiosa* requires polygalacturonase for colonization and pathogenicity in *Vitis vinifera* grapevines. Mol Plant Microbe Interact 20:411-419.

Schreiber, H. L., Koirala, M., Lara, A., Ojeda, M., Dowd, S. E., Bextine, B., and Morano, L. 2010. Unraveling the First *Xylella fastidiosa* subsp *fastidiosa* Genome from Texas. Southwestern Entomologist 35:479-483.

Schuenzel, E. L., Scally, M., Stouthamer, R., and Nunney, L. 2005. A multigene phylogenetic study of clonal diversity and divergence in North American strains of the plant pathogen *Xylella fastidiosa*. Appl Environ Microbiol 71:3832-3839.

Simpson, A. J. G., Reinach, F., Arruda, P., Abreu, F., Acencio, M., Alvarenga, R., Alves, L. C., Araya, J., Baia, G., and Baptista, C. 2000. The genome sequence of the plant pathogen *Xylella fastidiosa*. Nature 406:151-157.

Van Horn, C., Chang, C.-J., and Chen, J. 2017. De Novo Whole-Genome Sequence of *Xylella fastidiosa* subsp. *multiplex* Strain BB01 Isolated from a Blueberry in Georgia, USA. Genome Announc 5:e01598-01516.

Van Sluys, M. A., de Oliveira, M. C., Monteiro-Vitorello, C. B., Miyaki, C. Y., Furlan, L. R., Camargo, L. E., da Silva, A. C., Moon, D. H., Takita, M. A., Lemos, E. G., Machado, M. A., Ferro, M. I., da Silva, F. R., Goldman, M. H., Goldman, G. H., Lemos, M. V., El-Dorry, H., Tsai, S. M., Carrer, H., Carraro, D. M., de Oliveira, R. C., Nunes, L. R., Siqueira, W. J., Coutinho, L. L., Kimura, E. T., Ferro, E. S., Harakava, R., Kuramae, E. E., Marino, C. L., Giglioti, E., Abreu, I. L., Alves, L. M., do Amaral, A. M., Baia, G. S., Blanco, S. R., Brito, M. S., Cannavan, F. S., Celestino, A. V., da Cunha, A. F., Fenille, R. C., Ferro, J. A., Formighieri, E. F., Kishi, L. T., Leoni, S. G., Oliveira, A. R., Rosa, V. E., Jr., Sassaki, F. T., Sena, J. A., de Souza, A. A., Truffi, D., Tsukumo, F., Yanai, G. M., Zaros, L. G., Civerolo, E. L., Simpson, A. J., Almeida, N. F., Jr., Setubal, J. C., and Kitajima, J. P. 2003. Comparative analyses of the complete genome sequences of Pierce's disease and citrus variegated chlorosis strains of *Xylella fastidiosa*. J Bacteriol 185:1018-1026.

Zhang, S., Flores-Cruz, Z., Kumar, D., Chakrabarty, P., Hopkins, D. L., and Gabriel, D. W. 2011. The *Xylella fastidiosa* biocontrol strain EB92-1 genome is very similar and syntenic to Pierce's disease strains. J Bacteriol 193:5576-5577.

Table S6-2. Sequencing and assembly statistics of the genomes sequenced in this study.

Strain	#Reads[a]	#Reads post-trim[b]	Read length	Covg[c]	#Ctgs[d]	Size (Mbp)[e]	N50[f]	L50[g]	Refseq identity[h] (%)
WM1-1	2942684	2587777	138.7	145.2	113 34[i]	2.45 2.47[i]	148434 238450[i]	5 4[i]	99.7
AlmaEM3	722996	654360	135.7	35.8	100 30[i]	2.46 2.48[i]	115714 271106[i]	7 4[i]	96.3
TemL (Alma) Rec1	1268086	1143060	131.1	59.4	120	2.52	115978	7	99.3
TemL (Alma) Rec2	1234660	640702	150.5	27.6	402	2.74	103360	6	99.9
TemeculaL	2140558	1334223	113.8	57.4	162	2.54	93631	8	99.8
Temecula1*	1960132	1751487	153.9	109.7	113	2.45	99386	6	100
pglA-Km^R(Fetzer)	818192	741373	127.4	37.9	146	2.49	97642	6	99.8
NS1-Cm^R	319068	316673	158.8	20.0	254	2.51	27752	29	99.7
TemL (NS1 pglA) Rec 1	1400214	1285143	151.0	76.8	124	2.53	135060	5	99.9
KlN59.3 (GFP) (Temecula1)	3415272	3090572	146.2	183.6	117	2.46	103359	6	100
WM1-1 (GFP) Rec1	3133800	2842830	147.6	171.2	105	2.45	134853	6	99.6
WM1-1 (GFP) Rec2	3048060	2730936	140.4	156.2	125	2.45	134871	6	99.6
BBI64	98736	75586	5547.5	23	104	2.88	219218	6	NA
BB08-1	84733	62746	5392.5	24	98	2.92	175843	4	NA
CCPM1	58951	41019	5286.5	21	88	2.82	168016	5	NA
PD7202	8775306	NA	NA	401,2	3	2.63	2566522	1	NA
PD7211	9134670	NA	NA	405.9	3	2.65	2587308	1	NA

[a]Number of reads produced by the sequencing run.
[b]Number of reads that survived trimming.
[c]Average depth of coverage.
[d]Number of contigs.
[e]Genome size.
[f]Size of the contig such that more than half of the assembly is contained in contigs longer than this value.
[g]Number of contigs that contain more than 50% of the total assembly.
[h]Percent identity with the reference Temecula1 genome based on reference mapping. NA, Reference assembly was not performed as only PacBio reads were available.
[i]Assembly statistics of a hybrid assembly from Illumina and PacBio reads.
NA: Not available.

Table S6-3. Annotation results of the genomes sequenced in this study.

Strain	# Genes	CDS[a] (total)	CDS[a] (coding)	rRNA[b]	tRNA[c]	ncRNA[d]	Pseudo[e]	GC[f] (%)
WM1-1	2,334	2,275	2,161	2	49	4	114	51.6
AlmaEM3	2,341	2,281	2,117	2	50	4	164	51.7
TemL (Alma) Rec1	2,454	2,394	2,272	2	50	4	122	51.5
TemL (Alma) Rec2	2,584	2,520	2,396	2	50	4	124	51.1
TemeculaL	2,479	2,419	2,296	2	50	4	123	51.5
Temecula1*	2,374	2,320	2,211	1	47	4	109	51.5
pglA-Km^R (Fetzer)	2,433	2,373	2,240	2	50	4	133	51.5
NS1-Cm^R	2,533	2,478	2,347	1	48	4	131	51.5
TemL (NS1-pglA) Rec	2,463	2,403	2,272	2	50	4	131	51.5
KlN59.3 (GFP-Temecula1)	2,387	2,329	2,216	1	47	4	113	51.6
WM1-1 (GFP) Rec1	2,368	2,310	2,200	1	47	4	110	51.5
WM1-1 (GFP) Rec2	2,383	2,325	2,212	1	47	4	223	51.5
BBI64	2,863	2,774	2,378	3	69	4	396	51.7
BB08-1	2,834	2,751	2,357	4	63	6	394	51.8
CCPM1	2,720	2,642	2,336	3	59	6	306	51.8
PD7202	NA	NA	2,544	6	49	NA	NA	52.1
PD7211	NA	NA	2,562	6	49	NA	NA	52.2

[a]Coding sequence numbers.
[b]Number of ribosomal RNAs.
[c]Number of transfer RNAs.
[d]Number of non-coding RNAs.
[e]Number of pseudo genes.
[f]GC content expressed as percentage.
NA: Not available.

Table S6-4. Extent and origin of recent recombination in each strain of *X. fastidiosa* analyzed in this study using fastGEAR.

Strain name	Total length recombinant region (bp)	Recent recombination events (#)	Recombination origin: Total length of recombination region (number of events)				
			morus/sandyi	*multiplex*	*fastidiosa*	*pauca*	outside
morus/sandyi							
MUL0034	679015	164	0 (0)	329585(93)	348615 (68)	636 (2)	179 (1)
Mul-MD	656429	163	0 (0)	323899(92)	331715 (68)	636(2)	179 (1)
Ann-1	31415	23	0 (0)	3925(5)	27490 (18)	0 (0)	0 (0)
XFC033	671454	232	0 (0)	48615(42)	565554 (119)	38968 (41)	18317 (30)
multiplex							
Dixon	530	1	0 (0)	0 (0)	530(1)	0 (0)	0 (0)
CFBP8417	530	1	0 (0)	0 (0)	530(1)	0 (0)	0 (0)
CFBP8418	530	1	0 (0)	0 (0)	530(1)	0 (0)	0 (0)
M12	1107	2	577(1)	0 (0)	530(1)	0 (0)	0 (0)
Griffin-1	1107	2	577(1)	0 (0)	530(1)	0 (0)	0 (0)
CFBP8416	1107	2	577(1)	0 (0)	530(1)	0 (0)	0 (0)
ATCC35871	193473	135	104878(71)	0 (0)	87392(61)	660(1)	543(2)
SY-VA	166902	118	81539(61)	0 (0)	83649(54)	650(1)	1064(2)
BB01	289626	213	155027(108)	0 (0)	133431(103)	660(1)	508(1)
BB08-1	279510	222	144963(111)	0 (0)	133526(108)	660(1)	361(2)
BBI64	309987	232	169038(117)	0 (0)	139489(112)	660(1)	800(2)
AlmaEM3	287031	211	155450(108)	0 (0)	130428(101)	660(1)	493(1)
fastidiosa							
CCPM1	31035	14	414(1)	30621(13)	0 (0)	0 (0)	0 (0)
TemL(Alma)Rec1	35168	13	0 (0)	35168(13)	0 (0)	0 (0)	0 (0)
TemL(Alma)Rec2	30506	9	0 (0)	30506(9)	0 (0)	0 (0)	0 (0)
Temecula1	21347	8	0 (0)	21347(8)	0 (0)	0 (0)	0 (0)
TemeculaL	30138	8	0 (0)	30138(8)	0 (0)	0 (0)	0 (0)
Temecula1*	21347	8	0 (0)	21347(8)	0 (0)	0 (0)	0 (0)
NS1-CmR(TemeculaL)	30210	10	0 (0)	30151(9)	0 (0)	0 (0)	59(1)
TemL(NS1pglA)Rec1	30126	9	0 (0)	30087(8)	0 (0)	0 (0)	39(1)
pglA-KmR(Fetzer)	56747	26	1514(2)	54812(23)	0 (0)	0 (0)	421(1)
KLN59.3(GFP)	21296	8	0 (0)	21296(8)	0 (0)	0 (0)	0 (0)
WM1-1(GFP)Rec1	29831	16	5308(3)	24523(13)	0 (0)	0 (0)	0 (0)
WM1-1(GFP)Rec2	29888	17	5308(3)	24580(14)	0 (0)	0 (0)	0 (0)
WM1-1	29801	16	5308(3)	24493(13)	0 (0)	0 (0)	0 (0)
DSM10026	29345	17	5308(3)	23931(13)	0 (0)	0 (0)	106(1)
ATCC35879	29201	15	5308(3)	23893(12)	0 (0)	0 (0)	0 (0)
M23	32062	15	0 (0)	32062(15)	0 (0)	0 (0)	0 (0)
GB514	15384	4	0 (0)	15384(4)	0 (0)	0 (0)	0 (0)
EB92-1	24193	11	19917(7)	4276(4)	0 (0)	0 (0)	0 (0)
CFBP8073	494914	277	474384(229)	5215(12)	0 (0)	6696 (14)	8619 (22)
Stags Leap	34280	11	0 (0)	34280(11)	0 (0)	0 (0)	0 (0)
pauca							
9a5c	24357	52	8002(12)	2078(8)	1636(8)	0(0)	12641(24)
U24D	24465	53	8226(13)	2091(8)	1594(8)	0(0)	12554(24)
Fb7	46360	78	12239(19)	2992(10)	2417(10)	0(0)	28712(39)
Xf3124	19250	47	6807(17)	1678(9)	1414(5)	0(0)	9351(16)
Xf32	19304	47	6883(17)	1686(9)	1414(5)	0(0)	9321(16)
11399	9810	15	3782(6)	751(3)	574(2)	0(0)	4703(4)

J1a12	9797	15	3763(6)	757(3)	574(2)	0(0)	4703(4)
CVC0251	9838	15	3763(6)	757(3)	574(2)	0(0)	4744(4)
CVC0256	9810	15	3782(6)	751(3)	574(2)	0(0)	4703(4)
Pr8x	19845	46	4591(11)	2012(9)	1662(8)	0(0)	11580(18)
6c	19805	46	4591(11)	1977(9)	1646(8)	0(0)	11591(18)
COF0324	19831	46	4591(11)	2004(9)	1656(8)	0(0)	11580(18)
Hib4	57630	131	20319(35)	3719(16)	3471(17)	0(0)	30121(63)
COF0407	62932	91	20671(24)	5871(16)	11093(18)	0(0)	25297(33)
De Donno	62886	91	20553(24)	5891(16)	11104(18)	0(0)	25338(33)
CoDiRo	63153	91	20671(24)	5874(16)	11199(18)	0(0)	25409(33)
OLS0478	62932	91	20599(24)	5874(16)	11125(18)	0(0)	25334(33)
OLS0479	62978	91	20624(24)	5874(16)	11125(18)	0(0)	25355(33)
CFBP8072	250277	376	102349(123)	17508(48)	58911(77)	0(0)	71509(128)

Table S6-5. Ancestral recombination events in the core genome of *X. fastidiosa* predicted by fastGEAR. Lineages 1 and 2 are the lineages between which an ancestral recombination is detected. The direction of recombination is not identifiable in case of ancestral recombination.

Number of ancestral recombination events	Length of ancestral recombination region	Lineage1	Lineage2
91	877kb	*fastidiosa*	*morus/sandyi*
3	1.5kb	*pauca*	*morus/sandyi*
22	58kb	*multiplex*	*morus/sandyi*
37	47kb	*fastidiosa*	*multiplex*
1	1.5kb	*pauca*	*multiplex*
5	1.5kb	*pauca*	*fastidiosa*

Table S6-6. Complete list of genes under recent recombination used for Table 6-1, organized by COG numbers and description.

Category in the table	Gene	COG number	Description
Movement	*pilU*	COG5008	Tfp pilus assembly protein, ATPase PilU Cell motility, Extracellular structures
	pilT	COG2805	Tfp pilus assembly protein PilT, pilus retraction ATPase Cell motility, Extracellular structures
	pilY1	COG3419	Tfp pilus assembly protein, tip-associated adhesin PilY1 Cell motility, Extracellular structures
	pilQ	COG4796	Type II secretory pathway, component HofQ; Tfp secretin Intracellular trafficking, secretion, and vesicular transport
	fimT	COG4970	Tfp pilus assembly protein FimT Cell motility, Extracellular structures
	pilE	COG4968	Tfp pilus assembly protein PilE Cell motility, Extracellular structures
	pilA	COG4969	Tfp pilus assembly protein, major pilin PilA Cell motility, Extracellular structures
	Type 4 prepilin-like proteins leader peptide-processing enzyme	COG1989	Prepilin signal peptidase PulO (type II secretory pathway) or related peptidase Cell motility, Intracellular trafficking, secretion, and vesicular transport
Attachment	*smf-1*	COG3539	Pilin (type 1 fimbria component protein) Cell motility (?)
	yadV	COG3121	P pilus assembly protein, chaperone PapD Extracellular structures
	xadA1	COG5295	Autotransporter adhesin Intracellular trafficking, secretion, and vesicular transport, Extracellular structures
	xadA2	COG5295	Autotransporter adhesin Intracellular trafficking, secretion, and vesicular transport, Extracellular structures
	hsf	COG5295	Autotransporter adhesin Intracellular trafficking, secretion, and vesicular transport, Extracellular structures
	Fimbrial adhesin precursor	COG3539	Pilin (type 1 fimbria component protein) Cell motility (?)
Colonization degrading enzymes	*pulD*	COG1450	Type II secretory pathway component GspD/PulD (secretin) Intracellular trafficking, secretion, and vesicular transport
	gspE	COG2804	Type II secretory pathway ATPase GspE/PulE Cell motility, Intracellular trafficking, secretion, and vesicular transport, Extracellular structures
	pulF	COG1459	Type II secretory pathway, component PulF Cell motility, Intracellular trafficking, secretion, and vesicular transport, Extracellular structures
	pulG	COG2165	Type II secretory pathway, pseudopilin PulG Cell motility, Intracellular trafficking, secretion, and vesicular transport, Extracellular structures

	Xylan 1,4-xylosidase	COG1472	Periplasmic beta-glucosidase and related glycosidases Carbohydrate transport and metabolism
Regulation and signaling	*rpfF*	COG1024	Enoyl-CoA hydratase/carnithine racemase Lipid transport and metabolism
	rpfC	COG0642	Signal transduction histidine kinase Signal transduction mechanisms
	rpfG	COG3437	Response regulator c-di-GMP phosphodiesterase, RpfG family, contains REC and HD-GYP domains Signal transduction mechanisms
	luxQ	COG3292	Periplasmic ligand-binding sensor domain Signal transduction mechanisms
	ubiB	COG0661	Predicted unusual protein kinase regulating ubiquinone biosynthesis, AarF/ABC1/UbiB family Coenzyme transport and metabolism, Signal transduction mechanisms
	regB	COG0642	Signal transduction histidine kinase Signal transduction mechanisms
	cckA	COG0642	Signal transduction histidine kinase Signal transduction mechanisms
	pkn1	COG1262	Formylglycine-generating enzyme, required for sulfatase activity, contains SUMF1/FGE domain Posttranslational modification, protein turnover, chaperones
	barA	-	Histidine kinase-, DNA gyrase B-, and HSP90-like ATPase
	basS	COG0642	Signal transduction histidine kinase Signal transduction mechanisms
	qseC	COG0642	Signal transduction histidine kinase Signal transduction mechanisms
	phoP	COG0745	DNA-binding response regulator, OmpR family, contains REC and winged-helix (wHTH) domain Signal transduction mechanisms, Transcription
	phoQ	COG0642	Signal transduction histidine kinase Signal transduction mechanisms
	btuB	-	Iron complex outermembrane receptor protein
	btuB	COG1629	TonB-dependent receptor for iron transport Inorganic ion transport and metabolism
	hfq	COG1923	sRNA-binding regulator protein Hfq Signal transduction mechanisms
Nutrient acquisition	Tryptophan synthase alpha chain	COG0159	Tryptophan synthase alpha chain Amino acid transport and metabolism
	Tryptophan synthase beta chain	COG0133	Tryptophan synthase beta chain Amino acid transport and metabolism
	trpR	COG2973	Trp operon repressor Transcription
	Tryptophan tRNA ligase	COG0180	Tryptophanyl-tRNA synthetase Translational, ribosomal structure and biogenesis
	pstB	COG1117	ABC-type phosphate transport system, ATPase component Inorganic ion transport and metabolism
	phoR	COG5002	Signal transduction histidine kinase Signal transduction mechanisms

	phoH	COG1702	Phosphate starvation-inducible protein PhoH, predicted ATPase Signal transduction mechanisms
	phoB	COG0745	DNA-binding response regulator, OmpR family, contains REC and winged-helix (wHTH) domain Signal transduction mechanisms, Transcription
	pstA	COG0581	ABC-type phosphate transport system, permease component Inorganic ion transport and metabolism
	pstC	COG0573	ABC-type phosphate transport system, permease component Inorganic ion transport and metabolism
	pstS	COG0226	ABC-type phosphate transport system, periplasmic component Inorganic ion transport and metabolism
	phoU	COG0704	Phosphate uptake regulator Inorganic ion transport and metabolism
Adaptation to new conditions	*recO*	COG1381	Recombinational DNA repair protein (RecF pathway) Replication, recombination and repair
	recF	COG1195	Recombinational DNA repair ATPase RecF Replication, recombination and repair
	recA	COG0468	RecA/RadA recombinase Replication, recombination and repair
	recB	COG1074	ATP-dependent exoDNAse (exonuclease V) beta subunit (contains helicase and exonuclease domains) Replication, recombination and repair
	recC	COG1330	Exonuclease V gamma subunit Replication, recombination and repair
	recD	COG0507	ATP-dependent exoDNAse (exonuclease V), alpha subunit, helicase superfamily I Replication, recombination and repair
	recR	COG0353	Recombinational DNA repair protein RecR Replication, recombination and repair
	rdgC	COG2974	DNA recombination-dependent growth factor C Replication, recombination and repair
	mgsA	COG2256	Replication-associated recombination protein RarA (DNA-dependent ATPase) Replication, recombination and repair
	tRNA (cytidine(34)-2'-O)-methyltransferase	COG0219	tRNA(Leu) C34 or U34 (ribose-2'-O)-methylase TrmL, contains SPOUT domain Translation, ribosomal structure and biogenesis
	tRNA (guanine-N(1)-)-methyltransferase	COG0336	tRNA G37 N-methylase TrmD Translation, ribosomal structure and biogenesis
	tRNA (guanine-N(7)-)-methyltransferase	COG0220	tRNA G46 methylase TrmB Translation, ribosomal structure and biogenesis
	ttcA	COG0037	tRNA(Ile)-lysidine synthase TilS/MesJ Translation, ribosomal structure and biogenesis
	tRNA dimethylallyltransferase	COG0324	tRNA A37 N6-isopentenylltransferase MiaA Translation, ribosomal structure and biogenesis

	mnmE	COG0486	tRNA U34 5-carboxymethylaminomethyl modifying GTPase MnmE/TrmE Translation, ribosomal structure and biogenesis
	tRNA pseudouridine synthase A	COG0101	tRNA U38,U39,U40 pseudouridine synthase TruA Translation, ribosomal structure and biogenesis
	tRNA pseudouridine synthase B	COG0130	tRNA U55 pseudouridine synthase TruB, may also work on U342 of tmRNA Translation, ribosomal structure and biogenesis
	tsaB	COG1214	tRNA A37 threonylcarbamoyladenosine modification protein TsaB Translation, ribosomal structure and biogenesis
	tsaE	COG0802	tRNA A37 threonylcarbamoyladenosine biosynthesis protein TsaE Translation, ribosomal structure and biogenesis
	tRNA threonylcarbamoyladenosine dehydratase	COG1179	tRNA A37 threonylcarbamoyladenosine dehydratase Translation, ribosomal structure and biogenesis
	tRNA-2-methylthio-N(6)-dimethylallyladenosine synthase	COG0621	tRNA A37 methylthiotransferase MiaB Translation, ribosomal structure and biogenesis
	tRNA-dihydrouridine(20/20a) synthase	COG0042	tRNA-dihydrouridine synthase Translation, ribosomal structure and biogenesis
	ygfZ	COG0354	Folate-binding Fe-S cluster repair protein YgfZ, possible role in tRNA modification Posttranslational modification, protein turnover, chaperones
	mnmA	COG0482	tRNA U34 2-thiouridine synthase MnmA/TrmU, contains the PP-loop ATPase domain Translation, ribosomal structure and biogenesis
	tRNA(Ile)-lysidine synthase	COG0037	tRNA(Ile)-lysidine synthase TilS/MesJ Translation, ribosomal structure and biogenesis
Cell envelope structure	Biosynthetic peptidoglycan transglycosylase	-	monofunctional biosynthetic peptidoglycan transglycosylase
	rlpA	COG0797	Rare lipoprotein A, peptidoglycan hydrolase digesting "naked" glycans, contains C-terminal SPOR domain Cell wall/membrane/envelope biogenesis
	ftsI	COG0768	Cell division protein FtsI/penicillin-binding protein 2 Cell cycle control, cell division, chromosome partitioning, Cell wall/membrane/envelope biogenesis
	mrdA	COG0768	Cell division protein FtsI/penicillin-binding protein 2 Cell cycle control, cell division, chromosome partitioning, Cell wall/membrane/envelope biogenesis
	Peptidoglycan-N-acetylglucosamine deacetylase	COG4249	Uncharacterized protein, contains caspase domain General function prediction only

	UDP-2,3-diacylglucosamine hydrolase	COG2908	UDP-2,3-diacylglucosamine pyrophosphatase LpxH Cell wall/membrane/envelope biogenesis
	UDP-3-O-(3-hydroxymyristoyl)glucosamine N-acyltransferase	COG1044	UDP-3-O-[3-hydroxymyristoyl] glucosamine N-acyltransferase Cell wall/membrane/envelope biogenesis
	UDP-3-O-acyl-N-acetylglucosamine deacetylase	COG0774	UDP-3-O-acyl-N-acetylglucosamine deacetylase Cell wall/membrane/envelope biogenesis
	UDP-3-O-acylglucosamine N-acyltransferase	-	-
	UDP-glucose 4-epimerase	COG0451	Nucleoside-diphosphate-sugar epimerase Cell wall/membrane/envelope biogenesis
	tuaD	COG1004	UDP-glucose 6-dehydrogenase Cell wall/membrane/envelope biogenesis
	UDP-N-acetyl-alpha-D-glucosamine C6 dehydratase	COG1086	NDP-sugar epimerase, includes UDP-GlcNAc-inverting 4,6-dehydratase FlaA1 and capsular polysaccharide biosynthesis protein EpsC Cell wall/membrane/envelope biogenesis, Posttranslational modification, protein turnover, chaperones
	UDP-N-acetyl-D-glucosamine 6-dehydrogenase	COG0677	UDP-N-acetyl-D-mannosaminuronate dehydrogenase Cell wall/membrane/envelope biogenesis
	UDP-N-acetylenolpyruvoylglucosamine reductase	COG0812	UDP-N-acetylenolpyruvoylglucosamine reductase Cell wall/membrane/envelope biogenesis
	UDP-N-acetylglucosamine 1-carboxyvinyltransferase	COG0766	UDP-N-acetylglucosamine enolpyruvyl transferase Cell wall/membrane/envelope biogenesis
	UDP-N-acetylglucosamine 4-epimerase	COG0451	Nucleoside-diphosphate-sugar epimerase Cell wall/membrane/envelope biogenesis
	UDP-N-acetylglucosamine--N-acetylmuramyl-(pentapeptide) pyrophosphoryl-undecaprenol N-acetylglucosamine transferase	COG0707	UDP-N-acetylglucosamine:LPS N-acetylglucosamine transferase Cell wall/membrane/envelope biogenesis
	UDP-N-acetylmuramate--L-alanine ligase	COG0773	UDP-N-acetylmuramate-alanine ligase Cell wall/membrane/envelope biogenesis
	UDP-N-acetylmuramate--L-alanyl-gamma-D-glutamyl-meso-2,6-diaminoheptandioate ligase	COG0773	UDP-N-acetylmuramate-alanine ligase Cell wall/membrane/envelope biogenesis
	UDP-N-acetylmuramoyl-L-alanyl-D-glutamate--2,6-diaminopimelate ligase	COG0769	UDP-N-acetylmuramyl tripeptide synthase Cell wall/membrane/envelope biogenesis
	UDP-N-acetylmuramoyl-tripeptide--D-alanyl-D-alanine ligase	COG0770	UDP-N-acetylmuramyl pentapeptide synthase Cell wall/membrane/envelope biogenesis
	UDP-N-acetylmuramoylalanine--D-glutamate ligase	COG0771	UDP-N-acetylmuramoylalanine-D-glutamate ligase Cell wall/membrane/envelope biogenesis
	Lipopolysaccharide assembly protein B	COG2956	Lipopolysaccharide biosynthesis regulator YciM, contains six TPR domains and a predicted metal-binding C-terminal domain Cell wall/membrane/envelope biogenesis
	rfaQ	COG0859	ADP-heptose:LPS heptosyltransferase Cell wall/membrane/envelope biogenesis
	lptB	COG1137	ABC-type lipopolysaccharide export system, ATPase component Cell wall/membrane/envelope biogenesis

	lptF	COG0795	Lipopolysaccharide export LptBFGC system, permease protein LptF Cell wall/membrane/envelope biogenesis, Cell motility
	lptG	COG0795	Lipopolysaccharide export LptBFGC system, permease protein LptF Cell wall/membrane/envelope biogenesis, Cell motility
	lptA	COG1934	Lipopolysaccharide export system protein LptA Cell wall/membrane/envelope biogenesis
	lptC	COG3117	Lipopolysaccharide export system protein LptC Cell wall/membrane/envelope biogenesis
	fabG	COG1028	NAD(P)-dependent dehydrogenase, short-chain alcohol dehydrogenase family Lipid transport and metabolism, Secondary metabolites biosynthesis, transport and catabolism, General function prediction only
	3-oxoacyl-[acyl-carrier-protein] synthase 2	COG0304	3-oxoacyl-(acyl-carrier-protein) synthase Lipid transport and metabolism, Secondary metabolites biosynthesis, transport and catabolism
	3-oxoacyl-[acyl-carrier-protein] synthase 3	COG0332	3-oxoacyl-[acyl-carrier-protein] synthase III Lipid transport and metabolism
	3-oxoacyl-[acyl-carrier-protein] synthase 3 protein 2	COG0332	3-oxoacyl-[acyl-carrier-protein] synthase III Lipid transport and metabolism
Recombined sequences from *in vitro* recombinants	GTP-binding protein TypA/BipA	COG1217	Predicted membrane GTPase involved in stress response Signal transduction mechanisms
	Lipase/alpha-beta hydrolase	-	-
	Putative Ctpa-like serine protease/peptidase S41	COG0793	Carboxyl-terminal protease Posttranslational modification, protein turnover, chaperones
	Extracellular serine protease	COG4625	Uncharacterized conserved protein, contains a C-terminal beta-barrel porin domain Function unknown
	Putative Ctpa-like serine protease/ C-terminal processing protease CtpA/Prc, contains a PDZ domain	COG0793	Carboxyl-terminal protease Posttranslational modification, protein turnover, chaperones
	Translocation and assembly module TamA/ outer membrane protein assembly factor/ Surface antigen D15/ pathogenicity protein from Temecula1	COG0729	Autotransporter secretion outer membrane protein TamA Cell wall/membrane/envelope biogenesis

Table S6-7. Frequency of recent recombination events per gene of strains belonging to each *X. fastidiosa* subspecies.

Avalaible online at: https://www.nature.com/articles/s41396-019-0423-y#Ack1

Chapter 7

Concluding remarks

This study describes the growth behavior of '*Candidatus* Liberibacter asiaticus' (CLas) in vitro when cultured in commercial grapefruit juice, as well as the contribution of many conditions and compounds to improve its culturability in laboratory conditions. Additionally, the role of every TFP molecular component on natural competence and twitching motility of *Xylella fastidiosa*, and the genes that have been recombined by intersubspecific homologous recombination within wild-type strains of this pathogen, were determined.

When cultured in commercial grapefruit juice amended with compounds predicted to be important to fulfill the nutrient requirements of CLas, this bacterium presented a common growth behavior in which growth ratios were inversely proportional to the initial inoculum concentration. The dilution of samples allowed growth to resume, suggesting that this growth behavior is likely regulated by a cell density-dependent mechanism. Subculturing at short intervals and incubation under flow conditions were performed aiming at reducing the cell density of CLas. This allowed cells to multiply and reach a maximum growth as fast as 3 days post inoculation, but no sustained exponential growth was observed in any tested condition, and cultures unfortunately lost viability over time, being only transient. An ex vivo system to grow CLas from periwinkle calli initiated from infected leaves was also established and allowed cells to reach a high population. Together, our results describe a set of conditions and compounds that could improve the axenic growth of CLas, and we hope our findings may aid further efforts toward culturing this bacterium.

In *X. fastidiosa*, a comprehensive set of 38 type IV pili genes were analyzed to establish their functional role on the natural competence and twitching motility of this pathogen. Ten core genes were identified as being essential for both functions. These include the dedicated ATPases PilB (extension) and PilT (retraction), the prepilin peptidase PilD, the platform protein PilC, the entire alignment subcomplex PilMNOP, the secretin PilQ and the regulatory protein PilZ. Moreover, we identified that the minor pilin FimT3 is the DNA receptor of the *X. fastidiosa* TFP, which binds DNA non-specifically through a surface-exposed electropositive stripe. The function of TFP molecular components in other important phenotypes of the pathogen was also determined, including growth, cell aggregation and biofilm formation. Besides, whole genome analyses allowed the identification of recently recombined genes involved in host colonization, regulation and signaling, host evasion, and nutrient acquisition, which are all important for the ecology of *X. fastidiosa*. Our findings help to elucidate an important mechanism required for acquisition of exogenous DNA that contributes to the expansion of genetic diversity within *X. fastidiosa* and provide insights into how intersubspecific homologous recombination events may affect the evolution and adaptation of this pathogen to colonize its host's environments.